TECHNISCHE
UNIVERSITÄT
WIEN
Vienna University of Technology

Institut für Verfahrenstechnik,
Umwelttechnik und
Technische Biowissenschaften

DISSERTATION

"Hydrogen from Biomass for Industry - Industrial Application of Hydrogen Production Based on Dual Fluid Gasification"

written at the Vienna University of Technology,

for the purpose of obtaining the academic degree
"Dr. techn." supervised by

Univ.Prof. Dipl.-Ing. Dr.techn. Tobias Pröll
E166, Institute of Chemical Engineering

Univ.Prof. Dipl.-Ing. Dr.techn. Hermann Hofbauer
E166, Institute of Chemical Engineering

approved by the

Faculty of Technical Chemistry

Ing. Dipl.-Ing. Stefan Müller
0425596
Preindlgasse 3/6
1130 Vienna

April 15th, 2013 ____________________

Imprint

stefan.mueller@alumni.tuwien.ac.at,
Institute of Chemical Engineering,
Vienna University of Technology,
Getreidemarkt 9/166,
1060 Vienna,
Austria,

Dissertation:

"Hydrogen from Biomass for Industry-
Industrial Application of a Hydrogen Production
Based on Dual Fluid Gasification"

ISBN: 978-3-9502754-5-2

Printed by: Institute of Chemical Engineering in Vienna, April 15th, 2013
Reproduction requires color print

Distributed by:
Vienna University of Technology,
Institute of Chemical Engineering,
Getreidemarkt 9/166,
1060 Vienna
Austria

+43 158801 16600
www.vt.tuwien.ac.at

…
Because the truth is, that promoting science isn't just about providing resources, it's about protecting free and open inquiry. It's about ensuring that facts and evidence are never twisted or obscured by politics or ideology. It's about listening to what our scientists have to say, even when it's inconvenient, especially when it's inconvenient. Because the highest purpose of science is the search for knowledge, truth, and a greater understanding of the world around us, …, if we support science education to create the next generation of scientists and engineers, … if we have the vision to believe and invest in the things unseen, then we can lead the world into a new future of peace and prosperity …

44th President of the United States of America
…

Preface

Mankind today is facing major fundamental challenges. Our undiminished rising energy and resource consumption is destined to lead to an ecological and social upheaval which could in the near future endanger the peaceful growth and development of our world's society. Therefore, a major change in our behavioral patterns is necessary, leading ultimately to a time of transition. In the years ahead, we need to execute a major move away from our exploding resource consumption to a sustainable way of living that assures the peaceful survival of future generations. The scientific results within this dissertation are a small contribution to coping with the huge challenges which lie ahead of us.

The availability of usable energy was a major requirement for the development of today's wealthy society. In the past century, we were witness to an economic miracle that led to impressive prosperity in some parts of our world. Our energy supply for this wealth was mainly based on primary fossil energy resources like coal, oil and natural gas. Historically speaking, Europe has always been confronted with a shortage of resources due to the fact that only a limited amount of these required resources can be found within Europe's boundaries. For this reason, large amounts of resources and more than 50% of the primary energy demand have to be imported from countries outside of the European Union. Only an efficient utilization of all used resources can ensure that the future wealth of Europe can be maintained at a high level. Consequently, the sustainable utilization of renewable energy sources like water, wind, sun and biomass are seen today as an essential way to improve the prospects for our future energy supply. Our future energy system needs to ensure our mobility, the supply of electricity, the heating and cooling of our houses as well as the operation of our industry. While water, wind and sun have been so far mainly used for the generation of electricity, biomass is a renewable energy source with special properties and strengths. In comparison to wind, water and sun, biomass is the only renewable energy source which contains chemical energy and this fact leads to some significant advantages with regard to its utilization. The investigations in this work examine different concepts for the application of biomass as energy resources for the production of hydrogen for industrial processes. The investigations were carried out with a special focus on biomass gasification technology which offers a technological bridge from solid biomass feedstock to high quality clean energy carriers.

The creation of scientific results for a "Dissertation" demands curiosity, enthusiasm, discipline and persistence. The results thus obtained would not have been possible without the support of my colleagues and friends. I should like to thank Martin Stidl for his instructions and his patience at the beginning of my scientific work. I also want to thank Michael Fuchs for his friendly guidance and support during my time at the institute. The work has been proof read by Johannes Schmid, Stefan Koppatz, Cornelia Müller and Maureen Steel. I thank all of them for their critical look at my results and their constructive feedback. I also have to thank Tobias Pröll and Hermann Hofbauer for the scientific direction during the development of the achieved results. And finally I want to acknowledge the wonderful support, love and patience of my girlfriend Kordula Krassel during this demanding time.

The following results are a small contribution which should help to cope with the huge challenges which lie ahead of us. I believe strongly in our scientific institutions and in our efforts for technological change. These should undoubtedly help to overcome the major challenges we are facing even though they sometimes seem to be insuperable.

Stefan Müller, Vienna, March 2013

Abstract

The present work provides a detailed investigation of production pathways for the supply of hydrogen from solid biomass for industrial production processes. The investigations carried out, were focused on the capabilities of:

- **dual fluidized bed steam gasification** (dual fluid gasification)
- and **sorption enhanced reforming** (SER).

These processes have been used to evaluate the large-scale generation of:

(1) hydrogen with high purity for a refinery and
(2) hydrogen-rich gas for iron production.

The investigations carried out included a discussion of:

- the state of knowledge in the field of biomass gasification
- the state of knowledge in the field of sorption enhanced reforming,
- existing experimental results,
- as well as operational data from existing plants,
- and an illustration of the economic environment.

Additional sorption enhanced reforming experiments were conducted to contribute specific data for the plant development. During the experiments, limestone, a commodity already in use within the iron production process, was applied as bed material. In the end, the collected data has been taken for the calculation of **two novel hydrogen production plants** by the deployment of process simulation software:

(1) The resulting mass and energy balances showed that **hydrogen with high purity can be produced from biomass for a refinery**. The production process used was based on conventional dual fluid gasification in combination with equipment well known from natural gas steam reforming. Results achieved, illustrated that 30 MW of hydrogen can be produced from 50 MW of woody biomass.

(2) Sorption enhanced reforming has been applied to calculate the production of a **hydrogen-rich reducing agent for an iron production**. The results showed that 133 MW of woody biomass are necessary to supply 100 MW of hydrogen-rich reducing agent.

Both "hydrogen production plants" have been considered suitable for pursuing implementation steps from a technological point of view. The economic assessment of both production processes showed that the success of the elaborated plants is strongly dependent on the future development of feedstock prices. The current price level of biomass in Austria (~22,5 €/MWh, wood chips) in comparison to the price level of natural gas (~29 €/MWh) is not supporting a hydrogen production from biomass. In the case of an **iron production**, an economic parameter analysis showed, that a fuel price below 12 €/MWh would create preferable economic precondition for the realization of the proposed plant. The results showed, that further research activities in the field of gasification technology need to concentrate on high fuel flexibility towards low price feedstock.

Kurzfassung

Die vorliegende Dissertation umfasst eine detaillierte Untersuchung von Anlagenkonzepten für die Erzeugung von Wasserstoff aus Biomasse zur Einbindung in großindustrielle Produktionsprozesse. Der Fokus der Arbeit lag dabei auf den Einsatzmöglichkeiten:

- der „Zweibett-Wirbelschicht-Dampfvergasung“ (dual fluid Vergasung),
- sowie von „Sorption Enhanced Reforming“ (SER).

Die genannten Prozesse wurden im Rahmen der Arbeit eingehend untersucht und für die Entwicklung neuer Anlagenkonzepte zur Produktion:

(1) von hochreinem Wasserstoff für eine Raffinerie, und
(2) von wasserstoffreichem Reduktionsgas für die Eisenproduktion

eingesetzt. Als Ausgangsbasis für die Entwicklung der Anlagenkonzepte wurden umfassende Analysen durchgeführt:

- „Stand der Technik“ im Bereich Biomassevergasung,
- „Stand der Technik“ im Bereich Sorption Enhanced Reforming,
- bestehende experimentelle Ergebnissen,
- Betriebsdaten bestehender Großanlagen,
- sowie eine umfassende Darstellung des ökonomischen Umfelds.

Des Weiteren wurden im Zuge der Arbeit „Sorptionen Enhanced Reforming“-Versuche durchgeführt, um spezifische Daten für die Untersuchungen zu erhalten. Die Experimente wurden dabei mit Kalkstein durchgeführt, der bereits als Zuschlagsstoff in der Roheisenerzeugung eingesetzt wird. Die gewonnen Daten sowie die Erkenntnisse der Literaturrecherche wurden schlussendlich für die Modellierung von zwei neuen Anlagenkonzepten für die Wasserstofferzeugung genutzt:

(1) Die Ergebnisse zeigten, dass mittels konventioneller dual fluid Vergasungstechnologie und mit Hilfe der technischen Elemente der Erdgasreformierung hochreiner **Wasserstoff für eine Raffinerie** erzeugt werden kann. Die Ergebnisse zeigten des Weiteren, dass für die Herstellung von 30 MW Wasserstoff, 50 MW an holzartiger Biomasse benötigt werden.

(2) Der „Sorption Enhanced Reforming“-Prozess wurde für die Modellierung eines Anlagenkonzepts zur **Bereitstellung von wasserstoffreichem Gases für die Roheisenerzeugung** eingesetzt. Die Ergebnisse zeigten, dass für die Herstellung von 100 MW wasserstoffreichem Reduktionsgas, 133 MW an holzartiger Biomasse benötigt werden.

Die Untersuchungen ergaben, dass sich beide Konzepte aus technischer Perspektive für weitere Umsetzungsschritte eignen. Der ökonomische Erfolg ist im Wesentlichen von der Entwicklung der Rohstoffpreise abhängig. Das derzeitige Preisniveau von Biomasse in Österreich (~22,5 €/MWh für Waldhackgut) im Vergleich zu Erdgas (~29 €/MWh) macht eine Umsetzung aus ökonomischer Sicht nicht sinnvoll. Die Analyse der ökonomischen Parameter zeigte aber, dass im untersuchten Fall der Roheisenerzeugung, ein Brennstoffpreis unter 12 €/MWh bereits einen wirtschaftlichen Betrieb ermöglichen könnte. Die weitere Entwicklung der Vergasungstechnologien sollte sich daher auf kostengünstige Festbrennstoffe und erhöhte Brennstoffflexibilität konzentrieren.

Publications

Journal articles

I. Müller, S., Stidl, M., Pröll, T., Rauch, R., Hofbauer, H., 2011, "Hydrogen from Biomass - Large Scale Hydrogen Production Based on a Dual Fluidized Bed Steam Gasification System", Biomass Conversion and Biorefinery, (2011) 1, 55-61.

Peer-reviewed article as conference contributions

II. Müller, S., Kotik, J., Pröll, T., Rauch, R., Hofbauer, H., 2011, "Hydrogen from Biomass for Industry - Biomass Gasification for Integration in Refineries", in: Proceedings of the International Conference on Polygeneration Strategies (ICPS11), 30 August - 1 September 2011, Wien, Austria.

III. Müller, S., Pröll, T., Hofbauer, H., 2012, "A Thermodynamic Investigation of Dual Fluidized Bed Biomass Gasification with Sorption Enhanced Reforming", in: Proceedings of the 21st International Conference on Fluidized Bed Combustion (FBC), 3.-6. June 2012, Naples, Italy, pp.781-788, ISBN978-88-89677-83-4

Abstract reviewed article as conference contributions

IV. Müller, S., Stidl, M., Pröll, T., Rauch, R., Hofbauer, H., 2010, "Hydrogen from Biomass - Large Scale Hydrogen Production Based on a Dual Fluidized Bed Steam Gasification System", in: Proceedings of the International Conference on Polygeneration Strategies (ICPS10), 7 - 9 September 2010, Leipzig, Germany.

Directed master thesis

V. Jentsch R., Master Thesis, to be published 2013, Sorption Enhanced Reforming within the Next Generation Dual Fluid Gasifier, Institute of Chemical Engineering, Vienna University of Technology (written in German).

Relevant technical reports

VI. Müller, S., Stidl, M., Pröll, T., Fuchs, M., Rauch, R., Hofbauer, H., 2011 "BioH2 4Refineries - Simulationsergebnisse zur Erzeugung von Wasserstoff für Raffinerien mittels Biomassevergasung", Internal Report, Institute of Chemical Engineering, Vienna University of Technology (written in German)

VII. Müller, S., Kotik, J., Pröll, T., Hofbauer, H., 2011, "Hydrogen Production from Residues of Palm Oil Industry", Project Report H2 SIM GUO, Institute of Chemical Engineering, Vienna University of Technology.

VIII. Stidl, M., Müller, S., Kotik, J., Pröll, T., Hofbauer, H., 2011, "PRIMINREP - Primärressourcenreduzierte Roheisenproduktion - Integration eines Biomasse-Wirbelschicht-Dampfvergasers bei der Voestalpine Stahl GmbH", Technical Project Report PRIMINREP, Institute of Chemical Engineering, Vienna University of Technology (written in German).

IX. Stidl M., Müller S., Pröll T., Hofbauer H., 2010, "Integration eines Biomasse-Wirbelschichtdampfvergasers zur Erzeugung eines Produktgases zwecks Erdgassubstitution bei der SCA Hygiene Products GmbH", Technical Report, Project "Biomass to Gas", Institute of Chemical Engineering, Vienna University of Technology (written in German).

Acknowledgement

The present work summarizes the outcome of several **research projects** conducted at the Institute of Chemical Engineering at the Vienna University of Technology:

1. Neue Energien 2020, 821890, Biomass to Gas – Bewertung der technischen, ökonomischen und ökologischen Machbarkeit der Biomassevergasung zum Einsatz in der KWK-Anlage der SCA Hygiene Products GmbH
2. Neue Energien 2020, 818928 , Primärressourcen-minimierte Roheisenproduktion (PRIMINREP) – Integration eines Biomasse-Wirbelschicht-Dampfvergasers bei der Voestalpine Stahl GmbH
3. Industrial contract, Hydrogen Production from Residues of Palm Oil Industry (H2 SIM GUO)
4. Neue Energien 2020, 829907, Erzeugung von Wasserstoff für Raffinerien über Biomassevergasung (BioH2 4Refineries), together with OMV Refining & Marketing GmbH
5. Neue Energien 2020, 829904 , Erzeugung eines Produktgases aus Biomassereformierung mit selektiver CO_2-Abtrennung (ERBA) together with Voestalpine Stahl GmbH
6. Neue Energien 2020, 825490, Zweibettwirbelschicht Biomasse-Dampfvergaser der zweiten Generation (G-volution II), together with TECON Engineering GmbH

The results have been reached with financial support from the Austrian “Klima & Energiefonds” supported by the Austrian “Forschungsförderungsgesellschaft” (FFG) .

Special thanks are also given to all industrial partners who supported the development of the present work.

Table of Content

1. Introduction

In the past the availability of fossil energy resources has been a major reason for the successful development of wealthy societies in some parts of our world. Today, the excessive use of **fossil energy resources** could lead to significant negative impacts on our environment and our society in the near future.

According to the International Energy Agency (IEA), a change in our **energy system** is urgently needed to support energy supply security by an efficient utilization of used resources and in order to prevent a major change of the world's climate. Therefore, our energy system needs to be transformed to a **sustainable energy system** based on renewable energy sources. Especially Europe is suffering from a scarcity of resources and is therefore under pressure to find solutions for an efficient utilization of resources to prevent a future decline of wealth. For that reason, important international agreements such as emission targets have been set to reduce greenhouse gas emissions. These, made agreements are not enough to guarantee a limitation of global warming to an average increase of 2°C compared to the year 1850. But they are a first step in shaping a sustainable energy system for the future. To realize such a sustainable energy system, further development of **energy technologies** which enable the use of **renewable energy** is urgently required.[1]

Biomass is, among renewable energy sources, a source with special characteristics and strengths. Compared to wind, water and sun, biomass is the only renewable energy source which directly contains chemical energy. As a consequence, biomass would be a resource capable of replacing fossil fuels for mobility and industrial applications. At the same time, increased utilization of biomass would reduce fossil greenhouse gas emissions and energy imports. A promising energy conversion technology, which can enable a utilization of **biomass for industrial applications,** is **dual fluidized bed steam gasification** (dual fluid gasification). At the current stage of development the following key question arises: In which way can dual fluid gasification enable the most efficient utilization of biomass for industry?

Dual fluid gasification has made impressive development progress during recent years, which would support the integration of energy from biomass into industrial production processes. After the first demonstration of **dual fluid gasification** in a commercial plant in Güssing (Austria) 2002, ambitious research activities have focused on different **polygeneration concepts**. These polygeneration concepts aimed on the production of several (poly) fuels in one single plant. The investigations showed that products like synthetic natural gas[2] (SNG), synthetic diesel fuel[3] (Fischer-Tropsch-diesel fuel) and hydrogen[4] can be produced in one single plant beside electricity and heat. While commercial dual fluid gasification plants so far were built to produce electricity and heat, with our present knowledge, the production of hydrogen could also be applied. But at this point, the questions "How can hydrogen from biomass be produced by dual fluid gasification in the most economic and efficient way?" and "How can it be integrated in existing industrial plants?" have not yet been answered.

---

[1] cf. International Energy Agency (IEA), 2010, p45ff.

[2] cf. Rehling B., 2009, p7

[3] cf. Sauciuc A., 2011, p1

[4] cf. Mayer T., 2012, p125ff.;

1.1. Aim & Scope

The aim of the present work is to evaluate different concepts for the industrial application of a hydrogen supply based on dual fluid gasification. The evaluation of different application concepts should find answers to:

- How can "**conventional dual fluid gasification**" be deployed to produce pure hydrogen for a refinery on a large scale from biomass?
- How can "**sorption enhanced reforming**" be applied to provide a hydrogen rich gas for iron production on a large scale from biomass?
- What are the technological and economic advantages of **sorption enhanced reforming** over **conventional dual fluid gasification** for the production of a reducing agent?
- Are the hydrogen production costs achieved, sufficiently low to justify a further step aiming at the realization of large-scale plants?

1.2. Methodology

Fig. 1 shows the structure of the present work. To answer all the raised questions so far, the thesis starts with a discussion of the general economic surroundings of dual fluid gasification. In a further step, this thesis shows the current state of knowledge of biomass gasification and future possibilities of dual fluid gasification technology. Then the applied principles and methodology that are used for the investigation of different hydrogen production concepts are explained. In the result section, different hydrogen production concepts based on dual fluid gasification that enable the supply of hydrogen to existing industrial production plants are illustrated. The results achieved should lead to the successful further development of dual fluid gasification technology and reasonably contribute to the reduction of fossil resource consumption of industrial production processes. Furthermore, the results should point out pathways for using biomass as a renewable energy source in industry. This is realized by a precise description of opportunities and threats of different application concepts. The present work is carried out during a time strongly influenced by two major economic crises which occurred at the beginning of the years 2008 and 2011. Furthermore, a second major nuclear disaster after Chernobyl 1986 occurred at the beginning of 2011 in Fukushima, Japan.

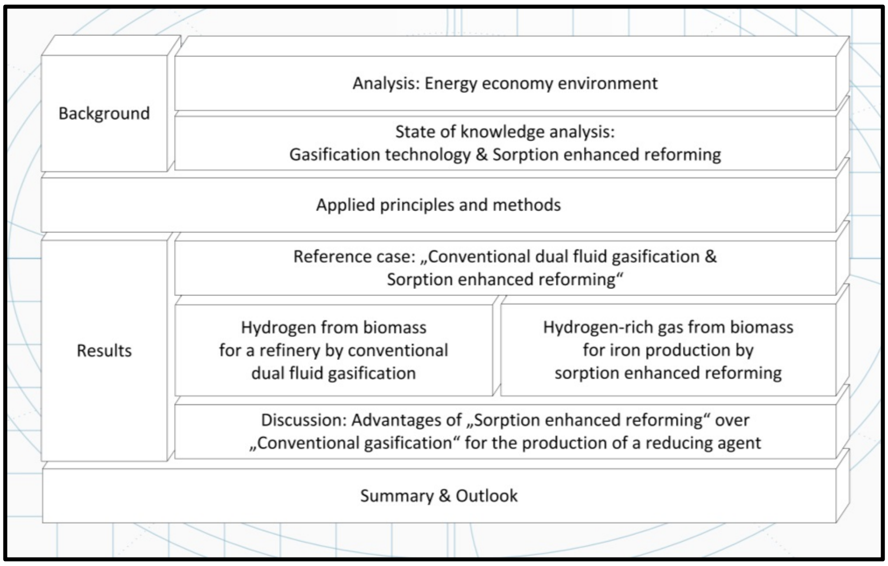

Fig. 1: Structure of present work

2. Energy Economy Environment

Large amounts of easily accessible primary energy resources have enabled the development of pleasant wealth in some parts of the world. The low-cost availability of energy provided the foundation for economic growth, wealth and power to shape our society. Nevertheless, energy was and still is a scarce economic commodity which needs to be treated with respect to its limited availability. Highly rising energy consumption already caused a rising amount of negative ecological impacts on the environment. Negative impacts like **global warming** or heavy nuclear disaster have raised a strong need for a major change of our energy system. Therefore, our current energy system needs to be transformed to a **sustainable energy system** with the aim of sustainable utilization of available energy resources. A change towards a sustainable energy system would mean a reduced consumption of fossil energy and a rising share of **renewable energy**. This would imply a fundamental change of the current **energy economy**, the **energy demand** and the **energy supply**. The preconditions for such a sustainable energy system, which will be accepted by the general public, need to be implemented by elected governments and political leaders.[1] The utilization of renewable energy sources needs to be enabled by **renewable energy technologies.**

2.1. Definitions

Renewable energy sources are energy sources which are considered to be inexhaustible in human dimensions. Solar radiation reaching the earth is responsible for the creation renewable energy like hydropower, wind and biomass.[2]

Primary energy is energy which exists in nature in its natural form without being effected by a technological conversion process. Examples for primary energy are crude oil, natural gas, coal, sun energy, water energy and wind energy.[3]

Final energy is energy which is formed out of primary energy with a technological conversion process. Examples for final energy are gasoline, electricity, wood pellets, district heating and hydrogen.[4]

Energy services are the result of energy conversion and represent the achieved benefits. Every energy conversion process includes energetic losses due to the conversion efficiency. Therefore, the achieved energy service includes energetic losses from every conversion process beforehand. Examples for such benefits from energy services are a comfortably heated room, a lighted room or an achieved transport from point A to point B.[5]

"**Sustainable development** is considered as a development that meets the needs of the present without compromising the ability of future generations to meet their own needs."[6]
A **sustainable energy system** enables energy supply to society without impairing future possibilities for the energy supply of future generations.

---

1 cf. Nakicenovic N., 2010, p1-3 – p1-4
2 cf. Hofbauer H., 2007, p3
3, 4, 5 cf. Nakicenovic N., 2010, p1-6
6 cf. Brundtland G., 1987, p54

2.2. Energy Demand

The EU-27 countries are responsible for about 15% (76 EJ, 1800 Mtoe) of the primary energy consumption worldwide (500 EJ, 11900 Mtoe).[1] **Fig. 2** gives an impression of the current energy demand in the European Union by displaying the final energy consumption of different sectors. European households, the transportation and the industrial sector are responsible for the main share of the overall energy demand. The energy demand of **households** in Europe is mainly driven by heating, cooling of houses and a smaller share of need for electricity. Room heating causes a significant demand for heat at a low temperature level. Therefore, common room heating systems demand energy from district heating networks, natural gas, wood, oil or even electricity. The **transportation** sector enables the transportation of goods and provides public and individual mobility services. To supply these services, the energy demand of the transportation sector implies a high demand for energy carriers with high energy density like final energy products from fossil crude oil.

The **industrial sector** operates industrial plants for the production of goods and commodities. **Fig. 2** shows that especially energy intensive industry like steel-, petrochemical-, food-, glass- and paper industry are responsible for the main share of energy demand in this sector. These industries require a large amount of low price fuels to operate their plants. At the same time low price fuels like coal and natural gas cause a significant amount of fossil CO_2 emissions. The energy demand of energy intensive industry leads to a strong need for an efficient operation of its production plants and the availability of a large amount of low price fuels. The legislation in the European Union tries to force industrial plants to reduce its energy consumption and fossil CO_2 emissions. A market-based **emission trading** system has been introduced within the European Union to reach set emission reduction goals. **These set reduction goals and the demand for energy supply security force the industrial sector to look out for new strategies to reduce fossil energy consumption.**

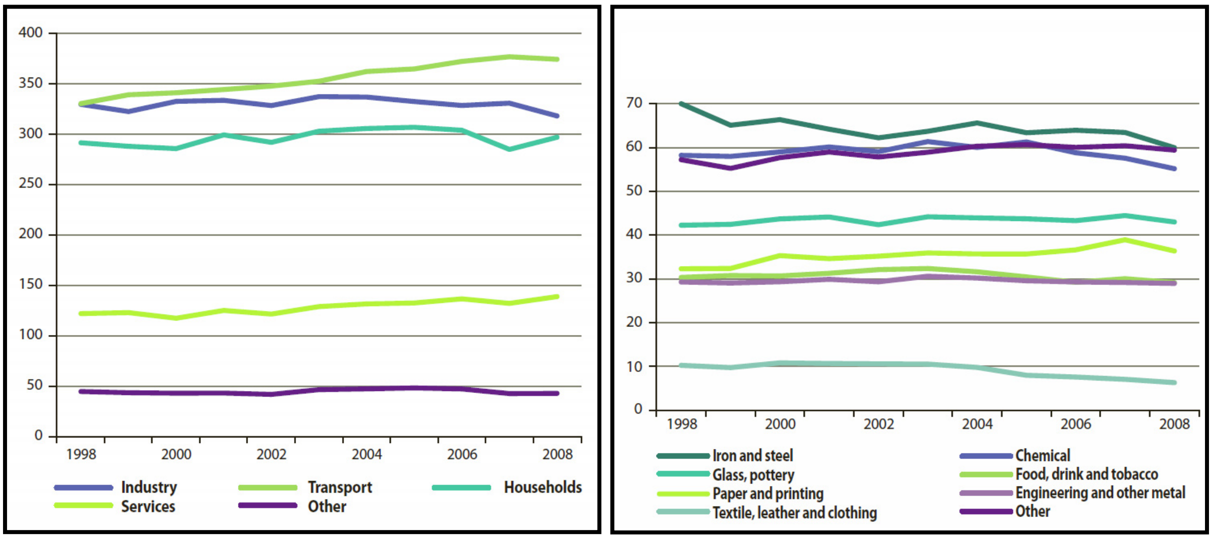

Fig. 2: EU-27: Final energy consumption by commercial sectors & by branch of industry (Mtoe)[2]

---

[1] cf. Nakicenovic N., 2010, p4-16ff
[2] figure: Eurostat, 2011, p49, p51

2.3. Energy Supply

Fig. 3 shows the development of the main European energy supply resources between 1998 and 2008. The current energy supply of the European Union is strongly dependent on fossil energy from oil, natural gas and coal. A main share of the overall energy supply is provided by imports from countries outside of the European Union. Only about 47% (~850 Mtoe, 36 EJ) of the 1800 Mtoe (76 EJ) primary energy demand have been supplied from resources within the European Union. This causes a strong dependence on energy supply from countries outside of the European Union. **Natural gas** imports from abroad are mainly covered by Norway, Russia and Algeria. **Crude oil** imports are mainly supplied by Russia, Norway, Libya, Iran and Saudi Arabia. And **hard coal** imports are primarily provided by South Africa, Russia, Australia and the United States of America.[1] **Fig. 3** further shows that **nuclear energy** is providing a nameable amount of primary energy to the EU-27 countries.

Beside fossil energy resources the energy supply from **renewable energy sources** (RES) started to growth recognizable from a low level. This renewable energy includes energy from hydro-, wind-, biomass-, solar- and geothermal sources.[2] The energy supply for the **industrial sector** within the European Union is mainly provided by fuels shown in **Fig. 3**. The industrial production in Europe is primarily operated with natural gas and electricity. But also oil products and solid fuels like coal provide a large part of the demanded energy. The importance of fuels from renewable energy sources started to grow in the industrial sector from a low level. The legislation of the European Union has set the target to raise the amount of renewable energy sources. **This forces industrial plant operators to look out for new renewable energy sources, which at the same time could induce higher production costs. The availability of energy at affordable prices and energy supply security is a main factor for the location of an industrial production plant.** And at that point high energy prices and a lack of supply security could result in a reallocation of industrial production to countries outside of the European Union.

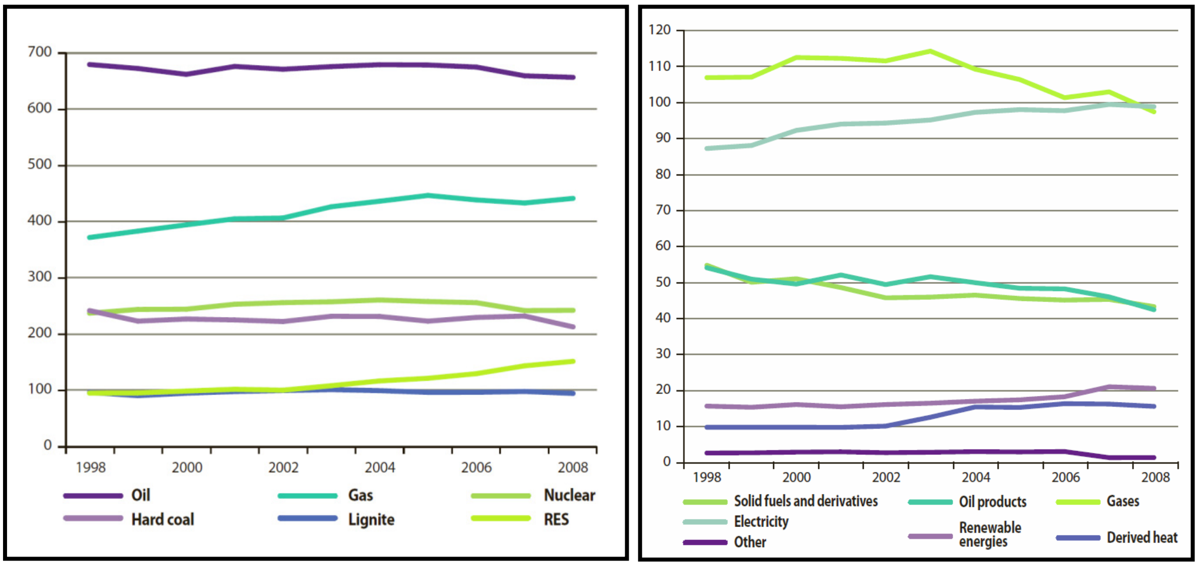

Fig. 3: EU-27: Gross inland primary energy consumption by source & final energy consumption in industry by fuel (Mtoe)[2]

---

[1] Eurostat, 2011, p37ff

[2] figure: Eurostat, 2011, p39, p53

2.3.1. Energy Sources

High energy demand in industrial countries requires **energy sources** with predictable security of supply. Several energy crises in the past have shown the economical and the potential social impact of high energy prices and energy shortages. Therefore, the **energy policy** within the European Union aims at high security of supply and affordable energy prices. Energy reserves play a key role for the **security of supply.** At the same time, energy reserves strongly depend on current energy price and technological stage of development.

Fig. 4 summarizes a model of McKelvey from 1972. Within this model **energy reserves** are defined as identified sources which can be used with the current state of technology at an economic price. The relation between reserves and undiscovered resources strongly depends on the state of science of geology. **Energy resources** name all identified and undiscovered resources which are available at affordable costs or may become affordable in future with respect to the price level. The remaining part is defined as **unconventional sources**. Unconventional sources are not economic and are therefore not considered as energy resource. But energy crises in the past already showed that the relation between reserves, resources and unconventional sources can change very quickly with a higher price. During the last 50 years the global reserves of conventional crude oil were steadily growing because of the described relations.[1] Beside all proved reserves large amount of **unconventional sources** of fossil energy like oil and natural gas are expected. But the availability of fossil energy might become limited within this century if the technological development stagnates.[2]

The global **crude oil reserves** at the end of 2010 have been calculated by BP at 1383 billion barrels. The total global **production** in the same year has been 82 095 thousand barrels a day. These mentioned figures result in a worldwide **reserve-to-production ratio** of around 46.2 years at the end of 2010. In the last century the average crude oil price has been around 25 USD/bbl. Between 1990 and 2010 the crude oil price raised from 30 USD/bbl up to 100 USD/bbl.[1]

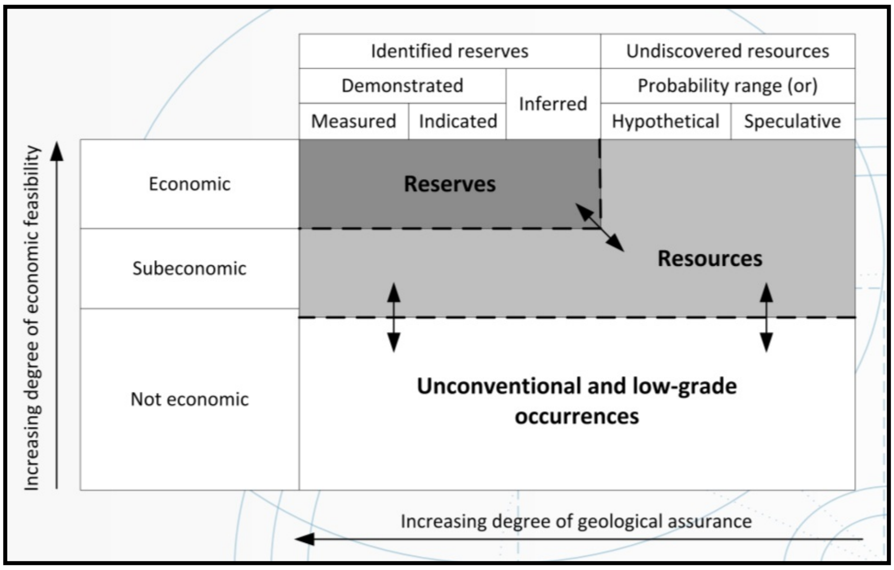

Fig. 4: McKelvey diagram for classifying energy reserves and resources[3]

---

[1] cf. BP, 2011, p6ff
[2] cf. Nakicenovic N., 2010, p6-1ff
[3] cf. figure: McKelvey V., 1972, p32-40

A similar situation can be observed in the sector of **natural gas reserves**. The natural gas reserves have been estimated by BP at 187 trillion cubic meters at the end of 2010. Simultaneously, the annual production has been named 3.2 trillion cubic meters per year. This leads to a reserve-to-production ratio of around 58.6 years for conventional natural gas. Between 1992 and 2010 the price for natural gas increased from 10 USD/MWh up to around 27 USD/MWh.[1] The natural gas price recently decreased in North America due to an increased production of shale gas. Global **coal reserves** at the end of 2010 are estimated by BP at 860 938 million tons. At the same time the annual production amounts to 7 296 million tons. The result for a calculation of the reserve-to-production ratio for coal therefore can be estimated with 118 years at the end of 2011. Between 1990 and 2010 the price for coal scored from 44$/t up to around 92$/t.[2]

Within the European Union the gross inland primary energy consumption is depending mainly on fossil energy source from oil, natural gas and coal. Nearly 80% (cf. **Fig. 3**) of the overall consumption is supplied by these fossil energy reserves. The remaining part is supplied by nuclear and renewable energy sources. The estimation of nuclear energy reserves can be realized in a same way like for fossil energy reserves. The estimation of renewable energy reserves implies a different approach. For the electricity generation with **nuclear power** fissile materials (natural uranium and thorium) are required. In the year 1998 fissile material reserves have been estimated 1 890 EJ and the annual consumption has been around 40 EJ. These numbers induce a reserve-to-production ratio of around 47 years for fissile materials for the operation of nuclear power plants.[3] **Tab. 1** illustrates a comparison of the so far discussed energy sources. **Tab. 2** shows results of an extensive calculation of the technical and theoretical potential of **renewable energy sources** carried out by H. Rogner.

Traditional energy sources	Crude oil	Natural gas	Coal	Nuclear
Occurrences (incl. unconvent. EJ)[4]	~ 80 000	~ 870 000	~ 140 000	-
Proven energy reserves (EJ)	~ 8 000	~ 7 000	~ 18 000	~ 1 890
Reserve / production ratio (a)	46	59	118	47
Current use (EJ/a, 2010) [5, 3]	170	120	150	40
Energy price (€/MWh, 2010)[6]	47	20	8	-
Energy density (MJ/Nm^3)	36 500	34	39 500	-
Carbon dioxide (tCO_2/MWh)[7]	0.29	0.20	0.34	indirect
Advantages	energy density	low CO_2 emiss.	availability, price	low CO_2 emiss.
Disadvantages	CO_2 emissions	energy density	CO_2 emissions	waste, risk

Tab. 1: Comparison of energy sources

Renewable energy source	Current use (2000)	Technical potential	Theoretical potential
Hydropower (EJ/a)	9	50	147
Biomass energy (EJ/a)	50	>276	2 900
Solar energy (EJ/a)	0.1	>1 575	3 900 000
Wind energy (EJ/a)	0.12	640	6 000
Geothermal energy (EJ/a)	0.6	5 000	140 000 000
Ocean energy (EJ/a)	n.a.	n.a.	7 400
Total	**56**	**>7 600**	**> 144 000 000**

Tab. 2: Renewable energy sources potential[8]

---

[1] cf. BP, 2011, p20ff; [2] cf. BP, 2011, p30ff [3] cf. Rogner H., 2000, p166 for open cycle in thermal reactors
[4] cf. Nakicenovic N., 2010, p6-3f; [5] cf. BP, 2011, p41; [6] Reference rate USD/EUR = 0.75;
[7] Rough references depending on exact fuel composition; [8] table: Rogner H., 2000, p168

2.3.2. Energy Source Biomass

Biomass is an example for a renewable energy source with certain strengths and characteristics. Biomass is the only renewable energy source mentioned in **Tab. 2** which can be used as **base material** and directly contains **chemical energy**, whereas the others represent mechanical, solar and heat energy. Chemical energy offers favorable properties due to the energy density. For this reason chemical energy is used to operate cars which demand for a significant amount of energy with high energy density. Biomass is a result of transformed solar energy.

The **definition of biomass** includes organic material from flora and fauna as well as dead parts of plants and animals as long as they are not considered as fossil material. Peat is in most countries already seen as fossil material and thus, marks the boundary between fossil material and biomass. Furthermore, biomass includes animal excrements and biogenous waste. Waste can also be considered as biomass if the waste is a result of the use of organic material from flora and fauna after a technological transformation of these materials.[1]

Woody biomass represents besides energy crops the most important type of biomass for the supply of energy. Within the EU27-countries around 177 757 000 ha of forest and wooded land was available in 2010. Overall the amount of forest in Europe is currently growing. In 2010 the increment in the growing stock was in excess of 770 million m^3 while the wood harvest reached approximately 485 million m^3.[2] These 485 million m^3 of dry wood are roughly equivalent to 4.5 EJ of energy.[3] The supplied wood has been consumed in different ways as products and services. Within the EU27-countries 42% of the overall wood consumption in 2010 was used for energy purposes. Further, 24% of the wood was used within the sawmill industry and additionally 17% were consumed by the pulp industry. The remaining amount of wood was used by the panel and plywood industry (12%), for processing solid fuels (3%) and for other material uses (2%).[4]

The market for energy from biomass is an immature market compared to historically important world markets like the coal or the crude oil market. Therefore, prices for energy from biomass are not as transparent as for example for coal. The price for energy from wood chips can be roughly named in Europe with 15–25 €/MWh strongly depending on location, quality and quantity.[5] In the future it is expected that the production costs of biomass can be reduced by better crops and better production systems. Improved production systems would involve large-scale energy forest plantations. But it has to be admitted that so far very little is known about managing large-scale energy forest plantations or even agricultural and forest residues for energy use.[6] The utilization of energy from biomass could reduce the amount of fossil CO_2 emissions. **Values mentioned before, show that biomass could supply a significant amount of demanded energy if the cost for biomass stays at an adequate level. Due to the strengths of biomass in comparison to other renewable energy sources, biomass especially could supply demanded renewable energy for the transport sector and industrial production processes.**

---

1 cf. Kaltschmitt M., 2009, p2
2 cf. Eurostat, 2011a, p13ff
3 calculation according to lhv and Nakicenovic N., 2010, p1-12ff
4 cf. Eurostat, 2011a, p20
5 cf. Meerman J.C., 2011, p245-p249;
6 cf. Tretter H., 2011, p9;
7 Rogner H., 2000, p162

2.3.3. Energy Infrastructure

Energy infrastructure can be seen as physical structures and necessary delivery systems which enable energy supply to the end users. Energy infrastructure includes power plants, the electrical power grid, pipelines for natural gas, refineries, fueling stations, transportation networks, roads and much more.[1] The components of the existing energy infrastructure today have been developed and built up over many generations in the past. The installation was consuming a significant share of available capital of all national economies in Europe. Figures below give an impression of the installed energy infrastructure in Europe today:

- Refineries in Europe (**Fig. 5**)[2],
- European electrical power grid (**Fig. 7**)[3],
- and the European natural gas network (**Fig. 8**)[4].

Taken efforts in the past enabled the supply of energy at affordable prices today. The infrastructure development was accompanied by the creation of necessary **regulations, technological standards and institutions**, which have a strong influence on the implemented energy supply concepts.[5] So far installed infrastructure served the needs of available energy reserves, energy supply concepts and available energy technologies in the past. Former energy supply concepts had a strong focus on centralized energy supply with large production units. **Existing energy infrastructure and regulations make it hard for renewable energy technologies to be competitive in comparison to traditional energy technologies.** At the same time, renewable energy technologies have to use the existing infrastructure in the best possible way to reach high efficiencies.

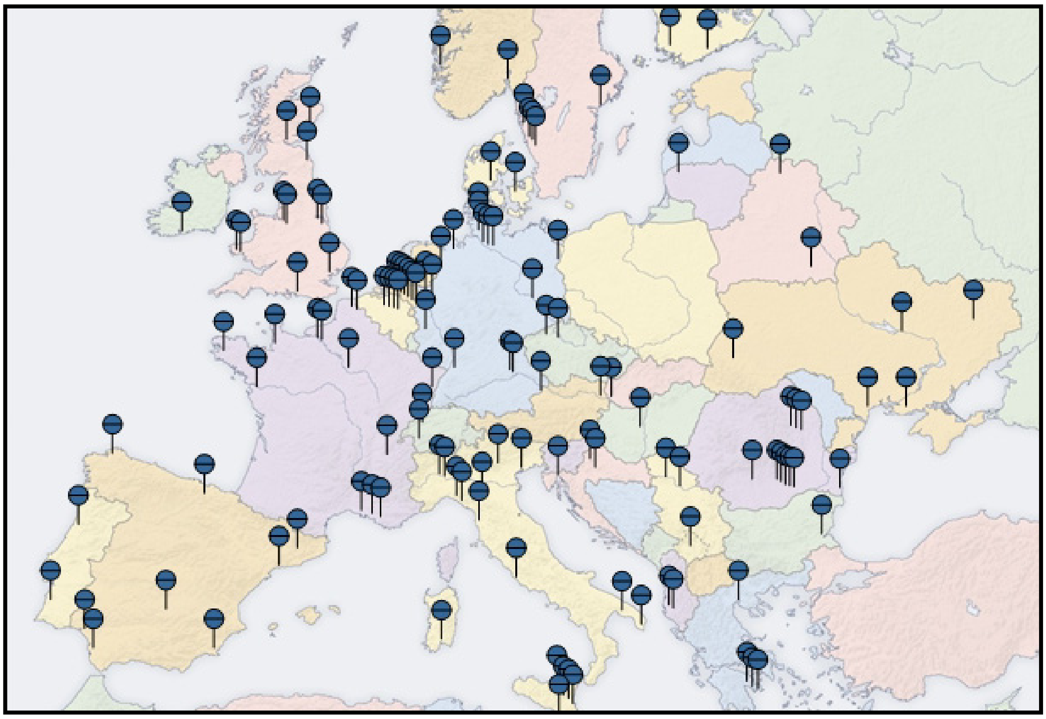

Fig. 5: Energy infrastructure - Refineries in Europe[2]

---

[1] cf. UNDP, 2000, p479

[2] Fig. 5: own survey Müller Stefan, Lichtscheidl Josef

[3] Fig. 7: https://www.entsoe.eu/resources/grid-map/ (read at Sept. 21st, 2011)

[4] Fig. 8: http://www.entsog.eu/mapsdata.html (read at Sept 21st, 2011)

[5] cf. Nakicenovic N., 2010, p5-2 ff.

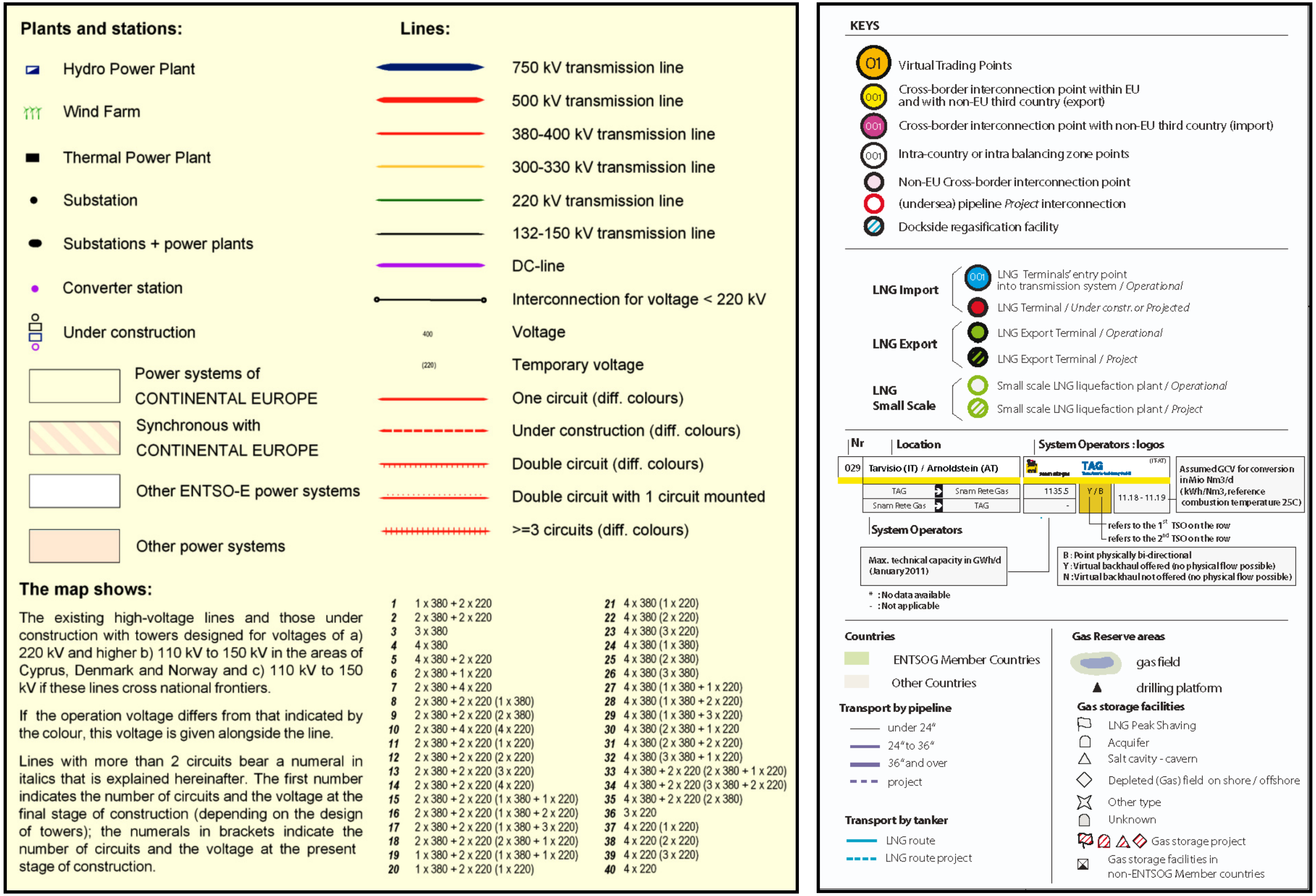

The map shows:

The existing high-voltage lines and those under construction with towers designed for voltages of a) 220 kV and higher b) 110 kV to 150 kV in the areas of Cyprus, Denmark and Norway and c) 110 kV to 150 kV if these lines cross national frontiers.

If the operation voltage differs from that indicated by the colour, this voltage is given alongside the line.

Lines with more than 2 circuits bear a numeral in italics that is explained hereinafter. The first number indicates the number of circuits and the voltage at the final stage of construction (depending on the design of towers); the numerals in brackets indicate the number of circuits and the voltage at the present stage of construction.

1	1 x 380 + 2 x 220	*21*	4 x 380 (1 x 220)
2	2 x 380 + 2 x 220	*22*	4 x 380 (2 x 220)
3	3 x 380	*23*	4 x 380 (3 x 220)
4	4 x 380	*24*	4 x 380 (1 x 380)
5	4 x 380 + 2 x 220	*25*	4 x 380 (2 x 380)
6	2 x 380 + 1 x 220	*26*	4 x 380 (3 x 380)
7	2 x 380 + 4 x 220	*27*	4 x 380 (1 x 380 + 1 x 220)
8	2 x 380 + 2 x 220 (1 x 380)	*28*	4 x 380 (1 x 380 + 2 x 220)
9	2 x 380 + 2 x 220 (2 x 380)	*29*	4 x 380 (1 x 380 + 3 x 220)
10	2 x 380 + 4 x 220 (4 x 220)	*30*	4 x 380 (2 x 380 + 1 x 220
11	2 x 380 + 2 x 220 (1 x 220)	*31*	4 x 380 (2 x 380 + 2 x 220)
12	2 x 380 + 2 x 220 (2 x 220)	*32*	4 x 380 (3 x 380 + 1 x 220)
13	2 x 380 + 2 x 220 (3 x 220)	*33*	4 x 380 + 2 x 220 (2 x 380 + 1 x 220)
14	2 x 380 + 2 x 220 (4 x 220)	*34*	4 x 380 + 2 x 220 (3 x 380 + 2 x 220)
15	2 x 380 + 2 x 220 (1 x 380 + 1 x 220)	*35*	4 x 380 + 2 x 220 (2 x 380)
16	2 x 380 + 2 x 220 (1 x 380 + 2 x 220)	*36*	3 x 220
17	2 x 380 + 2 x 220 (1 x 380 + 3 x 220)	*37*	4 x 220 (1 x 220)
18	2 x 380 + 2 x 220 (2 x 380 + 1 x 220)	*38*	4 x 220 (2 x 220)
19	1 x 380 + 2 x 220 (1 x 380 + 1 x 220)	*39*	4 x 220 (3 x 220)
20	1 x 380 + 2 x 220 (1 x 220)	*40*	4 x 220

Fig. 6: Legend to European electrical power grid (cf. Fig. 7) & European natural gas network (cf. Fig. 8)

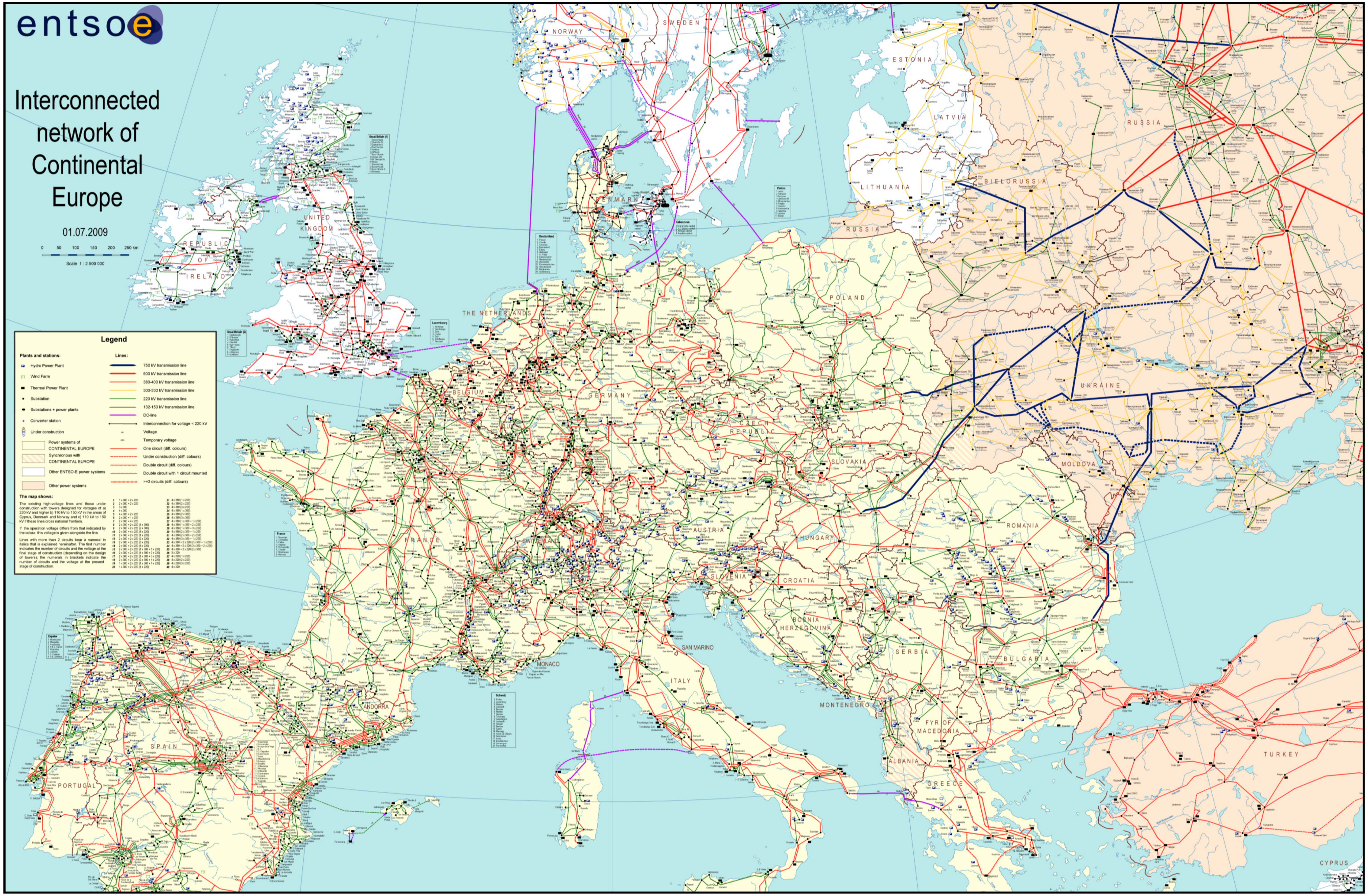

Fig. 7: Energy infrastructure – European electrical power grid

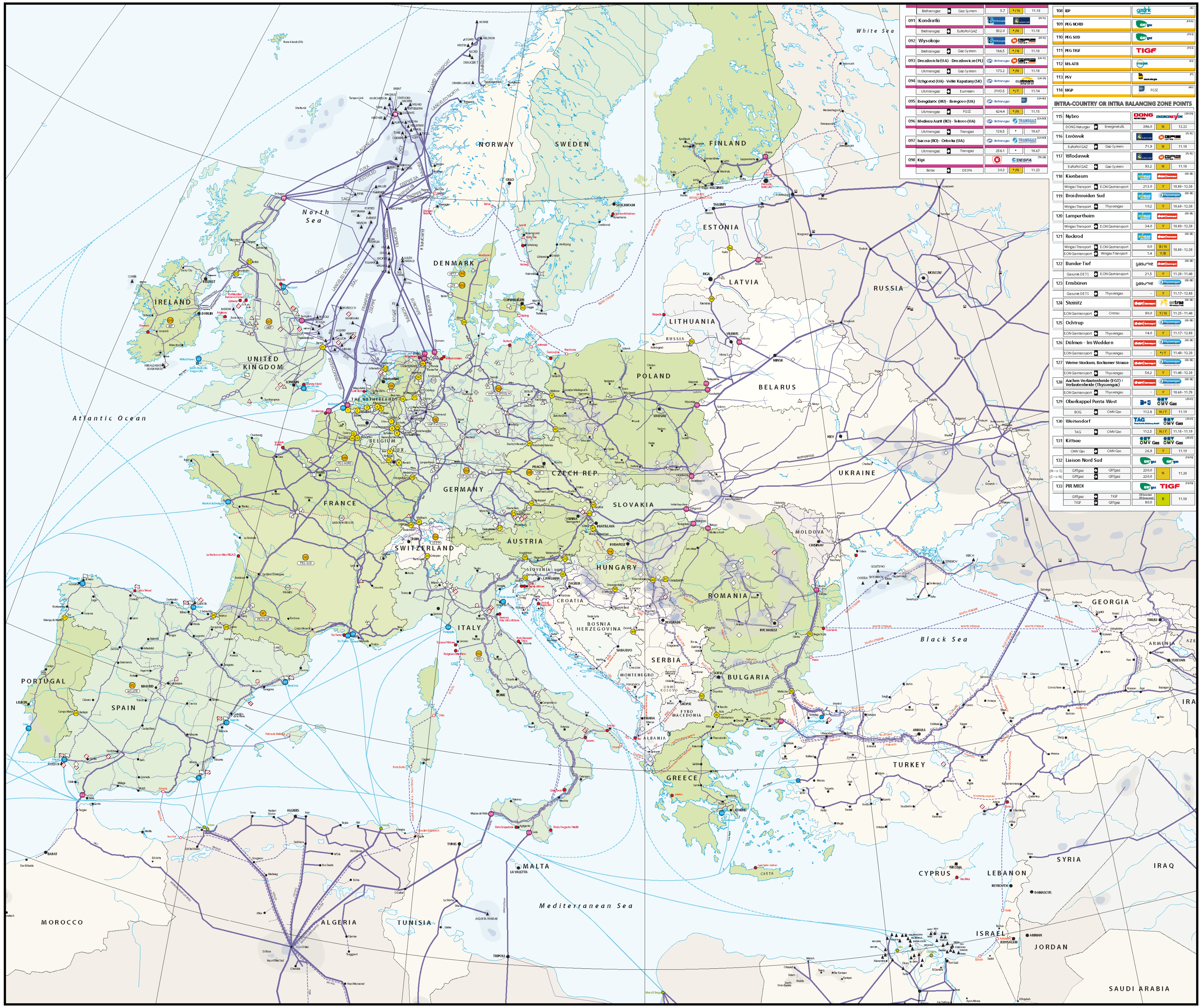

Fig. 8: Energy infrastructure – European natural gas network

2.3.4. Conventional Energy Technology

Energy technologies enable the supply of energy services to energy users. For this purpose energy transformation steps are necessary. The involved transformation steps start from primary energy, lead to the final energy followed by the final energy service. The different energy transformation steps require different energy technologies at different transformation stages. With regard to this perspective energy technologies can be divided into **exploitation technologies**, **conversion technologies** and **application technologies.** A power plant for electrical power is an example for a conversion technology, whereas a light bulb is an example for an application technology. Only high transformation efficiencies of all deployed technologies at every single stage can ensure an energy efficient supply of energy services to the energy user.[1]

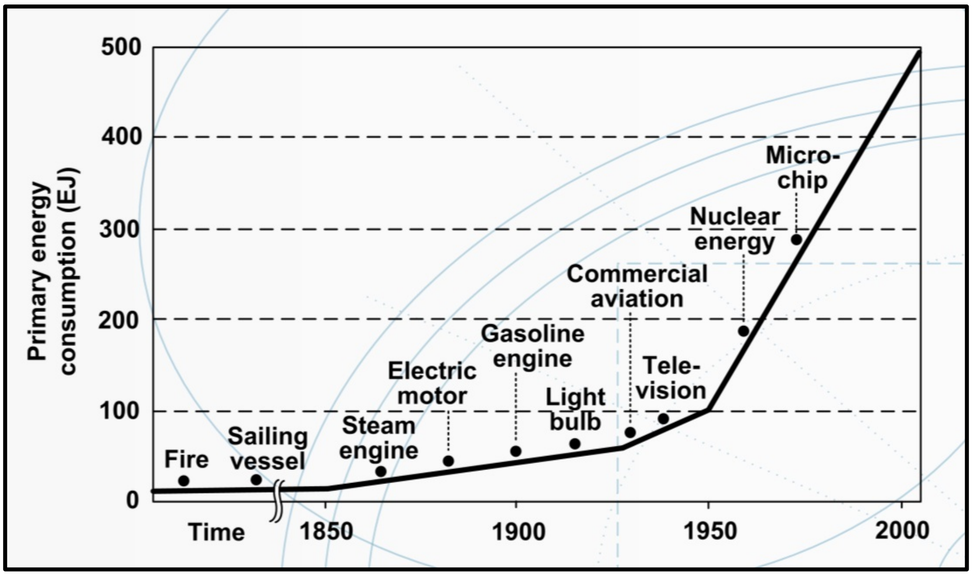

Fig. 9: Primary energy consumption worldwide in relation to main development steps of energy technologies[2]

The development of energy technologies in the past had strong influence on the primary energy consumption. **Fig. 9** shows an illustration of the world’s primary energy consumption versus main development steps of energy technology. Energy technologies can be divided into large-scale and small-scale units for centralized or decentralized applications. **Current research and development in the field of biomass gasification aims on the deployment of dual fluid gasification as conversion technology for decentralized applications from small- to medium-scale.** The primary energy exploitation and the energy conversion within the European Union today are mainly provided by a centralized energy system with large-scale supply units. The most important examples for energy conversion units in Europe are large-scale **refineries** (cf. **Fig. 5**) and large-scale **power plants for electricity generation**. Installed power plants within the European Union can be divided into thermal (460 000 MW), nuclear (130 000 MW), hydroelectric power plants (140 000 MW) and other types of power plants (65 000 MW).[3] As it can be seen in **Fig. 7** thermal power plants are responsible for the main share of produced electrical power within the European Union.

---

[1] cf. Nakicenovic N., 2010, p1-6ff

[2] cf. figure: Nakicenovic N., 2010, p3-1ff

[3] Data from 2008 cf. Eurostat, 2011, p60

Thermal power plants mainly use coal or natural gas as fuel. Applied technologies are coal-fired steam power stations and natural gas fired gas turbine combined cycle power stations. Ultra super critical steam cycle power plants, integrated gasification combined cycle power plants as well as carbon capture and storage techonlogies (CCS) are fields which are currently investigated to improve the state of the art of electricity production.[1] **Fig. 10** together with **Eq. 2.1** to **Eq. 2.8** shows the definition of expressions describing the energy flow through a thermal power plant.

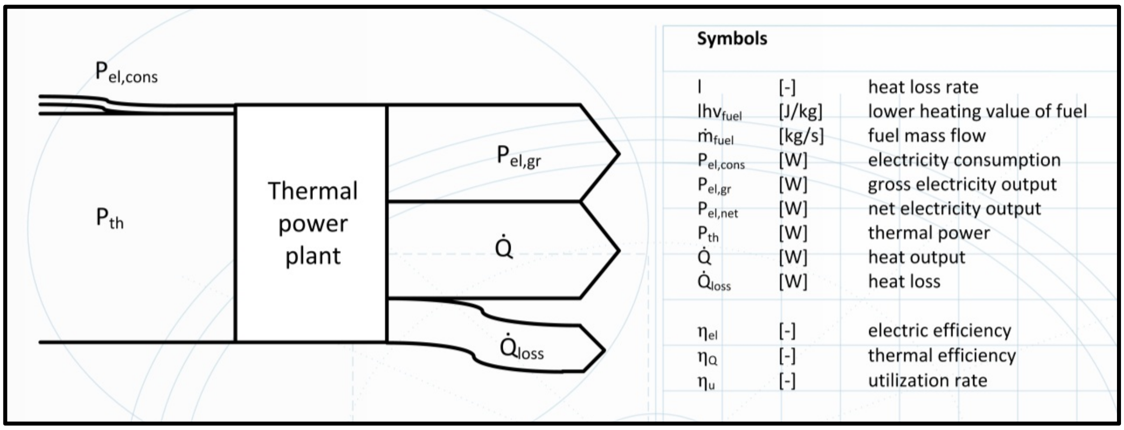

Symbols

l	[-]	heat loss rate
lhv_{fuel}	[J/kg]	lower heating value of fuel
$\dot{m}_{fuel}$	[kg/s]	fuel mass flow
$P_{el,cons}$	[W]	electricity consumption
$P_{el,gr}$	[W]	gross electricity output
$P_{el,net}$	[W]	net electricity output
P_{th}	[W]	thermal power
$\dot{Q}$	[W]	heat output
$\dot{Q}_{loss}$	[W]	heat loss
η_{el}	[-]	electric efficiency
η_{Q}	[-]	thermal efficiency
η_{u}	[-]	utilization rate

Fig. 10: Definitions describing the energy flow through a thermal power plant

Eq. 2.1: $$P_{th} = lhv_{fuel} \cdot \dot{m}_{fuel} \qquad [\,W\,]$$

Eq. 2.2: $$P_{th} = P_{el,net} + \dot{Q} + \dot{Q}_{loss} \qquad [\,W\,]$$

Eq. 2.3: $$P_{el,net} = P_{el,gr} - P_{el,cons} \qquad [\,W\,]$$

Eq. 2.4: $$\eta_{el} = \frac{P_{el,net}}{\dot{P}_{th}} \qquad [\,-\,]$$

Eq. 2.5: $$\eta_{Q} = \frac{\dot{Q}}{\dot{P}_{th}} \qquad [\,-\,]$$

Eq. 2.6: $$l = \frac{\dot{Q}_{loss}}{\dot{P}_{th}} \qquad [\,-\,]$$

Eq. 2.7: $$\eta_{el} + \eta_{Q} + l = 1 \qquad [\,-\,]$$

Eq. 2.8: $$\eta_{u} = \eta_{el} + \eta_{Q} < 1 \qquad [\,-\,]$$

A calculation of the average efficiency for thermal power plants within die EU27-countries for 2008 showed, that the average utilization rate of heat and power from thermal power plants was $\eta_u = \eta_{el} + \eta_Q = 48.5\%$.[2] The average electric efficiency of thermal power plants currently operating in Europe is named by different sources in the range of ~ $\eta_{el} = 35\%$.[3,4] The high fossil energy consumption is a main disadvantage of the installed power plants within the European Union. This leads to high primary energy imports [5] and high fossil CO_2 emissions. Already a small rise of the average thermal efficiency in Europe could contribute significantly to a reduction of the fossil energy consumption. Therefore, such a reduction is an integral part of the European energy strategy.[6] The European energy

---

[1] cf. Konstantin P., 2009, p271ff; cf. Walter H., 2011, p1-25ff
[2] Eurostat, 2011, p64; [3] Klaus T., 2009, p18
[4] http://www.enbw.com/content/de/der_konzern/enbw/forschung/co2_arme_kraftwerke/ (read at Feb. 21nd, 2013)
[5] cf. chapter 2.3; [6] cf chapter 2.7.3

strategy includes the development of new innovative energy technologies as high performance low-carbon technologies. This includes the development of carbon capture and storage (CCS) facilities for large-scale power plants. **Fig. 11** and **Tab. 3** show a rough insight about main characteristics of energy conversion technologies which are used today for electricity generation. New innovative energy technologies are investigated to improve the performance of the European energy system. At this stage renewable energy and low-carbon technologies have to compete with the performance of traditional energy conversion technologies.

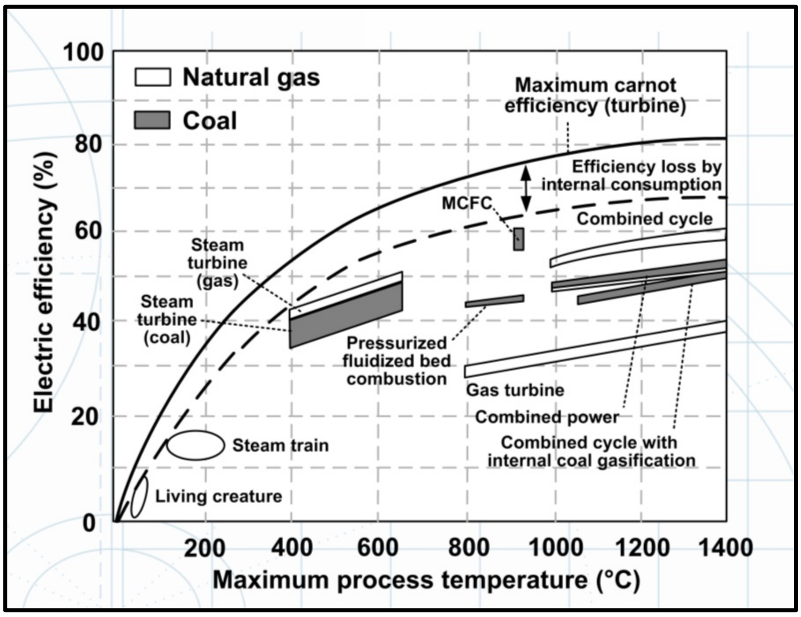

Fig. 11: Comparison of electric efficiencies of different technologies for electricity production (Illustration based on lhv, 600 MW net electrical power, condensation pressure 0.03 bar)[1]

Traditional power plants	Fuel	Electrical power	Electrical efficiency	Invest costs [MEUR]	Operator	Contractor
Steam power stations Lippendorf/Germany (1999)[2]	brown coal	1 840 MW_{el}	42 %	2 300	Vattenfall	Siemens AG
Combined cycle gas & steam power Hamm Uentrop/Germany (2007)[3]	natural gas	850 MW_{el}	58 %	450	Trianel	Siemens AG
Combined cycle gas & steam power Mellach/Austria (2011)[4]	natural gas	832 MW_{el}	59 %	400	Verbund	Siemens AG
Nuclear energy power plant Isar 2/Germany (1988)[5]	nuclear	1 410 MW_{el}	-	2 600	EON	Siemens AG
Hydro power plant, Vienna Freudenau/Austria (1997)[6]	hydro run of ricer	172 MW_{el}	-	930	Verbund	ARGE DKWF
Hydro power plant Kaprun/Austria - Haupt- & Oberstufe – (1953)[7]	hydro pump-storage	355 MW_{el}	-	-	Verbund	Tauern-kraftwerke AG

Tab. 3: Traditional power plants – Rough overview about main characteristics

---

1 cf. figure: Hlubleck W., 1996, p6-14
2 www.vattenvall.de (read at July. 30th, 2012); 3 www.trianel-hamm.de (read at July. 30th, 2012);
4 www.verbund.com (read at July. 30th, 2012); 5 www.eon-kernkraft.com (read at July. 30th, 2012);
6 www.verbund.com (read at July. 30th, 2012); 7 www.verbund.com (read at July. 30th, 2012);

2.4. Renewable Energy Technologies

Traditional energy technologies are the foundation of the existing energy system. The desired creation of a sustainable energy system as well as the intended reduction of the European Union`s dependency on energy imports raises a strong demand for alternative technologies which enable the utilization of "**renewable energy sources**" such as:

- hydropower, wind power,
- biomass, waste,
- solar power and geothermal energy.

The recreation of an existing energy system takes many generations and renewable energy technologies are confronted with strong competition for limited investment capital within the existing energy system against traditional energy technologies. **Tab. 4** displays costs and expected learning rates for renewable energy technologies for the example of electricity generation. Additionally, **Tab. 5** shows data of existing plants to enable a comparison with traditional energy technologies. In comparison with conventional and other renewable energy technologies, dual fluid gasification can be pointed out as energy conversion technology which allows the production of multiple chemical products such as synthetic natural gas (SNG), Fischer-Tropsch diesel fuel, hydrogen as well as peak load electricity and much more.

Renewable energy technologies	Electricity generation costs [EUR 2009/MWh]	Learning rates: expected reductions of technology costs*
Hydro	60	1%
Geothermal	38	5%
Wind – onshore	68	7%
Wind – offshore	83	9%
Biomass	98	5%
Concentrating solar power	191	10%
Solar - Photovoltaic	270	17%
Marine	233	14%

Tab. 4: Electricity generation costs of renewable energy technologies[1]

Renewable energy technologies	Fuel	Electrical power	Electrical efficiency	Invest costs [MEUR	Operator	Supplier
Wind power park Scroby Sands – UK (2010)[2]	wind power - offshore	60 MW_{el}	-	109	EON	Vestas
Photovoltaic park Lieberose – Germany (2009)[3]	solar	53 MW_{el}	-	160	Juwi	First Solar
Biomass power plant Vienna - Austria(2006)[4]	wood chips	25 MW_{el}	37%	60	Wien Energie	Siemens AG
Waste gasification plant Lahti – Finland (2012)[5]	waste	50 MW_{el}	31%	150	Lahti Energia	Metso

Tab. 5: Comparison of renewable energy technologies

---

[1] cf. table: IEA, 2010, p310; (used reference rate USD/EUR = 0.75, * Learning rate represents reduced investment costs by doubling cumulative installed capacity)

[2] cf. www.eon.com (read at July. 30th, 2012); [3] cf. www.solarpark-lieberose.de (read at July. 30th, 2012)

[4] cf. www.wienenergie.at (read at July. 30th, 2012); [5] cf. www.lahtienergia.fi (read at July. 30th, 2012)

Fig. 12 depicts a simplified picture illustrating a holistic vision for a sustainable energy system which was developed by the European Commission in 2003. Used approach included all mentioned energy sources as well as carbon capture and storage facilities. Additionally, the authors were focusing on the usage of fuel cells and hydrogen as energy carrier. The illustrated vision includes many important elements which could be an essential part of a future energy system. The production of hydrogen itself from primary fuels such as natural gas, coal or biomass implies different conversion steps. The different conversion steps include several energetic losses which have to be considered. **Fig. 13** shows a simplified illustration of energy flows which are part of a hydrogen production. Detailed aspects of mass and energy flows as well as energetic losses are discussed in detail in the result section of present work to enable a specific assessment of hydrogen production from biomass.

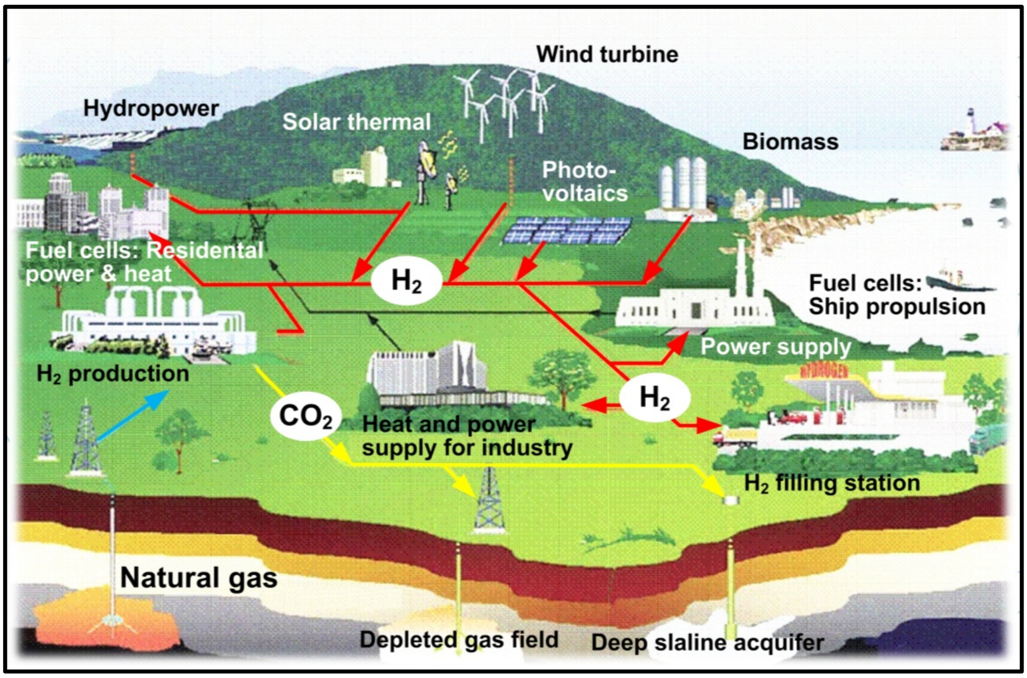

Fig. 12: Vision for future energy system based on hydrogen and fuel cells[1]

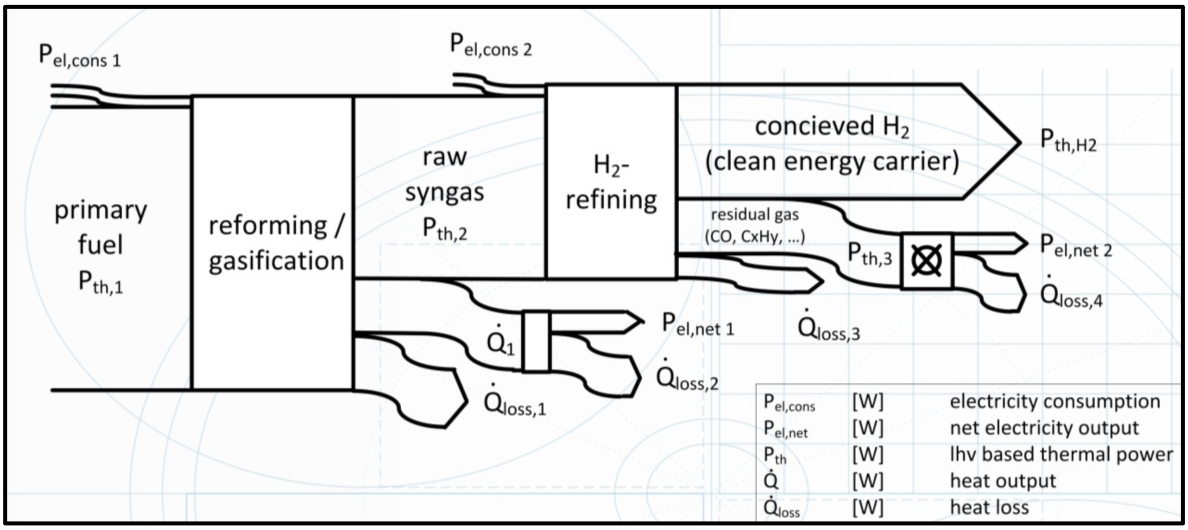

Fig. 13: Simplified illustration of energy flows in a hydrogen production for a hydrogen based system

---

[1] cf. figure: European Commission, 2003, p4

2.5. Renewable Energy Supply with Dual Fluid Gasification

Biomass gasification in a dual fluid gasifier system can be applied as a technology for the supply of renewable energy from biomass. It can be classified as a subtype of **gasification technologies** and is one possibility beside many others for the utilization of renewable energy from biomass. The gasification of solid fuels by thermo-chemical conversion supplies gaseous energy carriers for different ways of utilization in addition to the traditional forms of solid fuel combustion. Within a dual fluid gasification system steam is used as **gasification agent** for the gasification. The final product of a gasification system is named **product gas** and can be described as a gas with medium calorific value which offers beneficial properties for several synthesis processes as it contains the synthesis precursors carbon monoxide (CO) and hydrogen (H_2). Product gas can be used for the production of electricity and heat, as well as for polygeneration applications. It can be used for example for the Fischer-Tropsch-synthesis, the production of synthetic natural gas (SNG) or the generation of hydrogen.[1] At that point biomass gasification in a dual fluid gasifier provides advantages compared to other gasification technologies because of the achievable gas quality. But also other gasification technologies could be used for different applications. To enable an overview about strengths of weaknesses of different gasification technologies, a classification of gasification technologies and a detailed description of gasification itself are presented in **Chapter 3.**

Dual fluid gasification has made huge development steps during the last 30 years. Relevant progress in research and the offered possibilities of dual fluid gasification has led to the construction of several **commercial plants** based on this technology. **Tab. 6** gives an overview about commercial plants for the **production of heat and electricity**. Listed plants principally act as a supplier of synthesis gas including relevant amounts of hydrogen (H_2). Due to the economic environment and the funding framework the already realized plants focused on the production of electricity from wood chips. Water-, wind turbines and photovoltaic offer quite simple systems for the production of electricity from renewable sources, while dual fluid gasification requires quite complex overall plant configurations. Existing operating plants face challenges regarding high fuel costs and achievable operating hours. None the less so far realized plants enable the continuous production of electricity from renewable energy sources. Recent research activities focused on overall plant concepts which enable the production of synthesis products like synthetic natural gas[2] (SNG), hydrogen[3] or synthetic diesel fuel[4] (Fischer-Tropsch-diesel fuel) beside electricity and heat. Therefore, dual fluid gasification could enable in future commercial production of several common high quality energy carriers.

Location	Electricity production	Thermal-/ Electr. power	Start of operation	State	Estimated invest cost [MEUR] [5,6]
Güssing/AUT	Gas engine	8.0 MW_{th} / 2.0 MW_{el}	2002	Operating	10.7
Oberwart/AUT	Gas engine/ORC	8.5 MW_{th} / 2.8 MW_{el}	2008	Operating	16
Villach/AUT	Gas engine	15 MW_{th} / 3.7 MW_{el}	2010	Operating	23
Senden/GER[7]	Gas engine/ORC	15 MW_{th} / 5 MW_{el}	2012	Commissioning	33

Tab. 6: Commercial dual fluid gasification plants for the production of heat and electricity[8]

---

[1] cf. Kaltschmitt M., 2009, p600;
[2] cf. Rehling B., 2009, p7
[3] cf. Müller S., 2011, p55ff; [4] cf. Sauciuc A., 2011, p1;
[5] data: cf. Rauch R., 2012, p13
[6] data: http://www.energieburgenland.at/oekoenergie/biomasse/.. (read at March 15th, 2013)
[7] data: www.swu.de/uploads/tx_z7categorydownloads/Flyer_HGASenden.pdf (read at March 15th, 2013)
[8] cf. table: Hofbauer H., 2010, p7

2.6. Society & Environment

The availability of affordable energy is an important pre-condition for wealth, employment possibilities and the ability to follow modern living standards. The energy system today enabled the development of widespread prosperity in most of all industrialized countries. A lack of secure access to energy in the developing countries implies poverty, high fertility rates, high infant mortality, high illiteracy rates and low life expectancies. In industrialized countries energy poverty can lead to reduced living standards and reduced life expectancies. Therefore the future development of the energy system directly influences the further development of poverty, population growth, urbanization and the living standards in developing and industrialized countries.[1]

Furthermore, the current energy system is responsible for some major environmental problems with far-reaching global dimensions. **Fig. 14** shows a model for the effects of the transition of environmental problems during the development of societies and their wealth. Within this model urban pollution without safe water and sanitation services are the main environmental challenges of developing societies with a low standard of living. Increasing wealth leads to increasing urban air pollution accompanied by problems like deforestation by high urban concentrations of sulfur dioxide. Even additional increasing wealth within this model implies environmental burdens like rising **greenhouse gas emissions** which have a delayed global effect on the environment and can threat whole ecosystems.[2] Rising greenhouse gas emission already have today a significant impact on the global climate by the effect of **global warming**. Between 1850 and the year 2000 an increase of global mean temperature by 1°C has been observed. Until 2100 a further increase by another 3°C is expected (cf. **Fig. 14**). The main reasons for an increasing global mean temperature are continuously growing anthropogenic greenhouse gas emissions. The emission of radiation forcing components as CO_2, CH_4 and N_2O reinforce solar radiation on the global surface and are therefore acknowledged as major reason for global warming.[3] **Fig. 15** illustrates the effect of different radiation forcing components causing global warming as well as the development of carbon dioxide (CO_2) and methane (CH_4) concentration in the atmosphere over time. The negative consequences of global warming and a major change of the world’s climate can only be predicted roughly. The impact of global warming strongly depends on the further development of

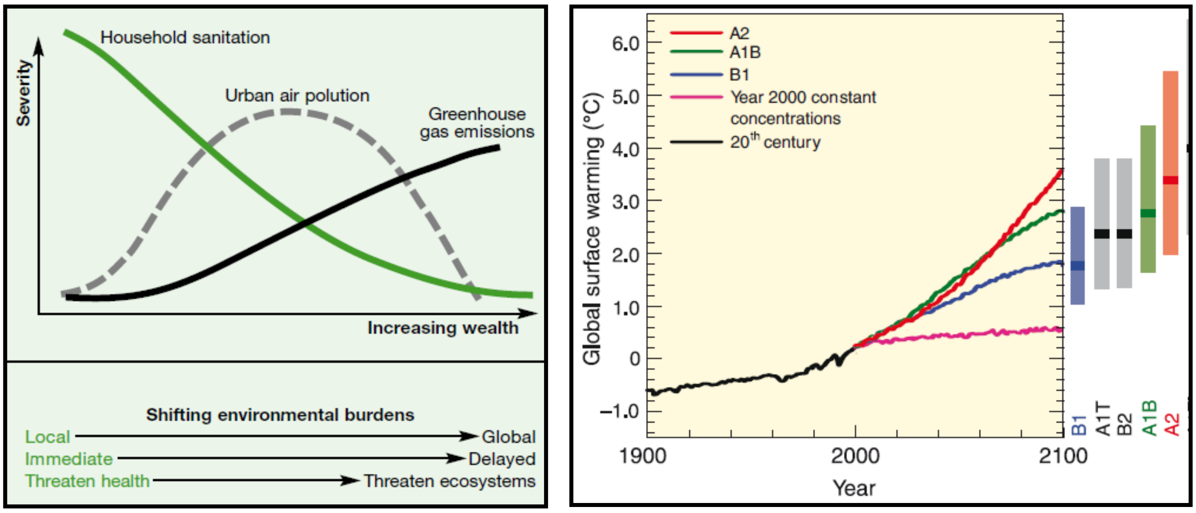

Fig. 14: Environmental risk transition[4] & Global surface warming scenarios until 2100[5]

---

[1] cf. Reddy A., 2000, p39ff; [2] cf. Holdren J., 2000, p95ff
[3] cf. IPCC, 2007, p30ff; [4] Fig. 14: McGranahan, G., 2000, p14ff; [5] Fig. 14: IPCC, 2007, p46

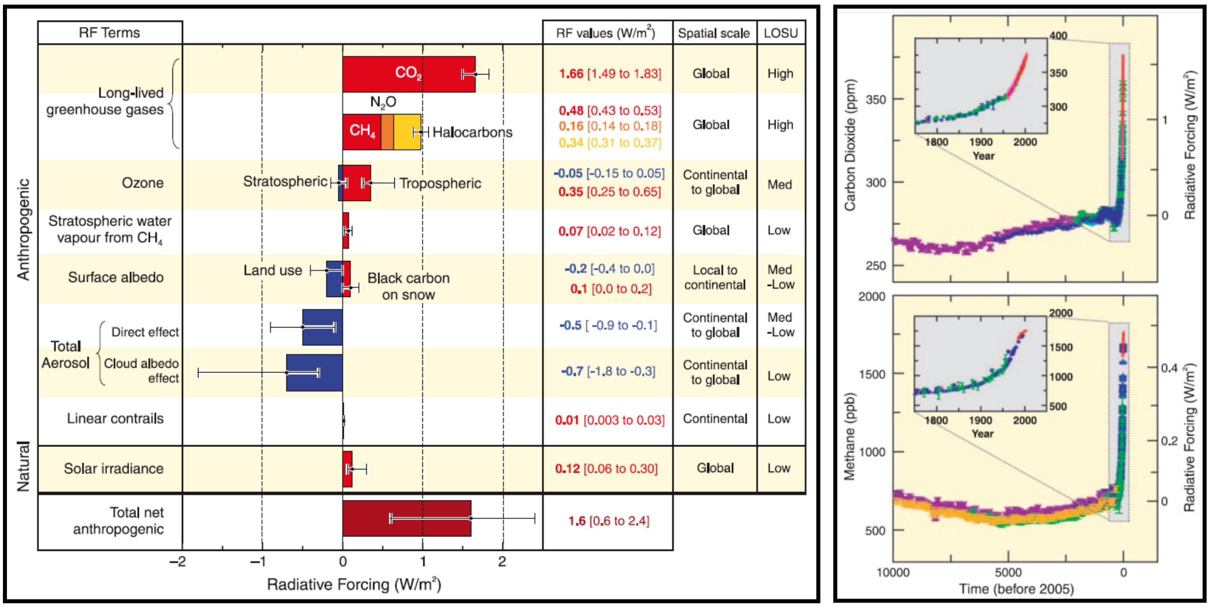

Fig. 15: Radiation forcing components[1] & CO_2 and CH_4 concentrations over the time[2]

greenhouse gas emissions. Therefore, the "Intergovernmental Panel on Climate Change" refers its conclusion to four reference scenarios (A1, A2, B1 and B2, cf. **Fig. 14**) which cover a wide range of demographic, economic and technological driving forces and resulting greenhouse gas emissions. The reference scenarios show that following negative consequences can be expected.

- a rising risk of extreme weather events,
- sea level rise and inundation of coastal lands,
- reduced crop yields and rising amount of drought periods,
- water supply shortages,
- affected forest compositions,
- loss of habitat and species and reduced functioning of vulnerable ecosystems.[3]

Because of that, an adequate response to the mentioned consequences is needed. This implies a reduction of greenhouse gas emissions to lower the impact of climate change. **Eq. 2.9** shows a model describing different approaches for a reduction of CO_2 emissions.[4]

Eq. 2.9:

$$\text{CO2 emissions} = \text{POP} \cdot \frac{\text{GDP}}{\text{POP}} \cdot \frac{\text{TOE}}{\text{GDP}} \cdot \frac{\text{CO2}}{\text{TOE}} \qquad [\,tCO_2\,]$$

According to the equation, CO_2 emissions can be seen as a product of population (POP), carbon content in energy (CO2/TOE), energy intensity of the economy (TOE/GDP) and the production per person (GDP/POP). Currently we face increasing population as well as increasing wealth (GDP/POP). Therefore, reduced CO_2 emissions can only be achieved by improved energy intensity (TOE/GDP) and reduced specific CO_2 emissions (CO_2/TOE) by high performance low-carbon technologies.

Additionally, society needs to adapt to the already upcoming negative outcomes of global warming and has to find a way for a more sustainable living. A strong need for a sustainable development in future was already mentioned by a report of the World Commission on Environment and Development called "Brundtland Report" in 1987.[4]

---

1 Fig. 15: IPCC, 2007, p39; 2 Fig. 15: IPCC, 2007, p38
3 cf. IPCC, 2007, p48ff; 4 Grübler A., 1994, p4; 5 cf. Brundtland G., 1987, p54

2.7. Politics

Energy policy in several countries tries to overcome economic, social and environmental challenges regarding future energy supply. The following chapter should give a short overview about main activities of energy policy in the USA, China and the EU.

2.7.1. United States of America

The primary energy consumption per-capita in the USA is twice as high as in the European Union and four times as high as in China.[1] Until 1960 the USA were self-sufficient regarding energy demand. Since that time the energy consumption and necessary energy imports, especially crude oil imports, were continuously growing. In 2009 the primary energy consumption reached 2400 Mtoe (101 EJ) and 24% of all energy consumed had to be imported. In comparison the EU had to import 53% of the primary energy demand. Main energy reserves consumed in the USA 2009 were crude oil (37EJ), natural gas (24EJ), coal (21EJ) and nuclear power (9EJ).[2] The USA are the leading country for energy related fossil greenhouse gas emissions with 21.4% of total global greenhouse gas emissions.[3] The energy strategy of the Obama Administration acknowledges a necessary reduction of greenhouse gas emissions and aims at energy supply security by the utilization of available energy resources within the United States. This implies the utilization of available offshore oil reserves, unconventional natural gas reserves, nuclear power and a rising share of biofuels. Furthermore, the strategy of the Obama Administration supports the development of new renewable energy technologies as a possibility to support economic growth and create new jobs.[4]

2.7.2. China

China has 1.3 billion inhabitants and is therefore currently the biggest country in the world. The national economy in China has achieved a growth of the gross domestic product (GDP) of around 10% nearly in each year since 1990. The increasing economic power of China is at the same time responsible for a fast increasing energy demand.[5] While the energy consumption per-capita is quite low compared to the USA and the European Union, the overall primary energy consumption 2008 reached after many years with high growing rates 2200 Mtoe (93 EJ)[6]. The rising energy demand lead to rising energy imports mainly from Africa. 70% of the energy demand in China is covered by coal which leads to relevant CO_2 emissions. Chinas energy policy is willing to support the reduction of greenhouse gas emissions only with a smaller contribution than leading industrial countries. According to Chinas point of view leading industrial countries have been responsible for the main share of greenhouse gas emission in the past. Chinas energy policy aims at efficient technologies for the energy supply by coal, large-scale hydro power plants and nuclear power. Furthermore the share of renewable energy should reach 16% until 2020 and afforestation should contribute to a reduction of greenhouse gases.[7]

---

[1] cf. International Energy Agency (IEA), 2010, p90

[2] cf. U.S. Energy Information Administration, 2009, p4ff

[3] Fischer, 2008, p508

[4] cf. Blueprint for a secure energy future (http://www.whitehouse.gov/energy, read at Sept. 30th, 2011)

[5] cf. Fischer, 2008, p100ff

[6] International Energy Agency (IEA), 2010, p85

[7] cf. Fischer, 2008, p104

2.7.3. European Union

Energy policy within the European Union aims at a competitive, sustainable and secure energy system. In order to reach such an energy system major challenges have to be addressed. The main challenges are increasing dependence on imports, climate change, the strain on energy reserves, energy prices and energy supply security.[1] In order to overcome these challenges the **European Commission for energy** takes several actions following the **energy strategy** of the European Union. The energy strategy includes

- achieving 20% energy savings by 2020,
- ensuring free movement of energy using internal markets,
- providing secure, safe and affordable energy,
- strengthening external energy links
- and developing innovative energy technologies

as new **high performance low-carbon technologies.**[2] The energy strategy is supported by market based instruments, by the development of energy technologies and by financial instruments. Market based instruments involve subsidies, taxes and a greenhouse gas emission allowance trading scheme. The energy technology development aims on high energy efficiency, renewable energy sources or low-carbon technologies. The research and development in this area is enhanced by the “Strategic Energy Technology Plan” (SET-Plan) and additionally by the support of large-scale demonstration projects. As a part of the financial instruments the “Seventh Framework Programme” and the “Competitiveness and Innovation Framework Programme” (CIP) have been installed starting in 2007 to strengthen regional development.[3] Described actions should support the achievement of the set targets. **Fig. 16** illustrates the situation of different member states with respect to the 2020 targets of the European Union.

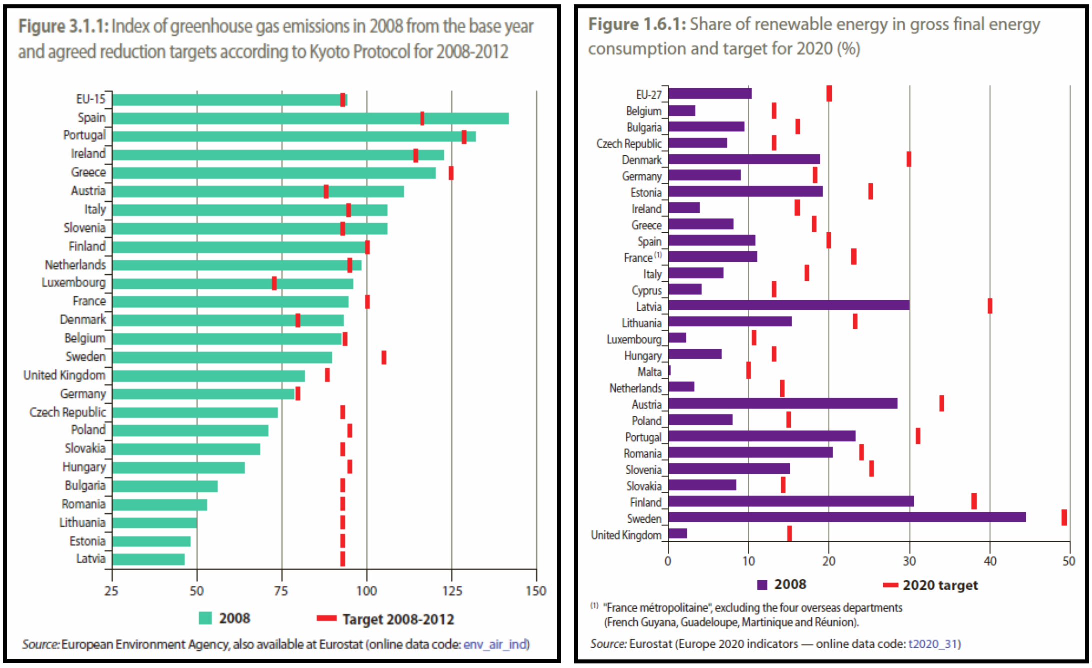

Figure 3.1.1: Index of greenhouse gas emissions in 2008 from the base year and agreed reduction targets according to Kyoto Protocol for 2008-2012

Source: European Environment Agency, also available at Eurostat (online data code: env_air_ind)

Figure 1.6.1: Share of renewable energy in gross final energy consumption and target for 2020 (%)

(1) “France métropolitaine”, excluding the four overseas departments (French Guyana, Guadeloupe, Martinique and Réunion).

Source: Eurostat (Europe 2020 indicators — online data code: t2020_31)

Fig. 16: Energy policy of the European Union – Renewable energy and emission reduction targets [4]

---

[1] cf. http://europa.eu/legislation_summaries/energy/index_en.htm (read at Sept. 30th, 2011)
[2] cf. http://europa.eu/legislation_summaries/energy/european_energy_policy/ (read at Sept. 30th, 2011)
[3] http://europa.eu/legislation_summaries/energy/european_energy_policy/.. (read at Sept. 30th, 2011)
[4] Fig. 16: Eurostat, 2011, p139, p73

2.8. Energy Economy Environment Summary

Chapter 2 gave a concise overview about relevant dimensions of the current state of the energy economy. The overview gave an impression of the major surrounding conditions relevant for the further development of dual fluid gasification within the European Union.

- Europe in its history always faced a lack of local available resources. Today, the EU has to import 53% of its primary energy demand of about 76 EJ. The European energy strategy today aims at free movement of energy at a safe and affordable price. At the same time, the energy strategy includes 20% energy savings, a reduction of greenhouse gas emissions by 20% and the development of new innovative energy technologies, as new high performance low-carbon technologies until 2020.

- Renewable energy technologies face strong competition for limited investment capital within the existing energy system against traditional energy technologies. In comparison to other renewable and traditional energy technologies, dual fluid gasification can be pointed out as energy conversion technology which allows the production of multiple chemical products such as synthetic natural gas, Fischer-Tropsch diesel fuel and hydrogen as well as peak load electricity. Hydrogen is discussed as a future energy carrier if it can be produced with adequate production efficiencies.

- Today the European industry is responsible for a final energy consumption of about 13.5 EJ and the used energy is mainly based on natural gas (4.2 EJ) and electricity (4.2 EJ). Most energy consumption arises by the steel (2.5 EJ) and chemical industry (2.3 EJ). Set reduction goals force the industrial sector to look out for new strategies to reduce its energy consumption by high performance low-carbon technologies.

- Although there are still large amounts of fossil energy reserves available, renewable energy sources are a major possibility to support set reduction goals. Biomass is the only renewable energy source which directly contains chemical energy. 4.5 EJ of the primary energy demand in the EU are covered with woody biomass. Today, forestry in Europe could supply up to 7 EJ of the demanded primary energy. In future, biomass especially could be used to supply the demanded clean energy carriers with high energy density for the transport sector as well as for industrial production processes.

The analysis of the energy economy environment showed that industry in Europe demands for final energy in form of natural gas, electricity and oil products. Compared to wind, water and sun, biomass is the only renewable energy source which directly contains chemical energy. As a consequence, biomass would be a resource capable of replacing fossil fuels for mobility and industrial applications. Biomass gasification enables the production of gaseous energy carrier from renewable feedstock. Dual fluid gasification in particular offers advantages compared to other gasification technologies because of the achievable gas quality. For this reasons **current research and development in the field of biomass gasification should aim on the deployment of dual fluid gasification as conversion technology for industrial applications.** This way biomass gasification technology could be used to reach the targets of the European energy strategy.

3. Gasification Technology

Gasification in general enables the conversion of a solid fuel into a gaseous fuel. The following chapter describes main facts about gasification, and should give a concise overview about

- the basic principles of gasification,
- the principles of dual fluid gasification,
- existing biomass power plants based on dual fluid gasification,
- and different pathways for the utilization of **product gas**.

3.1. Definitions

The thermo-chemical conversion of solid or liquid fuel into gaseous fuel is defined as **gasification.** Main driving force for the conversion process is the action of heat. A complete combustion, a full oxidation, of the fuel particle is prevented because of a lack of available oxygen.[1]

Biomass gasification can be carried out within different gasifier systems like fixed bed, fluidized bed, entrained flow or dual fluid gasifier systems (cf. **Fig. 17**). For the gasification of solid fuels air, oxygen, hydrogen, carbon dioxide or steam can act as **gasification agent.**[2] Gasification of solid biomass in the presence of hot steam as gasification agent is defined as **biomass steam gasification.**[3]

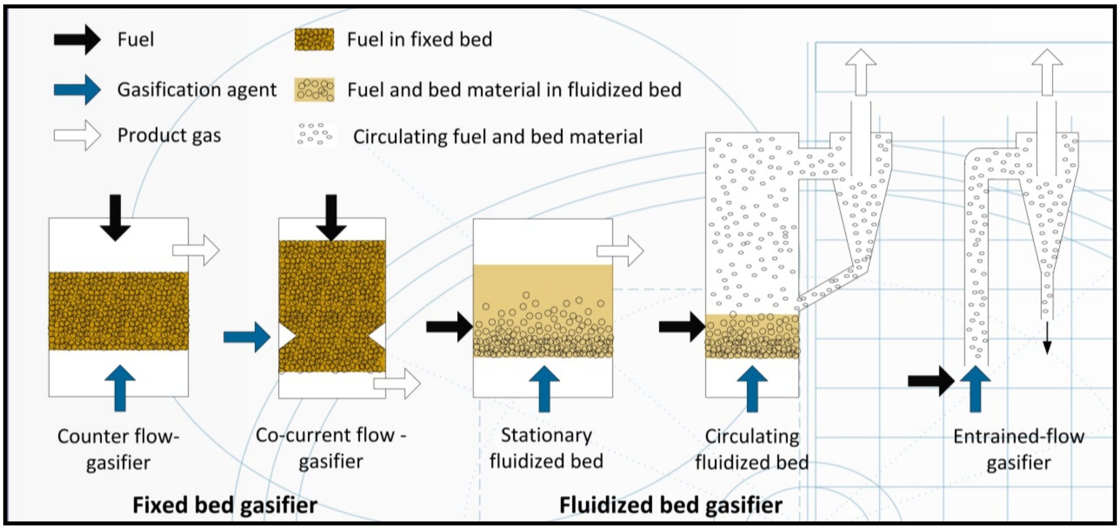

Fig. 17: Classification of gasifier types by occurring hydrodynamics[4]

The gaseous product of a gasifier system is called **product gas**. Main components of product gas are carbon monoxide (CO), carbon dioxide (CO_2), hydrogen (H_2), methane (CH_4), steam (H_2O) and, depending on the applied gasification agent, diluting nitrogen (N_2). Generally, the product gas additionally contains ammonia (NH_3), hydrogen sulfide (H_2S), certain amounts of **dust** and **condensable hydrocarbons** called **tar**[5]. The exact composition of the product gas is strongly dependent on the used fuel, on the used gasification agent, occurring process conditions and the used gasification technology.

---

1 cf. Kaltschmitt M., 2009, p4f; 2 cf. Hofbauer H., 2007a, p187ff
3 cf. Kaltschmitt M., 2009, p606; 4 cf. Hofbauer H., 2010a, p2ff; 5 cf. Kaltschmitt M., 2009, p395

Fluidized bed gasifiers additionally contain bed material. A gasifier bed inventory is represented by all solid particles present within a gasifier reactor. This includes solid fuel, ash and **bed material particles** with the largest share of above 90 wt.-%. Used bed material particles can have a catalytic influence on occurring chemical reactions and can reduce the tar content of the product gas. Initial bed material can consist of solid particles based on materials like silica sand (SiO_2), limestone (~ 90% $CaCO_3$), dolomite ($CaMg(CO_3)_2$) or olivine ($(Mg,Fe)_2SiO_4$).[1]

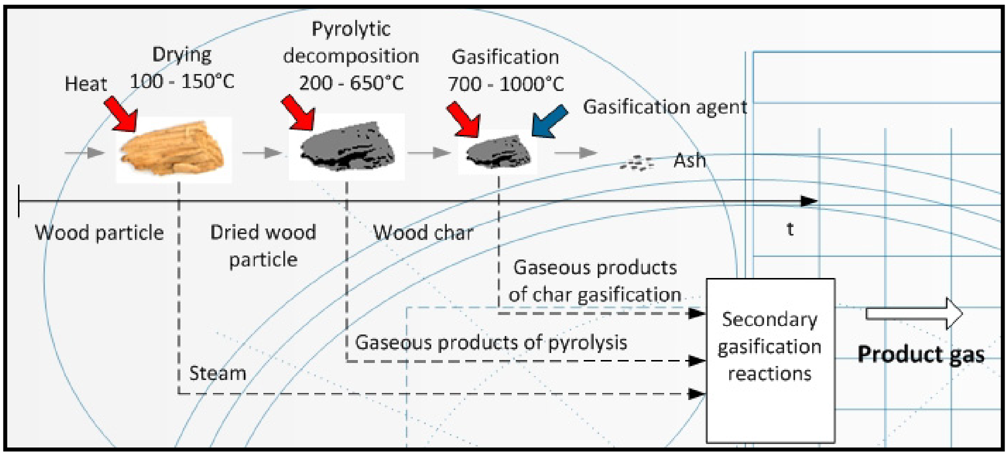

Fig. 18: Stages of biomass gasification[2]

Fig. 18 shows the different stages during the gasification of a solid wood particle. At the beginning of the gasification process a fresh wood chip contains relevant amounts of water. The thermo-chemical conversion of a solid wood chip into product gas is driven by the action of heat combined with a lack of available oxygen, which is preventing a full oxidation of the fuel particle. At the first stage the wet wood particle gets dried and hot steam volatilizes. Secondly, the dried wood particle gets decomposed by heat into wood char and gaseous products of pyrolysis. Finally the gasification itself takes place. The left over wood char gets gasified in the presence of a **gasification agent,** which is influencing the **gasification reactions**. Gaseous products of each single stage at the end react with each other in secondary gasification reactions.

All types of **solid fuel** which are applicable for combustion are technically also qualified as a fuel for gasification. Therefore, following solid fuels as fuel for gasification:

- coal,
- biomass,
- and waste materials [1]

Tab. 7 shows typical fuel compositions of wood and coal. Overall listed numbers represent rough values as guidance. A precise description of fuel can be achieved by an ultimate fuel analysis.

Eq. 3.1 to **Eq. 3.5** are defined as primary gasification reactions.[4] Gasification with oxygen within fixed bed gasifier is dominated mainly by reactions shown in **Eq. 3.1**, **Eq. 3.2** and **Eq. 3.4** whereas biomass fluidized bed steam gasification mainly is based on **Eq. 3.3** and **Eq. 3.4.**

---

1 cf. Pfeifer et al., 2011, p63ff
2 cf. figure: Kaltschmitt M., 2009, p394
3 cf. Hofbauer H., 2007, p96ff; 4 Kaltschmitt, 2009, p390ff

		Wood[1]	Coal[2]	Unit
Fuel properties	Water	< 60	< 60	wt.-%
	Ash	0.3-3.0	1-50	wt.-%$_{db}$
	Share of volatiles	80-90	5-70	wt.-%
	Lower heating value (lhv)	15-20	20-30	MJ/kg$_{db}$
	Ash softening temperature	1 250-1 450	1 000 - 1 300	°C
Elementary composition	Carbon (C)	46-52	60-95	wt.-%$_{db}$
	Hydrogen (H)	5-7	2-9	wt.-%$_{db}$
	Oxygen (O)	38-46	2-30	wt.-%$_{db}$
	Nitrogen (N)	0.1-0.6	0.5-3	wt.-%$_{db}$
	Sulfur (S)	0.01-0.1	0.5-3	wt.-%$_{db}$
	Chlorine (Cl)	0.002-0.02	0.1-1.0	wt.-%$_{db}$
	Calcium (Ca)	0.3-1.3	-	wt.-%$_{db}$
	Potassium (K)	0.1-0.4	-	wt.-%$_{db}$
	Magnesium (Mg)	0.02-0.2	-	wt.-%$_{db}$
	Phosphor (P)	0.01-0.1	-	wt.-%$_{db}$
Micronutrients	Arsenic (As)	0.01-1.0	1-1 000	mg/kg
	Cadmium (Cd)	0.05-1.0	-	mg/kg
	Chrome (Cr)	0.1-25.0	1-5 000	mg/kg
	Copper (Cu)	1-10	1-1 000	mg/kg
	Mercury (Hg)	0.001-0.150	-	mg/kg
	Lead (Pb)	0.01-50	1-30 000	mg/kg
	Zinc (Zn)	2-200	1-7 000	mg/kg
Molecular structure	Cellulose	40-50	-	wt.-%
	Hemi cellulose	18-27	-	wt.-%
	Lignin	20-30	-	wt.-%
	Resin/fat	0.5-3.5	-	wt.-%

Tab. 7: Values describing fuel composition and fuel characteristics of wood and coal

Eq. 3.1: $C + O_2 \leftrightarrow CO_2$ $\Delta H = -395.5$ kJ/mol

Eq. 3.2: $2\ C + O_2 \leftrightarrow 2\ CO$ $\Delta H = -221.0$ kJ/mol

Eq. 3.3: $C + H_2O \leftrightarrow CO + H_2$ $\Delta H = +118.5$ kJ/mol

Eq. 3.4: $C + CO_2 \leftrightarrow 2\ CO$ $\Delta H = +159.9$ kJ/mol

Eq. 3.5: $C + 2\ H_2 \leftrightarrow CH_4$ $\Delta H = -87.5$ kJ/mol

Eq. 3.6 to **Eq. 3.8** show typical reactions occurring between the gaseous products of char gasification and gaseous pyrolysis products.[3] These reactions are defined as secondary gasification reactions.

Eq. 3.6: $CO + H_2O \leftrightarrow CO_2 + H_2$ $\Delta H = -40.9$ kJ/mol

Eq. 3.7: $CH_4 + H_2O \leftrightarrow CO + 3\ H_2$ $\Delta H = 203.0$ kJ/mol

Eq. 3.8: $C_xH_y + x\ H_2O \leftrightarrow x\ CO + (x + \frac{y}{2})\ H_2$ $\Delta H > 0$ kJ/mol

---

[1] values: Kaltschmitt, 2009, p333ff

[2] values: Hofbauer, 2007, p96ff.; Kaltschmitt, 2009, p333ff; Benthaus, 1978, p7

[3] Kaltschmitt, 2009, p390ff

Gas cleaning facilities are used to reduce impurities like dust and tar to a lower level. Facilities like cyclones, fabric filters, wet scrubbers, electrostatic precipitators, catalytic high temperature gas cleaning facilities can be applied to reduce impurities to the limiting values demanded by the product **gas utilization.**[1]

In the past **coal gasification** has dominated the activities in the field of gasification technologies and was established as a technology for municipal energy supply.[2] Today modern coal gasification facilities are used for the large-scale production of electricity based on the integrated gasification combined cycle process (IGCC), for the production of Fischer-Tropsch diesel fuel and also for the production of a wide range of other chemicals. A review about the state of the art of plants currently in operation can be found elsewhere.[3] Coal gasification is an attractive opportunity because of its low fuel costs. But at the same time the utilization of coal leads to significant fossil CO_2 emissions.

Therefore, the development of gasification technologies within the last few years focused its activities more and more on biomass gasification. **Tab. 8** summarizes a rough description of advantages and disadvantages of different gasifier types using wood as feedstock.

Gasification characteristics for … using wood as feedstock		Fixed bed (co-current)	Fixed bed (counter-current)	Circulating fluidized bed	Dual fluid[x] gasification	Entrained flow gasification[7]
Gasification agent		air	air	air	steam	oxygen
Hydrogen (H_2)	vol.-%$_{db}$	15 – 21	10 - 14	15 - 22	35 – 45	29 – 35
Carbon monoxide (CO)	vol.-%$_{db}$	10 – 22	15 - 20	13 - 15	20 – 30	35 – 44
Carbon dioxide (CO_2)	vol.-%$_{db}$	11 – 13	8 - 10	13 – 15	18 – 25	17 – 22
Methane (CH_4)	vol.-%$_{db}$	1 – 5	2 - 3	2 – 4	8 – 12	< 1
Non condensable C_xH_y	vol.-%$_{db}$	0.5 – 2	n.a.	n.a.	2 – 3	n.a
Nitrogen (N_2)	vol.-%$_{db}$	40 - 60	40 – 60	40 – 60	**< 3**	3-9
Dust particles	g/Nm³	0.1 – 8 (1)	0.1 – 3 (1)	8 – 100 (20)	**60 – 100 (50)**	< 0.5
Tar	g/Nm³	0.1 – 6 (0.5)	10 – 150 (50)	1 – 30 (8)	**1 – 10 (2)**	n.a.
Ammonia (NH_3)	ppm	120 – 1000*				
Hydrogen cyanide (HCN)	ppm	20 – 500*				
Hydrogen sulfide (H_2S)	ppm	70 – 150*				
Lower heating value (lhv)	MJ/Nm³	4.0 – 5.6	3.7 – 5.1	3.6 – 5.9	**12 - 15**	n.n.
Cold gas efficiency	%	65 - 75	50 - 70	70 - 85	65 – 85	n.n.
x cf. chapter 3.2 ; () values in brackets indicate mean values; * dependent on fuel composition						

Tab. 8: Product gas composition for different atmospheric gasifier types[4, 5]

Dual fluid gasifier systems produce a gas with low nitrogen content which is an important advantage compared to other gasifier types. Low nitrogen content is especially favorable if the product gas is used for different synthesis[6] aiming at endproducts like synthetic natural gas or Fischer-Tropsch diesel fuel.

---

[1] cf. Kaltschmitt M., 2009, p629
[2] cf. Medek, 1984, p27;
[3] cf. Minchener A,, 2005, p2222ff
[4] Bolhar-Nordenkampf, 2004, p14;
[5] cf. Pröll, 2004, p17;
[6] cf. Bolhar-Nordenkampf, 2004, p51ff;
[7] values: Kaltschmitt, 2009, p620ff

3.2. Dual Fluid Gasification of Biomass

Fig. 19 illustrates the basic principle of a dual fluid gasification system. The gasifier system consists of two different reactors, which each operates a fluidized bed. The thermo-chemical conversion starts when solid fuel particles enter the gasification chamber, where drying, devolatilization and partially char gasification takes place. Within the gasification reactor steam is used for the fluidization and as gasification agent. The necessary heat for the gasification is provided by circulating bed material based on olivine ($(Mg,Fe)_2SiO_4$). The bed material is circulating between the gasifier and a second fluidized bed reactor, which is used as a combustion chamber. Within the combustion chamber remaining wood char from gasification is combusted and the bed material is heated up to ~900°C. The hot bed material leaves the combustor at the top as it is operated as a circulating fluidized bed. Afterwards the hot bed material is separated from the hot exhaust gas stream with a cyclone and returned to the gasification reactor. This closed loop enables the heat exchange between the two reactors at adequate operation temperatures and a regeneration of the bed material.[1] A reference for the achievable product gas composition of this system has already been shown in **Tab. 8**.

The described dual fluid gasification system provides a product gas nearly free of nitrogen, which is favorable for the production of several chemicals. Disadvantages of the gasification system in comparison to other gasifier types are an increased complexity and higher dust contents in the product gas stream.[2] The overall favorable characteristics of the described gasification system lead to the construction of several commercial plants based on this technology for the production of heat and electricity within the last years (cf. **Tab. 6**). Additionally, several research activities started to investigate the production of different end products like Fischer-Tropsch diesel fuel, synthetic natural gas, hydrogen.

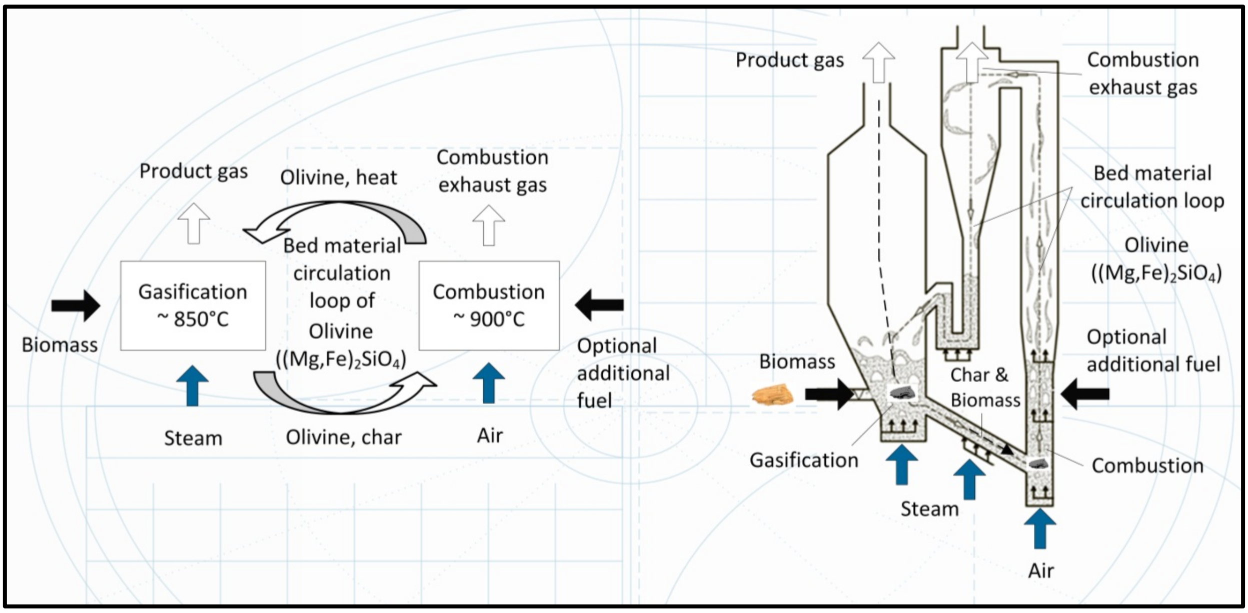

Fig. 19: Dual fluid gasification[3, 4, 5]

---

1 cf. Pröll T., 2004, p21
2 cf. Bolhar-Nordenkampf M., 2004, p47ff
3 cf. figure: Kreuzeder A., 2005, p9
4 cf. figure: Kaiser S., 2001, p10
5 cf. figure: Schmid, J.C., 2012, p206

3.3. Commercial Plants

Fig. 20 shows pictures of two commercial plants located in Güssing and Oberwart (Austria) based on dual fluid gasification. Both plants have been installed for the production of electricity and heat for local demand. The plant in Güssing was the first plant of its type and started operation in 2002. The plant in Oberwart started operation six years later in 2008 and was designed based on achieved know-how in Güssing. **Fig. 21** and **Fig. 22** illustrate layouts of the entire plants in Güssing and Oberwart. The realized production process for both plants can be subdivided into six different sections:

- fuel supply,
- gasification,
- gas cooling,
- gas cleaning,
- gas utilization,

and utilization of process heat. The main difference of Oberwart compared to Güssing is an **advanced process heat utilization** by

- a wood chip dryer to improve the overall plant efficiency and
- an organic rankine cycle (ORC) for an improved electricity output.[1]

The **fuel supply** for both plants is based on wood chips from local forestry. Delivered wood chips in general contain significant amounts of water in the range of ~40 wt.-% in dependence on storage and actual weather conditions. The wet wood chips are transported by conveyor equipment from the roofed incoming storage to the gasifier system. In Oberwart the conveyed wood chips additionally pass a dryer, where the water content is lowered to a value of 15-25 wt.-%. Within the gasifier system the actual **gasification** as already described in **Chapter 3.2** takes place. The achieved product gas leaves the gasifier with a temperature of around 850°C and the produced exhaust gas leaves the combustor with a temperature of around 900°C. The **gas cooling** of the hot product and exhaust gas stream consists of several heat exchangers for the utilization of process heat. Both gas streams are cooled down to temperatures in the range of 200°C.[1, 2] The **gas cleaning** section consists of an exhaust gas filter, a product gas filter and a

Fig. 20: Commercial dual fluid gasification plants: Güssing (left) and Oberwart (right)

---

[1] cf. Stidl M., 2012, p56ff

[2] cf. Pröll T., 2004, p31ff

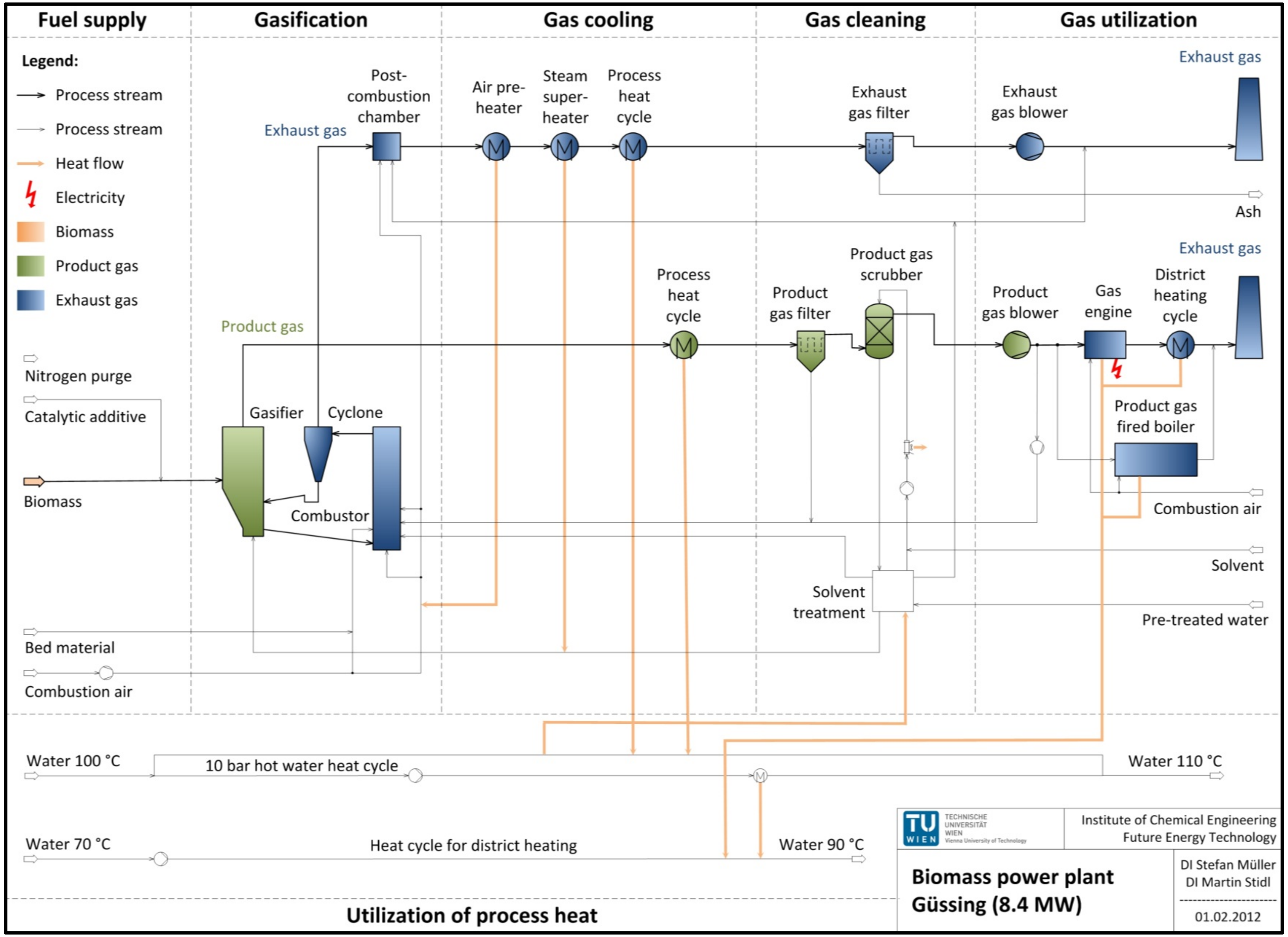

Fig. 21: Plant layout of Güssing (cf. Pröll T., 2004, p33)

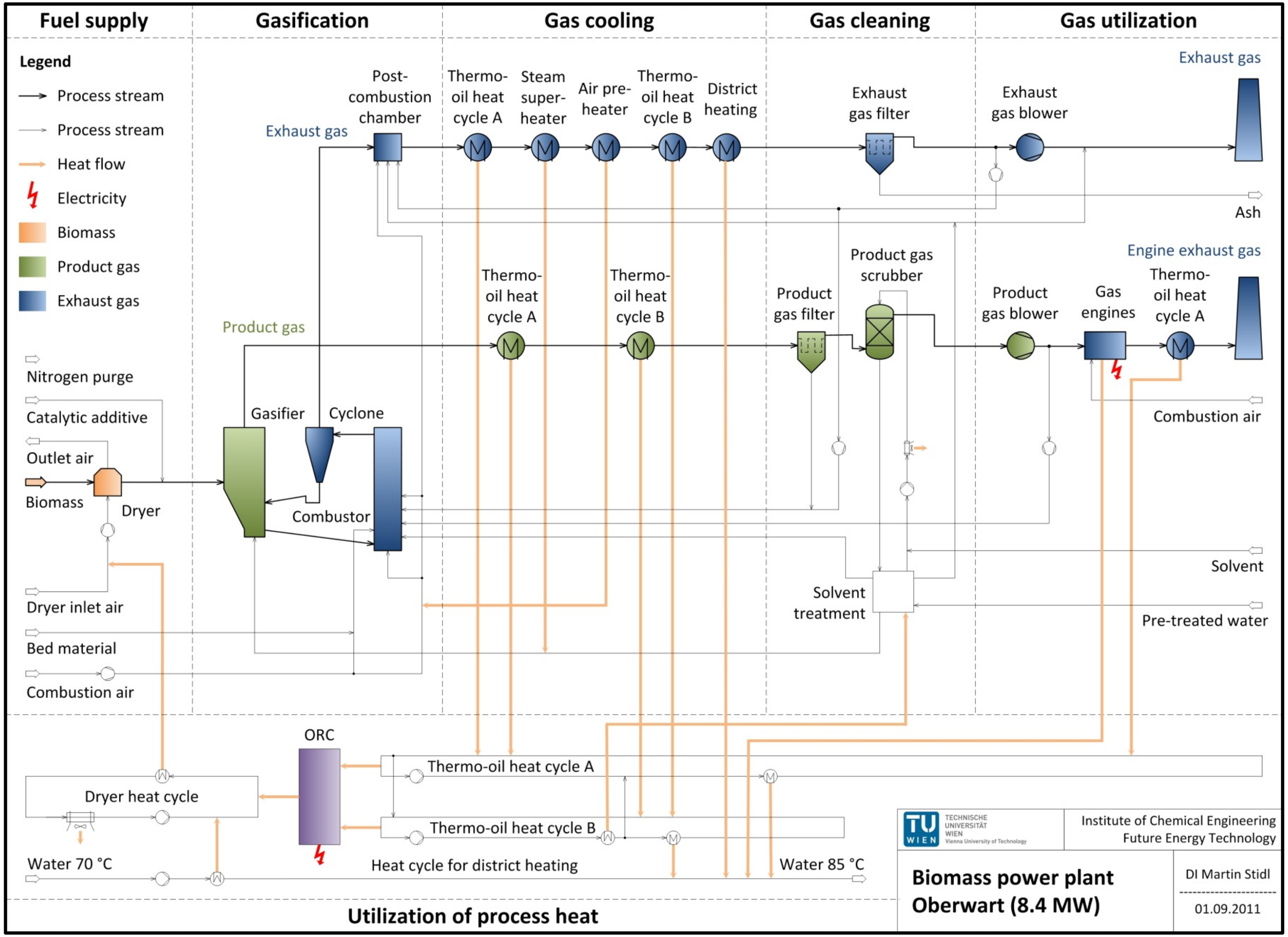

Fig. 22: Plant layout Oberwart (cf. Stidl M., 2012, p110)

product gas scrubber. The installed filters reduce the dust content within the gas streams and the product gas scrubber is used to condense water and solve tar from the product gas stream. The used solvent rapeseed methyl ester (RME) is recycled several times after a treatment process and is finally disposed in the combustor. After the gas cleaning section the conditioned product gas is prepared for the **product gas utilization.** In both plants, Güssing and Oberwart, the product gas is mainly combusted in gas engines for the production of electricity. Additionally, small amounts of the product gas are recycled to the combustor to enable an adjustment of the combustion temperature. Dependent on the time of the year and the actual heat demand, both plants can be operated with focus on electricity or heat production. The **utilization of process heat** is an essential part of the achievable overall plant efficiency. The available process heat is used in both plants:

- to pre-heat the combustion air,
- for the production of steam for fluidization of the gasifier,
- to superheat the steam for fluidization,
- for the solvent treatment,
- and for the supply of district heating.

Additionally, the plant in Oberwart has the possibility to use the available process heat for drying of supplied wood chips and for raised electricity output by the utilization of process heat with an organic rankine cycle (ORC).[1, 2, 3] **Tab. 9** summarizes main operation data of the two plants. **Tab. 10** shows the composition of the produced gas.

Operation parameter	Unit	Güssing (Austria)		Oberwart (Austria)	
Start up	a	2002		2008	
Estimated Investment Cost[9]	€	10 700 000		16 000 000	
Contractor		REPOTEC		ORTNER	
Plant operator		BK Güssing		Energie Burgenland	
Operation hours per year[4,5]	h/a	~7 000 – 7400		~ 6 800	
Subsequent data according to	Unit	Operation point: 11.12.2003[6]	Status 01.10.2013[5]	Operation point: 02.11.2010[7]	Status 01.10.2013[5]
Plant input					
Biomass (lhv based)	MW	7.8	~ 8.25	8.4	~ 8.4
Biomass (water content)	wt.-%	20	~ 33	35.9	~ 35
Biomass (wood chips)	kg/h	2 065	~ 2 610	2 783	~ 2760
Electricity consumption	MW	0.2	~ 0.25	0.42	~ 0.4
Scrubber solvent (RME)	kg/h	17	15	6	n.n
Nitrogen (N_2) purge[8]	Nm^3/h	75		75	
Limestone (dolomite)[8]	kg/h	10		5	
Fresh bed material (olivine)[8]	kg/h	40		20	
Water	kg/h	500	600	150	0
Plant output					
Electricity	MW	2.0	2.0	2.4	2.4
District heating	MW	4.2	4.1	0.9	2.5

Tab. 9: Operational data of commercial dual fluid gasification plants

---

1 cf. Pröll T., 2004, p31ff; 2 cf. Kotik J., 2010, p37ff
3 cf. Stidl M., 2012, p56ff; 4 status 1.10.2012
5 cf. interview with Kirnbauer F., March 21st 2013, (friedrich.kirnbauer@bioenergy2020.eu);
6 Pröll T., 2004, p154ff (optimized operation: $\mu_{H2O,BrSt} = 20\%$);
7 cf. Stidl M., 2012, p121; 8 data of additives according to Kirnbauer F.;
9 cf. Tab. 6

Product gas composition for Güssing and Oberwart after product gas scrubber		
Feedstock		wood chips
Gasification agent		steam
Hydrogen (H_2)	vol.-%$_{db}$	28 – 35
Carbon monoxide (CO)	vol.-%$_{db}$	22 – 24
Carbon dioxide (CO_2)	vol.-%$_{db}$	25 – 29
Methane (CH_4)	vol.-%$_{db}$	10 – 12
Non condensable C_xH_y	vol.-%$_{db}$	3 – 4
Nitrogen (N_2)	vol.-%$_{db}$	~ 2
Tar	g/Nm³	~ 1

Tab. 10: Product gas composition of Güssing and Oberwart[1,2,5]

Apart from this rough description of the plants in Güssing and Oberwart, an exact description of the plants and the operation characteristics can be found in further literature.[1, 2, 3]

3.3.1. Strengths and Weaknesses of Commercial Plants

The realization of commercial dual fluid gasification plants in Güssing and Oberwart enabled the utilization of local energy sources and an increase in prosperity within the immediate region. At the same time, the plants enabled relevant progress in research and the development of dual fluid gasification technology.

As a consequence of the novelty of the realized plants in Güssing and Oberwart, potential for further improvement still exists. Relatively **high fuel prices** and an unsure development in the future, put the plant operators under economic pressure to enable an 8000 hours operation of the plants per year. While the plant operators in Güssing are on the way to get close to a full time operation without the energetic advantages of a fuel dryer and the additional option of an organic rankine cycle, the plant operators in Oberwart still take several actions to reach the desired operation time per year and an improved energetic efficiency. Therefore, recent actions in Oberwart aimed at an improvement of

- the fuel conveying systems,
- the fuel dryer,
- the heat allocation between sources and heat user,
- the operation of the organic rankine cycle,
- the setup of used control- and automation systems,
- design deficiencies,
- and the electricity consumption.[3, 4]

As a further consequence of the novelty of the realized plants, the experience at the operation of the described plants is still growing and new findings enable a step by step improvement of the plants.

---

[1] Pröll T., 2004, p31ff
[2] Stidl M., 2012, p121ff
[3] cf. Kotik J., 2010. P138ff
[4] cf. Stidl M., 2012, p193ff
[5] cf. interview with Kirnbauer F., March 21st 2013, (friedrich.kirnbauer@bioenergy2020.eu)

3.4. Product Gas Utilization

The favorable product gas composition of dual fluid gasification offers many possibilities for the utilization of the product beside the production of electricity and heat. Product gas from dual fluid gasification can be used for the production of:

- electricity and heat,
- synthetic natural gas,
- Fischer-Tropsch diesel fuel
- gasoline,
- hydrogen,
- mixed alcohols,

and other chemicals like ammonia, aldehydes and isobutane.[1] The production of different products in one single plant is named polygeneration. Polygeneration concepts aim at the production of many (poly) equally important products.[2]

3.4.1. Production of Electricity and Heat

The production of electricity and heat through gas engines from product gas of dual fluid gasification has been demonstrated in Güssing and Oberwart. The results show that 2.0 MW of electricity and 4.5 MW of district heating can be produced from 8.4 MW wood chips (cf. **chapter 3.3**). The production of electricity could also be accomplished by the application alternative energy utilization technologies like gas turbines or fuel cells.

3.4.2. Synthetic Natural Gas

The production of synthetic natural gas from product gas of dual fluid gasification has been demonstrated at the BioSNG-plant in Güssing in 2009.[3] An evaluation of the achieved results showed that 0.87 MW BioSNG can be produced from 1 MW product gas. The produced synthetic natural gas meets the specification of the Austrian natural gas grid and the operation of a compressed natural gas (CNG) car has been demonstrated.[4] Achieved results and findings encouraged the construction of a 32 MW gasifier for the production of 20 MW BioSNG in Goteborg, Sweden. Scheduled start of operation is planned for 2013.

3.4.3. Fischer-Tropsch Diesel Fuel

The production of Fischer-Tropsch diesel fuel from product gas of dual fluid gasification has been demonstrated at a fully automated Fischer-Tropsch-pilot plant in Güssing 2010. The results demonstrated that Fischer Tropsch diesel fuel can be produced from wood chips and used as fuel for regular cars.[5] Preliminary studies already indicated that up to 0.55 MW of Fischer-Tropsch liquids can be produced from 1 MW of dry biomass dependent on the applied production concept.[6]

---

[1] cf. Rauch R., 2011, (oral presentation, 19th BEPS Meeting, 28th September 2011);
[2] cf. Fürnsinn S., 2007, p32;
[3] cf. Fuchs M., 2010, p116;
[4] cf. Rehling B., 2011, p111ff;
[5] cf. Sauciuc A., 2011a, p189ff;
[6] cf. Fürnsinn S., 2007, p80ff

3.4.4. Production of Hydrogen

The production of hydrogen from product gas of dual fluid gasification has been demonstrated with experimental facilities in Oberwart in 2011. The results showed that hydrogen with high purity can be produced from product gas of biomass gasification. Achieved experimental results enabled an insight into a potential large-scale production route.[1]

Hydrogen is often discussed as a potential future energy carrier for several applications. Discussions about hydrogen as energy carrier often lead to a situation where substantial properties of hydrogen and thermodynamic characteristics are not considered adequately. **Tab. 11** shows essential data describing the physical properties of hydrogen. Hydrogen (H_2) is a very light and very small molecule which implies significant challenges with respect to the storage of hydrogen. Different methods for storage of hydrogen are currently investigated by several research groups in the world. These methods include liquidation, compression as well as chemical or physical hydrogen storage systems. All named storage approaches demand additional energy input and face the challenge of leakages due to the diffusion of stored hydrogen.

Physical gas properties			Hydrogen (H_2)[2]	Methane (CH_4)[2]
Flammable range		vol.-%	4.0 – 77.0	4.4 – 17.0
Inflammation point		°C	560	595
Molar mass		kg/kmol	2.02	16.04
Gas density (0°C, 1.013 bar)		kg/m^3	0.09	0.72
Boiling point (1.013 bar)	Temperature	K	20.39	111.63
	Vaporization heat	kJ/kg	445.6	510.3
Lower heating value[3]		MJ/kg	120	50
Energy density (0°C, 1.013 bar)		MJ/m^3	10.8	36.0

Tab. 11: Physical gas properties of hydrogen in comparison with methane

Hydrogen enables the formation of high-explosive gas mixtures with a low inflammation point.[4] The volumetric energy density of hydrogen is low compared to methane. Therefore, the compression of hydrogen to high pressures includes a higher specific "energy penalty" than the compression of natural gas. The combustion of hydrogen itself is free of CO_2 emissions (cf. **Eq. 3.9**)[5], while predominant hydrogen production methods can include significant fossil CO_2 emissions (cf. **Tab. 31**).

Eq. 3.9: $$2\,H_2 + O_2 \quad \leftrightarrow \quad 2\,H_2O \qquad \Delta H = -484\ \text{kJ/mol}$$

Hydrogen produced from biomass avoids fossil CO_2 emissions. A large-scale hydrogen production process always needs to consider the necessary pressure level and hydrogen purity demanded by the hydrogen utilization route beside the physical properties of hydrogen in order to avoid additional efficiency penalties. Furthermore, direct utilization of hydrogen without a storage step is recommended in order to avoid energetic losses of storage systems. The present work investigates specific hydrogen production routes from dual fluid gasification. The findings of this investigation can be found in the result section of this work.

---

[1] cf. Mayer T, 2012, p125ff.
[2] Air Liquide, 2006, p362, p408
[3] cf. chapter 5.3 property data IPSEpro
[4] Air Liquide, 2006, p408
[5] Hubacek H, 1994, p79

3.4.5. Production of Alternative Fuels and Chemicals

Product gas from dual fluid gasification can be further used for the production of alternative fuels and chemicals. Experimental facilities for the production of mixed alcohols have been put into operation in Güssing in 2011. The production of methanol, ammonia, aldehydes and isobutane from product gas of dual fluid gasification has not been demonstrated so far but is discussed as an additional opportunity in the near future.

3.4.6. Direct Utilization of Product Gas

The direct utilization of the product gas of dual fluid gasification would reduce energetic losses due to additional conversion steps. Preliminary studies have investigated pathways for the integration of a dual fluid gasifier system into the existing infrastructure of a

- lime plant
- and a paper mill.

The results show that product gas of dual fluid gasification is capable to substitute a significant share of the used natural gas. High wood chip prices and an unsure development in the future can be identified as a major risk for the demonstration of the investigated concepts.[1]

3.5. Outlook & Potential Development

Dual fluid gasification demonstrated its capability as a part of electricity production and as a conversion technology for the production of several fuels and chemicals. Current research activities in the field of dual fluid gasification mainly aim at

- fuel flexibility,
- tar reduction,
- application of alternative bed materials,
- an improvement of the reactor design for increased gas-solid contact,
- increased possibilities for the product gas utilization,
- optimization and automation of existing plants,

and a reduction of the complexity of overall plants.[2] **Fig. 23** displays the learning curve of combined heat power plants (CHP) in comparison of historic learning curves of photovoltaics, wind mills and gas turbines. As it can be seen, the production of electricity based on dual fluid gasification is still at an early stage of development and relatively low capacities have been installed so far. The production of synthetic natural gas, Fischer-Tropsch diesel fuel and hydrogen is also still at a very early stage of development. Fuel flexibility can be defined as one key factor for the further development of dual fluid gasification.

---

[1] cf. Stidl M., 2012, p146ff

[2] cf. Stidl M., 2012, p201ff

The following materials are currently investigated regarding their suitability as fuel for gasification:

- hard coal, lignite,
- saw dust, wood/straw blended pellets, wheat bran,
- reed pellets, sugarcane bagasse, empty palm fruit bunches, fresh garden waste,
- waste wood, plastic from solid municipal waste, plastic from end-of-life cars,
- polyethylene, polystyrene, poly propylene,[1]
- and sewage sludge.

Additionally, alternative bed materials could lead to an improved product gas composition. Therefore, silica sand, Fe-olivine and limestone are currently investigated as possible bed materials for the application beside olivine.[2] The operation of a dual fluid gasifier system with limestone as bed material would be a pathway to lower the CO_2 content of the product gas by selective transport of CO_2 from the gasifier to the combustor (cf. sorption enhanced reforming). Findings in all mentioned and highlighted key areas can potentially improve the capability of dual fluid gasification as key energy conversion technology in the future.

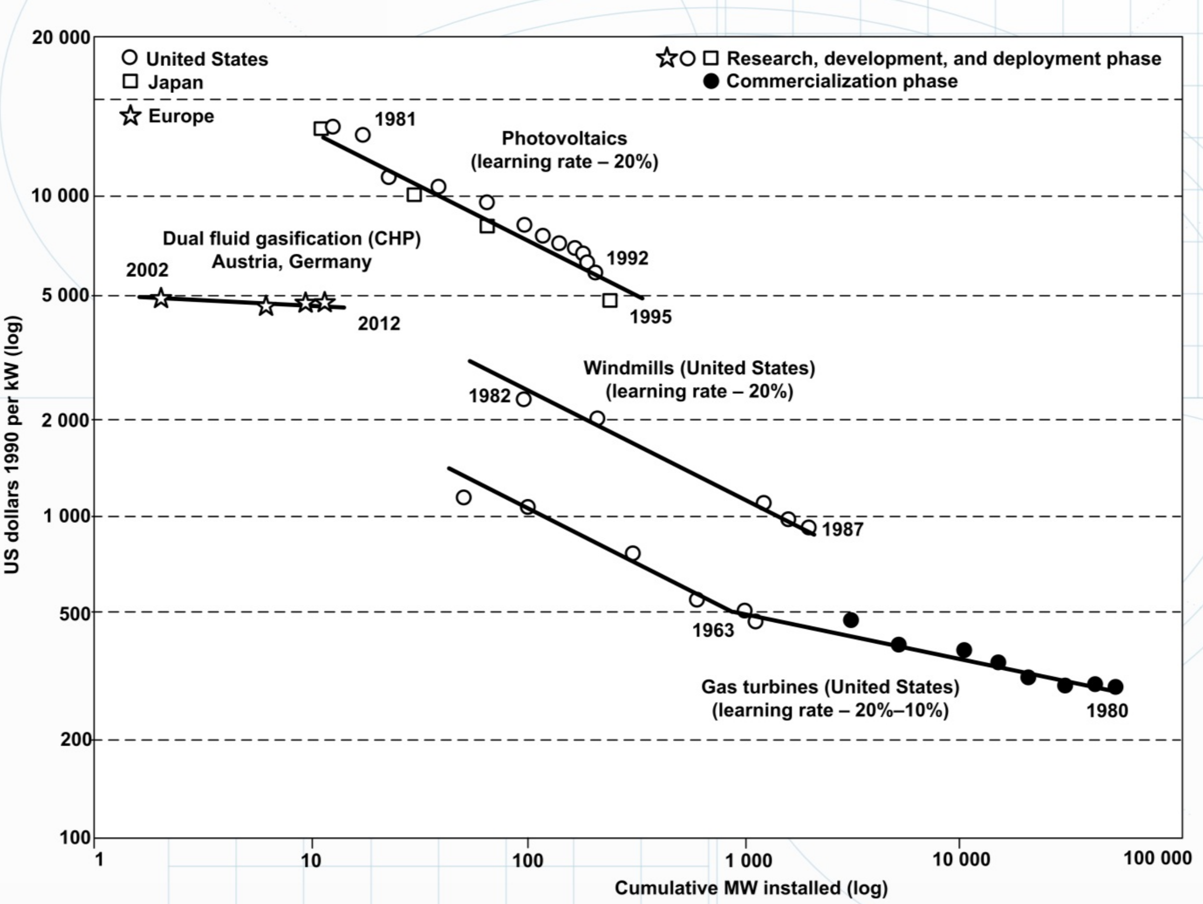

Fig. 23: Learning curves for the electricity production from combined heat power plants based on dual fluid gasification in comparison with photovoltaics, windmills and gas turbines[3]

---

[1] cf. Wilk V., 2011, p57
[2] cf. Koppatz S., 2011, p63ff
[3] cf. figure: UNDP, 2000, p16
(CHP Data added based on values shown in Tab. 6, USD inflation rate = 2.6 % according to OECD, Exchange Rate EUR/USD = 1.20)

3.6. Gasification Technology Summary

Chapter 3 gave a rough overview about the current state of knowledge in the field of biomass gasification. The presented literature review reflected main relevant facts of gasification technology with respect to the industrial application.

- Dual fluid gasification enables, in comparison with other gasification technologies, a favorable product gas composition for the production of several high quality clean energy carriers such as synthetic natural gas, Fischer-Tropsch diesel fuel, mixed alcohols, methanol, other fuels, basic chemicals and hydrogen. The technical demonstration of mentioned pathways is currently investigated by several research activities.

- So far realized commercial plants focused on the production of electricity. The production of electricity has been supported by the structure of national funding frameworks which offered a subsidized electricity prize for electricity from renewable energy sources. Realized plants demonstrated their capability for long time operation. At the same time, plant operators are forced to improve the reachable operation hours per year, the setup of used control- and automation system and the energetic efficiency of their operated plants. High fuel prices, an unsure development in the future, and the character of the legal funding scheme frameworks put plant operators under economic pressure to improve the performance of operated plants.

- Future development of overall plant concepts needs to focus on increased fuel flexibility, reduced plant complexity, a reduction of necessary gas cleaning equipment and an efficient production of multiple pure end products following the idea of a biorefinery. Especially, increased fuel flexibility could improve the economic situation of plants by the utilization of low cost fuels from waste materials.

- Several pathways are in theory possible for the utilization of biomass as a renewable energy source for energy intensive industry by the application of dual fluid gasification. Further research activities need to identify the most promising pathways and overcome remaining technological limitations within overall energy supply concepts.

Overall plant concepts for industry need to find solutions for existing technical limitations and consider site-related factors for a successful integration of renewable energy sources by the application of dual fluid gasification. Dual fluid gasification offers beneficial characteristics for the implementation of renewable chemical energy from biomass. So far investigated concepts did not reveal promising pathways and did not lead to an integration in energy intensive industry. Therefore, **a precise investigation of further overall concepts is necessary to prepare the realization of a suitable overall plant concept.** Within the present work concepts for the industrial production of hydrogen based on dual fluid gasification are investigated.

4. Sorption Enhanced Reforming

Biomass gasification by **sorption enhanced reforming** (SER) can be named as a promising pathway for the further development of dual fluid gasification. Sorption enhanced reforming aims at producing a gas with high hydrogen content reached by the application of bed materials based on limestone. High hydrogen content of the product gas is reached by a reduction of the CO_2 content due to a selective CO_2 transport enabled by the operated bed material. At the same time sorption enhanced reforming can lead to reduced tar content in the product gas stream through catalytic activity of limestone. Due to this fact, the application of sorption enhanced reforming enables an improved product gas composition and can increase the possibilities for product gas utilization.[1] The following chapter gives an overview about the current state of knowledge in the field of sorption enhanced reforming regarding

- the basic principles,
- occurring chemical reactions and thermodynamics,
- requirements concerning used solid particles,
- the application possibilities for dual fluid gasification,
- existing experimental results

and pathways for further improvement of the sorption enhanced reforming process.

4.1. Definitions

Adsorption is defined as a physical process by adhesion of gaseous or liquid fluids to a surface of a porous, surface active solid substance. Vice versa, the discharging process of gaseous or liquid fluids is defined as **desorption.**[2]

Absorption is defined as a chemical process in which atoms, molecules, or ions enter the bulk phase of a gas, liquid or solid material.[3]

Reforming can be defined as a conversion process of gaseous or fluid hydrocarbons into a gas mixture based on hydrogen and carbon monoxide. The conversion process is stimulated by a catalyst and or heat. Reforming as a term is mainly used in the area of petrochemical processes of a refinery.

Sorption enhanced reforming is defined as a product gas reforming process supported by absorption. Sorption enhanced reforming is applied for the reformation of a product gas from biomass gasification. Calcium based bed materials enable the selective transport of CO_2 from the product gas stream to an exhaust gas stream.[4] Sorption enhanced reforming leads to a reduced CO_2 content in the product gas stream.

---

[1] cf. Soukup G., 2009, p56

[2] cf. Kast W., 1988, p1

[3] cf. McMurry J., 2003, p409ff

[4] cf. Soukup G., 2009, p56ff

4.2. Basic Principles

First research activities in 1868 by Tessie Du Motay and Marechal studied main basic principles of the sorption enhanced reforming process. Carried out experiments at that time aimed at the production of hydrogen by steam reforming of hydrocarbons with the aid of calcium based sorbents.[1] Years later research activities carried out by Curran[2], Lin[3], Florin[4], Weimer[5], Johnson[6], Balasubramanian[7], Shimizu[8] and Höftberger[9] contributed further important research results to today's state of knowledge of sorption enhanced reforming.

Fig. 24 illustrates the basic principle of sorption enhanced reforming in comparison with conventional dual fluid gasification. Materials mainly consisting of limestone ($CaCO_3$, CaO) are used as bed material instead of olivine. The gasifier is operated at temperatures between 600 and 700°C enhancing the carbonation reaction (cf. **Eq. 4.1**). Solid wood particles enter the gasifier, where drying, devolatilization, and partially char gasification take place. Necessary heat is provided by the circulating calcium based bed material and by the exothermal carbonation reaction. The bed material is circulating between the gasifier and a second fluidized bed reactor, which is used as a combustion chamber enhancing the endothermal calcination reaction (cf. **Eq. 4.2**). Within the combustion chamber significant amounts of remaining wood char are combusted at temperatures between 800 to 900°C to provide heat for the gasification and for the calcination reaction. The described process configuration enables selective transport of CO_2 from the product gas stream to the exhaust gas stream and as a result an improvement of the product gas composition is obtained. Additionally, the selective removal of CO_2 stimulates the generation of hydrogen by the water-gas shift reaction (cf. **Eq. 4.3**).[10]

Eq. 4.1: $CaO + CO_2 \leftrightarrow CaCO_3 \qquad \Delta H = -181{,}4\ \mathrm{kJ/mol}$

Eq. 4.2: $CaCO_3 \leftrightarrow CaO + CO_2 \qquad \Delta H = 181.4\ \mathrm{kJ/mol}$

Eq. 4.3: $CO + H_2O \leftrightarrow CO_2 + H_2 \qquad \Delta H = -40.9\ \mathrm{kJ/mol}$

Fig. 25 shows important considerations regarding the thermodynamic equilibrium of the calcination and carbonation reaction. Highlighted thermodynamic limitations are important boundaries for the achievable product gas composition. The illustrated equilibrium function points out that sorption enhanced reforming only can be operated

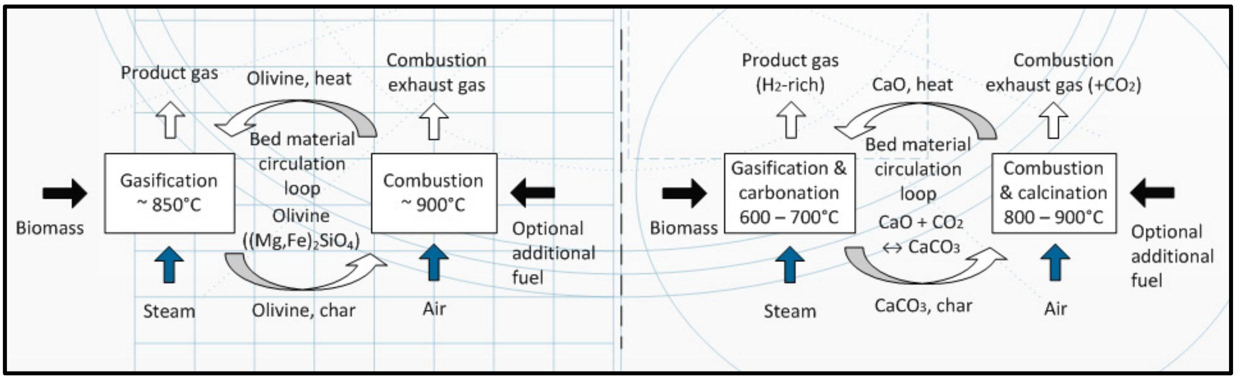

Fig. 24: Conventional dual fluid gasification vs. sorption enhanced reforming[10]

---

1 Tessie Du Motay M., 1868
2 Curran G.P., 1964, p128ff; 3 Lin S., 2002, p1283ff; 4 Florin N.H, 2007, p4119ff; 5 Weimer T., 2008, p1678ff;
6 Johnson K., 2006, p1195ff, 7 Balasubramanian B., 1999, p3543ff 8 Shimizu T., 1999, p62ff,
9 Höftberger E., 2005; 10 cf. figure: Koppatz S., 2009, p914ff

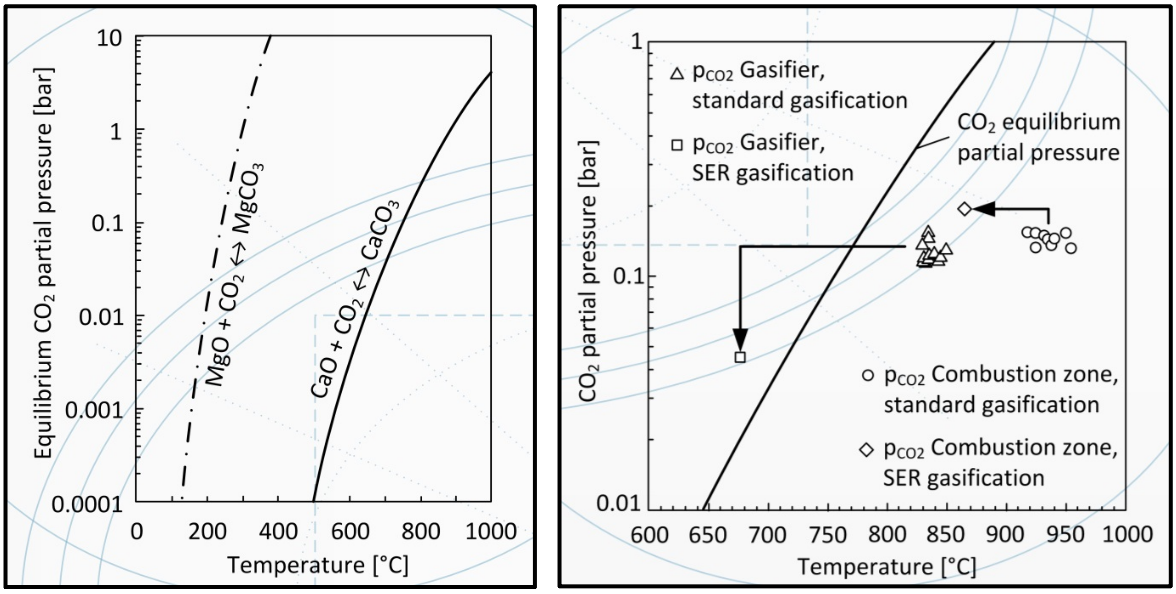

Fig. 25: Equilibrium partial pressure for carbonation (left)[1] and operation points of conventional gasification with olivine in comparison with sorption enhanced reforming (SER), (right)[2]

in a specific temperature range in relation to the actual partial pressure of CO_2. **Fig. 25 to the left** shows a comparison between the equilibrium function of the calcium carbonation reaction in comparison with the magnesium carbonation reaction. **Fig. 25 on the right** presents operating points of conventional gasification with olivine in comparison with sorption enhanced reforming with calcium based bed materials. As it can be seen, sorption enhanced reforming has to be operated at lower gasification temperatures. Additionally, a certain distance to the equilibrium has to be maintained to enable rapid reaction rates at low residence times of present bed material particles. At this point, the performance of operated bed material particles is an important factor for the operation of the overall process. Within **Fig. 25 right**, the vertical distance of SER operation points (□; ◊) to conventional gasification operation points (Δ; ○) represent change of the carbon dioxide (CO_2) partial pressure due to absorption and release.

4.3. Bed Material Requirements

Fig. 24 already showed the importance of operated bed material particles. The **circulating bed material** needs to offer sufficient characteristics to maintain the hydrodynamics in a dual fluid gasifier system at high temperatures. Furthermore, operated bed material needs to enable the heat exchange between the two reactors, should lead to low tar contents and offer a high resistance against attrition.

Attrition leads to a reduced particle size during the operation of solid particles in a fluidized bed. **Fig. 26** depicts different phenomena which result in particle breakage. Attrition phenomena like particle chipping, particle splitting and particle disintegration result in high demand for a renewal of the operated bed material.[3] High bed material renewal at the same time means high bed material consumption and reduced cold gas efficiency. Therefore, the used bed material particles should offer a high resistance against attrition.

---

1 figure: Soukup G., 2009a, p349

2 figure: Koppatz S., 2009, p919; 3 cf. Scala F., 2007, p2571

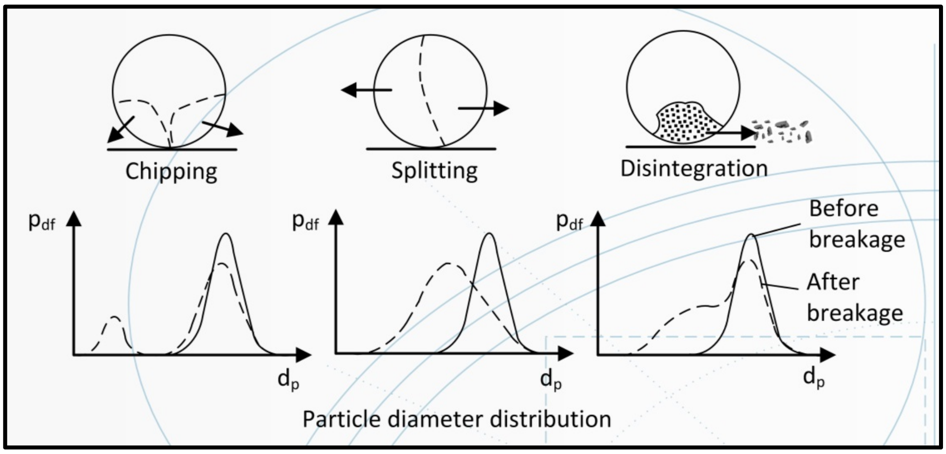

Fig. 26: Particle breakage patterns and characteristic particle diameter distributions[1]

Sorption enhanced reforming requires bed material which enables the selective transport of CO_2. **Eq. 4.4** shows a specification of the transport ability of solid particles based on calcium oxide (CaO) defined as **"CO_2 load"**.

Eq. 4.4:

$$X_{CaO} = \frac{\dot{n}_{CO_2}}{\dot{n}_{CaO} + \dot{n}_{CaCO_3}} \qquad \frac{[mol_{CO_2}]}{[mol_{CaO}]}$$

The CO_2 load of bed materials based on calcium oxide (CaO) is limited to 1.0 mol CO_2 per mol CaO due to the chemical composition and the molar mass of the reactants (cf. **Eq. 4.1**). Therefore, the absorption of CO_2 by a calcium oxide particle (CaO) cannot exceed 0.785 kg_{CO2} per kg_{CaO}.[2] The stated value can only be reached in theory due to several mechanisms which prevent a full carbonation of the calcium oxide (CaO) particles. Main reasons for a reduced CO_2 load are

- a low CO_2 diffusion rate,
- the development of a calcium carbonate ($CaCO_3$) surface layer,
- sintering
- and a reduced porosity after many carbonation and calcination cycles.[3]

Fig. 27 shows different models describing the mechanisms which lead to a reduced CO_2 load. The absorption of CO_2 by calcium oxide particles (CaO) induces on the one side a reduction of porosity and on the other side to the development of a layer of calcium carbonate ($CaCO_3$) which reduces the CO_2 diffusion rate. A detailed mathematical description of relevant mechanisms reducing the reaction activity can be found within the shrinking core model according to Levenspiel.[4] **Fig. 28 (left)** illustrates the described reduction of micro porosity of a calcium oxide particle surface (CaO) after many carbonation cycles by pictures of a scanning electron microscope (SEM). The described mechanisms cause a reduced CO_2 load which also can be observed within practical experimental tests. **Fig. 28 (right)** shows experimental results on the decay of CO_2 loading of different limestone after several calcination and carbonation cycles. The results show a significant decay of the reactivity of tested limestone after a low number of cycles. A recognizable decay can be a relevant factor for the application of different limestone for the sorption enhanced reforming process.

---

[1] figure: Scala F., 2007, p2571
[2] cf. Koppatz S., 2009, p914ff
[3] cf. Soukup G., 2009, p60ff
[4] Levenspiel O., 1999, p1ff

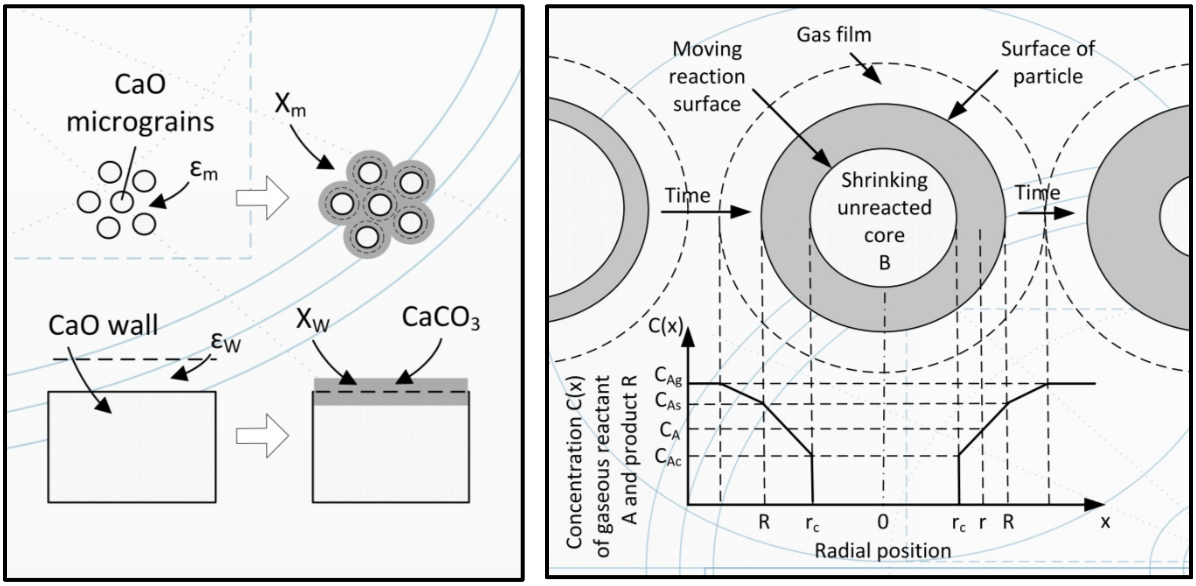

Fig. 27: Mechanisms for reduced CO_2 load (left)[1] and shrinking core model (right)[2]

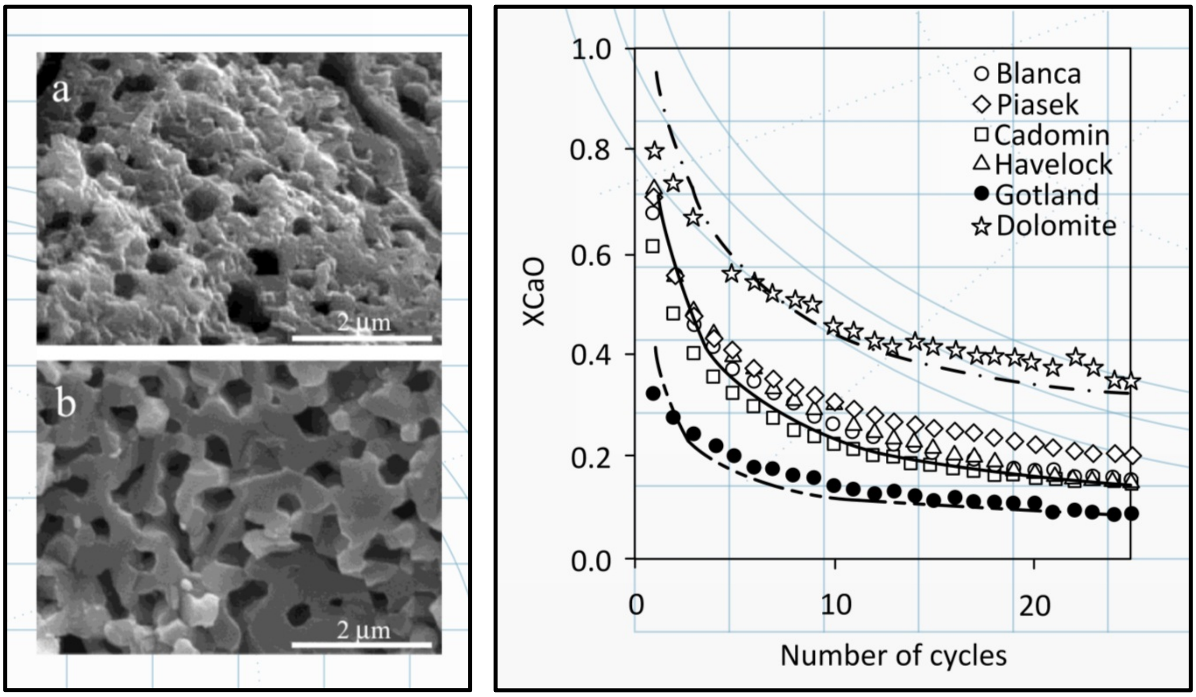

Fig. 28: SEM pictures illustrating the decay of micro porosity (left)[1] and experimental results about the decay of CO_2 load (XCaO) for different limestone (right)[3]

Sorption enhanced reforming is dependent on bed materials which are capable to maintain low attrition rates and constantly high CO_2 load during long time operation. **Chapter 4.3** described degeneration phenomena which imply major constraints for the practical achievable performance of the sorption enhanced reforming process. Therefore, the practical performance of used bed materials is an important factor for the efficient operation of the process. Specific bed materials for the operation of the process need to be selected by the results of representative degeneration tests.

---

1 figure: Abanades J. C., 2003, p313

2 figure: Levenspiel O., 1999, p1ff; 3 figure: Grasa G.S., 2006, p8848

4.4. Performance of Different Calcium Based Bed Materials

In **Chapter 4.4** results of bed material degeneration tests are presented. These degeneration tests have been carried out to assess the capability of several calcium based bed materials before sorption enhanced reforming experiments in a 100 kW test facility. **Fig. 29** shows results of this assessment for different calcium based bed materials regarding attrition and CO_2 load. Tested bed materials have been named by the authors according to an internal notation. As it can be seen, dolomites ($CaMg(CO_3)_2$; code D) showed less attrition than limestone ($CaCO_3$) name code C). Whereas the CO_2 load of tested bed materials has been quite similar after 20 carbonation and calcination cycles in a fluidized bed.[1] Bed materials **C1**, **C14**, **C35**, **C13**, **C15** and **C38** showed favorable characteristics due to relatively high resistance against attrition and a low degeneration of their CO_2 load. Therefore, these bed materials have been identified by the author as promising bed materials for the sorption enhanced reforming process. In 2008 practical sorption enhanced reforming experiments were carried out at a 100 kW dual fluid gasifier. **Tab. 12** shows the chemical composition of used bed materials which had been chosen by the responsible research team for practical experiments.[3]

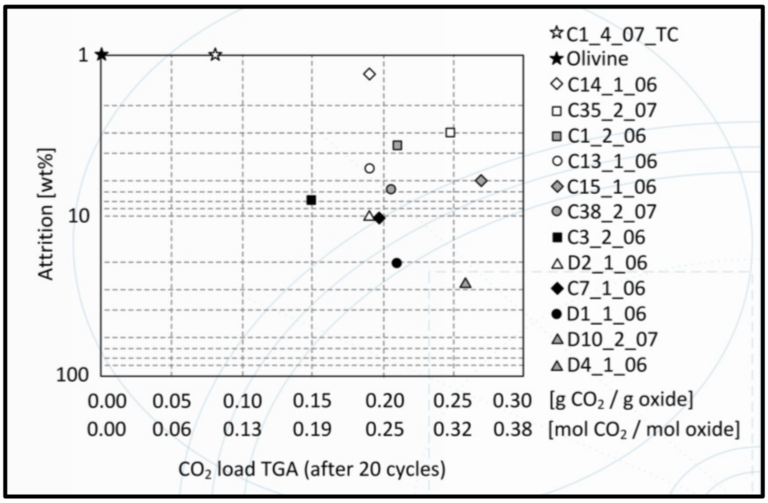

Fig. 29: Attrition during flash calcination in a fluidized bed[2]

Bed material	Unit	$CaCO_3$	CaO	$MgCO_3$	SiO_2	Al_2O_3	Fe_2O_3	MgO	Trace elements
Limestone									
C1	wt.-%	94	-	-	2.77	1.4	0.6	0.7	0.53
C14	wt.-%	98.1	-	0.9	0.55	0.35	0.08	-	0.57
C35	wt.-%	97.4	-	-	0.46	0.48	-	-	1.66
C38	wt.-%	94.8	-	0.7	-	1.95	2.5	-	0.05
C58	wt.-%	94.17	-	-	4.03	0.64	0.19	0.49	0.48
Pretreated limestone									
C1_a	wt.-%	22.75	71.25	-	2.77	1.4	0.6	0.7	0.53
C1_b	wt.-%	40.95	53.05	-	2.77	1.4	0.3	0.7	0.53
Olivine									
fresh[5]	wt.-%	-	0.9	-	39.8	0.4	10.3	46.8	2.30

Tab. 12: Chemical composition of tested bed materials in comparison with olivine[4]

---

1 Koppatz S., 2009, p916; 2 figure: Koppatz S., 2009, p916;
3 Soukup G., 2009a, p351; 4 table: Soukup G., 2009a, p351; 5 Kirnbauer F., 2011, p3795

4.5. Practical Experiences of Process Operation

The current state of knowledge regarding the practical operation of the sorption enhanced reforming includes

- experimental campaigns with a 100 kW dual fluid gasifier in Vienna,[1]
- experimental campaigns with a 200 kW dual fluid gasifier in Stuttgart,[2]
- and experiments at the 8 MW dual fluid gasifier in Güssing.[3]

Carried out experiments demonstrated a stable operation of the sorption enhanced reforming process. **Tab. 13** shows the gas composition achieved with sorption enhanced reforming in the 100 kW dual fluid gasifier in Vienna. Used bed materials are shown in **Tab. 12**. The results of the experimental campaign showed a significant increase of the hydrogen content in the product gas stream compared to conventional gasification. At the same time decreasing CO_2 and tar contents have been observed. The used gasifier system has not been designed for the operation of sorption enhanced reforming. Therefore, to maintain the necessary hydrodynamics at low circulation rates, more steam fluidization was used than preferable for the gasification reactions. This leads to high water contents in the product gas stream. The demonstration of sorption enhanced reforming at a 100 kW dual fluid gasifier lead to further experimental activities at the 8 MW dual fluid gasification plant in Güssing. During an experiment 5 hours of steady state sorption enhanced reforming operation has been achieved.[3] The composition of the product stream has been measured as illustrated in **Tab. 13**.

Product composition for …		Conventional gasification (100kW)[4, 6]	Gasification by SER (100kW)[4, 6]	Gasification by SER (200kW)[7]	Gasification by SER (8MW)[5]
Fuel		wood pellets	wood pellets	wood pellets	wood chips
Gasification agent		Steam	Steam	Steam	Steam
Water (H_2O)	vol.-%	30 – 45	50 - 65	n.a.	n.a.
Hydrogen (H_2)	vol.-%$_{db}$	36 – 42	55 – 75	72	50
Carbon monoxide (CO)	vol.-%$_{db}$	19 – 24	4 – 11	11	12
Carbon dioxide (CO_2)	vol.-%$_{db}$	20 – 25	6 – 20	5	17
Methane (CH_4)	vol.-%$_{db}$	9 – 12	8 – 14	11	13
Non condensable C_xH_y	vol.-%$_{db}$	2.3 – 3.2	1.5 – 3.8	2	6
Dust particles	g/Nm³	10 – 20	20 - 50	n.a.	n.a.
Tar	g/Nm³	4 – 8	0.3 – 0.9	14	1.0
Bed material		olivine	limestone	limestone	limestone (C1_b)*
Particle size	mm	0.4 – 0.6	0.5 – 1.3	0.3 – 0.7	0.5 – 1.3
* cf. composition of limestone "C1_b" shown in Tab. 12 in chapter 4.4					

Tab. 13: Product gas composition of conventional gasification compared to sorption enhanced reforming with the 100 kW dual fluid gasifier in Vienna[4], 200 kW in Stuttgart[7] & 8 MW in Güssing[5]

So far conducted experiments highlighted the potential of sorption enhanced reforming for increased hydrogen content in the produced gas. Carried out experiments also showed that further optimization of the process is possible. The optimization of the process can be maintained by used solid separators, adapted geometries of the used gasifier system and by the used limestone.

1Pfeifer C., 2009, p5073ff
2 Poboss N., 2011, p363ff; 3 Koppatz S., 2009, p914ff; 4 Pfeifer C., 2008, p807
5 Koppatz S., 2009, p919ff; 6 Pröll T., 2008, p1209; 7 Hawthorne C., 2012, p224

During the large-scale experiment at the 8 MW gasifier in Güssing reduced feedstock gasification, increased amounts of residual char and incomplete char combustion were reported. For this reason, an adaption of the gasifier system design could be used to improve hydrodynamics, residence times and bed material circulation rates.

4.6. Potential Process Improvement

Further optimization potential based on before presented experimental results has been investigated by Pröll T. in 2008 with a process modeling approach illustrated in **Fig. 30**. The results of his work reflect

- reachable product gas compositions,
- consequences of sorption enhanced reforming on bed material circulation rate **(cf. Eq. 4.5)** and residence time,
- and reachable cold gas efficiencies **(cf. Eq. 4.6).**[1]

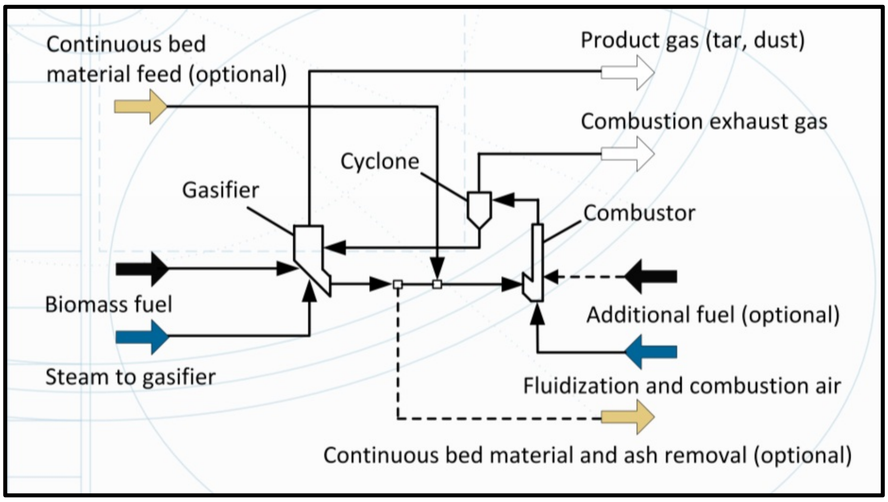

Fig. 30: Overall structure of process simulation model used by Pröll T.[2]

Eq. 4.5: $$r_{circ} = \frac{\dot{m}_{bed,G,in}}{\dot{m}_{fuel} \cdot (1 - \omega_{H2O,fuel} - \omega_{ash,fuel})} \qquad \frac{[kg]}{[kg_{fuel(waf)}]}$$

Eq. 4.6: $$\eta_{chem} = \frac{P_{chem,PG}}{P_{th}} = \frac{\dot{m}_{PG} \cdot lhv_{PG}}{\dot{m}_{fuel} \cdot lhv_{fuel}} \qquad [-]$$

Presented results indicated that the bed material circulation rate (r_{circ}) has to be one magnitude lower during sorption enhanced reforming compared to the conventional process to maintain the high temperature difference between gasifier and combustor. As a consequence, the mean solids residence time in the gasifier needs to increase about the same factor. This way, the hydrogen content could reach up to 80 vol.-%$_{db}$ if used bed materials are capable to maintain high CO_2 load.[3] Therefore, a design optimization of the used gasifier system for sorption enhanced reforming would require to concentrate on necessary hydrodynamics for lower bed material circulation rates, increased residence times and longtime bed material performance. This would lead to a reduced water content within the product gas stream, lower bed material consumption and a lower demand for additional fuel input to the combustion chamber.

---

[1] Pröll T., 2008, p1207ff

[2] figure: Pröll T., 2008, p1210

[3] Pröll T., 2008, p1215

4.6.1. Bed material

The practical performance of used bed materials is important for an efficient operation of the process. Therefore, Florin N.H. and Harris A.T. reviewed possibilities to enhance the multi-cycle reactivity of calcium oxide (CaO) for sorption enhanced reforming. As a result of their review five main methods have been considered to enhance the reactivity of used calcium oxide (CaO) for high CO_2 load at long time operation:

- mild calcination conditions,
- sorbent hydration,
- nano-sized sorbent particles,
- incorporation of calcium oxide (CaO) in inert porous matrix,
- and increased surface due to precipitated calcium carbonate ($CaCO_3$).[1]

Research activities investigating the mentioned methods showed first successful results. At the same time, used methods are still to inconvenient for the large-scale application as an industrial process.

4.6.2. Next Generation Dual Fluid Gasifier Design

A novel gasifier design potentially offers favorable characteristics for the sorption enhanced reforming process. First experimental results with a cold flow model showed that the improved design of the gasification chamber leads to an improved gas-solid contact due to well mixed flow conditions along the full reactor height. Additional in future, the changed design should enable increased residence times for solid particles and gas, reduced tar contents and a sufficient gas conversion.[2] For sorption enhanced reforming the characteristics of the next generation dual fluid gasifier design are expected to improve the preconditions for the CO_2 load of used calcium oxide (CaO) due to an improved gas-solid contact. This effect would be equal to increased residence times of important reactants and would potentially increase the process performance.

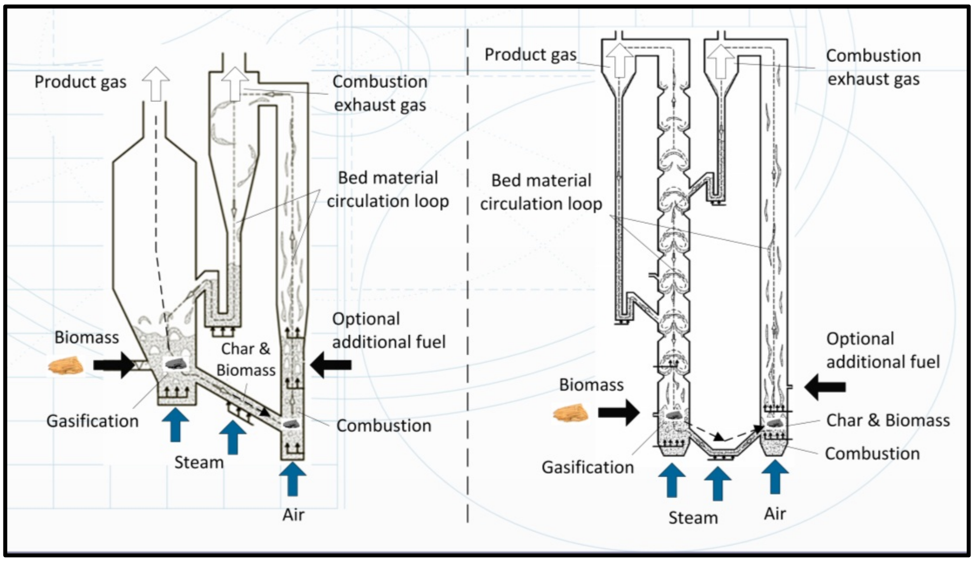

Fig. 31: Conventional dual fluid gasification in comparison with the next generation gasifier design[3]

---

[1] cf. Florin N.H., 2008, p307ff
[2] cf. Schmid J.C., 2012a, p229ff
[3] cf. figure Schmid J.C., 2012a, p234

4.7. Summary

Chapter 4 gave an overview about the current state of knowledge regarding sorption enhanced reforming. The presented overview explained basic principles, necessary thermodynamics and bed material requirements. Additionally, existing experimental data were presented to illustrate application possibilities for sorption enhanced reforming.

- Biomass gasification by sorption enhanced reforming enables an improved product gas composition by using calcium based bed materials. The achieved product gas contains high amounts of hydrogen and reduced amounts of tar and CO_2. Lower gasification temperatures lead to improved cold gas efficiency and used calcium based bed materials are available in large quantities at a low price.

- Sorption enhanced reforming is dependent on bed materials with high reactivity and high resistance against attrition. Different degeneration phenomena like particle disintegration or the decay of CO_2 loading imply major constraints for the practical achievable process performance. Especially the decay of CO_2 load after many carbonation and calcination cycles causes a high demand of bed material renewal. Experimental results of representative degeneration tests have been presented in **Chapter 4.4** for different calcium based bed materials.

- Sorption enhanced reforming has been successfully demonstrated in 2008 at a 100 kW dual fluid gasifier in Vienna, at a 200 kW dual fluid gasifier in Stuttgart and at an 8 MW dual fluid gasifier in Güssing. The results of the experiments carried out showed that sorption enhanced reforming can be operated in an industrial facility at large-scale. The achieved product composition confirmed the expected increase of the hydrogen content.

- Carried out experiments opened up further potential for process optimization. The optimization of the process can be maintained by a redesign of used solid separators, adapted reactor geometries of the used gasifier system and by the used limestone.

- A next generation dual fluid gasifier design could be an option for operating the sorption enhanced reforming process at favorable conditions. Improved gas-solid contact and hydrodynamics of a new gasifier design potentially leads to longer residence times and improved CO_2 load of the operated bed materials.

Further activities of research and development need to focus on the necessary adaption of currently used gasifier systems for a commercial long time operation of sorption enhanced reforming at industrial scale.

5. Applied Principles and Methods

The aim of the present work is to evaluate different concepts for the industrial application of a hydrogen production based on dual fluid biomass gasification. Within **Chapter 5** necessary methods are explained which are used to evaluate different concepts for the integration of dual fluid gasification into existing industrial production processes. **Chapter 5** addresses:

- principles of modeling dual fluid gasification plants,
- the possibilities of the process simulation software IPSEpro,
- existing experiences regarding the simulation of new plant concepts,
- and investment decisions supported by net present value calculations.

The listed methods are used to compare different hydrogen production concepts for the integration of dual fluid gasification into existing industrial production plants.

5.1. Definitions

A **model** can be defined as a simplified reproduction of reality focused on the investigation of important existing relations and observed behavior. Modeling of important relations by mathematical equations enables a predictive calculation of future behavior with respect to existing boundary conditions. **Modeling** can be described as the creation of a model based on an existing system of important observed relations.[1]

Process simulation predicts the behavior of a process by calculating the results of a mathematical model describing the process by the use of a computer. Therefore, necessary simulation models need to be implemented in simulation software. Simulation of processes in the field of energy technologies typically bases on a description of physical or chemical interactions of modeled mass- and energy flows.[2] The present work focuses on modeling with the process simulation software IPSEpro. Further, well established process simulation software are: Aspen Plus, ChemCAD, CHEMASIM, Aspen Hysys, HSC Sim - Chemistry, System7, UniSim, and many more.

5.2. Modeling of Dual Fluid Gasification

The development of dual fluid gasification technology has been accompanied by the development of several models describing the occurring processes within a dual fluid gasification plant. Results of the model development can be consulted in literature.[3] Pröll T. chose, based on previous work by Schuster G. et al. 2001 and Kaiser S. 2001, the **process simulation software IPSEpro** as software environment for the model development. Created models are based on an equation orientated calculation of mass and energy balances for steady states and describe gasification based processes in the surrounding of dual fluid gasification plants. Therefore, the created model units include beside the dual fluid gasifier also further equipment like pumps, turbines, heat exchangers, separators and additional chemical reactors in order to represent entire plant configurations.[4] The model development within IPSEpro enabled the creation of simulation models describing entire dual fluid gasification plants through the creation of flow charts within IPSEpro projects.

---

[1] cf. VDI, 1993, p1ff

[2] cf. Pröll T., 2008a, p2; [3] Pröll T., 2008a; [4] cf. Pröll T., 2008a, p1

5.3. Simulation with IPSE Pro

Fig. 32 shows the structure of the simulation software IPSEpro. IPSEpro consists of a model development area and a kernel used as analyzer and solver. A simulation model describing a process can be created as a flow chart within an individual project. Results are calculated by the solver in connection with property data (dynamic link libraries) for implemented substance streams like water/steam, ideal gases, inorganic solids and organic mixtures. The equations are provided by single unit-models which are grouped in model libraries. Single unit-models are formed by an equation system describing the occurring processes within a device (e.g. turbine, engine, heat exchanger). Unit-models in the surrounding of biomass gasification have been grouped within the **biomass gasification library** (BG-Lib). Unit models within the BG_Lib are based on the calculation of **mass- and energy balances**. The mass balance differs according to the nature of the substance conversion inside a specific unit:

- as a balance of chemical elements if chemical reactions take place,
- as a balance of chemical compounds if no chemical reactions take place,
- or as total mass flow balance if a stream passes without changing its composition.[1]

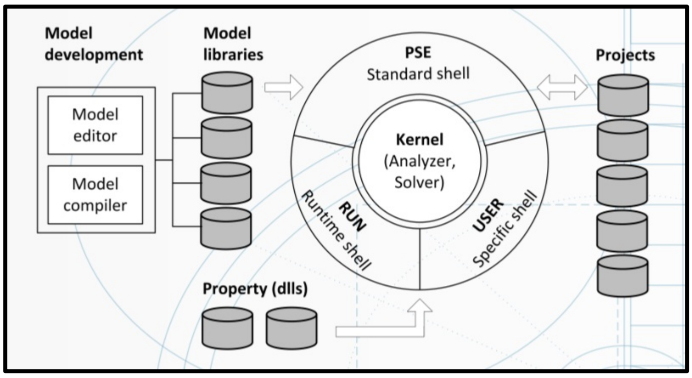

Fig. 32: Structure of process simulation software IPSEpro[2]

Eq. 5.1: $$\dot{\boldsymbol{Q}} + \boldsymbol{P} = \sum_{i=1}^{Z}[\dot{\boldsymbol{n}}_i \cdot \boldsymbol{H}_i^* \,(\boldsymbol{p}_i, \boldsymbol{T}_i)]$$

Energy balance calculations are based on total enthalpy as shown by **Eq. 5.1.** Gravity potential and kinetic energy are generally neglected.[2] The solution of the equation system are dependent on property data provided by dynamic link libraries (dll). Biomass gasification simulation projects refer to property data from several sources. Property data for water and steam are formulated based on real property data from IAPWS-IF97.[3] Data used for gases are based on ideal gas data related to the JANAF-Tables.[4] Necessary data for inorganic solids are calculated according to data reported by Ihsan Barin. And the description of organic substances like biomass, charcoal and fuel oil is based on elementary analyzes.[5]

Within biomass gasification library different unit-models can be used for several processes in the surrounding of a gasification plant. Dual fluid processes are represented by a gasification reactor and a connected combustion reactor. A description of the gasifier models, combustion reactor models and further unit-models for equipment like pumps, heat exchangers, separators and chemical reactors can be found in literature.[5, 6]

---

1 Pröll T., 2008a, p6;

2 cf. figure: Pröll T., 2008a, p4 adapted from Simtech, 2003, p2-2;

3 cf. Wagner W., 1998; 4 cf. Chase M., 1985; 5 cf. Pröll T., 2008a, p12ff; 6 Pröll T., 2008, p1210

5.4. Simulation of new Concepts for Gasification Plants

Unit-models within the biomass gasification library (BG_Lib) have been validated through experimental results and data from operating plants like Güssing and Oberwart. This enables predictive calculations of new plants. The results allow an evaluation of new concepts at an early stage of development. Examples for new concepts for dual fluid gasification plants simulated can be found in literature. 2004 Pröll T. calculated several different concepts for an improvement of electricity and heat generation.[1] In 2010, Stidl M. modeled several concepts to supply energy from biomass gasification for the pulp and paper industry.[2] Aside from that, different pathways of product gas utilization have been investigated by process simulation in the past.[3] **Fig. 33** shows an example for an IPSEpro project which was used for calculating an improved concept for a gasification plant.

5.5. Investment Decision - Net Present Value

Mass- and energy balances are the main result of a simulated plant concept as shown in **Fig. 33**. The results enable a decision about further steps for a realization by assessing expected plant input and plant output. The **construction of a new power plant** in general is associated with high investment costs and the expectation of plant operation over a long period of time. The decision about the realization involves economic uncertainties. Adequate methods accompanying the investment decision reduce the risk of an undesired outcome. **Capital budgeting methods** can support the economic aspects of an investment decision. Calculations which are used to support an investment decision are:

- payback calculations,
- return of investment calculations,
- internal rate of return calculations,
- or net presents value calculations.[1]

Listed methods enable a comparison of different investment options. **Tab. 14** together with **Eq. 5.2** to **Eq. 5.4** show the net present value calculation for a new power plant.

Position	Symbol	Unit	Value
Boundary conditions			
Net capacity of new power plant	-	MW_{el}	555
Net electricity generation	-	GWh/a	4 163
Electricity price	-	€/MWh	38
Interest rate	i	%	8.00
Lifetime	n	a	25
Net present value calculation			
Investment cost incl. interest	I_0	€	594 000 000
Earnings	E	€/a	158 200 000
Operating expenses	A	€/a	77 200 000
Profit	P	€/a	81 000 000
Cumulative present value factor	BWSF	-	10.7
Net present value	NPV	€	270 700 000

Tab. 14: Net present value calculation[2]

---

1 cf. Pröll T., 2004, p172ff; 2 cf. Stidl M., 2012, p128ff; 3 cf. chapter 3.4;
4 cf. Konstantin P., 2009, p147ff; 5 cf. Konstantin P., 2009, p165ff

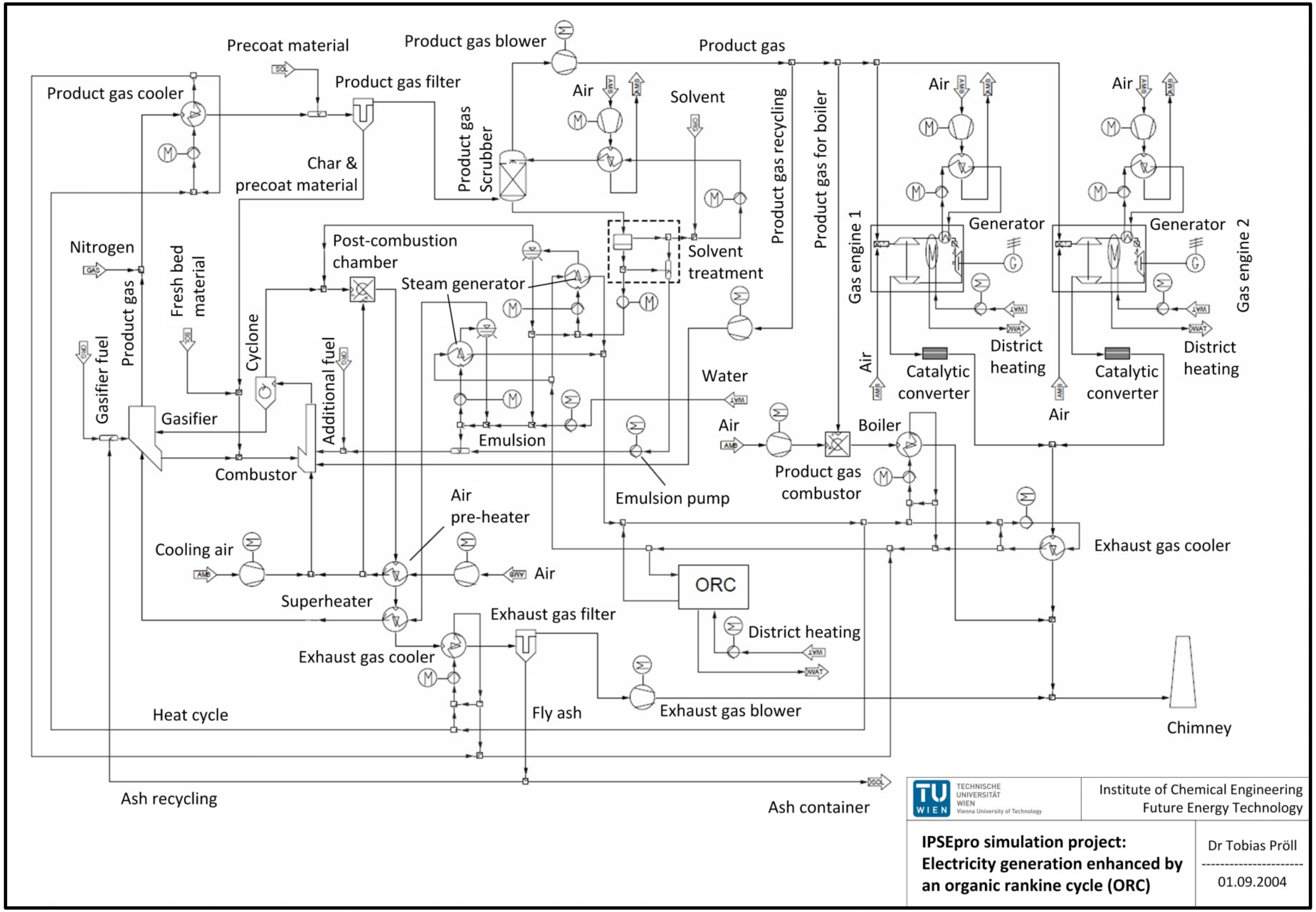

Fig. 33: Concept for improved electricity generation based on dual fluid gasification (cf. figure: Pröll T., 2004, p177)

Tab. 15 together with **Eq. 5.2** to **Eq. 5.8** show another example that rates 3 options for the energy supply of a paper mill through a net present value calculation.

Eq. 5.2: $$P_{\text{€}} = E - A \qquad [\tfrac{\text{€}}{a}]$$

Eq. 5.3: $$BWSF = \frac{(1+i)^n - 1}{(1+i)^n \cdot i} \qquad [-]$$

Eq. 5.4: $$NPV = -I_0 + BWSF \cdot P_{\text{€}} \qquad [\text{€}]$$

Position	Symbol	Unit	Option 0	Option 1	Option 2
Example: A paper mill has to decide about the future supply of electricity and heat. Future energy supply could be provided by: 0.) rehabilitation of the existing steam power and heat supply station, 1.) heat and power supply from a new gas turbine or 2.) a combined cycle power plant. **Investment decision:** Which option leads to an economic favorable supply of electricity and heat?					
Boundary conditions					
Investment cost incl. interest	$I_{Opt,X}$	€	16 000 000	40 000 000	48 000 000
Operating expenses					
Maintenance cost	A_1	€/a	640 000	1 000 000	1 200 000
Taxes on capital & insurance costs	A_2	€/a	80 000	200 000	240 000
Labor costs	A_3	€/a	500 000	500 000	500 000
Fuel costs (natural gas)	A_4	€/a	11 714 000	17 833 000	19 462 000
Costs for additional electricity	A_5	€/a	1 512 000	0	0
Backup power costs	A_6	€/a	305 000	526 000	425 000
Earnings from electricity surplus	E_1	€/a	0	- 9 406 000	- 12 552 000
Sum operating expenses	$C_{Opt,X}$	€/a	**14 750 000**	**10 653 000**	**9 274 000**
Net present value calculation					
Cumulative present value factor	BWSF	-	8.56	8.56	8.56
Additional investment costs	ΔI_X	€	0	24 000 000	32 000 000
Operating expenses savings	ΔC_X	€/a	0	4 098 000	5 476 000
Net present value	ΔNPV_X	€	0	11 073 000	14 875 000

Tab. 15: Comparison of different energy supply options by net present value calculation[1]

Eq. 5.5: $$C_{Opt,X} = \sum A_i - E_i \qquad [\tfrac{\text{€}}{a}]$$

Eq. 5.6: $$\Delta I_X = I_{Opt,X} - I_{Opt,0} \qquad [\text{€}]$$

Eq. 5.7: $$\Delta C_X = C_{Opt,0} - C_{Opt,X} \qquad [\tfrac{\text{€}}{a}]$$

Eq. 5.8: $$\Delta NPV_X = NPV_{Opt,X} - NPV_{Opt,0} \qquad [\text{€}]$$

Option 0 in general represents a business as usual scenario. The option with the highest net present value should be preferred for further realization steps. As a result of the comparison in **Tab. 15** Option 2 reaches the highest net present value and therefore should be favored for further realization steps. But economic aspects are only one important perspective out of many which have to be considered. Additionally, the technological feasibility, strategic considerations, macroeconomic aspects and the expected impact on the local surrounding have to be part of the decision. Technological risks can be acknowledged by risk assessment methods as described in literature.[2] Moreover decisions can be supported by multi-criteria decision making methods as stated in literature[3] if many different criteria have to be taken in consideration.

---

1 cf. Konstantin P., 2009, p168; 2 cf. Wildemann H., 2006, p120ff; 3 cf. "Nutzwertanalyse" Haas G., 2005, p94ff

5.6. Applied Methodology

Chapter 5 gave a short overview about available principles and methods to investigate new energy supply concepts based on dual fluid gasification. The aim of the present work is to evaluate different hydrogen production concepts for the industrial application of dual fluid gasification.

Present thesis should find answers to following questions:

- How can "**conventional dual fluid gasification**" be deployed to produce pure hydrogen for a refinery on a large scale from biomass?
- How can "**sorption enhanced reforming**" be applied to provide a hydrogen rich gas for iron production on a large scale from biomass?
- Are the hydrogen production costs achieved, sufficiently low to justify a further step aiming at the realization of large-scale plants?

The structure of the present work shown in **Fig. 34** aims on answering the above mentioned questions. Dual fluid gasification is investigated as a technology for the production of hydrogen. A reference case reflecting the current state of knowledge and the results of an environment analysis is created to form a foundation for novel concepts for the supply of hydrogen to industrial facilities. Novel hydrogen production concepts are created according to the demands of a modern refinery as well as a modern raw iron production. Conventional dual fluid gasification as well as sorption enhanced reforming are used as primary process for the hydrogen production. A comparison of both processes illustrates which process is preferable for the hydrogen output of each concept. A final discussion summarizes achieved results and findings.

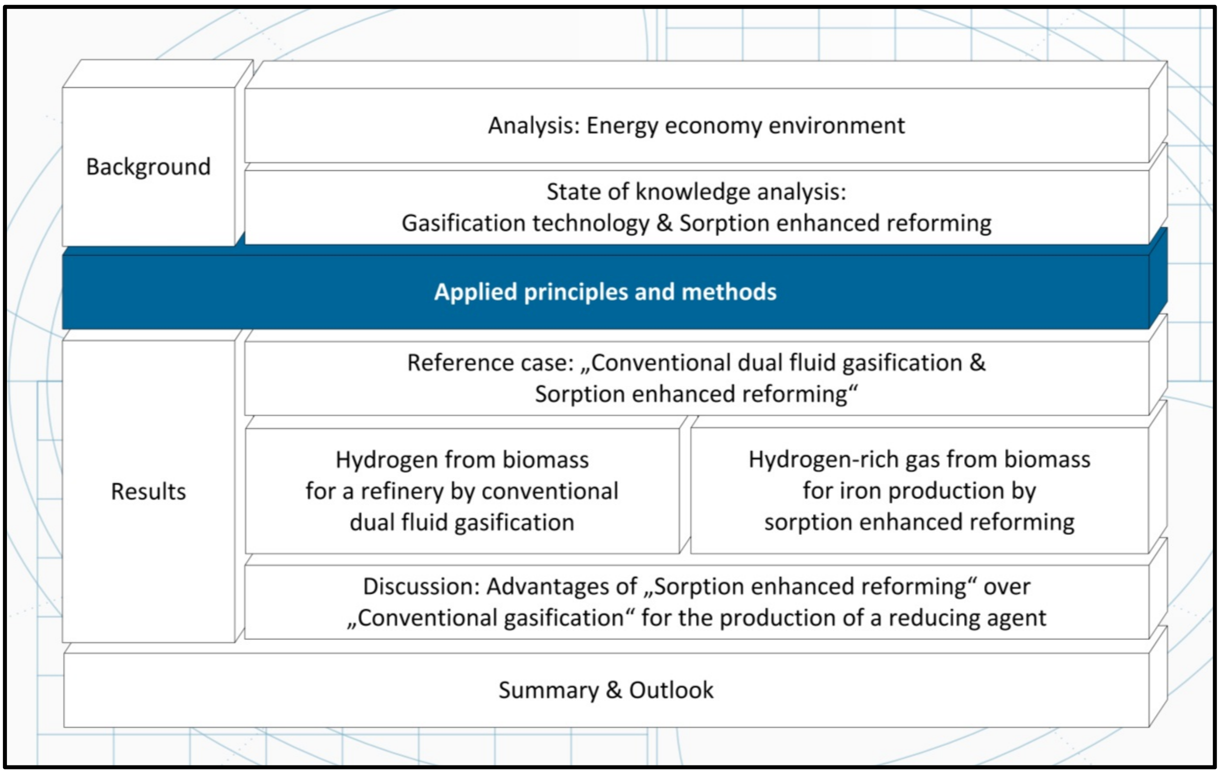

Fig. 34: Applied evaluation method to investigate the formulated research questions

6. Reference Case – Conventional Dual Fluid Gasification & Sorption Enhanced Reforming

In **Chapter 6** available data is conjoined to a "reference case". Included data sources set the foundation for the calculation of concepts for the

1. production of hydrogen with high purity for a refinery, and for the
2. production of a hydrogen-rich agent for iron ore reduction.

These novel concepts are calculated based on the **reference case** which is **formed by available data from electricity generation** (cf. **Tab. 9**) and **experimental data** (cf. **Chapter 4**). Therefore, **Chapter 6** includes

- basic data for the calculation of novel concepts,
- a reference case for conventional dual fluid gasification,
- an economic evaluation of conventional dual fluid gasification,
- a reference case for sorption enhance reforming,
- and an analysis of the impact of key figures of sorption enhanced reforming

Illustrated **basic data** should state equal preconditions for the calculation of novel concepts. Under these conditions a reproduction of achieved results is possible.

6.1. Basic Data for the Calculation of Novel Concepts

Equal preconditions for the calculation of novel concepts are assured by the use of equal default values for

- ambient conditions,
- compositions of important organic fuel mass flows (fuel, char, tar, solvent, …),
- efficiency factors (blower, pumps, …),
- equal key process figures describing the process operation
- as well as an equal consideration of pressure and heat losses.

Tab. 16 to **Tab. 20** illustrate consulted values within this work for the calculation of novel concepts. Beside the shown values, following considerations are used for heat and pressure losses. **Heat losses** within a biomass gasification plant raise the fuel demand and reduce the amount of available process heat. In the present work heat loss is considered with **4 % of the gasifier fuel input** (wood chips) referenced by the lower heating value.[1]

Pressure losses are important values for blower performance calculations. Within the present work pressure losses are summarized for whole plant sections in single devices. **Pressure losses** of the product stream for example are summarized in the product gas filter with **50 mbar.**[1] For that reason, the results of a simulation deliver the expected electricity consumption of blowers. But this way, the used simulation model does not provide a precise pressure profile of the calculated plant.

---

[1] cf. Stidl M., 2012, p111ff

Ambient conditions			
Altitude above sea level	m	150	for Vienna
Temperature	°C	10	mean annual temperature
Pressure	mbar	1000	-
Relative air humidity	%	80	-

Tab. 16: Ambient conditions

Air composition [1]		
Nitrogen (N_2)	vol.-%$_{db}$	78.10
Oxygen (O_2)	vol-%$_{db}$	20.95
Argon (Ar)	vol-%$_{db}$	0.92
Carbon dioxide (CO_2)	vol-%$_{db}$	0.03

Tab. 17: Air composition

Composition		wood chips [2]	char [2]	tar [2]	scrubber solvent (RME) [2]
Water (H_2O)	Weight%	40	-	-	-
Carbon (C)	Weight%wf	48	84.8	94	93
Hydrogen (H)	Weight%wf	6	3.2	6	5
Nitrogen (N)	Weight%wf	0.2	0.0	0	2
Oxygen (O)	Weight%wf	45	12	0	0
Sulfur (S)	Weight%wf	0.01	0	0	0
Chlorine (Cl)	Weight%wf	0.001	0	0	0
Ash	Weight%wf	0.8	0	0	0
Lower heating value	kJ/kg$_{db}$	17 503	31 248	38 490	36 874

Tab. 18: Composition of important organic fuel mass flows

Efficiency factors		Product gas blower [3]	Flue gas blower [3]	Air blower [3]
Isentropic efficiency	%	50	65	65
Mechanical efficiency	%	98	98	98
Drive system				
Electrical efficiency	%	90	90	90
Mechanical efficiency	%	100	100	100

Tab. 19: Efficiencies of used blower units

Efficiency factors		Pumps within gas cooling, gas cleaning [3]	Pumps within process heat utilization [3]
Isentropic efficiency	%	50	70
Mechanical efficiency	%	98	98
Drive system			
Electrical efficiency	%	80	90
Mechanical efficiency	%	100	100

Tab. 20: Efficiencies of used pumps

---

[1] EN ISO 6976, 2005, p34

[2] cf. Data: Pröll T., 2004, p213ff

[3] cf. Data Stidl M., 2012, p111ff

A further important precondition is the way of calculating mass- and energy flows within the dual fluid gasifier system. **Fig. 35** shows a sketch of the structure of the used simulation model. Shown arrows represent relevant mass and energy streams which are calculated within the simulation model. **Tab. 21** shows important key figures describing the operation of the gasifier system. Listed values are used as important key figures for the calculation of performance aspects of novel concepts. Further important data for performance calculations reflecting fuel supply, gas cooling, gas cleaning and gas utilization is in general provided by:

- experimental results,
- operation data from the process control system of existing plants,
- and by technical data from equipment manufacturer.

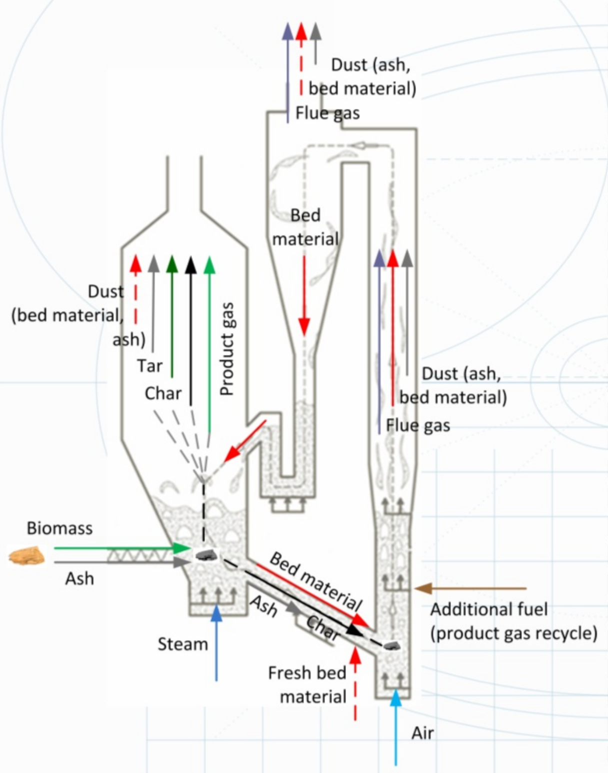

Symbols

lhv_{fuel}	[kJ/kg]	Lower heating value of biomass (fuel)
$lhv_{add\ fuel}$	[kJ/kg]	Lower heating value of additional fuel
lhv_{PG}	[kJ/kg]	Lower heating value of product gas
$\dot{m}_{air}$	[kg/h]	Air massflow
$\dot{m}_{char,bed}$	[kg/h]	Char massflow from gasifier to combustor
M_{CO}	[kg/mol]	Molar weight of carbon monoxide (CO)
$\dot{m}_{add\ fuel}$	[kg/h]	Additional fuel massflow
$\dot{m}_{flue,g}$	[kg/h]	Flue gas massflow
$\dot{m}_{fluid}$	[kg/h]	Fluidisation massflow gasifier (steam)
$\dot{m}_{fuel}$	[kg/h]	Biomass (fuel) massflow
M_{O2}	[kg/mol]	Molar weight of oxygen (O_2)
$\dot{m}_{PG}$	[kg/h]	Product gas massflow
$\dot{m}_{PGre}$	[kg/h]	Product gas recycle massflow
$w_{ash.fuel}$	[-]	Ash content of biomass
$w_{H.fluid}$	[-]	Elementary hydrogen content of gasifier fluidization
$w_{H.fuel}$	[-]	Elementary hydrogen content of biomass
$w_{H2O.fluid}$	[-]	Water content of gasifier fluidization
$w_{H2O.fuel}$	[-]	Water content of biomass
$w_{H2.PG}$	[-]	Hydrogen content of product gas
$w_{H2O.PG}$	[-]	Water content of product gas
$X_{H2O.rel}$	[kg/kg_{waf}]	Relative water conversion rate
$X_{H2O.abs}$	[kg/kg]	Absolute water conversion rate
η_{H2}	[-]	Hydrogen productivity rate
η_g	[-]	Cold gas efficiency
φ_{char}	[kg/kg_{waf}]	Char combusted in combustion chamber
φ_{SF}	[kg/kg_{waf}]	Steam to fuel ratio
λ	[-]	Air ratio
$\mu_{O2,air}$	[kg_{O2}/kg]	Oxygen content in combustion air
$\mu_{O2,adf}$	[kg_{O2}/kg]	Oxygen content in additional fuel
$\mu_{CO,fluegas}$	[kg_{CO}/kg]	Carbon monoxide content in flue gas stream
$\mu_{O2,fluegas}$	[kg_{O2}/kg]	Oxygen content in flue gas stream

Fig. 35: Structure of used simulation model for the dual fluid gasification system

Eq. 6.1:

$$\eta_g = \frac{\dot{m}_{PG} \cdot lhv_{PG} - \dot{m}_{PGre} \cdot lhv_{PG}}{\dot{m}_{fuel} \cdot lhv_{fuel} + \dot{m}_{add\ fuel} \cdot lhv_{add\ fuel}} \qquad [-]$$

Eq. 6.2:

$$\varphi_{SF} = \frac{\dot{m}_{fluid} \cdot w_{H2O.fluid} + w_{H2O.fuel} \cdot \dot{m}_{fuel}}{(1 - w_{H2O.fuel} - w_{ash.fuel}) \cdot \dot{m}_{fuel}} \qquad [\frac{kg_{H2O}}{kg_{fuel,waf}}]$$

---

1 cf. Stidl M., 2012, p166

Eq. 6.3: $$\varphi_{char} = \frac{\dot{m}_{char.bed}}{(1 - w_{H2O} - w_{ash}) \cdot \dot{m}_{fuel}} \qquad [\frac{kg_{char}}{kg_{fuel,waf}}]$$

Eq. 6.4: $$\lambda \cdot \dot{m}_{flue\,g} \cdot \left(\mu_{O2,flue\,g} - \frac{M_{O2}}{2 \cdot M_{CO}} \cdot \mu_{CO,flue\,g}\right) = (\lambda - 1) \cdot \left(\dot{m}_{air} \cdot \mu_{O2,air} + \dot{m}_{add\,fuel} \cdot \mu_{O2,adf}\right)$$

Eq. 6.5: $$X_{H2O.rel} = \frac{\dot{m}_{fluid} \cdot w_{H2O.fluid} + \dot{m}_{fuel} \cdot w_{H2O.fuel} - \dot{m}_{PG} \cdot w_{H2O.PG}}{(1 - w_{H2O.fuel} - w_{ash.fuel}) \cdot \dot{m}_{fuel}} \qquad [\frac{kg_{H2O}}{kg_{fuel,waf}}]$$

Eq. 6.6: $$X_{H2O.abs} = \frac{\dot{m}_{fluid} \cdot w_{H2O.fluid} + \dot{m}_{fuel} \cdot w_{H2O.fuel} - \dot{m}_{PG} \cdot w_{H2O.PG}}{\dot{m}_{fluid} \cdot w_{H2O.fluid} + \dot{m}_{fuel} \cdot w_{H2O.fuel}} \qquad [\frac{kg_{H2O}}{kg_{H2O}}]$$

Eq. 6.7: $$\eta_{H2} = \frac{\dot{m}_{PG} \cdot w_{H2.PG}}{\dot{m}_{fluid} \cdot w_{H.fluid} + \dot{m}_{fuel} \cdot w_{H.fuel}} \qquad [\frac{kg_{H2}}{kg_H}]$$

Notation			Equation	Citation Eq.
Cold gas efficiency	η_g	%	Eq. 6.1	-
Steam to fuel ratio	φ_{SF}	$kg_{H2O}/kg_{fuel,waf}$	Eq. 6.2	BG_Lib
Char combusted in combustion chamber	φ_{char}	$kg_{char}/kg_{fuel,waf}$	Eq. 6.3	BG_Lib
Air ratio	λ	-	Eq. 6.4	BG_Lib
Relative water conversion rate	$X_{H2O.rel}$	$kg_{H2O}/kg_{fuel,waf}$	Eq. 6.5	BG_Lib
Absolute water conversion rate	$X_{H2O.abs}$	kg_{H2O}/kg_{H2O}	Eq. 6.6	-
Hydrogen productivity rate	η_{H2}	kg_{H2}/kg_H	Eq. 6.7	-

Tab. 21: Key figures describing the dual fluid gasification system

6.2. Reference Case – Conventional Dual Fluid Gasification

Chapter 3.3 presented a rough description of the existing plants in Güssing and Oberwart in terms of operational data. Within the present chapter data from these plants are used for the illustration of a reference plant. A layout for this reference plant can be found in **Fig. 36**. It consists of a regular fuel supply section, gasification, gas cooling, gas cleaning and gas utilization. The gas utilization is focused on the production of electricity in gas engines. Beside electricity the plant offers a significant amount of process heat at high temperature level. The reference plant is containing process heat utilization as district heating only due to the fact that the usage of available process heat is strongly depending on the local circumstances and the local demand during the year.

Tab. 22 shows the used data for the reference plant. The illustrated reference values have been calculated based on an optimized operation point for Güssing published by Pröll T. 2004. This published operation point has been recalculated to a 10 MW reference plant and extended by a fuel dryer system. The fuel dryer is used to improve the overall plant performance through a reduction of the water content of the supplied feedstock. At the same time, the amount of available low temperature heat is reduced and the necessary blower leads to a slightly increased electricity consumption. The influence of the fuel dryer system on the reference plant has been recalculated with IPSEpro. **Tab. 23** shows used data for a fuel dryer system as it is currently operated in Oberwart.

Listed reference values are used as a starting point for all further investigations within the present work. These investigations are focused on the achievable hydrogen output. **Cold gas efficiency** and **air ratio** are used as important key figures for the energetic efficiency of the operated gasifier system. "**Char combusted in combustion chamber**" represents the net fuel flow from the gasifier to the combustor as share of the total biomass fed to the system.

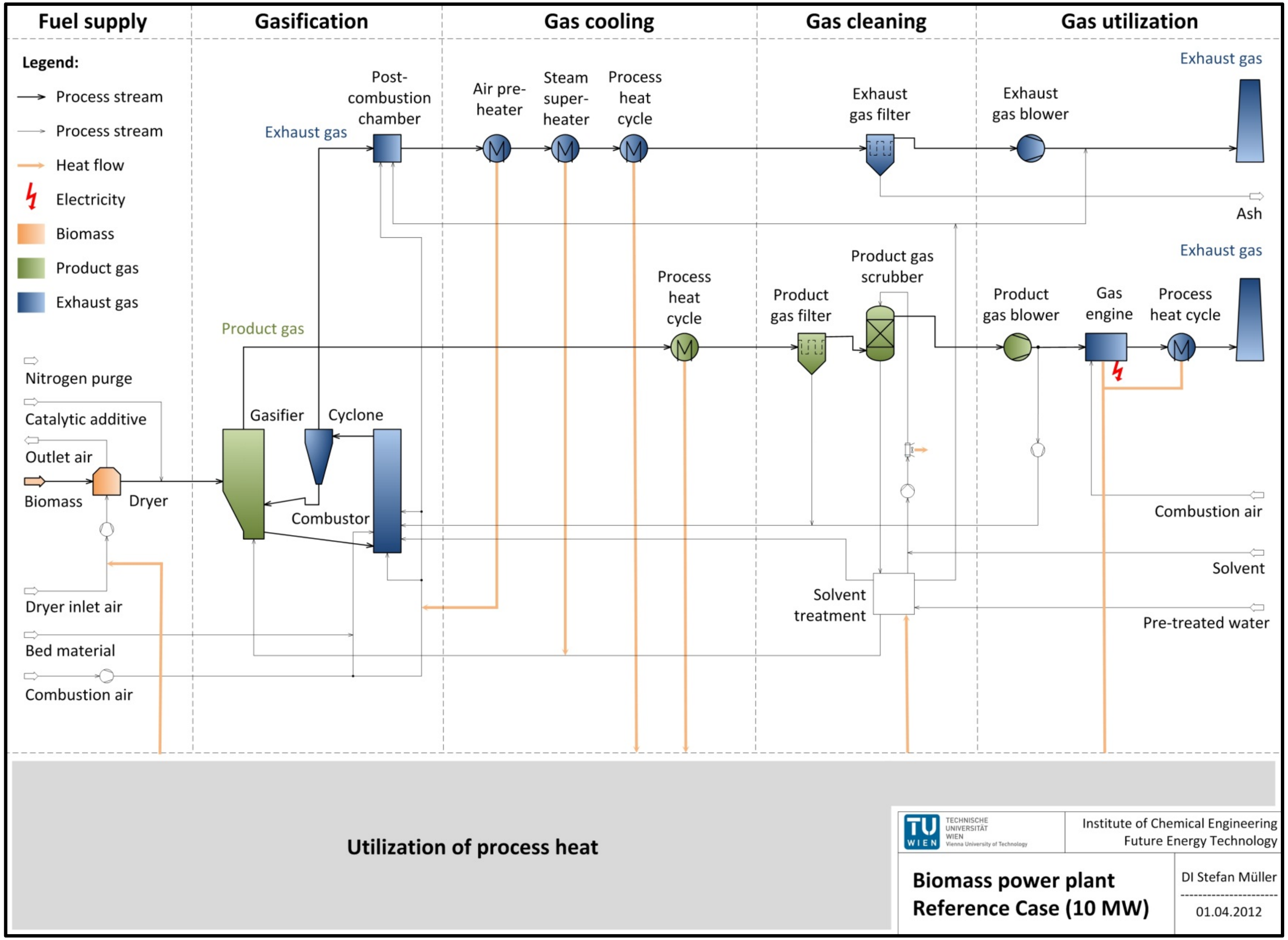

Fig. 36: Layout of the created reference case

Operation parameter	Unit	Güssing (Austria)	Oberwart (Austria)	Reference Plant
Plant input		Optimized point: $\mu_{H2O,BrSt} = 20\%$[1]	Operation point: 02.11.2010[2]	Reference val.
Thermal power gasifier (lhv)	MW	7.8	8.4	10.0
Biomass fuel (wood chips)	kg/h	2065	2783	3530
Biomass fuel water content	wt.-%	20.0	35.9	40.0
Water content after dryer	wt.-%	20.0	26.4	20.0
Electricity consumption	MW	0.2	0.42	0.35
Scrubber solvent (RME)	kg/h	17	6	20
Nitrogen purge[3]	Nm^3/h	75	75	100
Limestone/burnt limestone[3]	kg/h	10	5	5
Fresh bed material (olivine)[3]	kg/h	40	20	25
Water[7]	kg/h	500	150	180
Plant output				
Electricity	MW	2.0	2.4	2.5
District heating[7]	MW	4.2	0.9 (2.5)	4.3
Ash	kg/h	178.4	78.0	100
Key figures				
Cold gas efficiency	%	70.3	67.9	~ 70
Steam to fuel ratio	$kg_{H2O}/kg_{fuel,waf}$	0.55	0.62	0.55
Char combusted in combustion chamber	$kg_{char}/kg_{fuel,waf}$	0.11	0.16	0.10
Air ratio	-	1.05	1.21	1.05
Rel.water conversion rate	$kg_{H2O}/kg_{fuel,waf}$	0.09	0.02	~ 0.08
Abs. water conversion rate	kg_{H2O}/kg_{H2O}	0.16	0.03	~ 0.15
Hydrogen productivity rate	kg_{H2}/kg_{H}	0.30	0.28	~ 0.30

Tab. 22: Reference values for the setup of novel concepts

Operation parameter			Reference Values [4,5,6]
	Water content of biomass before dryer	wt.-%	40.0
	Water content of biomass after dryer	wt.-%	20.0
	Dryer inlet air temperature	°C	80.0
	Dryer outlet air temperature	°C	30.0
	Pressure loss of dryer system	mbar	35.0
	Humidity, saturation of dryer outlet air	%	90.0
Data for used heat exchanger	Heat loss	kW	0.0
	Necessary process heat consumption (Reference case)	kW	1 100
	Temperature of heat exchanger inlet	°C	115.0
	Temperature of heat exchanger outlet	°C	80.0
Data for used blower unit & drive system	Isentropic efficiency (blower)	%	50.0
	Mechanical efficiency (blower)	%	98.0
	Electrical efficiency (drive system)	%	90.0
	Mechanical efficiency (drive system)	%	100.0
	Additional electricity consumption (Reference case)	kW	100.0
	Dryer inlet air flow rate (Reference case)	Nm^3/h	35 150

Tab. 23: Reference data fuel dryer system

---

1 Pröll T., 2004, p154ff; 2 cf. Stidl M., 2012, p121
3 data of additives adjusted according to actual values
4 cf. Stidl M., 2012, p113ff; 5 cf. Jünger C., 2008, p72ff, p16ff, p103ff;
6 cf. Ringhofer T., 2011; 7 cf. Tab. 9

Steam is used for the fluidization of the gasifier to maintain the hydrodynamics. In addition, fed steam serves as gasification agent. The “**steam to fuel ratio**” describes the total water input in relation to the amount of dry fuel which is fed to the gasifier. In an ideal case, supplied water would be consumed to a large extent by gasification reactions and only a low amount of residual water remains within the product gas. **Absolute** and **relative water conversion rate** (cf. Eq. 6.5, Eq. 6.6) describe the share of water which is consumed by the gasification reactions. High conversion rates would be desired for an ideal hydrogen production. The **hydrogen productivity rate** is used for calculations reflecting the hydrogen production performance of the gasifier systems. Based on the reference values, it can be drawn the conclusion that, in the present case, hydrogen from biomass itself contributes most to the overall hydrogen production (η_{H2} = 0.30 kg_{H2}/kg_{H}). Whereas only a smaller share of hydrogen arises due to the conversion of water ($X_{H2O.abs}$ = 0.15 kg_{H2O}/kg_{H2O}). A explanation of this phenomenon is given in **Chapters 7.6**, **8.8** and **9**.

6.3. Economic Evaluation – Conventional Dual Fluid Gasification

Tab. 22 showed reference data for a 10 MW biomass gasification plant focused on the production of electricity. Illustrated data allow also an economic evaluation of the reference plant. Required cost rates for all further economic investigations within present work are listed in **Tab. 24.**

Parameter	Unit	Value	Data source
Investment cost (IC) incl. interest (NPV)	USD_{1990}/kW_{el}	4 500	Fig. 23
Investment cost (IC) incl. interest (NPV)	€	16 500 000	Fig. 23
Maintenance costs per year	% (IC) / a	2.0	cf. BMELV, 2006, p332
Insurance, administration & tax	% (IC) / a	2.5	cf. BMELV, 2006, p332
Number of employees	pers.	7	-
Cost of one employee per year	€/a	70 000	-
Operation hours per year	h/a	7 000	Tab. 9
Wood chip costs (per dry ton)	$€/t_{atro}$	100	Ehrig R., 2010, p48ff
Electricity costs	€/kWh	0.10	www.e-control.at (read May 25th 2012)
Scrubber solvent (RME)	€/t	960	according to information from OMV
Nitrogen (N_2)	$€/Nm^3$	0.10	according to information from Messer
Carbon dioxide (CO_2)	$€/Nm^3$	0.10	according to information from Messer
Oxygen (O_2)	$€/Nm^3$	0.07	according to information from Messer
Fresh bed material (olivine)	€/t	185	according to inf. from CHP Güssing
Limestone/ burnt limestone	€/t	30	according to inf. from CHP Güssing
Natural gas	€/MWh	28.8	www.e-control.at (read May 25th 2012)
Coal	€/MWh	10	cf. Tab. 1, cf. IEA 2010, p213
Fresh water	€/t	2	according to information from SCA
Costs for ash disposal	€/t	90	according to inf. from CHP Güssing
Earnings ash disposal (SER)	€/t	10	-
Emission allowances	$€/t_{CO2}$	20	www.eex.com (read May 25th 2012)
Subsidized electricity price	€/MWh	134.14	www.e-control.at (read May 25th 2012)
Earnings for district heating	€/MWh	25	according to inf. from CHP Güssing
Earnings for produced steam	€/t	25	according to information from OMV
Expected lifetime	a	20.0	cf. BMELV, 2006, p327
Interest rate	%	8.0	cf. BMELV, 2006, p326
Cumulative present value factor	-	10	-

Tab. 24: Cost rates for net present value calculations

The results of a net present value evaluation show the economic relations within the investigated business case (cf. **Tab. 25.**). Should a small community invest in a dual fluid gasification plant or buy electricity from a large energy provider? The results reveal that an investment of 16.5 million euro is only an option if earnings from electricity subsidies are high enough and there is a strong all-season demand for available process heat. Available process heat could be supplied at high temperature level as it is favored by most industrial facilities.

Business Case

Business Case: A small community in Austria has to decide about future electricity supply. The future supply of electricity supply could be provided: 0.) by a large national energy provider, 1.) by a new dual fluid gasification plant without utilization as district heating, or 2) by a new dual fluid gasification plant inclusive district heating **(reference case)**
Investment decision: Which option leads to an economic favorable supply of electricity?

Position	Symbol	Unit	Option 0	Option 1	Option 2
Boundary conditions					
Electricity supply		MWh/a	17 500	17 500	17 500
District heating supply		MWh/a	-	-	30 100
Investment cost incl. interest	$I_{Opt,X}$	€	0	16 500 000	16 500 000
Expenses					
Fuel cost (wood chips)	A_1	€/a	-	**1 482 665**	**1 482 665**
Electricity costs	A_2	€/a	**1 750 000**	245 000	245 000
Maintenance, insurance, admin., tax	A_3	€/a	-	742 500	742 500
Operating supplies	A_4	€/a	-	303 345	303 345
Labor costs	A_5	€/a	-	**490 000**	**490 000**
Earnings					
Earnings from electricity			-	2 347 450	2 347 450
Electricity consumption			-	- 1 750 000	- 1 750 000
Net earnings from subsidies	E_1	€/a		597 450	597 450
Earnings from district heating	E_2	€/a	-	-	752 500
Sum (Expenses – Earnings)	$C_{Opt,X}$	€/a	**1 750 000**	**2 666 060**	**1 913 560**
Net present value calculation					
Cumulative present value factor	BWSF	-	10	10	10
Additional investment costs	ΔI_X	€	-	16 500 000	16 500 000
Operating expenses savings	ΔC_X	€/a	-	-916 060	-163 560
Net present value	ΔNPV_X	€	0	-25 660 605	-18 135 605

Tab. 25: Comparison of different energy supply options by net present value calculation

Parameter Analysis

Parameter Analysis: The results illustrated in Tab. 25 show that following parameters are most important for the investment decision: 1.) subsidized electricity prices and 2.) wood chip price. A parameter variation of both parameters shows the necessary values with respect to the reference values to enable a positive investment decision for option X based on a positive "net present value".

Position	Reference Value	Unit	Option 0	Option 1	Option 2
Subsidized elec. price for pos. NPV	0.134	€/kWh	-	> 0.24 &	> 0.20 &
Wood chip price for positive NPV	100	€/t_{atro}	-	< 50	< 55

Tab. 26: Parameter analysis of the business case "electricity production"

The results of the economic evaluation are strongly dependent on the future development of wood chip and electricity price. Negative net present values of Option 1 and 2 imply that Option 0 should be favored from an economic point of view. The result of the parameter analysis shows that a **wood chip price below 55 €/t_{atro}** in combination with a

subsidized electricity price above 0.20 €/kWh is necessary to enable an investment decision favoring Option 2. The illustrated economic aspects have to be considered before the construction of a new plant. Even if the economic results show that electricity from biomass seems an expensive solution, an installation of a dual fluid gasification plant at the same time would create jobs within the community. Moreover, expenses for fuel would stay within the community if used wood chips are provided by local suppliers. Expenses for electricity from a national energy provider would not contribute to the development of wealth in the community. Therefore, the installation of a plant could be used to generate a positive impulse for the strategic development of a region. The illustrated reference case combined with an economic assessment showed important relations and preconditions for the installation of a new dual fluid gasification plant. The success of a biomass gasification plant for electricity production is highly dependent on the future development of prices for electricity, prices for wood chips and funding rates.

6.4. Reference Case – Sorption Enhanced Reforming

Chapter 6 so far illustrated important basic data for the simulation of traditional dual fluid gasification. A similar approach is now used for sorption enhanced reforming. The following pages reflect important key figures and basic data for the simulation of sorption enhanced reforming. Important aspects of sorption enhanced reforming have already been shown within **Chapter 4.** Calcium based bed materials enable the selective transport of CO_2 from the gasifier to the combustion chamber and influence the behavior of the gasifier system including the achieved product gas composition. This leads to some main differences in comparison with conventional dual fluid gasification using olivine as bed material. Therefore, the objective of the following paragraphs is to give

- a description of reference data for sorption enhanced reforming,
- a description of key process figures,
- and the results of variations illustrating the impact of these key figures.

Tab. 27 highlights important values for a gasifier system operating sorption enhanced reforming. Low gasification temperatures of around 650°C favor selective transport of CO_2 from the gasifier to the combustor due to the equilibrium of the carbonation reaction. The selective transport of CO_2 as well as the catalytic effect of calcium oxide leads to high H_2 content in the product gas stream. **Tab. 27** depicts common value ranges for product gas compositions based on experimental results.

Operation parameter	Symbol / Unit		Reference values	Data Source
Thermal power gasifier (lhv)	P_{th}	MW	10	-
Gasification temperature	T_G	°C	~ 650	cf. chapter 4
Combustion temperature	T_R	°C	~ 925	cf. chapter 4
Bed material in gasifier system	$m_{inventory}$	kg	3 000	according to Güssing
Bed material within gasifier	$m_{gasifier}$	kg	1 500	according to Güssing
Product gas composition				
Water (H_2O)	vol.-%		30 – 65	cf. Tab. 13, Steam to fuel
Hydrogen (H_2)	vol.-%$_{db}$		55 – 75	cf. Tab. 13, Eq. 6.14
Carbon monoxide (CO)	vol.-%$_{db}$		8 – 14	cf. Tab. 13, Eq. 6.14
Carbon dioxide (CO_2)	vol.-%$_{db}$		8 – 16	cf. Tab. 13, Eq. 6.14
Methane (CH_4)	vol.-%$_{db}$		8 – 12	cf. Tab. 13
Non condensable C_xH_y	vol.-%$_{db}$		2 – 3	cf. Tab. 13
Dust particles	g/Nm³		20 - 50	cf. Tab. 13
Tar	g/Nm³		0.3 – 0.9	cf. Tab. 13
Key figures				
Steam to fuel ratio	φ_{SF}	$kg_{H2O}/kg_{fuel,waf}$	~ 0.55	cf. Tab. 22
Air ratio	λ	-	~ 1.05	cf. Tab. 22
Rel. water conversion rate	$X_{H2O.rel}$	$kg_{H2O}/kg_{fuel,waf}$	0 05 - 0.3	Estimation
Abs. water conversion rate	$X_{H2O.abs}$	kg_{H2O}/kg_{H2O}	0.1 – 0.5	Estimation
Hydrogen productivity rate	η_{H2}	kg_{H2}/kg_H	0.25 – 0.5	Estimation
Bed material renewal rate	κ_{CaO}	h^{-1}	0.0 – 1.0	-
CO_2 load	X_{CaO}	$[mol_{CO2}/mol_{CaO}]$	0.0 – 0.55	-

Tab. 27: Reference values for sorption enhanced reforming

Experimental investigations summarized in **Tab. 13** already showed different results for different bed materials and experimental settings. Therefore, the product gas composition and key figures like cold gas efficiency, water conversion rate and hydrogen productivity rate are very sensitive to the practical performance of the operated bed material. Bed material performance variations imply a critical trade-off between CO_2 transport potential and global heat integration potential depending on the solids circulation rate operated. The bed material performance can be determined by key process figures like CO_2 load after a specific cycle number or necessary bed material renewal rate.

6.5. Key figures for Sorption Enhanced Reforming Operation

Operated calcium particles lose their capability to load CO_2 after N calcination and carbonation cycles, which is known as decay of CO_2 loading. High CO_2 load can only be maintained if the bed material is renewed after an adequate operation time. Because of that,

- **bed material renewal rate**,
- decay of **CO_2 loading**
- and **solids (calcium oxide) circulation rate**

are important key process figures. **Fig. 37** shows main mass and energy streams of the used simulation model for the calculation of these important process figures. The equations from **Eq. 6.8** to **Eq. 6.13** display a mathematical definition for mentioned figures describing main phenomena of sorption enhanced reforming.

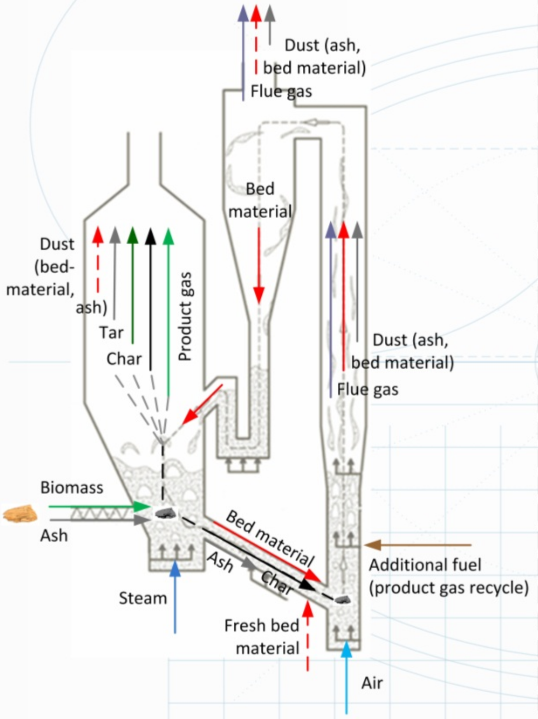

Symbols

$K_p(T)$	[-]	Equilibrium constant
$\dot{m}_{bed,fresh}$	[kg/h]	Fresh bed material ($CaCO_3$) entering circulation loop
$\dot{m}_{bed,G,in}$	[kg/h]	Massflow of bed material entering the gasifier from combustor
M_{CaCO3}	[g/mol]	Molar weight of $CaCO_3$
M_{CaO}	[g/mol]	Molar weight of CaO
M_{CO2}	[g/mol]	Molar weight of CO_2
$\dot{m}_{CO2,capt}$	[kg/h]	Massflow of CO_2 absorbed by bed material in gasifier
$m_{gasifier}$	[kg]	Amount of bed material within gasifier
$m_{inventory}$	[kg]	Total bed material within system
N	[-]	Mean cycles of particle within system
p_{CO}	[Pa]	Partial pressure of CO in product gas
p_{CO2}	[Pa]	Partial pressure of CO_2 in product gas
p_{H2}	[Pa]	Partial pressure of H_2 in product gas
p_{H2O}	[Pa]	Partial pressure of H_2O in product gas
X_{CaO}	$[mol_{CO2}/mol_{CaO}]$	CO_2 load
δ_{CaO}	$[s^{-1}]$	Calcium circulation rate
$\delta_{Eq.,WGS-shift}$	[-]	Logarithmic distance to equilibrium (water-gas-shift reaction, gasifier)
κ_{CaO}	$[s^{-1}]$	Bed material renewal rate
σ_{CO}	[mol/mol]	CO / CO_2 in combustor exhaust gas
τ_{CaO}	[s]	Mean time of particle within system
φ_{CaO}	$[kg_{CO2}/kg_{CaO}]$	CO_2 load
$\omega_{CaCo3,bed,fresh}$	$[kg_{CaCO3}/kg_{bed,fresh}]$,	$CaCO_3$ in fresh material
$\omega_{CaCo3,bed,G,in}$	$[kg_{CaCO3}/kg_{bed}]$,	$CaCO_3$ in bed material to gasifier from combustor
$\omega_{CaCo3,inventory}$	$[kg_{CaCO3}/kg_{bed}]$,	$CaCO_3$ in bed mat. inventory
$\omega_{CaO,bed,fresh}$	$[kg_{CaO}/kg_{bed,fresh}]$,	CaO in fresh bed material
$\omega_{CaO,bed,G,in}$	$[kg_{CaO}/kg_{bed}]$,	CaO in bed material to gasifier from combustor
$\omega_{CaO,inventory}$	$[kg_{CaO}/kg_{bed}]$,	CaO in bed mat. inventory

Fig. 37: Structure of used simulation model for the calculation of key process figures

The **calcium circulation rate** is introduced with respect to the performance of solid CaO particles. Therefore, following equation is used:

Eq. 6.8:
$$\delta_{CaO} = \frac{\dot{m}_{bed,G,in} \cdot \left(\frac{\omega_{CaO,bed,G,in}}{M_{CaO}} + \frac{\omega_{CaCO_3,bed,G,in}}{M_{CaCO3}}\right)}{m_{inventory} \cdot \left(\frac{\omega_{CaO,inventory}}{M_{CaO}} + \frac{\omega_{CaCO_3,inventory}}{M_{CaCO3}}\right)} \qquad [\,s^{-1}\,]$$

The calcium circulation rate describes the transition of a potential active mol of CaO on its way between carbonation and calcination within the overall gasifier system. The **bed material renewal rate** is another important key figure for the overall process performance. Following equation is used to calculate the bed material renewal rate:

Eq. 6.9:
$$\kappa_{CaO} = \frac{\dot{m}_{bed,fresh} \cdot \left(\frac{\omega_{CaO,bed,fresh}}{M_{CaO}} + \frac{\omega_{CaCO_3,bed,fresh}}{M_{CaCO3}}\right)}{m_{inventory} \cdot \left(\frac{\omega_{CaO,inventory}}{M_{CaO}} + \frac{\omega_{CaCO_3,inventory}}{M_{CaCO3}}\right)} \qquad [\,s^{-1}\,]$$

Additional fresh bed material is necessary to maintain the CO_2 load of CaO particles because of the decay of loading after N cycles as shown in **Fig. 28.** For this reason, fresh $CaCO_3$ is fed to the bed material circulation loop just before the combustion and calcination step. A high bed material renewal rate raises the CO_2 load of the bulk bed material in circulation, increases the selective transport of CO_2 from the gasifier but at the same time reduces the cold gas efficiency. The **CO_2 load** of the bed material is a further central key figure for the process. These equations are used for the calculation of the CO_2 load based on a mass and molar perspective:

Eq. 6.10:
$$\varphi_{CaO} = \frac{\dot{m}_{CO2,capt}}{\dot{m}_{bed,G,in} \cdot \left(\omega_{CaO,bed,G,in} + \omega_{CaCO_3,bed,G,in} \cdot \frac{M_{CaO}}{M_{CaCO3}}\right)} \qquad \left[\frac{kg_{CO2}}{kg_{CaO}}\right]$$

Eq. 6.11:
$$X_{CaO} = \frac{\frac{\dot{m}_{CO2,capt}}{M_{CO2}}}{\dot{m}_{bed,G,in} \cdot \left(\frac{\omega_{CaO,bed,G,in}}{M_{CaO}} + \frac{\omega_{CaCO_3,bed,G,in}}{M_{CaCO3}}\right)} \qquad \left[\frac{mol_{CO2}}{mol_{CaO}}\right]$$

High CO_2 load improves the selective transport of CO_2 from the gasifier to the combustion chamber and increases the product gas quality by reducing the CO_2 content of the product gas. The bed material operation time has to be kept at an adequate level to maintain the desired reactivity. **Eq. 6.12** and **Eq. 6.13** describe this operation time by the calculation of "mean time of particle within gasifier system" and "mean cycles of particle within gasifier system". All the described equations have been implemented in IPSEpro and enable a discussion of relevant parameters within the process simulation environment based on existing experimental data.

Eq. 6.12:
$$\tau_{CaO} = \frac{1}{\kappa_{CaO}} \qquad [\,s\,]$$

Eq. 6.13:
$$N = \tau_{CaO} \cdot \delta_{CaO} \qquad [\,-\,]$$

Notation			Equation
Calcium circulation rate	δ_{CaO}	s^{-1}	Eq. 6.8
Bed material renewal rate	κ_{CaO}	s^{-1}	Eq. 6.9
CO_2 load	φ_{CaO}	$[kg_{CO2}/kg_{CaO}]$	Eq. 6.10
CO_2 load	X_{CaO}	$[mol_{CO2}/mol_{CaO}]$	Eq. 6.11
Mean time of particle within gasifier system	τ_{CaO}	s	Eq. 6.12
Mean cycles of particle within gasifier system	N	-	Eq. 6.13

Tab. 28: Key process figures for sorption enhanced reforming

Beside these important figures, **Eq. 6.14** illustrates a function for the calculation of the equilibrium of the water-gas shift reaction. The water-gas shift reaction is a dominant reaction with strong influence on the product gas composition with respect to the water (H_2O), carbon dioxide (CO_2), carbon monoxide (CO) and hydrogen content (H_2) of the product gas stream. The deviation ($\delta_{Eq.WGS-shift} = 0$) from the equilibrium of this reaction determines an upper boundary for the achievable hydrogen content due to present thermodynamics.

Eq. 6.14:
$$10^{\delta_{Eq.WGS-shift}} \cdot K_p(\mathrm{T}) = \frac{p_{co2} \cdot p_{H2}}{p_{co} \cdot p_{H2O}} \qquad \delta_{Eq.WGS-shift} = 0$$

6.6. Variation of Key Figures of Sorption Enhanced Reforming

Variations of the described key process figures within IPSEpro are used to point out the thermodynamic behavior of dual fluid gasification by sorption enhanced reforming. **Fig. 38** shows the used flow chart of a simple simulation model for the investigation of three variation approaches described in **Tab. 29.**

Described variations have been carried out based on reference values shown in **chapter 6.4** with respect to achievable **cold gas efficiency**, **product gas composition**, **bed material consumption** and key parameters for the **design of experimental facilities**. During the variations thermodynamic equilibrium of the water-gas shift reaction was assumed for product gas composition at the exit of the gasifier (cf. **Eq. 6.14**).

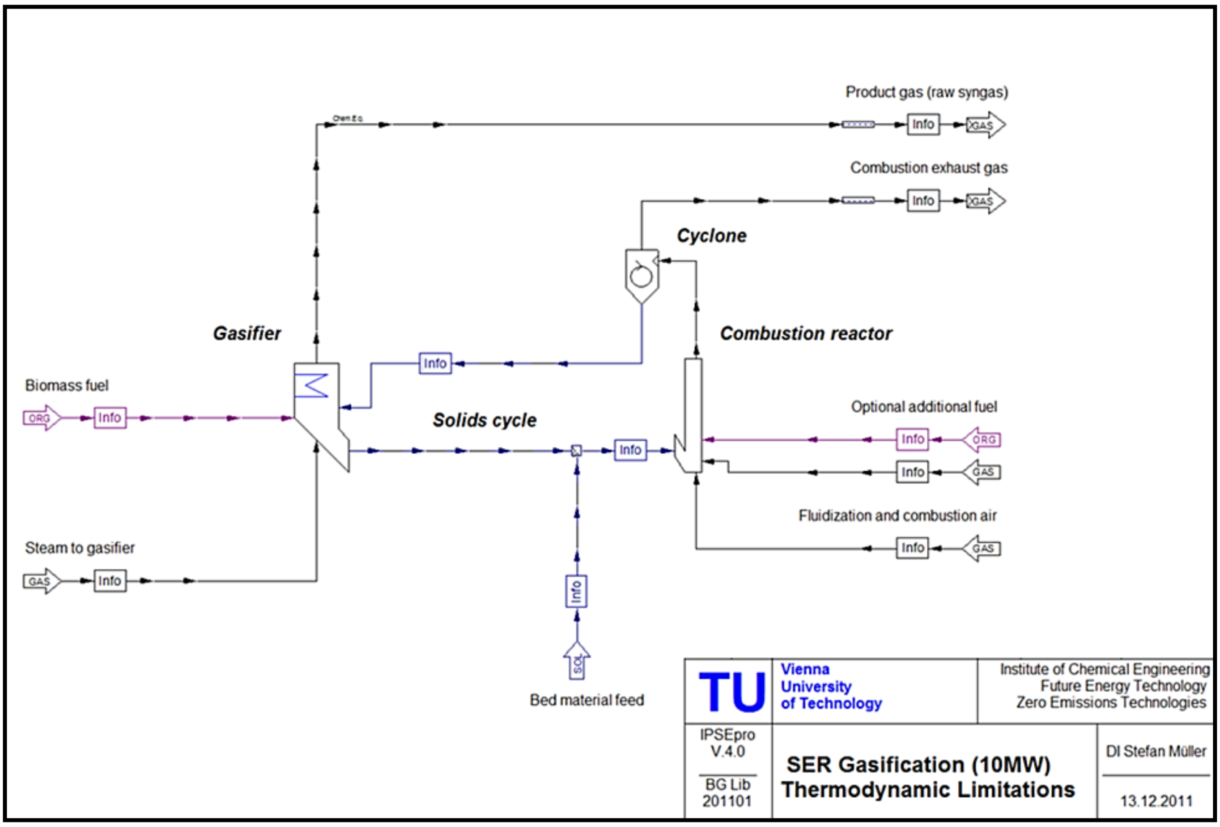

Fig. 38: Simulation model for the variation of key figures of sorption enhanced reforming

Nr.	Variation parameters			Value range	Results	Additional constants
1	CO_2 load	X_{CaO}	$[mol_{CO2}/mol_{CaO}]$	0.0 – 0.55	Fig. 39 (right), Fig. 41 (right), Fig. 43	$\kappa_{CaO} = 0.065$ equals $\dot{m}_{bed,fresh} \sim 200$ kg/h
2	CO_2 load bed material renewal	X_{CaO} κ_{CaO}	$[mol_{CO2}/mol_{CaO}]$ $[h^{-1}]$	0.1 – 0.8 0.0 – 1.0	Fig. 39 (left)	
3	CO_2 load mean cycle number	X_{CaO} N	$[mol_{CO2}/mol_{CaO}]$ [-]	0.0 – 0.85 5 - 100	Fig. 41 (left)	

Tab. 29: Variation of key process figures for sorption enhanced reforming

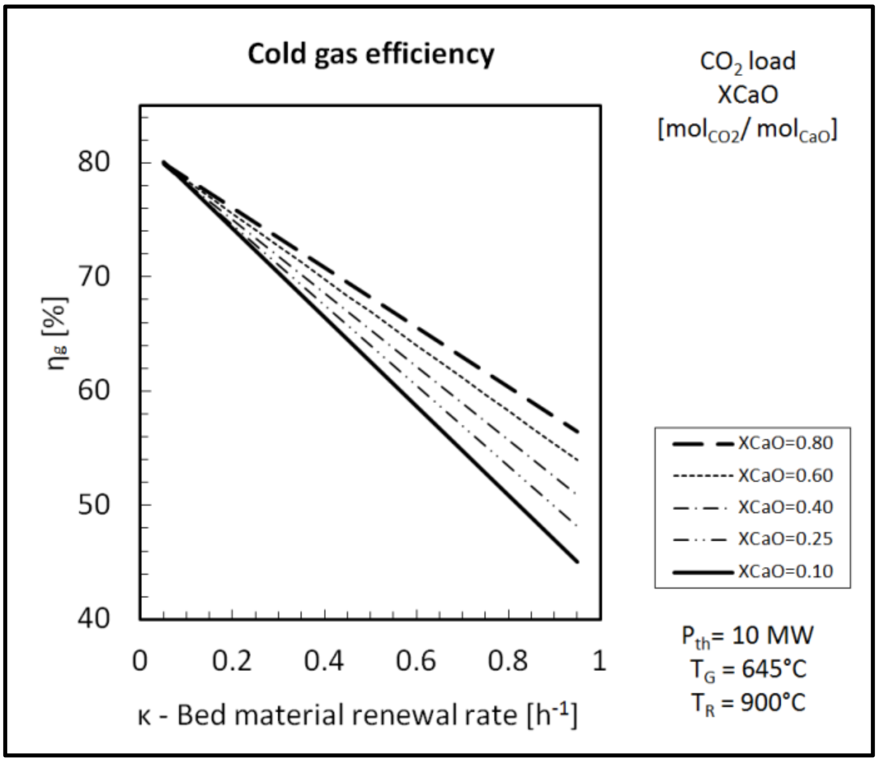

Fig. 39: Cold gas efficiency (η_g) depending on bed material renewal rate

Achievable **cold gas efficiency** is strongly determined by temperatures, fuel composition, fuel water content and heat losses. Cold gas efficiency is also depending on the bed material renewal rate as shown in **Fig. 39**. Large amounts of fresh $CaCO_3$ entering the system raise the heat demand in the combustion chamber for calcination and maintaining the necessary temperatures. Furthermore, low CO_2 load of the circulating bed material raises the necessary amount of circulating bed material to maintain the process. According to the described relationships bed material renewal rates should be kept on a low level in terms of cold gas efficiency.

The **product gas composition** is strongly depending on the selective transport of CO_2 from the gasifier to the combustion chamber. Therefore, the CO_2 load of the circulating bed material has major influence on the product gas composition. This dependency is shown in **Fig. 40**. The equilibrium of the water-gas-shift reaction has been an important precondition for the calculation of the composition of the product gas at the exit of the gasifier. Solid particles with high CO_2 load would raise the H_2 content in the product gas. At the same time high bed material renewal rates would be necessary to keep the load at high levels with respect to the decay of load (cf. **Fig. 28**). Favorable product gas compositions and high cold gas efficiency can therefore be identified as an important trade-off of gasification with sorption enhanced reforming.

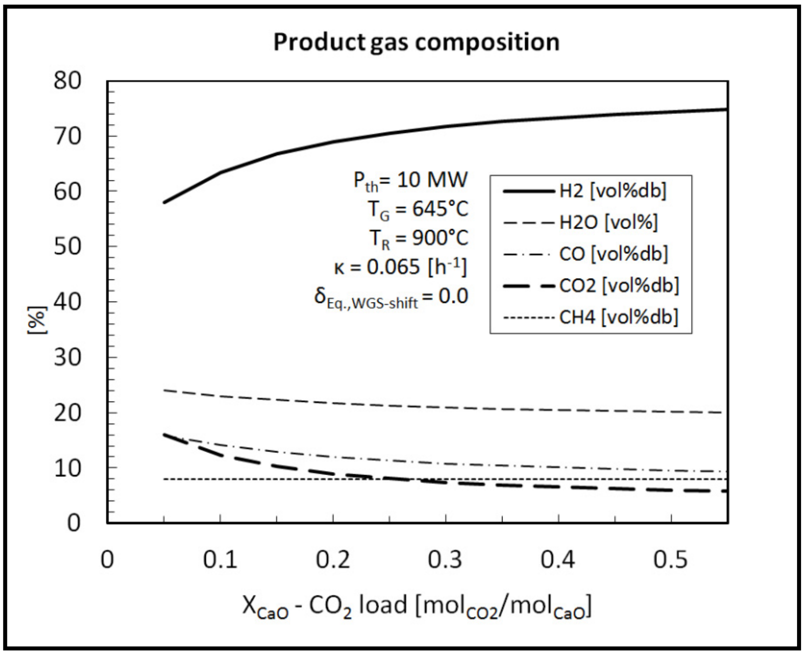

Fig. 40: Product gas composition depending on CO_2 load of circulating bed material

An improvement of product gas composition by the operation of higher bed material renewal rates leads to a reduction of cold gas efficiency. In specific cases this reduction of the cold gas efficiency can be prevented by arranging the process along industrial processes involving a certain lime and/or limestone throughput. CO_2 load of circulating solid particles is a limiting parameter for the overall process. The practical performance of different limestone has a strong influence on **bed material consumption**. Low load capacity after low cycle numbers (N) leads to a high demand for bed material renewal. The practical performance of solid particles directly influences bed material consumption and cold gas efficiency. **Fig. 41** shows necessary bed material renewal rates for different transport capacities of limestone particles after different mean cycle numbers completed.

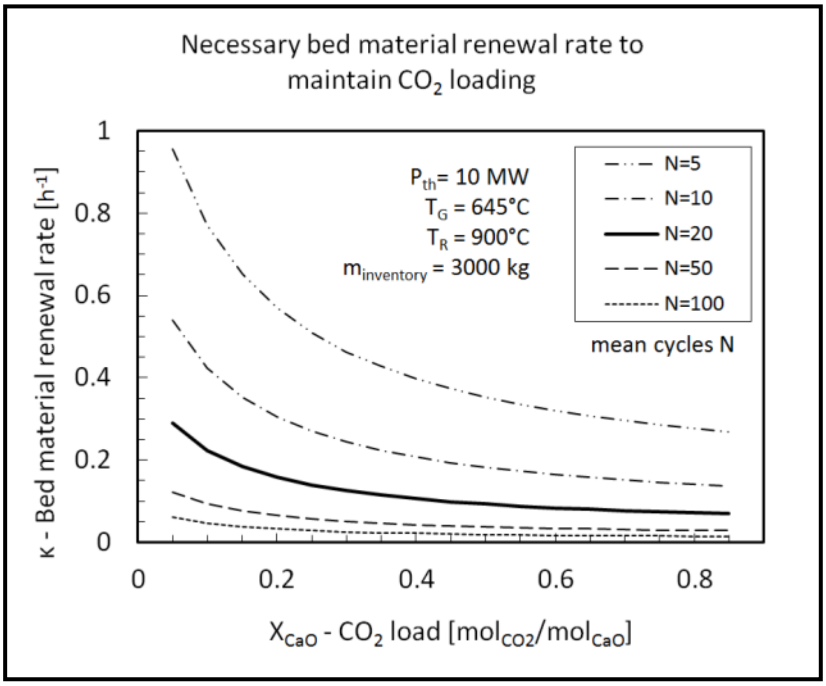

Fig. 41: Necessary bed material renewal for constant CO_2 load

A real system includes bed material inventory which consists of different fractions of solid particles which experienced a different number of cycles. Within the simulation model used for the variations the occurring cycle number distribution of the operating bed material is represented by the parameter N (mean cycle number). Furthermore, it has been assumed that solid particles are ejected at random and old solid particles are not discharged selectively from the operating bed material. This simplified approach has to be acknowledged during the evaluation of the results. As it can be seen, low CO_2 load of a certain limestone after low cycle numbers, leads to a high demand for bed material renewal. High bed material renewal rates at the same time reduce the cold gas efficiency.

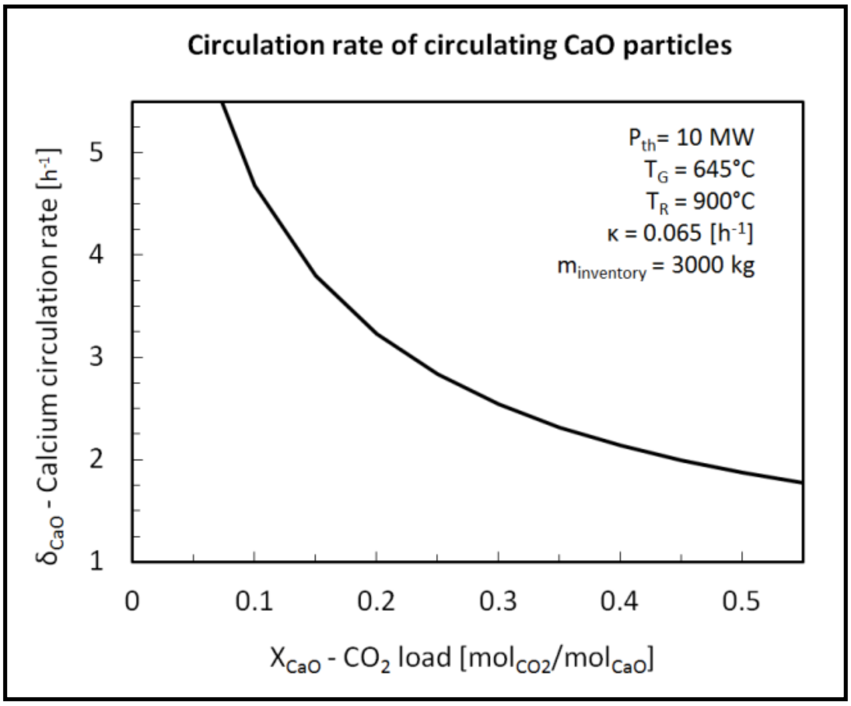

Fig. 42: Circulation rate of CaO particles

This relationship underlines once more the long time performance of circulating solid particles as a key factor for the overall process. Limestones with a low decay of CO_2 load after long time operation are needed for high cold gas efficiency and a desired product gas composition. Otherwise high bed material consumption could be a significant disadvantage for the realization of sorption enhanced reforming.

Fig. 42 shows the **calcium circulation rate** for solid CaO particles with different load capability. High CO_2 load enables a lower cycling rate because necessary heat for the gasification is transported in form of latent heat together with bound reaction energy of the carbonation reaction. Simulation results presented in **Fig. 42** show necessary circulation rates which were calculated for a fixed bed material renewal rate of κ_{CaO} = 0.065 per hour. This value equals ~ 200 kg of fresh bed material per hour according to the determined bed material inventory. A low bed material renewal rate is desired to keep cold gas efficiency high and bed material consumption low. Attrition and decay of CO_2 load can be limiting parameters which demand for higher bed material renewal rates. This tradeoff therefore has a strong influence on the necessary circulation rate depending on particle performance. The attrition of solid particles is at the same time strongly dependent on the used solids separation systems, the mechanical stability of used bed material and velocities maintained within the dual fluidized bed system.

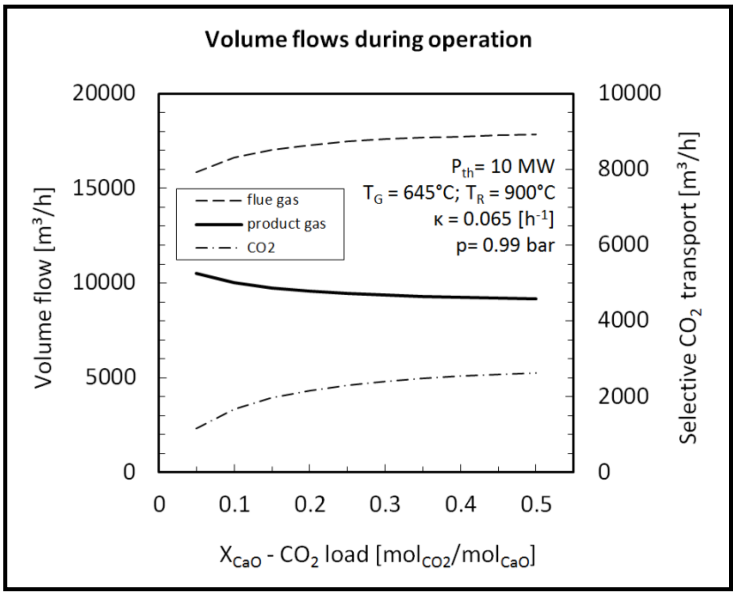

Fig. 43: Volume flows during operation

As it can be seen, selective transport of CO_2 has only a small impact on the operational volume flows. Nevertheless, changes of volume flows need to be considered regarding the influence on the fluid dynamics within the system. **Fig. 43** shows the necessary bed material circulation for the gasification by sorption enhanced reforming for different CO_2 transport capacities of the operating bed material. As can be seen from **Fig. 44**, the bed material circulation is strongly influenced by CO_2 transport. This relationship should be considered before the design of experimental facilities.

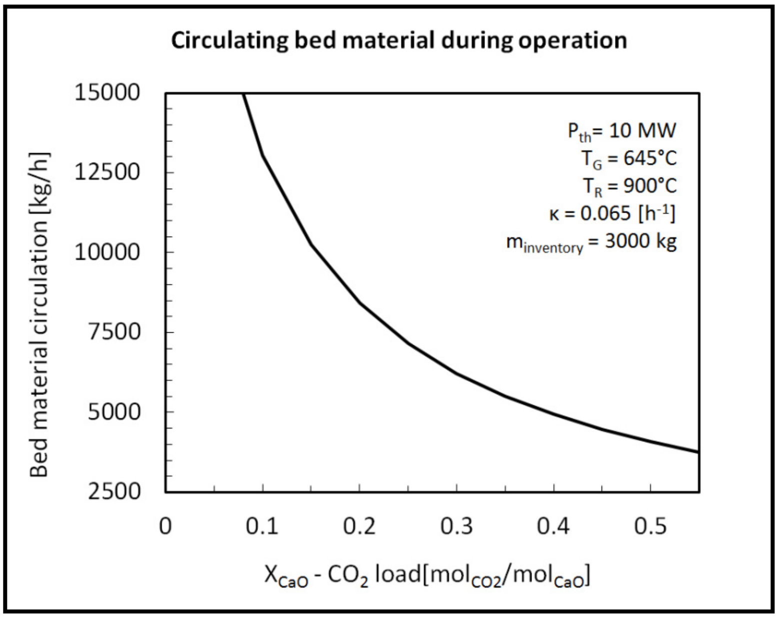

Fig. 44: Amount of circulating bed material during operation

The decay of CO_2 transport with an increased number of carbonation and calcination cycles has been previously identified as a key factor for the performance of gasification by sorption enhanced reforming. The optimum bed material circulation rate is determined by the energy balance of the system requiring the temperature levels for carbonation and calcination. As a consequence, the loading of the sorbent directly determines the achievable product gas composition.

Overall, carried out variations show import aspects of sorption enhanced reforming. High bed material renewal rate lead to reduced cold gas efficiency. A certain bed material renewal rate will always be required in order to compensate for attrition. Low mechanical stability of the used bed material therefore can be a further constraint for the process which would lead to reduced cold gas efficiency. Mechanical stability of different limestone itself has been beyond the focus of carried out variations. But, the effect of necessary bed material renewal on cold gas efficiency due to attrition can be estimated with the results shown in **Fig. 39**

Reduced cold gas efficiency can be compensated by other advantages in specific cases. If high H_2 contents are the primary aim, the process could be arranged along with industrial processes involving a certain limestone throughput. Illustrated results enable basic design considerations for novel plants based on sorption enhanced reforming. The results of the illustrated variations showed the impact of key process figures on the operation of sorption enhanced reforming. The meaning of these results needs to be accounted before a practical long time demonstration of sorption enhanced reforming is designed. Therefore, **Tab. 30** shows reference values for key process figures which are used for further investigations within the present work.

Notation			SER Reference Case
Calcium circulation rate	δ_{CaO}	h^{-1}	~ 3.2
Bed material renewal rate	κ_{CaO}	h^{-1}	~ 0.065
CO_2 load	φ_{CaO}	kg_{CO2}/kg_{CaO}	~ 0.16
CO_2 load	X_{CaO}	mol_{CO2}/mol_{CaO}	~ 0.20
Mean time of particle within gasifier system	τ_{CaO}	h	~ 15
Mean cycles of particle within gasifier system	N	-	~ 50

Tab. 30: Reference values for key process figures of sorption enhanced reforming

6.7. Summary

Within **Chapter 6** reference data for the calculation of novel concepts was presented.

- Novel concepts based on conventional dual fluid gasification can be calculated by the aid of existing data from commercial plants in Güssing and Oberwart. The created reference case (10 MW_{th}) is based on published data by Pröll T., Stidl M., Kotik J. and data provided by Kirnbauer F. reflecting the current status of both plants in October 2012.

- The following key figures have been introduced to compare important performance aspects for the operation and the simulation of a dual fluid gasifier system:

    - "cold gas efficiency",
    - "steam to fuel ratio",
    - "char combusted in combustion chamber",
    - "air ratio",
    - "water conversion rate",
    - "hydrogen productivity rate".

- An economic evaluation of the reference plant illustrated main parameters which need to be considered during an investment decision. The illustrated reference plant (10 MW_{th}) for electricity production demands a **wood chip price below 55 €/t_{atro}** in combination with a **subsidized electricity price above 0.20 €/kWh** to achieve a favorable economic result.

- Novel concepts based on sorption enhanced reforming can be calculated based on experimental results (cf. **Tab. 13**) together with theoretic considerations reflecting the existing knowledge in the field of conventional dual fluid gasification.

- Variations using a sorption enhanced reforming simulation model within **Chapter 6** enabled the calculation of reference values for following important key figures:

    - "bed material renewal rate",
    - "CO_2 load",
    - "mean cycles of particle within gasifier system".

- Carried out variations showed theoretically, with respect to the set preconditions, that a hydrogen content up to ~75 vol.-$\%_{db}$ can be reached in the product gas stream at the exit of the gasifier (cf. **Fig. 40**). The variations showed furthermore the importance of the used bed material. The used bed material needs to be capable to maintain high CO_2 loads over a long operation time to enable high hydrogen content in combination with high cold gas efficiency.

Presented data illustrates the actual state of knowledge and is used in **Chapter 7 & 8** for the calculation of novel concepts based on conventional dual fluid gasification as well as sorption enhanced reforming.

7. Hydrogen from Biomass for a Refinery by Conventional Dual Fluid Gasification

Mobility and transportation make up the largest share of energy consumption within the European Union (cf. **Fig. 2**). Required **crude oil**, for European refineries, is mainly **imported** from Russia, Norway, Libya, Iran and Saudi Arabia. Operated production processes in a refinery itself already cause significant fossil CO_2 emissions. European emission reduction targets put pressure on refinery operators to reduce the CO_2 emissions of the **refining process**. Therefore, refinery operators are forced to find new approaches to increase the process efficiency and to reduce the fossil "CO_2 – footprint" of produced fuels for aircrafts, trucks and cars. An increased share of renewable energy for the refining process would improve the fossil "CO_2-footprint" of produced fuels. Simultaneously, a rising share of fuels from rapeseed, wheat or sugar beets can change the characteristics of produced fuels and lead to reduced efficiency within the refining process.

Hydrogen is an important commodity for the refining process and large amounts of hydrogen are required for the production of fuels like gasoline, diesel fuel or kerosene. Today, hydrogen is mainly produced from natural gas which leads to significant fossil CO_2 emissions. These fossil CO_2 emissions could be reduced if renewable energy resources would be used as feedstock for the production of hydrogen. Pure hydrogen from renewable feedstock at the same time would not affect the characteristics of produced fuels. But possible hydrogen production processes from renewable feedstock are still uncertain and need to be investigated to find applicable process routes in the surrounding of a refinery. Within **Chapter 7** a novel process route for the production of hydrogen via dual fluid gasification is investigated. Carried out investigations include:

- a description of the initial situation, research tasks and aims,
- discussion of the process designs for the production of hydrogen,
- detailed description of the chosen process route,
- simulation of an overall hydrogen production plant,
- variations investigating key process figures influencing the hydrogen output,
- the expected results of the created hydrogen production plant,
- and an evaluation of the achieved results.

7.1. Initial Situation, Research Tasks & Aims

Refinery operators have identified hydrogen from renewable energy sources as a promising pathway to reduce the fossil CO_2 emissions within the refining process. An applicable hydrogen production process needs to enable the implementation of a large-scale pilot plant into a refinery as a first plant of its kind. Dual fluid gasification already demonstrated good characteristics as an energy conversion technology for the production of hydrogen in present applications. The product gas compositions achieved, already contain a significant share of hydrogen of about ~ 40 vol.-%$_{db}$ (cf. **Tab. 8**). A novel production process based on dual fluid gasification would have to enable the production of pure hydrogen (H_2 > 99.9 vol.-%) according to the demands of a modern refinery. To deliver this high purity, the achieved product gas needs to be cleaned and treated by several process steps. These process steps at the same time need to satisfy the requirements of an efficient production.

7.2. Process Design for a Hydrogen Production Process

The investigated **hydrogen production process** is based on conventional dual fluid gasification. Therefore, the overall production process can be devided into

- fuel supply,
- gasification,
- gas cooling,
- gas treatment
- and gas utilization.

Wood chips were chosen as feedstock for the production process. Wood chips are available in large quantities within the European Union and currently available at low prices compared to other renewable feed stocks. The gasification step is based on **conventional dual fluid gasification** using olivine as bed material. As a result of the gasification the product gas contains ~ 40 vol.-%$_{db}$ of hydrogen (cf. **Tab. 13**). Gasification by sorption enhanced reforming yields even higher hydrogen contents. But so far no large-scale plant is applying the sorption enhanced reforming process and therefore conventional dual fluid gasification has been chosen for the hydrogen production process for refineries.

The generated product gas stream has to be cooled and treated by several **gas cleaning** and **gas separation** steps in order to reach the pure hydrogen level. **Fig. 45** gives a rough overview about considered gas treatment steps in the present case. The required gas cleaning can be accomplished by **cyclone, filter** and **scrubber systems**. Different gas components can be separated by **membrane systems**, **pressure swing adsorption** (PSA) or **cryogenic processes**. And CO_2 can be removed from the product gas stream by **absorption into physical or chemical solvents.**

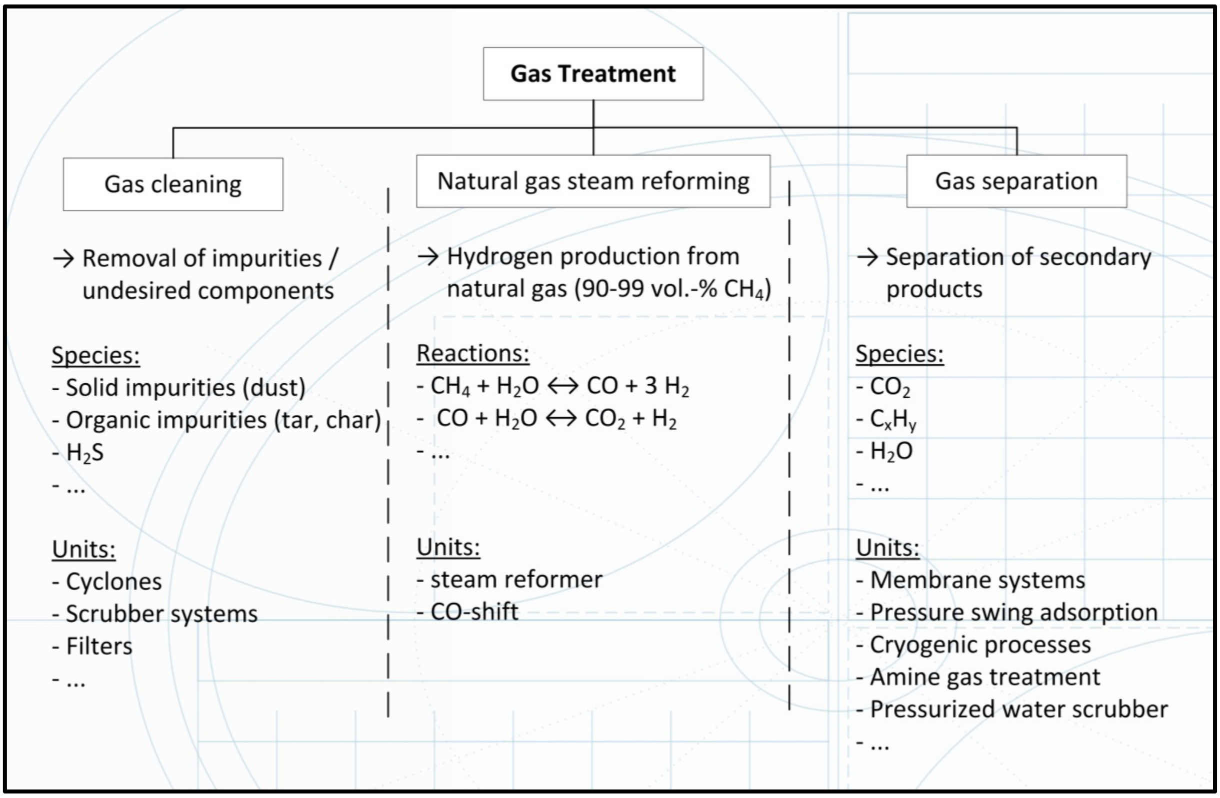

Fig. 45: Considered gas treatment possibilities

A decision about the required gas cleaning and gas separation steps depends on the desired **gas utilization**. And this also includes a decision about favored side products like electricity, Fischer-Tropsch diesel fuel or bioSNG. In this specific case, refinery operators demanded a production process mainly focused on hydrogen to maintain the benefit of low influence on the characteristics of produced fuels. Therefore, chosen gas treatment steps needed to ensure a high yield of pure hydrogen ($H_2 > 99.9$ vol.-%).

The most common production method for the generation of hydrogen is natural gas steam reforming. This production method is based on **steam reformer**, **CO-shift step** and **pressure swing adsorption** as represented in a simplified graphic in **Fig. 46**. A detailed description of this process can be found in literature.[1] Steam reforming of natural gas can be seen as bench mark in contrast to a novel process based on dual fluid gasification.

Tab. 31 shows operational data of a hydrogen production via natural gas steam reforming. Natural gas basically consists of methane (CH_4), whereas a product gas stream from dual fluid gasification consists of different gas components including impurities like dust and tar (cf. **Tab. 13**). For this reason, gas cleaning and the separation of different gas components are crucial process sections for hydrogen production.

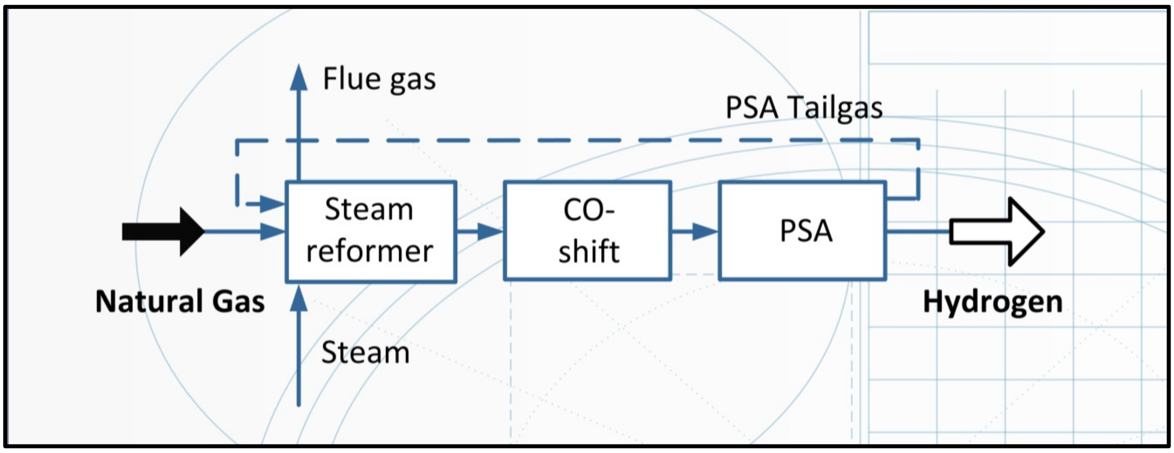

Fig. 46: Hydrogen production via natural gas steam reforming[1]

Plant input *			Plant output *		
Natural Gas**	Nm^3/h	3 822	Hydrogen	Nm^3/h	10 040
Natural Gas (lhv)	MJ/Nm^3	36.91	Hydrogen (lhv)	MJ/Nm^3	10.79
Natural Gas (chem. en.)	MW	39.2	Hydrogen (chem. en.)	MW	30
Electricity	MW	0.3	Steam (48 bar_{abs})	t/h	12.4
Steam (26 bar_{abs})	t/h	8.7			
* Plant size of source data[1] reduced to 30 MW H_2 Output (~ 16%)					
** Necessary electricity for natural gas compression to 23 bar: 0.76 MW					

Tab. 31: Operational data hydrogen production via natural gas steam reforming[2]

Several gas treatment steps have been calculated within IPSEpro for a suitable novel process design for an optimized hydrogen production from biomass. **Gas cleaning** steps need to ensure low dust and tar contents of the processed gas to protect subsequent equipment of an overall plant.

---

[1] cf. Spath P., 2001, p4

[2] cf. Spath P., 2001, p3ff

Gas cleaning in existing plants demonstrated that fabric filter based on polytetrafluoroethylen (PTFE), and scrubber operated with rapeseed methyl ester (RME), reached a sufficient gas quality for a long time operation of gas engines. Increased gas quality can be reached using **multi stage scrubber systems**. Additional, cooled scrubber solvents (e.g.: 10°C) can be used for an additional reduction of the water content of processed gas, undesired gas components as well as remaining dust and tar. Based on existing experience today the named gas cleaning methods can ensure a sufficient gas cleaning for the overall process.

An investigation of different **gas separation** methods showed that pressure swing adsorption is the favorable method for the production of pure hydrogen. Membrane systems can reach only low hydrogen purities and the achieved hydrogen-rich gas stream is gained at a low pressure. Cryogenic processes reach similar efficiencies as membrane systems. But additionally they need a complex gas pretreatment and are only favorable if the input gas stream offers low hydrogen contents.[1]

Gas separation by **pressure swing adsorption** enables the production of hydrogen with high purities ($H_2 > 99.9$ vol.-%). Different gases species are separated by adsorption under high pressure. A detailed description of the process can be found in literature.[2] A further advantage compared to other methods is that pressure swing adsorption supplies the produced hydrogen at high pressure and is an approved industrial process.

Product gas contains a significant amount of CO_2 of about 20 vol.-$\%_{db}$ (cf. **Tab. 13**). CO_2 can be removed from the product gas stream for instance by **amine gas treatment** or a **pressurized water scrubber**. Amine gas treatment is well known as a post-combustion method for the removal of CO_2. This gas treatment process requires a significant amount of heat in the range of 3.9 - 4.2 MJ/kg CO_2 and is based on absorption and desorption.[3]

CO_2 separation by a pressurized water scrubber works due to the solubility of CO_2 in water at high pressures and is well known as a process for the treatment of gas from fermentation plants. Pressurized water scrubber systems need large amounts of water.[4] Both described methods would be suitable for a hydrogen production process.

A novel **process design** for the production of hydrogen from biomass has been created based on the discussed characteristics of different possibilities for each single process step. Additionally, several calculations with IPSEpro supported the initial decision-making process concerning different possibilities for the process design. Calculations based on a process design using membrane separation, as one possibility out of many, can be found in literature.[5] The finally concluded design for a hydrogen production process can be seen in **Fig. 47**. The chosen process design is based on

- conventional dual fluid gasification system,
- polytetrafluoroethylen fabric filter,
- CO-shift step known from natural gas steam reforming,
- multi stage scrubber system with cooled solvents (RME, water),
- compressor,
- CO_2 separation unit,
- pressure swing adsorption (PSA),
- and a steam reformer.

---

1 cf. Pascalowska B., 1996, p55ff
2 Sircar S., 2009
3 cf. Walter H., 2011, chapter CCS, p9ff
4 cf. Kaltschmitt M., 2009, p899; 5 cf. Müller S., 2011

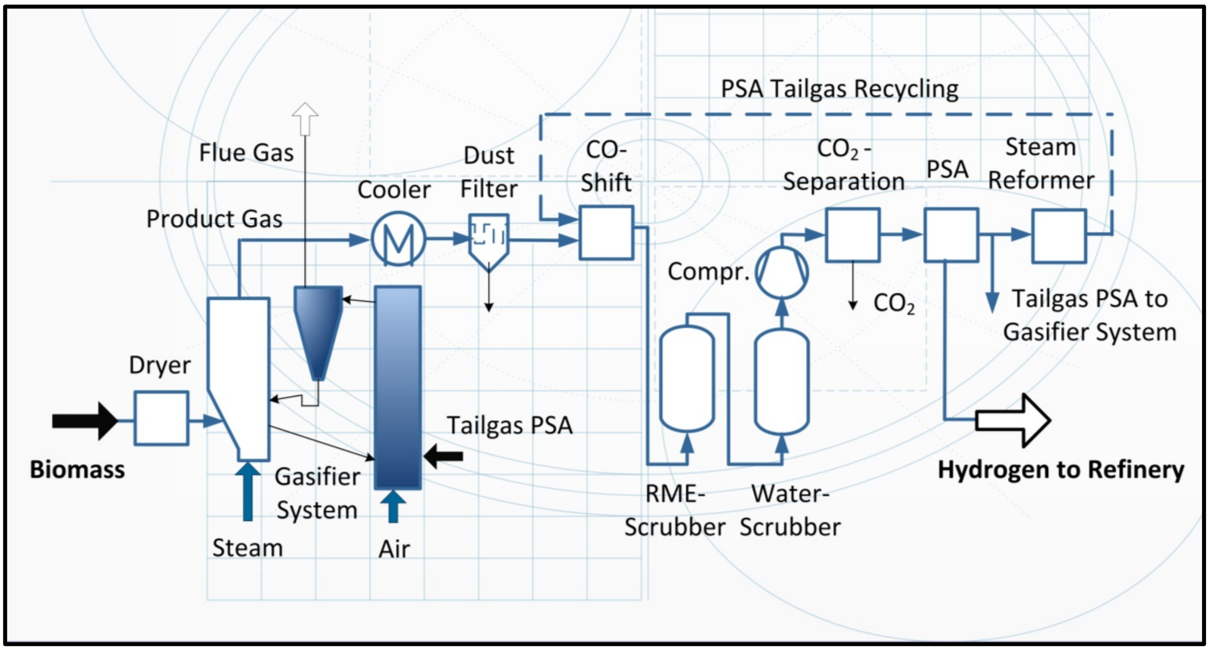

Fig. 47: Process design hydrogen production via dual fluid gasification

The chosen process design uses components which proved their reliability within industrial processes. The chosen process design enables the production of pure hydrogen according to the demands of a refinery. In the next step the process design is used for the creation of a layout for an overall plant. A simulation of an overall plant should show the process performance within an entire plant.

7.3. Hydrogen Production Plant for a Refinery

Fig. 48 shows the developed layout for a hydrogen production via a conventional dual fluid gasification system. Wood chips with a water content of 40 wt.-% are used as **fuel supply** for the hydrogen production process. Before the wood chips enter the gasifier system they are dried with a biomass dryer to lower the water content to 20 wt.-%.

Necessary heat for the dryer is supplied by available low temperature heat which is used to heat the dryer inlet air up to a temperature of about 80°C. The applied **drying system** can be constructed as a spiral-, cross flow chute or belt dryer. The dryer outlet air needs to be cleaned from dust before the used air can exit the plant.

After the drying, a screw conveyor is feeding the wood chips into the gasifier. Additionally, the screw conveyor is flushed with a small CO_2 stream to prevent that air enters the gasifier. At this position nitrogen (N_2) should not be used instead of CO_2 due to fact that nitrogen impairs the performance of gas separation by pressure swing adsorption (PSA).

Within the gasifier system the solid wood chips are converted into product gas (cf. **Chapter 3.2**). Steam for the fluidization of the gasifier is pre-heated by available process heat at a temperature of 450°C and olivine is used as bed material for the **gasification**. The gas produced has a temperature of 850°C and contains about ~ 40 g/Nm^3 dust, ~ 15 g/Nm^3 char and ~ 5 g/Nm^3 tar at the exit of the gasifier. These analyzed values are based on measured data at existing units in Güssing and Oberwart.

Downstream of the gasifier the product gas is **cooled**, **cleaned** and **separated** by several gas **treatment steps**. Directly after the gasification the product gas is cleaned in a bag filter and cooled in heat exchangers. The bag filter is operated as a fabric filter based on polytetrafluoroethylen (PTFE). Operation experience shows that this filter system reduce the dust content to ~ 10 mg/Nm^3 and the tar content to ~ 1 g/Nm^3. The temperature of the gas stream entering the bag filter is limited to 220°C.

Available process heat is used by heat exchangers to pre-heat PSA tail gas for the steam reformer and for the heat supply to the process heat cycle. The process heat cycle enables the heat transfer to vaporizer, steam generator, district heating and dryer.

After this first cooling and cleaning step, the product gas stream is mixed with steam and recycled PSA tail gas coming from the steam reformer. This gas mixture is transported to the **CO-shift** unit. At this stage the gas stream contains about 50 vol.-% of water (H_2O) and has temperature of ~275°C. Within the CO-shift unit, the carbon monoxide (CO) content of the gas mixture is reduced by a sulfur resistant catalyst which is catalyzing the water gas shift reaction (cf. **Eq. 3.6** in **Chapter 3**).

Eq. 3.6: $$CO + H_2O \leftrightarrow CO_2 + H_2 \qquad \Delta H = -40.9\ kJ/mol$$

As a result of this process step, the carbon monoxide (CO) content decreases and the hydrogen (H_2) content is increased. Subsequent to the shift stage, the gas stream is cooled by another heat exchanger and supplied to a **rape seed oil methyl ester (RME) scrubber** and a **water scrubber**. Within existing plants RME scrubber showed sufficient performance for reducing the tar content to ~ 25 mg/Nm^3. An additional water scrubber and cooled scrubber solvents condense water from the gas stream and cause a further reduction of remaining tars to protect the subsequent PSA against condensing tars.

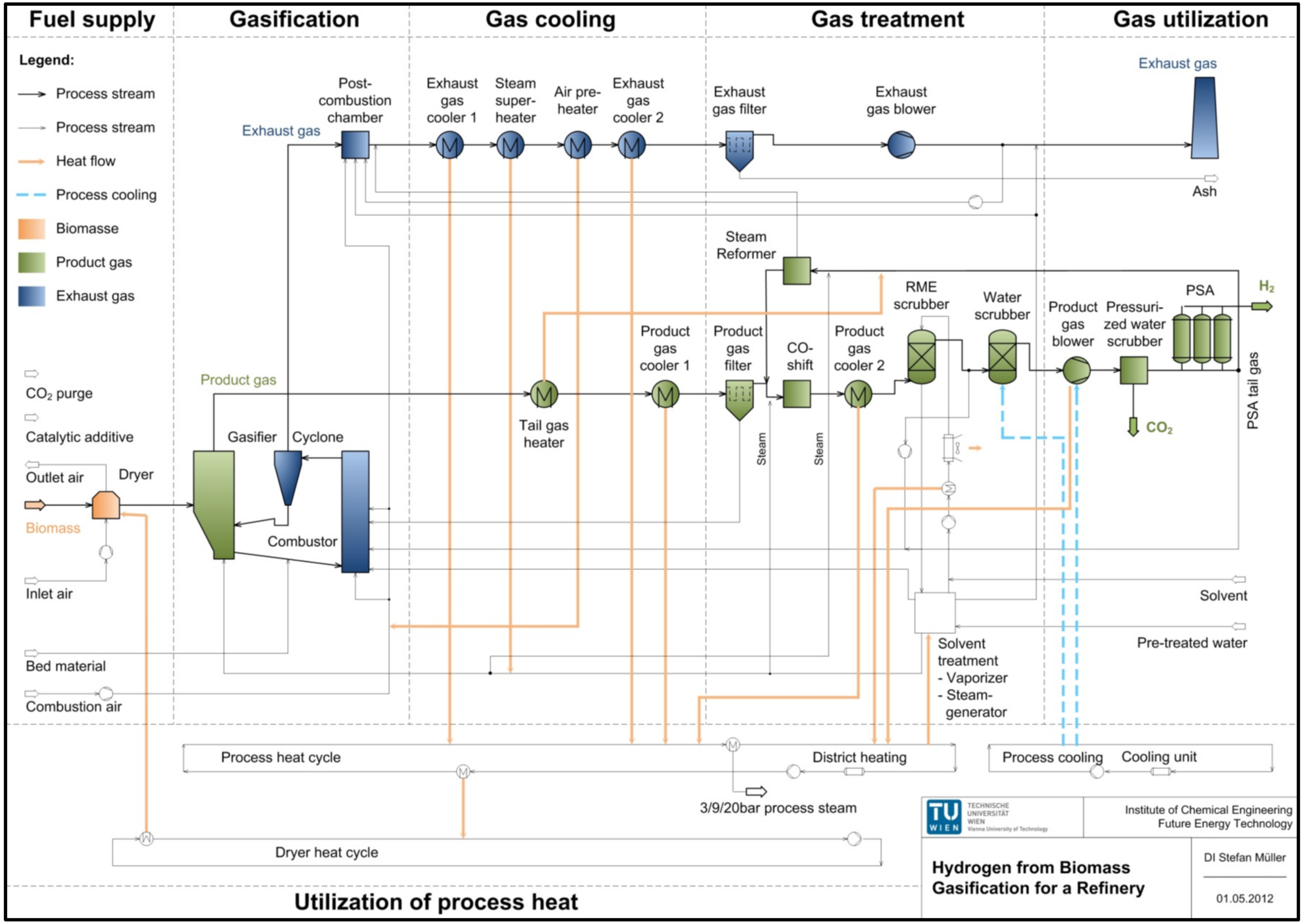

Fig. 48: Layout of an entire plant for hydrogen production via dual fluid gasification

After the cleaning steps, the gas is compressed to a pressure of 23 bar_{abs} and 85 % of CO_2 is removed by a pressurized water scrubber. Pressurized water scrubber proofed its reliability especially for the treatment of gas from fermentation plants.

The pressurized water scrubber is followed by a **pressure swing adsorption** system (PSA). Within the PSA, hydrogen is separated with high purity from the remaining gas components. The PSA system reaches a hydrogen separation efficiency of 85%, depending on the processed gas composition, and supplies hydrogen with a pressure of 22.3 bar_{abs} at the exit of the PSA system. The remaining gas stream is called **PSA tail gas** and still contains valuable gas components such as methane (CH_4), ethane (C_2H_6), and propane (C_3H_8) with high heating value. Therefore, the tail gas stream is used as additional fuel for the combustor and supplied in a larger extent to a steam reformer. The application of a **steam reformer** increases the hydrogen output mainly due to the reforming reaction shown in **Eq. 3.7** in **Chapter 3**.

Eq. 3.7: $$CH_4 + H_2O \leftrightarrow CO + 3\,H_2 \qquad \Delta H = 203.0\ \text{kJ/mol}$$

The endothermic reforming process of the PSA tail gas is operated by temperatures of about 800°C. For this reason, the tail gas stream is preheated with available process heat and mixed with superheated steam. Additionally a small share of tail gas is combusted to reach the desired process temperature. The reformed tail gas stream contains an increased share of carbon monoxide (CO) and hydrogen (H_2). The reformed tail gas stream is recycled before the CO-shift to the main gas treatment process. Overall, the described gas treatment process can be seen as a considerable modification of a process known as natural gas steam reforming.

Beside the product gas stream, the **exhaust gas stream** is a second main gas stream, which needs to be operated within the plant. The exhaust gas stream is resulting from the combustion of wood char and PSA tail gas within the combustion chamber. Additionally, a small share rises from a combustion process within the steam reformer. The overall exhaust gas stream contains dust and relevant amounts of heat. In order to clean the exhaust gas from dust, the gas stream is cleaned with a cyclone and a fabric filter. Several heat exchangers are used to transfer heat to the **process heat utilization.**

Generated process heat is used within the described hydrogen production plant for many different applications with the aim to improve the overall plant performance. In the present case, refinery operators agreed that steam and district heat for refinery facilities in the surrounding would be a useful additional outcome of the hydrogen production process. For this reasons, the described plant layout includes the utilization of process heat:

- for a fuel dryer,
- to pre-heat combustion air,
- to support heat for the gas treatment process,
- for solvent treatment,
- for the generation of super-heated steam for the gasification,
- and to provide steam and district heating to facilities co-located to the plant.

The illustrated layout for a hydrogen production plant was used to elaborate a simulation model. **Fig. 49** shows the created simulation model as an IPSEpro flow sheet. This simulation model enabled a calculation of mass- and energy flows based on basic data from **Chapter 6. Tab. 32** and **Tab. 33** show important additional data which are used for the calculations.

Term	Unit	Value	Char.[1]	Data source
Fuel supply				
Biomass supply (wood chips, lhv)	MW	50	S	demanded by refinery
Biomass water content before dryer	wt.-%	40	S	Tab. 23
Biomass water content after dryer	wt.-%	20	S	Tab. 23
Dryer inlet air temperature	°C	80	S	Tab. 23
Gasification				
Steam temperature for gasifier fluidization	°C	450	S	cf. Pröll T., 2004, p214
Combustion air temperature for combustor	°C	400	S	cf. Pröll T., 2004, p214
Gasification temperature	°C	850	S	Pröll T., 2004, p154
Combustion temperature	°C	935	S	cf. Pröll T., 2004, p214
Steam to fuel ratio	$kg_{H2O}/kg_{fuel,waf}$	0.55	S	Tab. 22
Char combusted in combustion chamber	$kg_{char}/kg_{fuel,waf}$	0.10	S	Tab. 22
Air ratio	-	1.05	S	Tab. 22
Product gas composition at the exit of the gasifier				
Water (H_2O)	vol.-%	34.1	R	cf. steam to fuel ratio
Hydrogen (H_2)	vol.-$\%_{db}$	39.9	R	cf. Tab. 10
Carbon monoxide (CO)	vol.-$\%_{db}$	22.5	S	cf. Tab. 10
Carbon dioxide (CO_2)	vol.-$\%_{db}$	24.1	R	cf. Tab. 10
Methane (CH_4)	vol.-$\%_{db}$	10.0	S	cf. Tab. 10
Ethene (C_2H_4)	vol.-$\%_{db}$	2.4	S	cf. Tab. 10
Ethane (C_2H_6)	vol.-$\%_{db}$	0.4	S	cf. Tab. 10
Propane (C_3H_8)	vol.-$\%_{db}$	0.4	S	cf. Tab. 10
Oxygen (O_2)	vol.-$\%_{db}$	0.15	S	cf. Tab. 10
Nitrogen (N_2)	vol.-$\%_{db}$	0.14	R	cf. biomass, Tab. 18
Hydrogen sulfide (H_2S)	vol.-$\%_{db}$	0.006	R	cf. biomass, Tab. 18
Ammonia (NH_3)	vol.-$\%_{db}$	0.0015	S	cf. Tab. 8
Hydrogen chloride (HCl)	vol.-$\%_{db}$	0.0005	R	cf. biomass, Tab. 18
Hydrogen cyanide (HCN)	vol.-$\%_{db}$	0.00015	S	cf. Tab. 8
Dust particles	g/Nm^3	40	S	cf. Pröll T., 2004, p213
Char particles	g/Nm^3	15	S	cf. Pröll T., 2004, p213
Tar	g/Nm^3	5	S	cf. Pröll T., 2004, p213
Gas cooling				
Product gas temperature after gas cooling	°C	150	S	cf. Pröll T., 2004, p213
Exhaust gas temperature after gas cooling	°C	160	S	cf. Pröll T., 2004, p214
Gas treatment – filter				
Filter - Dust content of product gas after filter	mg/Nm^3	10	S	CHP Güssing
Filter - Tar content of product gas after filter	g/Nm^3	1	S	cf. Pröll T., 2004, p213
Gas treatment – CO-shift				
Water content of gas entering CO-shift	vol.-%	50	S	manufacturer data
Temperature of gas entering CO-shift	°C	275	S	manufacturer data
Ethene (C_2H_4) conv. into ethane (C_2H_6)	%	100	S	manufacturer data
CO conversion (water gas shift reaction)	%	81	S	manufacturer data

Tab. 32: Values for the calculation of mass- and energy flows for a hydrogen production for a refinery

---

[1] Character of value: set value (S) or resulting value (R)

Term	Unit	Value	Char.	Data source
Gas treatment – RME scrubber				
Gas temperature before RME-scrubber	°C	150	S	cf. Pröll T., 2004, p213
Gas temperature after RME-scrubber	°C	40	S	cf. Pröll T., 2004, p213
Saturation of gas (water content) after scrubber	%	100	S	-
Tar content of gas after scrubber	mg/Nm³	25	S	CHP Güssing
Gas treatment – water scrubber				
Gas temperature after water-scrubber	°C	10	S	-
Saturation of gas (water content) after scrubber	%	100	S	-
Tar content of gas after scrubber	mg/Nm³	0	S	-
Gas treatment – compressor				
Gas pressure before compressor	bar_{abs}	1.1	R	manufacturer data, MAN
Gas pressure after compressor	bar_{abs}	23.0	S	manufacturer data, MAN
Isentropic efficiency	%	75	S	manufacturer data, MAN
Mechanical efficiency	%	98	S	manufacturer data, MAN
Electrical efficiency (drive system)	%	96	S	manufacturer data, MAN
Mechanical efficiency (drive system)	%	98	S	manufacturer data, MAN
Gas treatment – CO_2 separation (pressurized water scrubber)				
CO_2 separated from gas stream	%	85	S	cf. Urban W., 2009, p44ff
Gas treatment – pressure swing adsorption (PSA)				
Gas pressure at gas inlet	bar_{abs}	23.0	S	manufacturer data, UOP
Separation coefficient (hydrogen)	%	85	S	manufacturer data, UOP
Gas pressure at gas outlet (hydrogen)	bar_{abs}	22.3	S	manufacturer data, UOP
Gas pressure at gas outlet (tail gas)	bar_{abs}	1.3	S	manufacturer data, UOP
Gas treatment – steam reformer				
Temperature of gas at the steam reformer inlet	°C	400	S	-
Water content of gas entering steam reformer	vol.-%	35	S	-
Temperature in steam reformer	°C	800	S	-
Methane (CH_4) conv. (steam reforming reaction)	%	80	S	manufacturer data
Ethene (C_2H_4) conversion	%	95	S	manufacturer data
Ethane (C_2H_6) conversion	%	95	S	manufacturer data
Propane (C_2H_8) conversion	%	95	S	manufacturer data
Gas utilization (Hydrogen)				
Temperature of exiting hydrogen stream	°C	45	S	manufacturer data, UOP
Pressure of exiting hydrogen stream	bar_{abs}	22.3	S	manufacturer data, UOP
Hydrogen (H_2)	vol.-%	> 99.9%	D	refinery operator
Carbon monoxide (CO)	ppmV	< 10	D	refinery operator
Nitrogen (N_2)	vol.-%	< 0.2	D	refinery operator
Oxygen (O_2)	ppmV	< 2.5	D	refinery operator
Water (H_2O)	ppmV	< 2.5	D	refinery operator

Tab. 33: Values for the calculation of mass- and energy flows for a hydrogen production for a refinery

---

1 Character of value: set value (S), resulting value (R), or demanded by refinery (D)

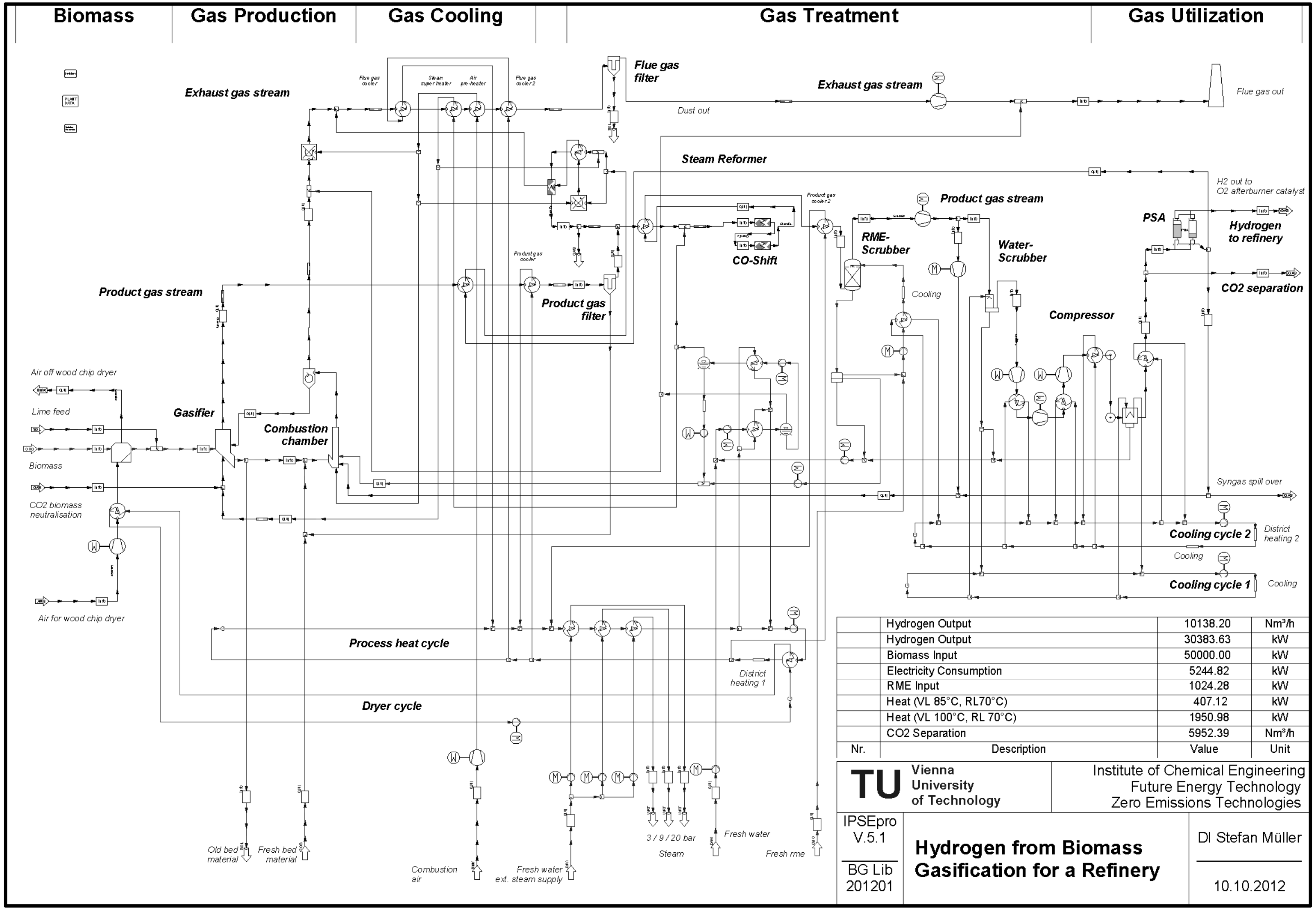

Nr.	Description	Value	Unit
	Hydrogen Output	10138.20	Nm³/h
	Hydrogen Output	30383.63	kW
	Biomass Input	50000.00	kW
	Electricity Consumption	5244.82	kW
	RME Input	1024.28	kW
	Heat (VL 85°C, RL70°C)	407.12	kW
	Heat (VL 100°C, RL 70°C)	1950.98	kW
	CO2 Separation	5952.39	Nm³/h

Fig. 49: Simulation flow sheet for an entire plant for hydrogen production via conventional dual fluid gasification

7.4. Simulation Results

The simulation model was used to calculate mass- and energy balances for the described hydrogen production process based on values listed in **Chapter 6.1** and **Chapter 7.3**. The results of this simulation are shown in **Tab. 34**.

Plant input			Plant output		
Term	Unit	Value	Term	Unit	Value
Biomass (wood chips)	kg/h	18 898	Hydrogen	Nm^3/h	10 138
Biomass water content	wt.-%	40	Hydrogen	kg/h	912
Biomass (lhv)	MJ/kg	9.6	Hydrogen (lhv)	MJ/kg	120
Biomass (chem. energy)	kW	50 000	Hydrogen (lhv)	MJ/Nm^3	10.79
Electricity consumption #	kW	5 244	Hydrogen (chem. energy)	kW	30 383
Fresh scrubber solvent (RME)	kg/h	100	Steam (20 bar_{abs}, 215 °C)	kg/h	2 000
Fresh bed material (olivine)	kg/h	100	Steam (9 bar_{abs}, 180 °C)	kg/h	2 328
Limestone (catalytic additive)	kg/h	15	District heating (VL 85°C, RL 70°C)	kW	2 357
Fresh water	kg/h	2 965	CO_2 from CO_2 separation	t/h	11.7
Air ##	Nm^3/h	58 226	Ash	kg/h	205
CO_2 purge	Nm^3/h	250	Exhaust gas	Nm^3/h	62 074
<u>Gasifier system:</u>					
Cold gas efficiency:		70.8 %			
Relative water conversion rate:		0.10 $kg_{H2O}/kg_{fuel.waf}$			
Absolute water conversion rate:		0.18 kg_{H2O}/kg_{H2O}			
Hydrogen productivity rate:		0.32 kg_{H2}/kg_{H}			
# excl. cooling & CO_2 separation; ## excl. dryer					

Tab. 34: Simulation results – Hydrogen production from biomass for a refinery

30 MW of pure hydrogen can be produced from **50 MW** of biomass with an electricity consumption of **5.2 MW**. Additionally, **2.4 MW** district heating and a significant amount of steam can be provided to facilities which are located nearby the hydrogen production. The achieved hydrogen purity meets the demands of a refinery. The calculated plant configuration is used to operate a novel innovative process based on well-proven industrial equipment. The process performance achieved needs to be compared with a hydrogen production via natural gas steam reforming (**cf. Tab. 31**).

7.5. Key Figures Describing the Hydrogen Output

Tab. 34 showed key figures describing the hydrogen output of the used gasifier system. The hydrogen production process consists of several process steps. Each single process step contributes to the overall hydrogen output. Illustrated values for the hydrogen output are moderately sensitive to the preset product gas composition. Beside

- relative water conversion rate ($kg_{H2O}/kg_{fuel,waf}$),
- absolute water conversion rate (kg_{H2O}/kg_{H2O}),
- and the hydrogen productivity rate (kg_{H2}/kg_{H}),
  (cf. definitions **Eq. 6.5** to **Eq. 6.7**)

also the performance of subsequent equipment influences the hydrogen output of the overall plant. Following parameters can be used to increase the overall hydrogen output:

- conversion rates of the water-gas-shift reaction within the CO-shift reactor,
- hydrogen separation efficiency of the pressure swing adsorption unit,
- and achievable conversion rates within the steam reformer.

Tab. 32 and **Tab. 33** showed preset values for the calculation of the above named parameters according to the experience of equipment manufacturer. A hydrogen mass flow analysis of each single process step shows the effect of each step with respect to the overall hydrogen output of the modeled plant.

7.6. Hydrogen Mass Flow Analysis

Fig. 50 shows a mass flow chart reflecting the elementary flow of hydrogen atoms through the gasifier system. Hydrogen atoms enter the gasifier bound in the biomass stream (C_xH_y – white) as well as in water (H_2O – blue) as fuel water content or through the fluidization of the gasifier as gasification agent. The produced gas stream contains hydrogen atoms as a part of water, C_xH_y (CH_4, C_2H_4, …, tar, char) and pure gaseous hydrogen (H_2 – red). **The presented hydrogen mass flow chart shows that the achieved gaseous hydrogen (H_2) within the product gas stream mainly arises from the conversion of dry biomass. And at the same time, only a small share of the generated gaseous hydrogen arises from water conversion.** The calculation results indicate an absolute water conversion rate of 0.18 kg_{H2O}/kg_{H2O}. Apart from that, a small share of hydrogen atoms leave the gasifier bound in char to the combustor.

The combustor supplies the required heat for the gasification reactions. Within the combustor hydrogen atoms bound in char and optional additional fuel are part of the combustion process. In this case, PSA tail gas is used as additional fuel for the combustion process. Involved hydrogen atoms leave the combustor after the combustion in the form of water as a part of the flue gas stream.

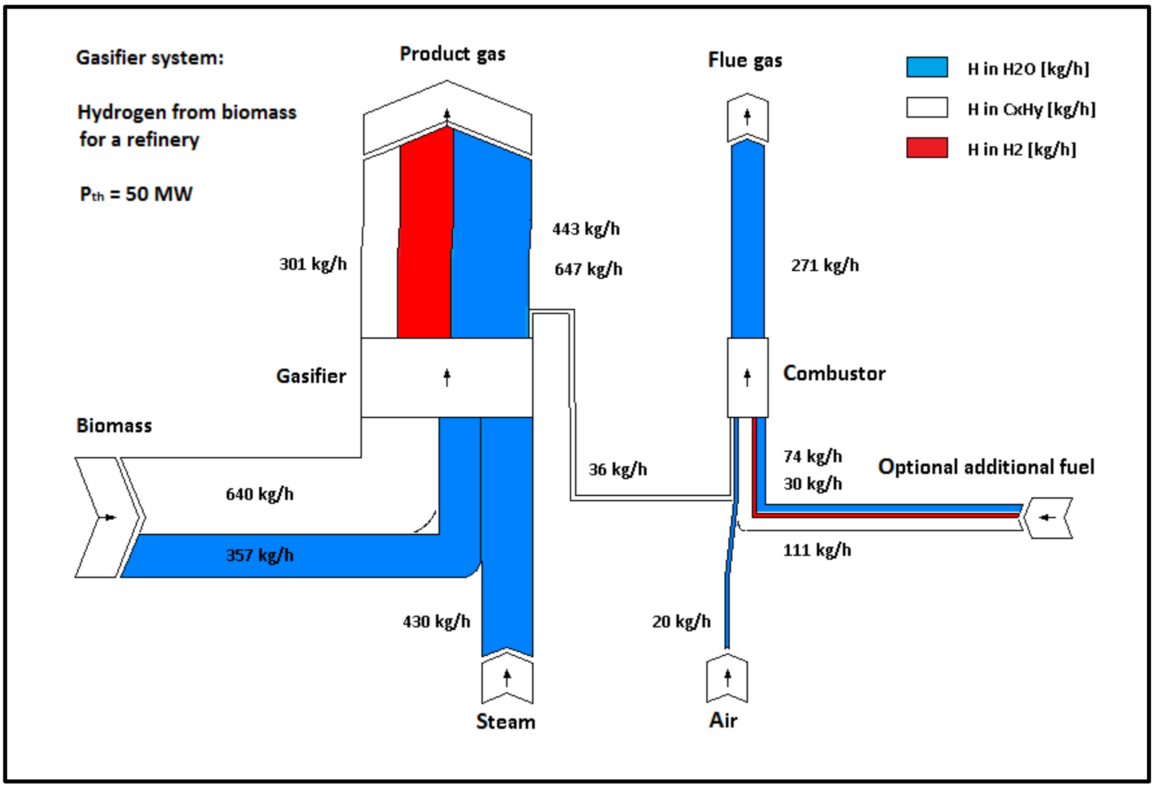

Fig. 50: Hydrogen mass flow chart for the used conventional gasifier system

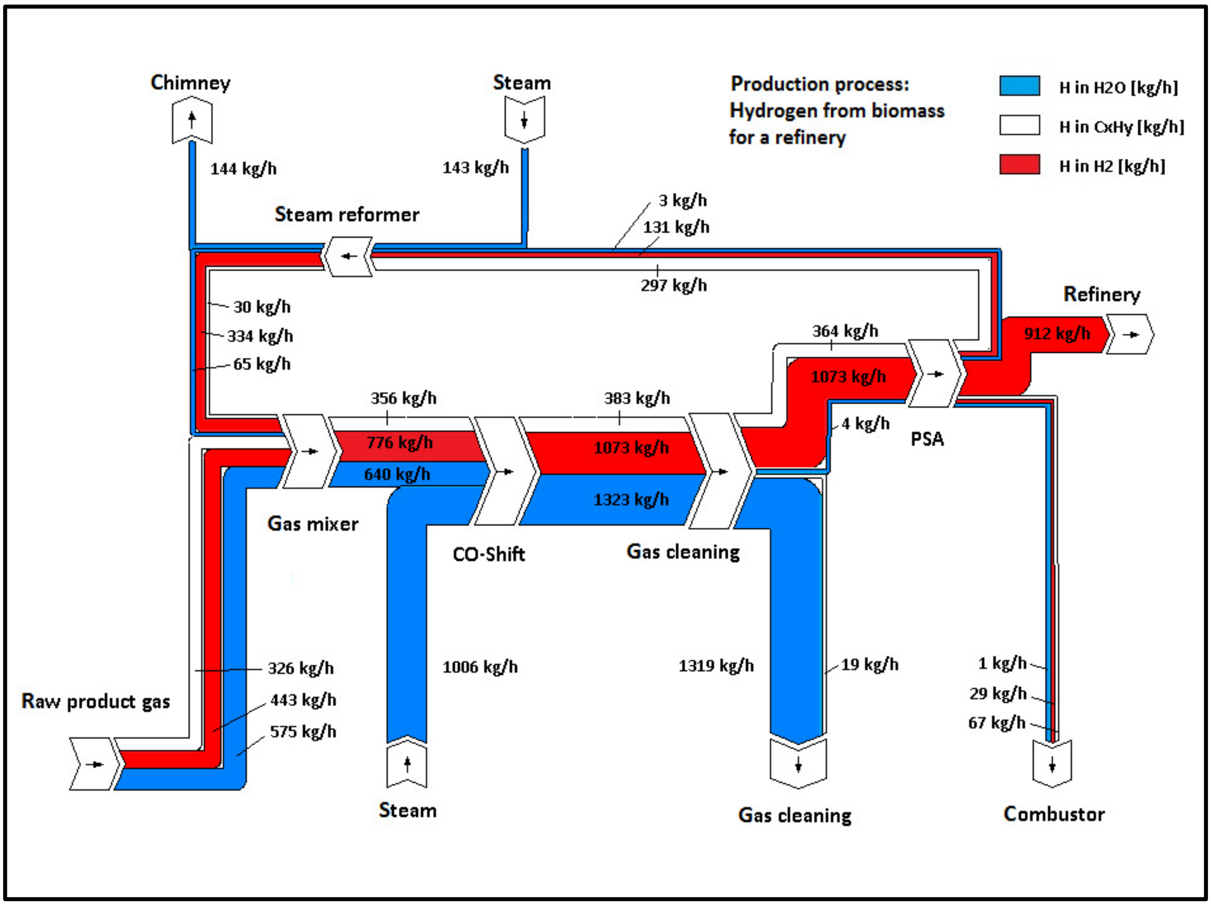

Fig. 51: Hydrogen mass flow chart for relevant gas treatment sections

Subsequent process steps convert the raw product gas stream into pure hydrogen. Within the CO-shift step the water gas-shift reaction is used to convert water (H_2O) together with carbon monoxide (CO) into carbon dioxide (CO_2) and hydrogen (H_2). Additional, ethylene (C_2H_4) is hydrated to ethane (C_2H_6). These reactions can be seen in the hydrogen mass flow chart as an increased mass flow of H_2 and a slightly increased mass flow of hydrogen bound in C_xH_y. The gas cleaning steps lead to a removal of water as well as hydrogen bound in C_xH_y in form of tar and remaining char particles.

Pressure swing adsorption (PSA) is used to separate pure hydrogen (H_2) from the remaining gas components. The PSA tail gas contains a high share of hydrogen, bound in C_xH_y gas components. A small share of the hydrogen atoms bound in the tail gas streams is lost as additional fuel for the combustor. The main share of the remaining hydrogen, bound in the PSA tail gas stream, can be recycled to the process after the treatment by a steam reformer. As can be seen, the steam reformer enables the production of gaseous hydrogen (H_2) from hydrogen bound in C_xH_y gas components as well as from water. This way, the steam reformer increases the hydrogen output of the overall process.

The total hydrogen output is determined by the performance of the gasifier combined with the efficiency of every subsequent process step. A variation of important process parameters shows the sensitivity of the process.

7.7. Variation of Sensitive Parameters

Variations have been conducted to estimate the sensitivity of the process with respect to a change of main process parameters. The steam to fuel ratio has been identified as an sensitive process parameter for the performance of the process. All calculations so far within the present chapter used a preset steam to fuel ratio of 0.55.

Fig. 52 illustrates the impact of a variation of the steam to fuel ratio on the hydrogen output of the plant. Carried out variations considered water-gas-shift reaction near equilibrium ($\delta_{Eq.WGS\text{-}shift}$ = -0.05; cf. definition **Eq. 6.14**) at the exit of the gasifier, as an important precondition corresponding to the preset product gas composition.

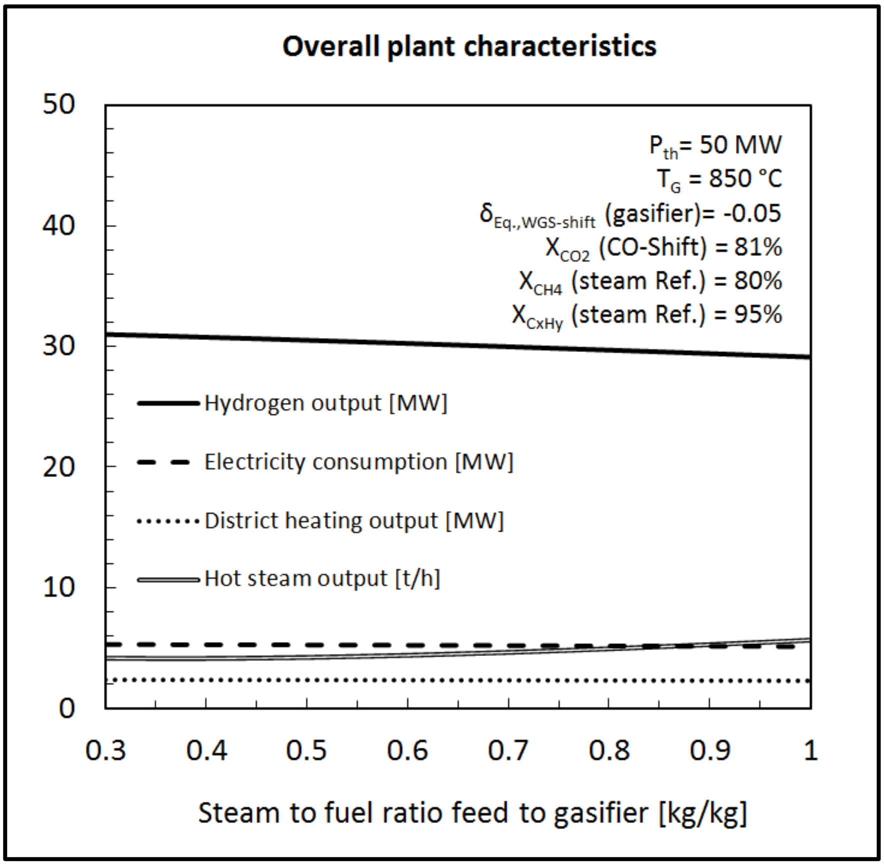

Fig. 52: Major plant characteristics as a function of the steam to fuel ratio feed to the gasifier

As can be seen, a changing steam to fuel ratio has small impact on the overall hydrogen output of the plant. Variations showed that the hydrogen output stays quite constant in the area of 30 MW. The results are at the same time not very sensitive to small changes of reaction rates within CO-shift and steam reformer. This can be explained by a collaborating process chain.

The included process steps form a quite robust process chain, which is not very sensitive to little changes of gas compositions and reaction rates. A lower steam to fuel ratio favors higher hydrogen output and a lower heat surplus of the plant. This can be explained by a lower heat demand of the gasifier due to fact that less steam needs to be heated up to the gasification temperature.

Fig. 53 additionally shows the correlation of product gas composition and steam to fuel ratio under the consideration of a constant distance to the thermodynamic equilibrium of the water-gas shift reaction. High hydrogen content at the exit of the gasifier does not directly lead to significantly increased hydrogen output of the overall process. This can be explained by the reason that vice versa higher carbon monoxide contents are used for an increased hydrogen production by the subsequent CO-shift step.

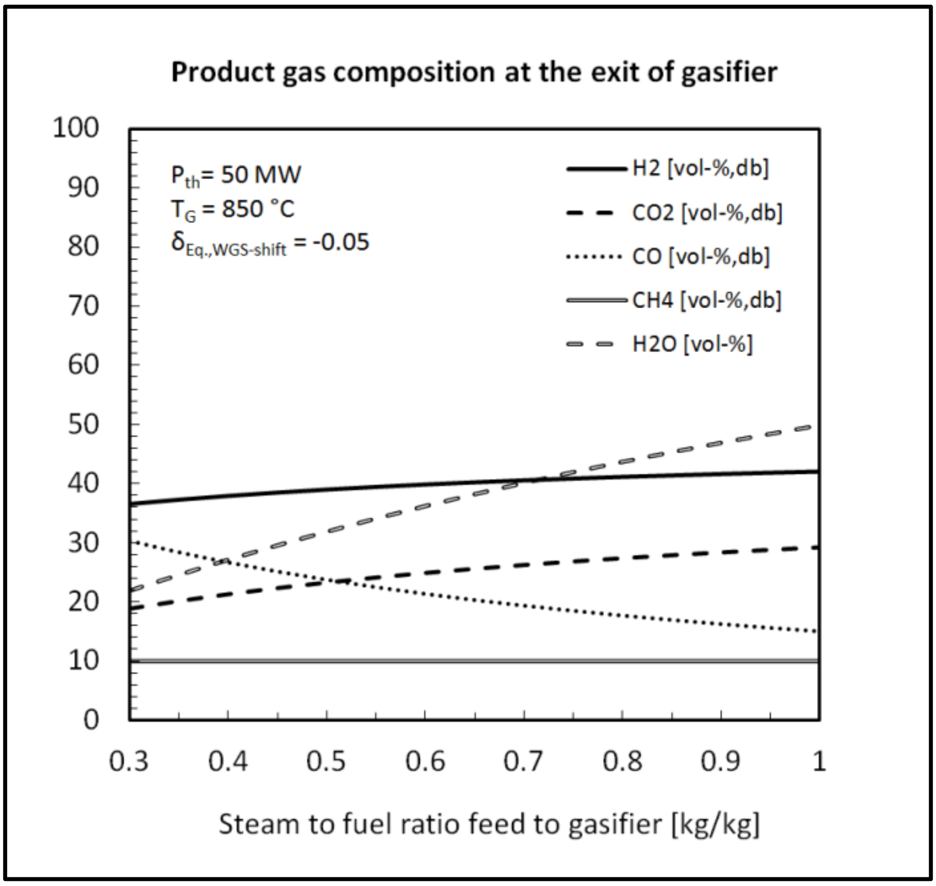

Fig. 53: Product gas composition at the exit of the gasifier close to water gas shift equilibrium

It can be concluded once more, that the included process steps form a quite robust process chain, which is not very sensitive to little changes of gas compositions and reaction rates.

7.8. Economic Evaluation – Hydrogen for a Refinery

The simulation results enabled an assessment of the hydrogen production by net present value calculations. Necessary cost rates are again taken from the reference case according to **Tab. 24**. Additional cost rates and expected investment costs for the described plant are shown in **Tab. 35**.

Parameter	Unit	Value	Data source
Investment cost incl. interest (NPV)	€	80 000 000	according to information from REPOTEC
Diesel fuel	€/t	600	according to information from OMV
Fatty acid ethyl esters (FAME)	€/t	960	according to information from OMV
Equivalent FAME utilization	t/a	45 907	according to information from OMV
Lower heating value FAME	MJ/kg	37.3	-

Tab. 35: Additional cost rates for net present value calculations

Business Case
Business Case: A refinery operator is forced to reach strategic targets of reducing fossil resource consumption and reduced fossil CO_2 emissions. Hydrogen demanded by the refinery so far was produced 0.) via natural gas steam reforming (40 MW). The refinery operator identified the following options as potential solutions to reach the strategic targets: 1.) increasing the share of processed biodiesel fuel (fatty acid ethyl esters - FAME) within the refinery or 2) installation of a hydrogen production from woody biomass (50 MW). 3.) The installation of a hydrogen production plant from woody biomass additionally could gain financial support by the European Commission funded by the revenues of a European greenhouse gas emission allowance trading scheme. Financial support would fund half of necessary operation and investment costs. **Investment decision:** Which investment option would reduce fossil CO_2 emissions at minimal costs?

Position	Symbol	Unit	Option 0	Option 1	Option 2	Option 3
Boundary conditions						
Natural gas consumption		MWh/a	280 000			
Biodiesel fuel consumption		t/a		45 907		
Biomass consumption (wood chips)		MWh/a			350 000	350 000
Hydrogen supply		MWh/a	210 000		210 000	210 000
Investment cost incl. interest	$I_{Opt,X}$	€	0	0	80 000 000	40 000 000
Expenses						
Fuel cost (natural gas)	A_1	€/a	**8 064 000**			
Fuel cost (FAME)	A_2	€/a		**16 526 520**		
Fuel cost (wood chips)	A_3	€/a			**7 937 229**	**7 937 229**
Electricity costs	A_4	€/a			3 670 800	3 675 700
Maintenance, insurance, admin.,tax	A_5	€/a			3 600 000	3 600 000
Operating supplies	A_6	€/a			1 150 310	1 150 310
Labor costs	A_7	€/a			**490 000**	**490 000**
Costs for CO_2 emission allowances	A_8	€/a	1 108 800			
Earnings						
Earnings from district heating	E_1	€/a			416 500	416 500
Earnings from steam supply	E_2	€/a			757 400	757 400
Granted financial support	E_3	€/a				4 632 969
Sum (Expenses – Earnings)	$C_{Opt,X}$	€/a	**9 172 800**	**16 526 520**	**15 674 439**	**12 215 369**
Net present value calculation						
Cumulative present value factor	BWSF	-	10	10	10	10
Additional investment costs	ΔI_X	€	0	0	80 000 000	40 000 000
Operating expenses savings	ΔC_X	€/a	7 353 720	0	852 081	4 311 151
Net present value	ΔNPV_X	€	73 537 200	0	-71 479 187	3 111 507

Tab. 36: Evaluation of the hydrogen production from biomass for a refinery by NPV calculations

The investigated business case compares a hydrogen production via natural gas steam reforming with a hydrogen production from biomass. **Tab. 36** shows the results of the evaluation. Due to the current energy policy within the European Union, the share of renewable energy sources in a refinery has to reach set targets until 2020 (cf. **Chapter 2.7.3**). A biomass based hydrogen production is one possibility out of many which could support the desired development. In the present case, the hydrogen production process is compared with an increased utilization of biodiesel fuel (Fatty acid ethyl esters - FAME) as bench mark, because biodiesel fuel could be used to reach an equivalent reduction of fossil energy.

Shown results give an important insight into the main relationships in the environment of the created hydrogen production concept. The economic feasibility of the created hydrogen production is strongly dependent on the price for wood chips, the natural gas price and the price for FAME. Beside fuel costs, high electricity consumption is an additional important cost factor. **Option 3** has a positive net present value compared to Option 1 due to the financial support by the European Commission.

Parameter Analysis

Parameter Analysis: The results illustrated in Tab. 36 show that following parameters are most important for the investment decision: 1.) wood chip price, 2.) natural gas price, 3.) FAME price. A ceteris paribus (cet. par.) variation of each parameter shows the necessary price in comparison to the reference values for a positive investment decision for option X based on a positive "net present value".

Position	Reference Value	Unit	Option 0	Option 1	Option 2	Option 3
Wood chip price for positive NPV	100	€/t_{atro}	-	-	< 10	< 108
Natural gas price for positve NPV	28.8	€/MWh	< 55	-	-	-
FAME price for positive NPV	960	€/t	> 800	-	> 1115	> 955

Tab. 37: Parameter analysis of the business case "hydrogen production from biomass for a refinery"

Tab. 37 shows the results of a ceteris paribus parameter analysis. Illustrated values indicate the necessary value of a single parameter to reach a positive net present value for Option X. For example, the net present value of Option 2 is positive at a wood chip price (cet. par.) below 10 €/t_{atro} **or** at a FAME price (cet. par.) above 1115 €/t.

From an economic point of view, **Option 3** should be favored at a FAME price of 960 €/t if

- the wood chip price is lower than 108 €/t_{atro} (24.3 €/MWh),
- and the natural gas price is higher than 55 €/MWh.

A realization of the created hydrogen production concept would support the strategic goals of the refinery operator as well as the European energy policy. Further realization steps need be accompanied by considerations with respect to feed stock price development to maintain financial risks at a low level. The installation of a hydrogen production plant from biomass can be used to generate a positive impulse for development of a region, if used wood chips are supplied from local suppliers. At the same time, alternative methods increasing the share of renewable energy in a refinery need to be observed and compared with the presented solution.

7.9. Results and findings

Chapter 7 presented a novel concept for the integration of conventional dual fluid gasification in a refinery. A hydrogen production based on biomass gasification would increase the share of renewable energy within the refining process and would improve the fossil "CO_2-footprint" of produced fuels without a negative influence on the characteristics of produced fuels.

- Used process design for the production of pure hydrogen is based on a conventional dual fluid gasification system, CO-shift step, multi stage scrubber systems, a CO_2 separation unit, pressure swing adsorption (PSA) and a steam reformer.

- Investigations supported by a detailed simulation model showed that 30 MW of pure hydrogen can be produced from 50 MW of biomass accompanied by an electricity demand of 5.2 MW. Additionally, 2.4 MW district heating and a significant amount of steam can be provided to facilities which are located nearby the hydrogen production site.

- A hydrogen mass flow analysis was carried out to identify the main driving force enhancing large hydrogen output. An investigation of the gasifier showed that the achieved gaseous hydrogen (H_2) at the exit of the gasifier, mainly arises from the conversion of dry biomass. Whereas, only a small share of the generated hydrogen originates from water conversion. Subsequent process steps form a robust process chain. Variations of important process parameters showed that the overall hydrogen output is not very sensitive with respect to little changes of gas compositions and conversion rates. Fluctuations within the process chain are compensated by the overall process.

- The calculated plant configuration consists of well-proven industrial equipment, which is used to operate a novel innovative process. Further experimental investigations can be used to test the practical performance of used gas cleaning and gas separation steps. Additionally, the influence of changing product gas composition, nitrogen, sulfur, chlorine, ammonia, as well as tar and dust on the efficiency of different process steps could be investigated in detail.

- Achieved mass and energy balances have been used for a financial assessment of the developed production concept by net present value calculations. The results show that hydrogen production is strongly dependent on the future development of feedstock price. A realization of the created plant concept should be favored at at a FAME price of 960 €/t if the wood chip price is lower than 108 €/t_{atro} (24.3 €/MWh), and the natural gas price is higher than 55 €/MWh. Achieved results need to be compared with other alternatives to increase the share of renewable energy in a refinery.

The created hydrogen production concept represents a first plant of its kind and a mature possibility to reduce the fossil energy consumption of a refinery. The novel process uses equipment with high reliability. An installation of a hydrogen production plant from biomass is a possibility to increase the share of locally available feedstock and reduces required energy imports for mobility applications. This way, the elaborated plant concept can be seen as a promising option to increase the share sustainable resources for mobility applications.

8. Hydrogen-rich Gas from Biomass for Iron Production by Sorption Enhanced Reforming

Iron and steel are important base materials for various industrial applications. Moreover, iron and steel production is one of the main industrial causes for fossil CO_2 emissions. A main share of these CO_2 emissions arise due to the energy demand and the chemical reactions for the reduction of iron oxide (Fe_xO_y) to raw iron in a blast furnace at high temperatures of up to 2000°C. Major reaction partners for the reduction of iron oxide (Fe_xO_y) are carbon monoxide (CO) and hydrogen (H_2) provided by fuels like coal, natural gas, oil and plastic waste materials. (cf. **Eq. 8.1** to **Eq. 8.6**)[1, 2]

Eq. 8.1: $3\,Fe_2O_3 + CO \leftrightarrow 2\,Fe_3O_4 + CO_2$ $\Delta H = -35.1$ kJ/mol

Eq. 8.2: $3\,Fe_2O_3 + H_2 \leftrightarrow 2\,Fe_3O_4 + H_2O$ $\Delta H = -1.0$ kJ/mol

Eq. 8.3: $Fe_3O_4 + CO \leftrightarrow 3\,FeO + CO_2$ $\Delta H = -9.7$ kJ/mol

Eq. 8.4: $Fe_3O_4 + H_2 \leftrightarrow 3\,FeO + H_2O$ $\Delta H = 43.8$ kJ/mol

Eq. 8.5: $FeO + CO \leftrightarrow Fe + CO_2$ $\Delta H = -16.9$ kJ/mol

Eq. 8.6: $FeO + H_2 \leftrightarrow Fe + H_2O$ $\Delta H = 17.2$ kJ/mol

Existing emission reduction targets force the iron and steel industry in Europe to find new approaches to reduce their fossil CO_2 emissions. Therefore, several solution pathways are currently investigated by the iron and steel industry to raise the production efficiency and reduce fossil resource consumption. At worst, missing solution pathways could lead to a transfer of the iron production to regions outside of the European Union, where environmental regulations are not considered in an equal way.

Biomass gasification by sorption enhanced reforming enables a product gas composition which consists of components which are favorable for the chemical reduction of iron oxide (Fe_xO_y). Therefore, product gas from sorption enhanced reforming offers suitable characteristics for the usage as reducing agent. Additionally, calcium oxide (CaO) is a well known additive for the iron production process improving slag formation. Sorption enhanced reforming has been successfully demonstrated during experimental campaigns in the past, but up to now there is no large-scale plant in continuous operation. Within **Chapter 8** a novel concept for the integration of sorption enhanced reforming in iron and steel production is investigated. These investigations include:

- description of the initial situation, research tasks and aims,
- discussion of the process design for the production of a reducing agent,
- experimental sorption enhanced reforming results
  using limestone well known from raw iron production,
- simulation of an overall sorption enhanced reforming plant,
- the expected results for the created production plant,
- variations investigating key process figures influencing the plant performance,
- and an evaluation of the achieved results.

---

[1] Hubacek, 1994, p137ff

[2] Reaction enthalpies for listed reactions calculated by the use of HSC Chemistry 6.12 for 800°C

8.1. Initial Situation, Research Tasks & Aims

Different types of limestone are already part of raw iron production. Therefore, available limestone can also be employed as bed material operating sorption enhanced reforming. Besides, used limestone can be recycled after its employment as bed material within the gasifier system to the raw iron production. (cf. **Fig. 54**)

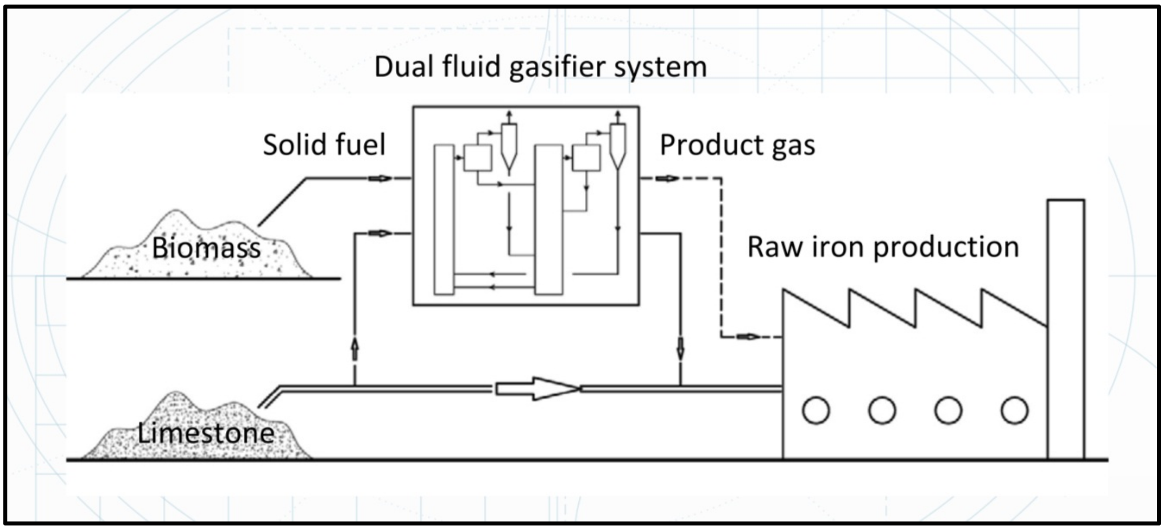

Fig. 54: Dual fluid gasifier system as a part of raw iron production[1]

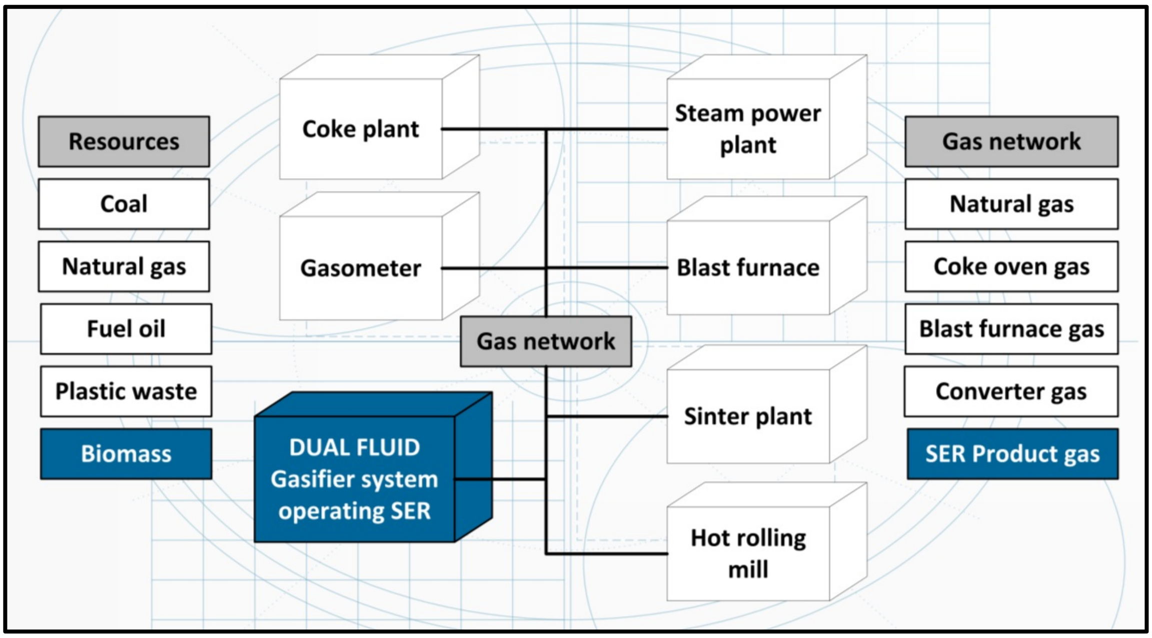

Fig. 55: Integration of a dual fluid gasifier into a metallurgical plant[2]

Fig. 55 shows a rough illustration of the gas network within a metallurgical plant which distributes different gas streams. **Tab. 38** lists values for different gas compositions distributed by the gas network. Whereas **Tab. 39** shows available limestone which are already part of the production process within the investigated metallurgical plant.

---

[1] illustration taken from the project proposal ERBA

[2] cf. Voestalpine, 2010, p49

Component / Property	Unit	Natural gas	Coke oven gas	Converter gas	Blast furnace gas
Hydrogen (H_2)	vol.-%$_{db}$	-	55 - 65	2 -4	2 – 4
Carbon monoxide (CO)	vol.-%$_{db}$	-	5 – 10	60 – 65	20 – 30
Carbon dioxide (CO_2)	vol.-%$_{db}$	-	-	10 – 15	20 – 25
Methane (CH_4)	vol.-%$_{db}$	90 – 99	20 – 25	-	-
Nitrogen (N_2)	vol.-%$_{db}$	-	5 – 10	15 – 20	45 – 60
Lower heating value	MJ/Nm³	~ 36	~ 18	~ 9	~ 4

Tab. 38: Rough gas compositions of gases operated within the gas network of a metallurgical plant

Limestone	$CaCO_3$	Particle size	Consumption
Unit	wt.-%	mm	t/a
KS_3	~88	1.0	36 000
KS_2	~94	1.0	74 000
KS_5	~98	1.1	3 700
KS_4	~94	0.5	8 000
KS_1	~93	2.2	524 000

Tab. 39: Limestone operated within the investigated metallurgical plant[1]

Within the present chapter a plant concept is investigated to enable the integration of a large-scale sorption enhanced reforming plant into the existing network of a metallurgical plant. The state of knowledge regarding sorption enhanced reforming already has been assessed before in **Chapter 4**. Additional experimental results achieved with limestone from raw iron production are used to calculate mass and energy balances for a novel plant concept with a thermal power of **100 MW**. The created plant concept aims for the production of a reducing agent with high reducing potential and high heating value.

8.2. Process Design for the Production of a Reducing Agent

Main sections for the production of a reducing agent by sorption enhanced reforming for raw iron production are

- fuel supply,
- gasification,
- gas cooling,
- gas treatment
- and gas utilization.

Wood chips are used as **fuel supply** and a wood chip dryer is used to maintain low fuel water content. For the **gasification** reactor limestone is used as bed material to follow the idea of the sorption enhanced reforming process. The consumed limestone can be reused outside of the described process as additive for example within the blast furnace. The application of sorption enhanced reforming enables hydrogen contents (H_2) within the product gas of 55-75 vol.-%$_{db}$ and leads to a gas composition which is comparable to coke oven gas. Even if the current state of knowledge regarding sorption enhanced reforming is mainly based on investigations using woody biomass as fuel, in future also waste materials could be a fuel supply option.

---

[1] according to information provided by Voestalpine

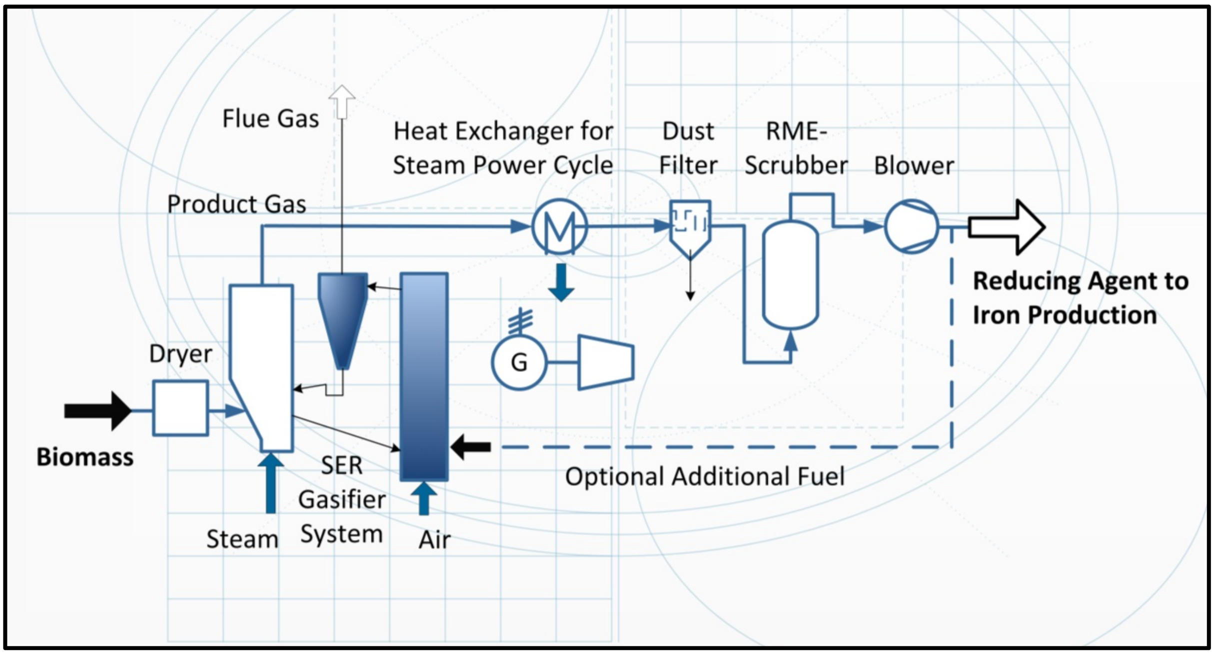

Fig. 56: Process design for the integration of a dual fluid gasifier running sorption enhanced reforming for raw iron production

Gas cooling is provided by heat exchangers arranged along the product gas stream. Available process heat is used for the existing demand within the gasification plant. Additionally, electricity has been identified by iron making operators as most valuable side product. Therefore, remaining high temperature process heat is used for the production of electricity by applying a steam power cycle. The **gas treatment section** includes a dust filter to remove dust, an RME-scrubber to remove tars and water from the gas stream. Finally, a blower provides the achieved reducing agent to the iron ore reduction. The combustor within the gasifier system can also operate oxyfuel combustion for subsequent carbon capture and storage (CCS) applications. The described overall process design has been used for the setup of a detailed plant layout.

8.3. Experimental Investigation Sorption Enhanced Reforming

Experimental investigations of sorption enhanced reforming in the past led to reliable data describing the process. This operation mode of the dual fluid gasifier has been proven at lab scale and industrial scale. At the same time, the achieved results pointed big differences between different types of limestone out with respect to achievable gas compositions and attrition.

As a part of present work, additional experiments have been carried out with “KS_1” to provide specific data for present investigations. “KS_1” is a type of limestone which is used as additive in blast furnaces as a part of raw iron production. Experimental investigations of sorption enhanced reforming with wood pellets and “KS_1_09_12”[1] were done from September to October 2012 with a 100 kW dual fluid gasifier at Vienna University of Technology. The same gasifier system has already been used for numerous experiments in the past. A precise description of the used gasifier can be found in literature.[2,3]

---

1 KS_1_09_12 stands for a specific batch of KS_1 from September 2012

2 Koppatz S., 2012, p10494

3 Schmid J.C., 2012, p207ff

On October 8th 2012 important process parameters were measured during a continuous sorption enhanced reforming operation with the limestone "KS_1_09_12". The measurements were performed to provide data for product gas composition, tar, dust and char content, as well as important process parameters like:

- hydrogen productivity rate,
- water conversion rate,
- bed material consumption,
- and CO_2 transport. (cf. definitions illustrated in **chapter 6**)

A precise description of used measurement systems and measuring methods can also be found in literature.[1] **Tab. 40** and **Tab. 41** show data for "KS_1_09_12" as it was used as bed material during the experiment. During the startup phase the bed material composition changed significantly because of the calcination reaction occurring above temperatures of 800°C. The weight of the bed material inventory changed significantly because of the release of CO_2. The exact bed material composition during the experiment can only be estimated by an analysis of used particles after the experiment, because so far, the experimental setup offers no possibility for solid samples during continuous operation.

Limestone	GLV wt.-%	CaO wt.-%	MgO wt.-%	SiO_2 wt.-%	Al_2O_3 wt.-%	Fe_2O_3 wt.-%	H_2O wt.-%
KS_1_09_12	44.4	51.7	3.6	0.1	0.1	0.1	0

Tab. 40: Chemical composition "KS_1_09_12"[2]

Term	Unit	Values before experiment	Values after experiment
Bed material particle density	kg/m³	2650	1800
Bed material bulk density	kg/m³	1400	980
Repose angle	°	23	23
Sauter mean diameter, d_{sv}	mm	0.425	0.385
Mean particle size, d_{p50}	mm	0.465	0.415
Size distribution d_{p10} –d_{p50} - d_{p90}	mm	0.375 – 0.465 - 0.550	0.315 – 0.415 - 0.540

Tab. 41: Characteristics of the particle inventory for the experiment "KS_1_09_12"

Tab. 42 depicts operational data for the used gasifier system during the experiment. The total experimental procedures were carried out between 06:00 am until 17:00 pm. During the experiment no fresh bed material was added.

Within **Fig. 57** data from the process control system can be found. The desired operation point has been identified during experimental tests before at September 10th 2012. On October 08th the same operation point was reached at 11:30 am and has been hold at a steady state until 13:15 pm for two tar measurements. Until 13:15 pm 3.3 kg of bed material left the gasifier system and were separated from a subsequent cyclone. This bed material loss is estimated by the use of the cyclone and exact numbers could not be measured. A bed material inventory loss of ~1.6 kg/h was registered by the described method.

---

[1] Schmid J.C., 2012, p207ff

[2] according to information provided by Voestalpine; GLV: glowing loss;

Operation parameter	Unit	Typical Values[1]	SER – Oct. 8th 2012
Bed material particles	-	Olivine	KS_1_09_12
Bed material particle density	kg/m³	2850	2650 – 1800
Bed material inventory	kg	100	100 (68)*
Gasification reactor			
Typical fluidization regime	-	bubbling bed	bubbling bed
Steam to fuel ratio	$kg_{H2O}/kg_{fuel,waf}$	0.8 – 1.1	0.9
Thermal power, feed gasifier (wood pellets)	kW	66 – 97	73
Temperature, gasifier	°C	800 – 810	650 – 720
Cross sectional area, gasifier	m^2	0.073	0.073
Superficial gas velocity, U	m/s	0.41 – 0.56	0.29 – 0.32
Fluidization ratio, U/U_{mf}	-	2.1 – 5.6	2.5 – 4.6
Fluidization ratio, U/U_t	-	0.06 – 0.12	0.06 – 0.1
Estimated gas residence time (bubbling bed)	s	0.27 – 0.37	0.4 – 0.5
Estimated gas residence time (freeboard)	s	3 – 4	5 – 6
Combustion reactor			
Typical fluidization regime	-	fast bed	fast bed
Thermal power, additional fuel to combustion	kW	22 – 31	7
Temperature, combustion zone	°C	840 – 900	820 – 860
Cross sectional area, combustor	m^2	0.0075	0.0075
Superficial gas velocity, U	m/s	8.8 – 10.1	6.9 – 7.7
Fluidization ratio, U/U_{mf}	-	44 – 100	90 - 170
Fluidization ratio, U/U_t	-	1.3 – 2.3	2.1 – 3.5
Estimated mean gas residence time	s	0.73 – 0.85	0.9 – 1.1
* value in brackets weight of inventory according to estimated composition after partial calcination			

Tab. 42: Operation data - 100 kW dual fluid gasifier – Conv. gasification compared to SER

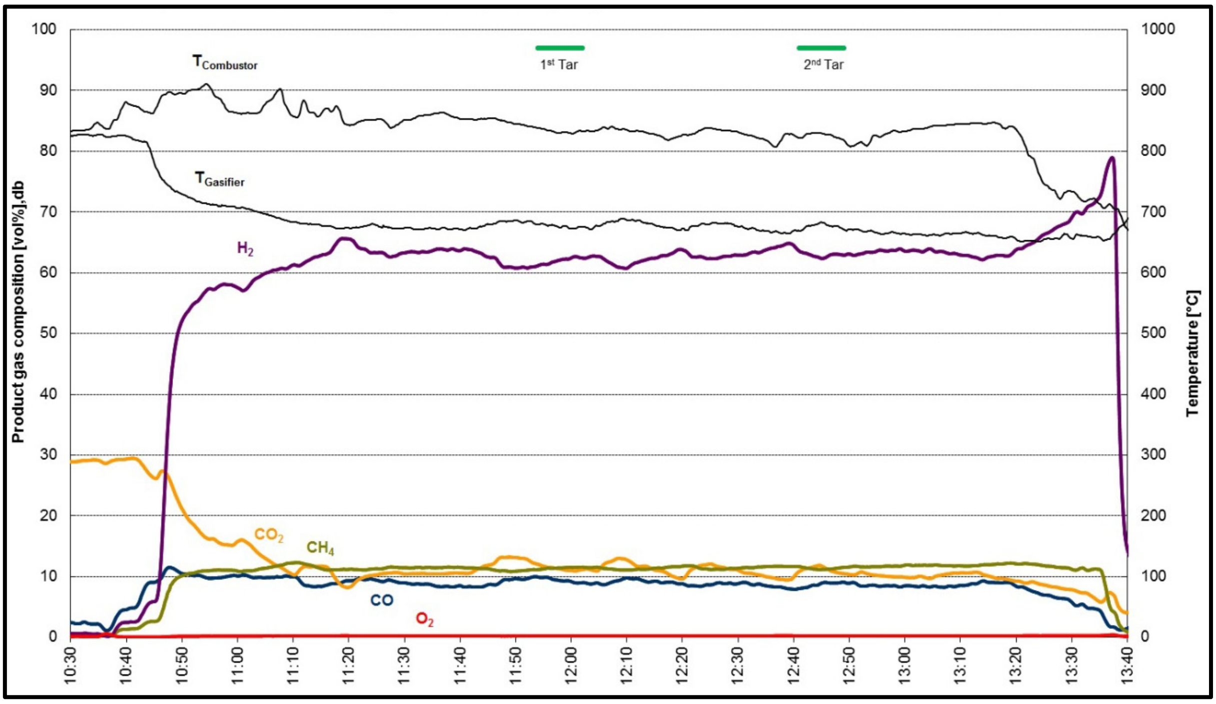

Fig. 57: Progress of experimental procedure according to process control system – October 08th 2012

---

[1] Schmid J.C., 2012, p207

Fig. 57 shows the progress of

- the temperature in gasifier and combustor,
- the composition of the product gas stream (H_2, CO_2, CH_4, CO, O_2),
- and the timing of the tar measurement points

during the experiment. Measured values between 11:30 am und 13:15 pm have been used for a detailed evaluation of the overall performance. Therefore, the collected data between 11:30 am and 13:15 pm has been analyzed by the use of

- mean value calculations of measured values with Microsoft excel,
- mass and energy balance data validation using IPSEpro,
- and the calculation of key figures describing the process performance.

Tab. 43 shows the results of this analysis in comparison with typical values of the experimental facility achieved conventional operation using olivine as bed material. The results show, that the experiment has been conducted with low thermal fuel power and lower bed material inventory. Only low amounts of additional fuel were fed to the combustor due to high amounts of remaining char from the gasification reactor. Low gasification temperatures have been conducted by a low bed material circulation rate controlled by the fluidization of upper and lower loop seal.

The achieved product gas composition can be described as a typical gas composition from sorption enhanced reforming. High steam to fuel ratio was required in order to maintain the hydrodynamics within the gasifier system. Consequently, high water content was measured within the product gas stream. The conducted tar measurements showed a comparably low tar content despite the low gasification temperatures.

Key process figures have been analyzed through an IPSEpro calculation of the entire mass and energy balance by using the experiment validation mode. The results show a high hydrogen production rate enforced by a relatively high water conversion rate. Additionally, sorption enhanced reforming enables improved cold gas efficiency due to the lower gasification temperature. Thermodynamic aspects of the process have been discussed already literature[1].

In comparison the performance of "**KS_1_09_12**" was better than an average limestone type with respect to the reducing potential of the achieved product gas composition. Simultaneously, only a small share of potential CO_2 load was activated during the experiment. There was no decay of CO_2 loading recognizable likely due to the short operation time. The registered loss of bed material was estimated with 1.6 kg/h together with an operated inventory of approximately 68 kg. This numbers equal a loss of bed material in the range of 2.5 wt.-%/h. During the experiment no fresh bed material was fed to the gasifier system.

Overall, the experiment demonstrated the capability of "KS_1_09_12" as bed material for sorption enhanced reforming. Further experimental investigations need to focus on an improved control of bed material circulation rate as well as on an investigation of long time particle performance with respect to the decay of CO_2 load. Achieved experimental results with „ KS_1_09_12 " are included into the considerations for the setup of a detailed plant layout based on the before described process design (cf. **Fig. 56**).

---

[1] cf. Müller S., 2012

Operation parameter	Unit	Typical Values[1,2]	SER – Oct. 8th 11:30 – 13:15 Measured	SER – Oct. 8th 11:30 – 13:15 IPSE Analysis[3]
Gasifier system				
Bed material	-	Olivine	"KS_1_09_12"	"KS_1_09_12"
Fuel type	-	wood pellets	wood pellets	wood pellets
Gasification temperature	°C	800 - 860	674	679
Combustion temperature	°C	840 - 940	836	838
Feedstock / fuel input gasifier (wood chips)	kg/h	15 - 20	15	15
Feedstock / fuel input gasifier (wood chips)	kW	74 - 97	73	73
Additional fuel to combustion reactor	kW	22 - 23	7	7
Overall fuel input	kW	98 - 120	80	80
Product gas yield	Nm^3/h	14 - 22	-	12
Lower heating value of product gas	MJ/Nm^3	12 - 14	-	13.6
Product gas power	kW	50 - 60	-	46
Steam fluidization gasifier	kg/h	5 - 11	6	8
Steam fluidization upper & lower loop seal	kg/h	3 - 10	8	8
Fluidization secondary air combustor	Nm^3/h	30 - 50	35	37
Ratio primary air to secondary air	-	0.08 - 0.1	0.13	0.12
Steam to fuel ratio	$kg_{H_2O}/kg_{fuel,waf}$	0.5 – 1.0	-	0.9
Product gas composition				
Hydrogen (H_2)	vol.-%$_{db}$	34 – 43	62.9	63.9
Carbon monoxide (CO)	vol.-%$_{db}$	22 - 30	8.8	8.9
Carbon dioxide (CO_2)	vol.-%$_{db}$	15 – 25	11.0	11.0
Methane (CH_4)	vol.-%$_{db}$	8 – 12	11.5	11.8
Ethene (C_2H_4)	vol.-%$_{db}$	1.5 – 3.5	1.2	1.3
Ethane (C_2H_6)	vol.-%$_{db}$	0.5 – 1.0	0.9	0.9
Propane (C_3H_8)	vol.-%$_{db}$	0.2 - 0.5	0.05	0.05
Water (H_2O)	vol.-%	32 – 49	51.7	50.3
Tar content (GC-MS/gravimetric)	g/Nm^3	3-9 / 2 - 4	5.3 / 2.3	6.4
Dust content	g/Nm^3	n.a.	7.7	7.4
Char content	g/Nm^3	n.a.	5.4	5.2
Key figures gasifier system				
Relative water conversion rate	$kg_{H_2O}/kg_{fuel,waf}$	0.07 – 0.14	-	0.23
Absolute water conversion rate	kg_{H_2O}/kg_{H_2O}	0.09 - 0.16	-	0.25
Logarithmic deviation from CO-Shift eq.	-	(-0.3) – (-0.5)	-	(-0.37)
Hydrogen productivity rate	kg_{H_2}/kg_H	n.a.	-	0.29
Cold gas efficiency experiment	%	50 – 55	-	58
Char combusted in combustion chamber	$kg_{char}/kg_{fuel,waf}$	n.a.	-	0.20
Air ratio combustor	-	n.a.	-	1.4

Tab. 43: Experimental data – sorption enhanced reforming October 08th 2012 compared to typical results of conventional dual fluid gasification with olivine

---

1 Koppatz S., 2012, p10494; 2 Schmid J.C., 2012, p207
3 according to used evaluation method research group gasification and gas cleaning

Operation parameter	Unit	Reference Values cf. Tab. 30	SER – Oct. 8th 11:30 – 13:15 Measured	SER – Oct. 8th 11:30 – 13:15 IPSE Analysis[3]
Key figures sorption enhanced reforming				
Calcium circulation rate	h^{-1}	~ 3.2	-	3
Bed material renewal rate	h^{-1}	~ 0.065	0	-
CO_2 load	kg_{CO2}/kg_{CaO}	~ 0.16	-	0.05
CO_2 load	mol_{CO2}/mol_{CaO}	~ 0.20	-	0.06
Operation time of particles within gasifier system	h	~ 15	2.5	-
Operated SER cycles within gasifier system	-	~ 50	-	8

Tab. 44: Experimental data – sorption enhanced reforming October 08th 2012

8.4. Plant Layout for the Production of a Reducing Agent

Fig. 58 shows the detailed plant layout for the described process. The illustrated plant layout is quite similar comparing to the reference case (cf. **Fig. 36**) and in comparison to the presented layout for a hydrogen production for a refinery (cf. **Fig. 48**). Main differences can be found in the gasification and gas cooling section.

The shown plant is based on limestone ("KS_1") instead of olivine as bed material to reach high hydrogen output and higher reducing potential of the product gas. The gasification temperature is reduced to 675°C to enable the sorption enhanced reforming process. Experimental results are used for the expected product gas composition. After gas cooling and gas cleaning the product gas is directly used as a reducing agent for the raw iron production.

The utilization of process heat is focused on electricity production by the use of a steam power cycle. Several heat exchangers in the product and exhaust gas stream enable the operation of the steam power cycle.[1] Many manufactures offer small size steam turbines for the illustrated application.[2] The chosen steam power cycle set-up is based on the results of an inquiry addressed to different manufacturers. Chosen set-up uses a two stage process including a middle- and a low-pressure turbine which additionally allows heat supply for the biomass dryer cycle at an adequate temperature level.

The created plant layout enabled the creation of a simulation model for the calculation of mass- and energy balances. Used initial values are based on the reference case (cf. **Chapter 6**) complemented by additional values shown in **Tab. 45** and **Tab. 46**, as well as the achieved experimental results with „ KS_1_09_12 ".

---

[1] cf. Strauß K., 2009, p249ff.

[2] cf. www.siemens.com/energy; www.mandieselturbo.com; www.geoilandgas.com; (read at July 1st, 2011)

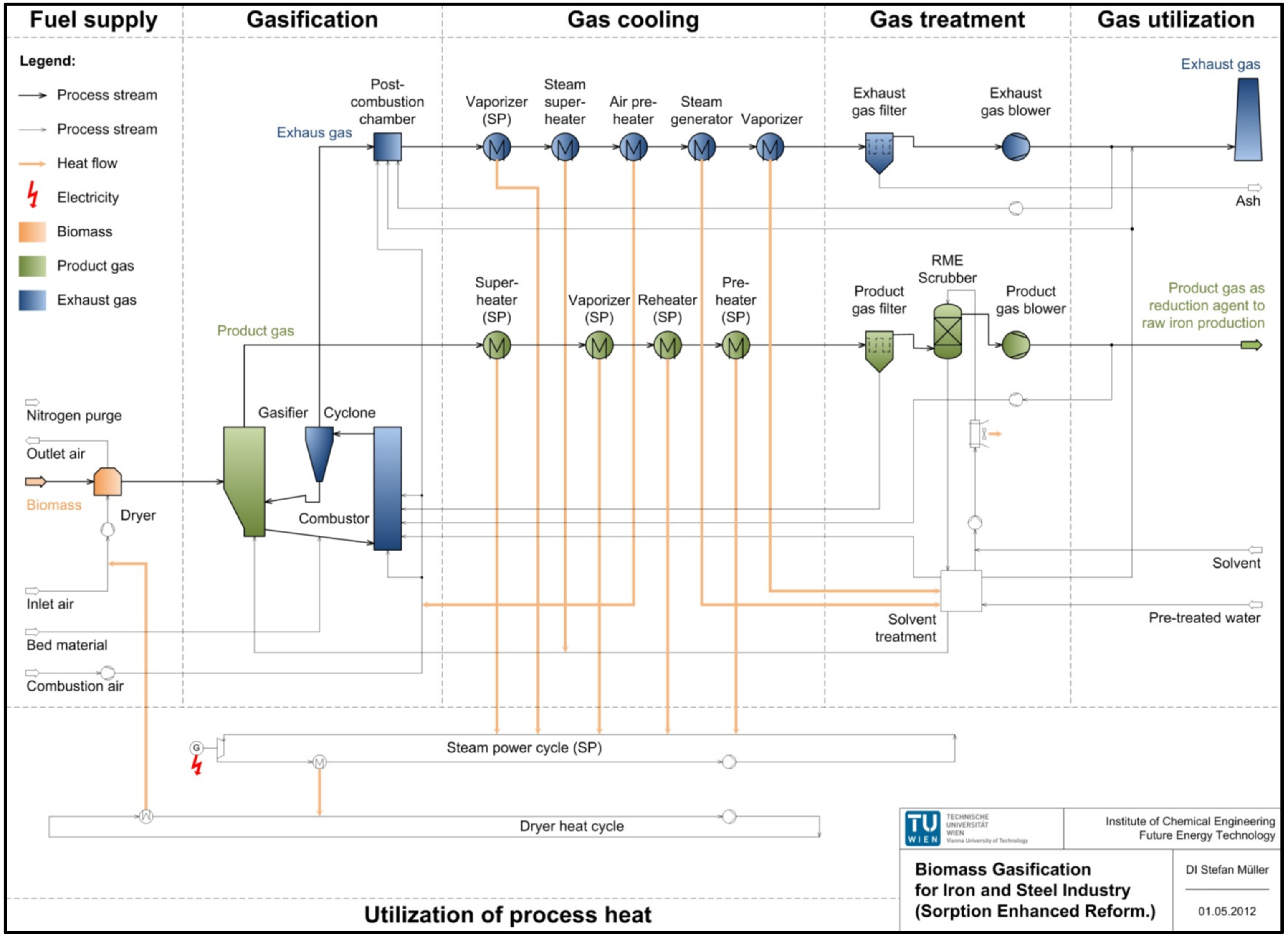

Fig. 58: Layout of a dual fluid gasification plant for the production of and reducing agent for the iron production

Term	Unit	Value	Char.[1]	Data source
Plant output				
Thermal power produced reducing agent	MW	100	S	demanded by operator
Fuel supply				
Biomass water content before dryer	wt.-%	40	S	Tab. 23
Biomass water content after dryer	wt.-%	20	S	Tab. 23
Dryer inlet air temperature	°C	80	S	Tab. 23
Gasification				
Steam temperature for gasifier fluidization	°C	450	S	cf. Pröll T., 2004, p214
Combustion temperature air for combustor	°C	400	S	cf. Pröll T., 2004, p214
Gasification temperature	°C	675	S	cf. chapter 4.2; Tab. 43
Combustion temperature	°C	900	S	cf. Pröll T., 2004; Tab. 43
Steam to fuel ratio	$kg_{H_2O}/kg_{fuel,waf}$	0.55	S	cf. Tab. 22; Tab. 43
Char combusted in combustion chamber	$kg_{char}/kg_{fuel,waf}$	0.18	S	cf. Tab. 22; Tab. 43
Air ratio	-	1.4	S	cf. Tab. 22; Tab. 43
Product gas composition at the exit of the gasifier				
Water (H_2O)	vol%	34.6	R	cf. steam to fuel ratio
Hydrogen (H_2)	vol.-%db	63.4	R	cf. Tab. 13; Tab. 43
Carbon monoxide (CO)	vol.-%db	9.1	S	cf. Tab. 13; Tab. 43
Carbon dioxide (CO_2)	vol.-%db	11.3	S	cf. Tab. 13; Tab. 43
Methane (CH_4)	vol.-%db	11.9	S	cf. Tab. 13; Tab. 43
Ethene (C_2H_4)	vol.-%db	1.3	S	cf. Tab. 13; Tab. 43
Ethane (C_2H_6)	vol.-%db	1.0	S	cf. Tab. 13; Tab. 43
Propane (C_3H_8)	vol.-%db	0.1	S	cf. Tab. 13; Tab. 43
Oxygen (O_2)	vol.-%db	0.15	S	cf. Tab. 10
Nitrogen (N_2)	vol.-%db	1.7	R	cf. N_2 purge
Hydrogen sulfide (H_2S)	vol.-%db	0.007	R	cf. biomass, Tab. 18
Ammonia (NH_3)	vol.-%db	0.0015	S	cf. Tab. 8
Hydrogen chloride (HCl)	vol.-%db	0.0007	R	cf. biomass, Tab. 18
Hydrogen cyanide (HCN)	vol.-%db	0.00015	S	cf. Tab. 8
Dust particles	g/Nm^3	5	S	cf. Tab. 13; Tab. 43
Char	g/Nm^3	5	S	Tab. 43
Tar	g/Nm^3	5	S	cf. Tab. 13; Tab. 43
Gas cooling				
Product gas temperature after gas cooling	°C	150	S	cf. Pröll T., 2004, p213
Exhaust gas temperature after gas cooling	°C	160	S	cf. Pröll T., 2004, p214
Steam power cycle				
Inlet pressure – middle pressure turbine	bar	80	S	cf. Siemens SST-200
Inlet temperature – middle pressure turbine	°C	460	R	cf. Siemens SST-200
Inlet pressure – low pressure turbine	bar	2.0	S	cf. Siemens SST-200
Inlet temperature – low pressure turbine	°C	120	R	cf. Siemens SST-200
Outlet pressure – low pressure turbine	bar	0.05	S	cf. Siemens SST-200
Isentropic efficiency	%	80	S	cf. Siemens SST-200
Electrical efficiency (drive system)	%	96	S	cf. Siemens SST-200
Mechanical efficiency (drive system)	%	98	S	cf. Siemens SST-200

Tab. 45: Values for the calculation of mass- and energy flows for the production of a reducing agent

---

[1] Character of value: set value (S) or resulting value (R)

Term	Unit	Value	Char.	Data source
Gas treatment – filter				
Filter - Dust content of product gas after filter	mg/Nm³	30	S	cf. Kirnbauer F., 2011a
Filter - Tar content of product gas after filter	g/Nm³	0.5	S	cf. Kirnbauer F., 2011a
Gas treatment – RME scrubber				
Gas temperature before RME-scrubber	°C	150	S	cf. Pröll T., 2004, p213
Gas temperature after RME-scrubber	°C	40	S	cf. Pröll T., 2004, p213
Saturation of gas (water content) after scrubber	%	100	S	-
Tar content of gas after scrubber	mg/Nm³	25	S	cf. Kirnbauer F., 2011a

Tab. 46: Values for the calculation of mass- and energy flows for the production of a reducing agent

8.5. Additional Oxyfuel Combustion for CCS Applications

The created plant layout for the production of a reducing agent prevents fossil CO_2 emissions by the utilization of biomass. Carbon capture and storage (CCS) technologies are used to enable a safe disposal of fossil CO_2 emissions. Therefore, carbon capture within a dual fluid gasification plant could be used to enable an additional reduction of CO_2 emissions. This reduction would lead to an additional improvement of plant emissions in terms of the European emission allowances trading scheme.

The created simulation model allows an investigation of the benefits of additional carbon capture. Hence, the simulation model has been used to calculate a plant operating the **oxyfuel combustion** process together with sorption enhanced reforming. Oxyfuel combustion process is currently considered as one of the most economic carbon capture processes. For the combustion process, pure oxygen mixed with exhaust gas is used instead of air. This way, the combustion process leads to high CO_2 contents in the exhaust gas stream and offers good characteristics for an efficient disposal.

An extension of the plant layout by the oxyfuel combustion process can be calculated by small changes within the simulation model. The combustion air stream is replaced by a stream of **pure oxygen mixed with exhaust gas**. This oxygen enriched exhaust gas is used for fluidization of the combustor and for the post-combustion chamber.

Oxyfuel combustion is a relatively new, complex and sensitive process. The process has been proven at lab and pilot scale.[1] An inappropriate operation can cause an inhomogeneous combustion with negative effects on reactor materials. Based on existing experimental results, the oxygen enrichment of the oxygen-exhaust gas mixture has been set to the maximum **oxygen content** of **30 vol.-%** and is preheated to a temperature of 350°C. These set operation parameters have been chosen as a balance between operation efficiency, operation safety and existing operation experience.[2]

---

[1] cf. Höltl W., 2010

[2] cf. Tondl G., 2013, p23ff, p61ff, p90ff

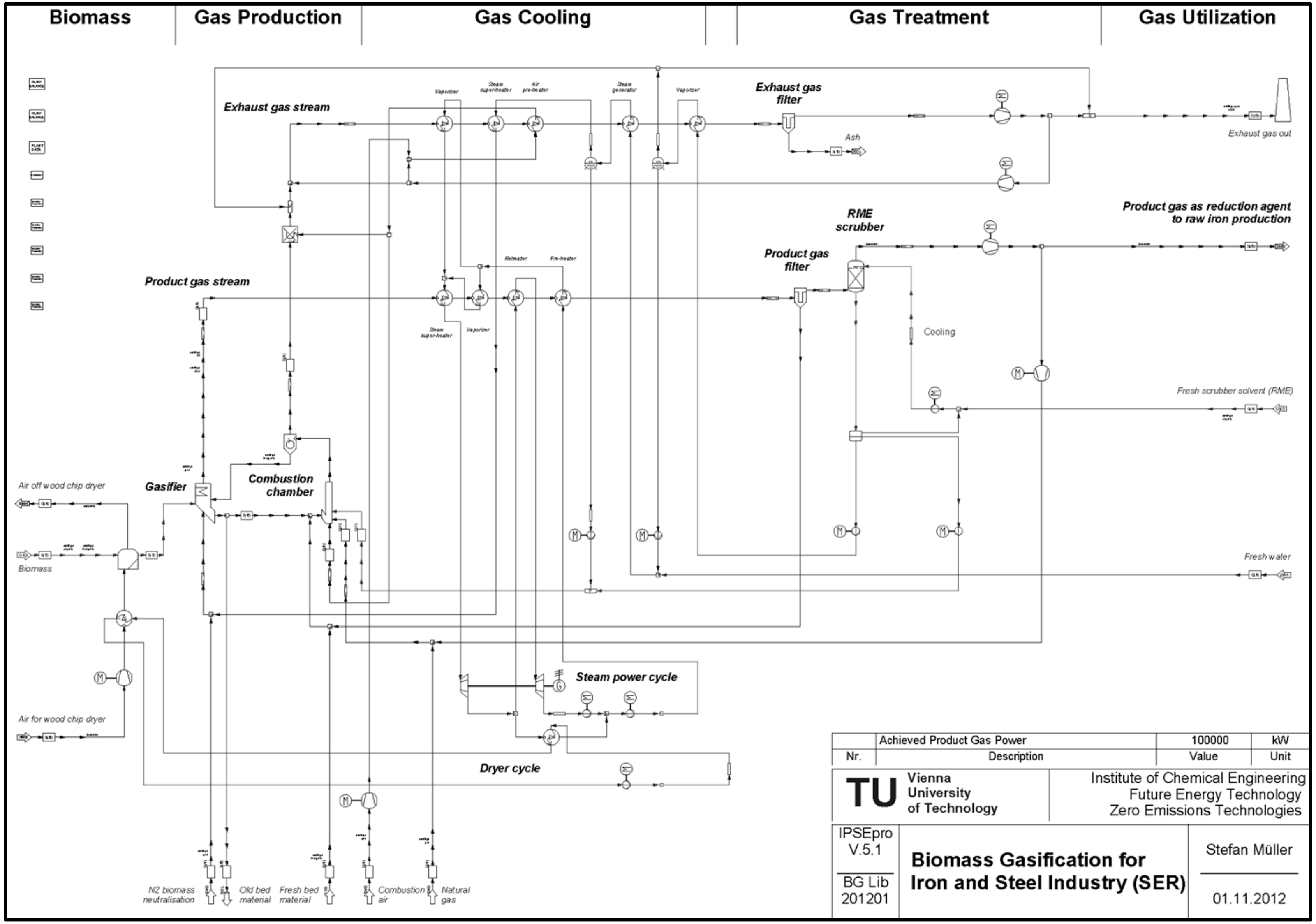

Fig. 59: Simulation flow sheet for an entire plant for the production of a reducing agent

8.6. Simulation Results

Fig. 59 depicts a flow chart of the simulation model used for the calculation of mass and energy balances for the production of a reducing agent by using the sorption enhanced reforming process. **Tab. 47** shows the results for a regular operation based on the described initial values (cf. **Tab. 45** and **Tab. 46**). Beside the regular operation illustrated in **Tab. 47**, an additional simulation run was carried out including the oxyfuel combustion process as described in **Chapter 4.5**. **Tab. 48** shows the results for this additional simulation run.

Plant input			Plant output		
Term	Unit	Value	Term	Unit	Value
Biomass (wood chips)	kg/h	50 341	Product gas (reducing agent)	Nm^3_{wet}/h	28 396
Biomass water content	wt.-%	40	Product gas (reducing agent - lhv)	MJ/kg_{wet}	22.88
Biomass (lhv)	MJ/kg	9.53	Product gas (reducing agent - lhv)	MJ/Nm^3_{wet}	12.68
Biomass (chem. energy)	kW	133 230	Product gas (water content)	vol%	7.81
Electricity consumption	kW	2 785	Product gas (red. agent - chem. en.)	kW	100 000
Fresh scrubber solvent (RME)	kg/h	200	Electricity – steam power (gross)	kW	5 544
Bed material inventory	kg	25 000	Electricity – steam power (net)	kW	2 758
Fresh bed material (limestone)	kg/h	5 000	Exhaust gas	kg/h	122 659
Fresh water	kg/h	378	Ash and dust from exhaust gas filter	kg/h	978
Natural gas	Nm^3/h	0	Old bed material out	kg/h	2500
Nitrogen (N_2) purge	Nm^3/h	500	Disposable CO_2	t/h	0
Oxygen (O_2)	Nm^3/h	0			

Gasifier system:

Cold gas efficiency:	71.9 %
Relative water conversion rate:	0.18 $kg_{H2O}/kg_{fuel.waf}$
Absolute water conversion rate:	0.33 kg_{H2O}/kg_{H2O}
Hydrogen productivity rate:	0.41 kg_{H2}/kg_{H}
Calcium circulation rate:	6.75 h^{-1}
Bed material renewal rate:	0.13 h^{-1}
CO_2 load:	0.11 kg_{CO2}/kg_{CaO}
CO_2 load:	0.14 mol_{CO2}/mol_{CaO}
Operation time of particles within gasifier system:	7.5 h
Operated SER cycles within gasifier system:	50

Tab. 47: Simulation results – production of a reducing agent for the iron and steel industry

The findings reveal that **100 MW** of product gas can be produced from **133.2 MW** of wood chips. Additional, **2.8 MW** of electricity can be supplied as a net plant value. The product gas consists of **63 vol.-%$_{db}$ of hydrogen (H_2)**, of 9 vol.-%$_{db}$ of carbon monoxide (CO) and 12 vol.-%$_{db}$ of methane (CH_4). Mentioned gas components determine the reducing potential of the supplied gas stream. Low gasification temperature leads to an increased char transport from the gasifier to the combustor. Fresh bed material is fed to the gasifier system to maintain demanded CO_2 load capability. In the present case, operated bed material is expected to provide a CO_2 load of 0.14 mol_{CO2}/mol_{CaO} after 50 cycles. Worse performance would demand for more fresh bed material and would induce reduced cold gas efficiency. High performing bed material maintaining high CO_2 load would allow an additional improvement of the gas composition favorable for the iron ore reduction. The simulation results display a comparably high hydrogen productivity rate for the sorption enhanced reforming process.

Plant input			Plant output		
Term	Unit	Value	Term	Unit	Value
Biomass (wood chips)	kg/h	50 404	Product gas (reducing agent)	Nm^3_{wet}/h	28 396
Biomass water content	wt.-%	40	Product gas (reducing agent - lhv)	MJ/kg_{wet}	22.88
Biomass (lhv)	MJ/kg	9.53	Product gas (reducing agent - lhv)	MJ/Nm^3_{wet}	12.68
Biomass (chem. energy)	kW	133 398	Product gas (water content)	vol%	7.81
Electricity consumption	kW	2 458	Product gas (red. agent - chem. en.)	kW	100 000
Fresh scrubber solvent (RME)	kg/h	200	Electricity – steam power (gross)	kW	6 604
Bed material inventory	kg	25 000	Electricity – steam power (net)	kW	4 147
Fresh bed material (limestone)	kg/h	5 000	Exhaust gas	kg/h	40 226
Fresh water	kg/h	378	Ash and dust from exhaust gas filter	kg/h	1 054
Natural gas	Nm^3/h	0	Old bed material out	kg/h	2 500
Nitrogen (N_2) purge	Nm^3/h	500	Disposable non fossil CO_2	t/h	36.1
Oxygen (O_2)	Nm^3/h	11 024			

**Tab. 48: Simulation results including oxyfuel combustion –
production of a reducing agent for the iron and steel industry**

Oxyfuel combustion within the combustor of the gasifier system enables the subsequent disposal of CO_2 as "Carbon Capture & Storage" application. The additional oxygen consumption causes increased operation costs. Oxyfuel combustion at the same time leads to a reduced exhaust gas stream. Furthermore, the combustion process is operated at a higher combustion temperature of about 950°C to provide the necessary conditions for the calcination reaction in the surrounding of high partial pressure of CO_2. High combustion temperature and high specific heat factor (C_p) of CO_2 raise the overall fuel demand of the gasifier system. Simultaneously, an efficient operation of the combustion chamber by the set configuration of combustion parameters can compensate this higher fuel demand. Illustrated values within **Tab. 48** enable an evaluation of a potential integration of the oxyfuel combustion process.

8.7. Key Figures Describing the Hydrogen Output

The illustrated simulation results indicate a higher hydrogen productivity of sorption enhanced reforming compared to conventional gasification. The hydrogen output is dominated by the remaining thermodynamic distance to the equilibrium of the water gas shift reaction (cf. **Eq. 6.14**). Thermodynamic equilibrium ($\delta_{(Eq.WGS-shift)} = 0$) enables

- high water conversion rates,
- and because of that high hydrogen productivity rate

dependent on the present gasification temperature and the catalytic influence of used bed materials. The following parameters could be used to increase the hydrogen output:

- improved cold gas efficiency,
- low bed material renewal rate,
- gasification temperature,
- catalytic influence of used bed materials,
- better gas-solid contact in the gasification reactor,
- higher residence times for gas as well as fuel and bed material particles

The outcome depicted in **Tab. 47** indicates that a hydrogen productivity of 0.41 kg_{H2}/kg_{H} has been obtained.

8.8. Hydrogen Mass Flow Analysis

Fig. 60 shows a mass flow chart reflecting the elementary mass flow of hydrogen atoms through the gasifier system operating in sorption enhanced reforming mode. Presented illustration is based on a similar approach as already described within **Chapter 7.6**. Achieved gaseous hydrogen (H_2 – red) within the product gas stream mainly arises from the conversion of dry biomass (C_xH_y – white) as well as from the conversion of water (H_2O – blue). Beforehand presented simulation results indicated an absolute water conversion rate of 0.33 kg_{H2O}/kg_{H2O}. This comparably high water conversion rate can be explained by

- a lower gasification temperature with a favorable influence on the thermodynamic equilibrium of the water gas shift reaction,
- increased hydrogen (H_2) production by continuous removal of carbon dioxide (CO_2) following the principle of "Le Chateliers",
- and catalytic effects of the used bed material favoring hydrogen (H_2) production due to catalyzed water gas shift reaction.[2,3,4]

These effects can be seen within the hydrogen mass flow chart as a comparably large hydrogen mass flow (1511 kg/h H_2 – red) and reduced water mass flow (1263 kg/h H_2O – blue). Besides, low gasification temperatures, in the present case 675°C, imply higher amounts of residual char (C_xH_y – white) which is transported to the combustion chamber.

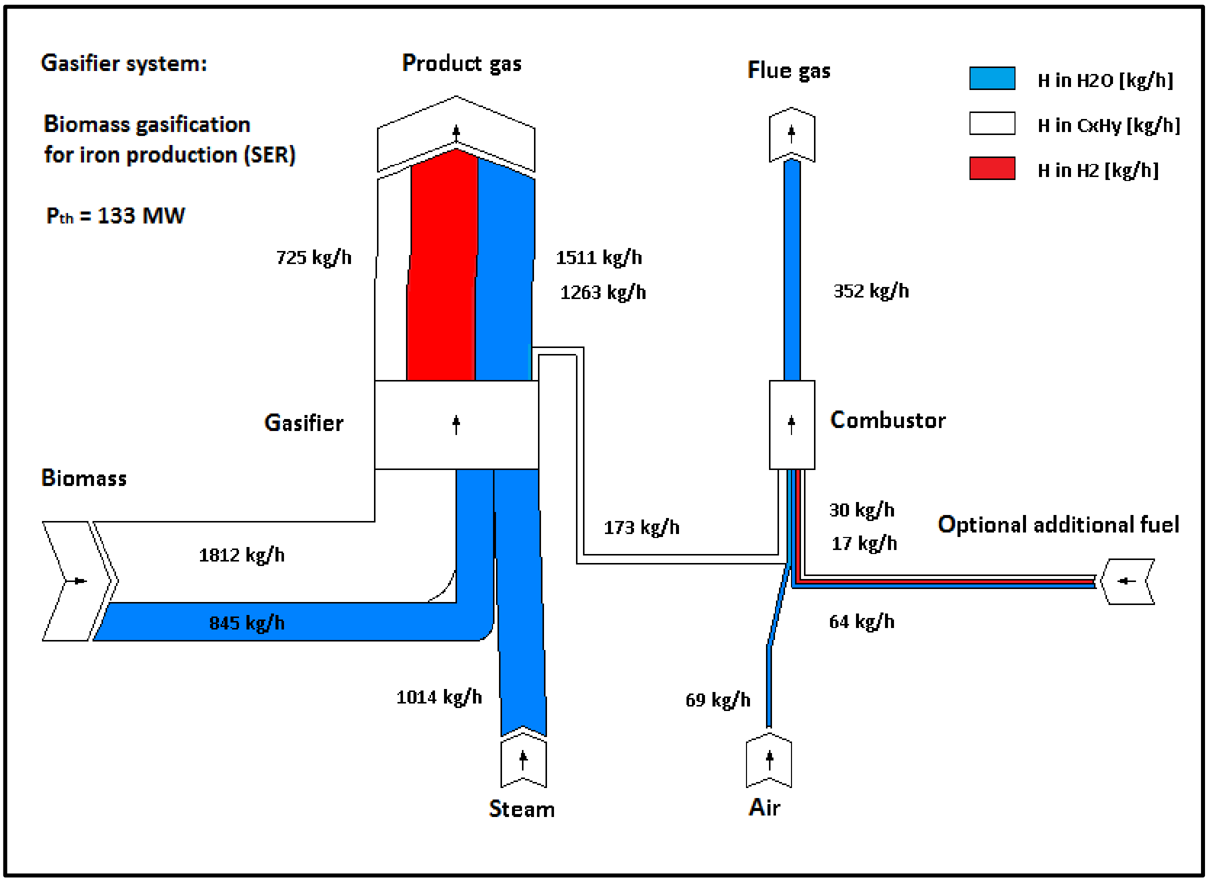

Fig. 60: Hydrogen mass flow chart for the used gasifier system operating SER

---

[1] cf. Eq. 3.6 in Chapter 3

[2] cf. S. Koppatz, 2009a, p712ff.

[3] cf. Z. Abu El-Rub, 2004, p6911ff.

[4] cf. D. Sutton, 2001, p155ff.

8.9. Variation of Sensitive Parameters

IPSEpro enables ceteris paribus variations of important process parameters to show the influence of single parameters on the plant behavior. **Fig. 61** depicts results of variations carried out to show the impact of main parameters relevant for the overall plant performance. Necessary bed material renewal and maintained CO_2 load have strong influence on the plant efficiency as well as on the product gas composition.

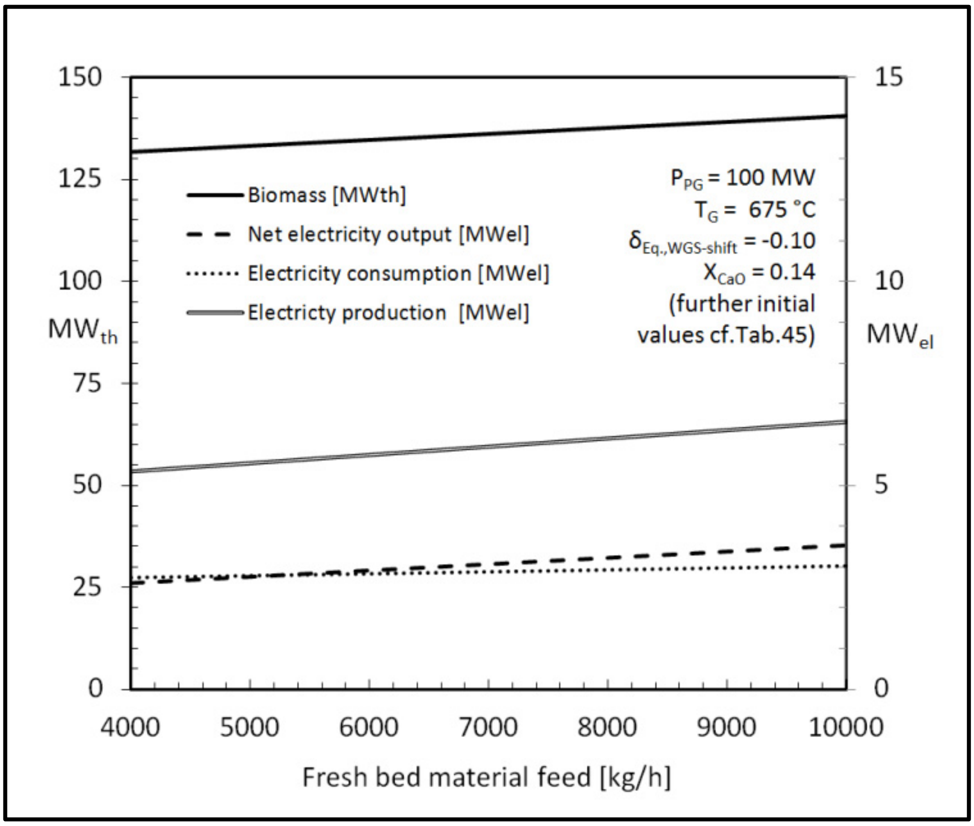

Fig. 61: Major plant characteristics as a function of the CO_2 load of the used bed material

So far, the used bed material "KS_1" has only be used to operate sorption enhanced reforming within experimental facilities. At the current stage of development, the long time performance of "KS_1" within a large-scale dual fluid gasifier system has not been measured. Necessary bed material renewal and maintained CO_2 load can only be estimated by theoretical considerations as well as the indicated results of the experimental investigations.

Fresh bed material fed to the gasifier system can be used to maintain high CO_2 load (cf. **Chapter 4.3**). High amounts of fresh bed material are at the same time a drawback due to the fact that cold gas efficiency is reduced by a raising stream of fresh cold bed material which needs to be heated up to the present temperatures within the gasifier system. **Fig. 61** depicts the influence of fresh material on biomass consumption, electricity consumption as well as electricity production. Reduced cold gas efficiency results in increased electricity consumption due to higher loads on blowers and to increased electricity production due to a higher share of available heat.

Fig. 62 shows the influence of the operated CO_2 load on the product gas composition with respect to the reaction partners of the water gas shift reaction.

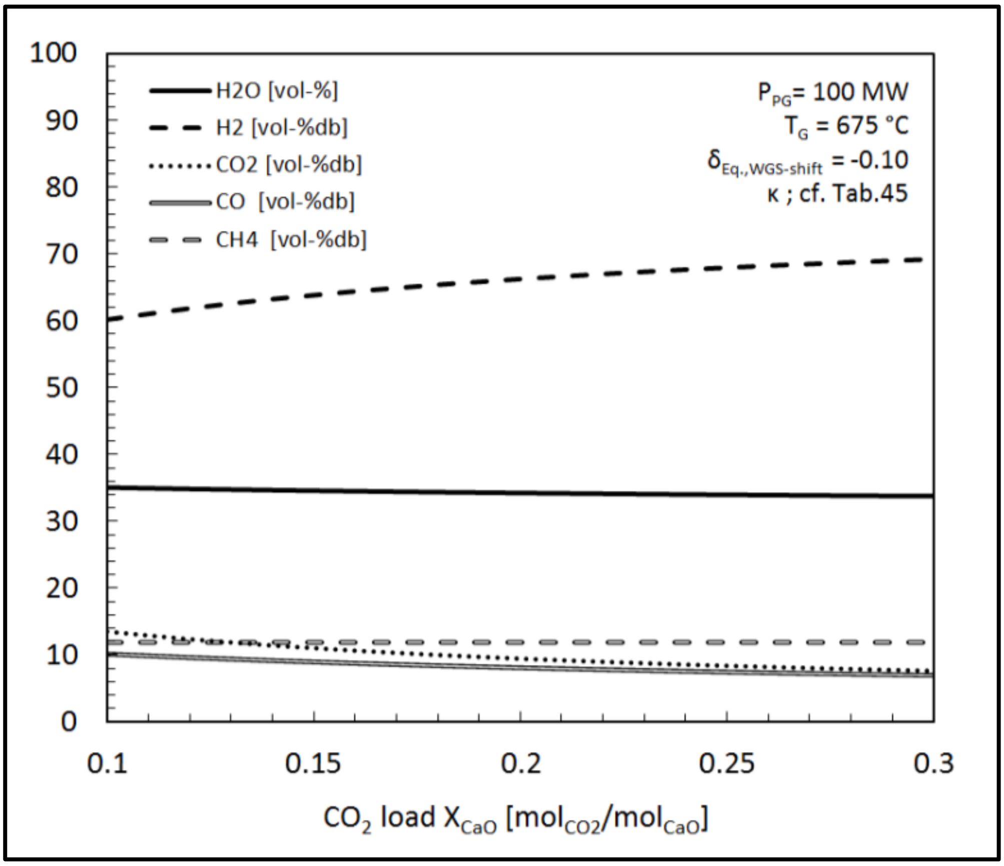

Fig. 62: Product gas composition as a function of the CO_2 load of the used bed material

High CO_2 load can be used to improve the hydrogen content in the product gas. Therefore, limestone particles are desired which maintain high CO_2 load over long operation times. The practical long time performance of "KS_1" needs to be investigated on small-scale before the implementation in a large-scale facility to ensure adequate process efficiency.

Within the present case used bed material particles can be reused within the raw iron production process. This way, the drawback of high bed material consumption can be reduced by the local preconditions.

8.10. *Economic Evaluation – Reducing Agent from SER*

Achieved simulation results enable an assessment by net present value calculations. Necessary cost rates are again taken from the reference case according to **Tab. 24**. Additional cost rates and expected investment costs for the described plant are shown in **Tab. 49**. The investigated business case compares the traditional utilization of coal and natural gas with the setup plant concept. **Tab. 50** shows the results of the evaluation.

Parameter	Unit	Value	Data source
Investment cost incl. interest (NPV) – regular operation	€	80 000 000	Estimation, cf. Tab. 6
Investment cost incl. interest (NPV) – oxyfuel operation	€	85 000 000	Estimation, cf. Tab. 6
Limestone cost splitting between SER / raw iron prod.	%	50	-
Specific carbon dioxide emissions of coal	t_{CO2}/MWh	0.34	cf. Tab. 1
Electricity consumption for final CO_2 disposal	kWh/t_{CO2}	140	cf. Haider, 2009, Tab. 5.2

Tab. 49: Additional cost rates for net present value calculations

Business Case
An operator of a raw iron production is forced to reach strategic targets by aiming at reduced fossil resource consumption and reduced fossil CO_2 emissions. So far 0.c) coal or 0.) natural gas was used as reducing agent. The production of a reducing agent by 1.) sorption enhanced reforming has been identified as a possibility to reduce fossil energy consumption. 2) A combined operation of sorption enhanced reforming together with the oxyfuel combustion process would enabled the disposal of CO_2 emissions and lead to an improved plant operation with respect to the European Unions emission allowances trading scheme. **Investment decision:** Which investment option would minimize fossil CO_2 emissions at minimal costs?

Position	Symbol	Unit	Option 0.c	Option 0	Option 1	Option 2
Boundary conditions						
Coal consumption		MWh/a	700 000			
Natural gas consumption		MWh/a		700 000		
Reducing agent from SER		MWh/a			700 000	700 000
Investment cost incl. interest	$I_{Opt,X}$	€	0	0	80 000 000	85 000 000
Expenses						
Fuel cost (coal)	A_1	€/a	**7 000 000**			
Fuel cost (natural gas)	A_2	€/a		**20 160 000**		
Fuel cost (wood chips)	A_3	€/a			**20 989 051**	**21 015 318**
Electricity costs CO_2 disposal	A_4	€/a				3 568 396
Maintenance, insur., admin., tax	A_5	€/a			3 600 000	3 825 000
Operating supplies	A_6	€/a			2 224 292	2 224 292
Labor costs	A_7	€/a			**490 000**	**490 000**
Costs CO_2 emission allow.	A_8	€/a	4 760 000	2 772 000		
Oxygen costs	A_9	€/a				5 401 760
Earnings						
Earnings from electricity	E_1	€/a			2 589 707	3 893 950
Earnings CO_2 emission allow.	E_2	€/a				5 097 708
Earnings from ash production	E_3	€/a				
Sum (Expenses – Earnings)	$C_{Opt,X}$	€/a	**11 760 000**	**22 932 000**	**24 713 636**	**27 533 107**
Net present value calculation						
Cumulative present value factor	BWSF	-	10	10	10	10
Additional investment costs	ΔI_X	€	0	0	80 000 000	85 000 000
Operating expenses savings	ΔC_X	€/a	11 172 000	0	-1 781 636	-4 601 107
Net present value	ΔNPV_X	€	111 720 000	0	-97 816 358	-131 011 073

Tab. 50: Evaluation of a reducing agent from biomass for iron production by NPV calculations

Tab. 50 shows the results of the economic evaluation of the created plant layout. Shown results give an important insight into main relationships in the surrounding circumstances of iron production. The findings reveal that fuel prices dominate the feasibility of the different supply options.

Coal is a comparably cheap reducing agent which at the same time induces most fossil CO_2 emissions. But low costs for emission allowances at a price level of 20 €/t_{CO2} still have a low impact on the results. Iron ore reduction by the aid of natural gas (Option 0) or by a reducing agent from sorption enhanced reforming (Option 1) achieves quite similar operation costs per year. The investment costs for the investigated plant concepts have been estimated. A detailed inquiry on investment cost from a plant manufacturer has not been part of present investigations. **Tab. 51** shows the results of a ceteris paribus parameter analysis of important parameters of the illustrated business case.

Parameter Analysis

Parameter Analysis: The results illustrated in Tab. 50 show that following parameters are most important for the investment decision: 1.) wood chip price, 2.) coal price, 3.) natural gas price, 4.) price of CO_2 emission allowances. A ceteris paribus (cet. par.) variation of each parameter shows the necessary price in comparison to the reference values for a positive investment decision for option X based on a positive "net present value".

Position	Reference Value	Unit	Option 0.c	Option 0	Option 1	Option 2
Wood chip price for positive NPV	100	€/t_{atro}	-	-	< 54	< 37
Coal price for positive NPV	10	€/MWh	< 26	-	-	-
Natural gas price for positive NPV	28.8	€/MWh	> 13	-	> 43	> 48
Price of CO_2 emission allowances for positive NPV	20	€/t_{CO2}	< 132	-	> 91	> 54

Tab. 51: Parameter analysis of the business case "reducing agent from biomass for iron production"

The parameter analysis illustrated in **Tab. 51** shows that Option 1 is favorable from an economic point of view if

- the wood chip price is lower than 54 €/t_{atro} (12 €/MWh),
- the natural gas price is higher than 29 €/MWh,
- and the coal price is higher than 26 €/MWh.

The economic feasibility of an operation including the oxyfuel combustion process (Option 2) is strongly dependent on the price level of emission allowances. Additional costs for oxygen and CO_2 disposal can only be justified if the prices of emission allowances exceed the additional operation costs. A ceteris paribus parameter variation of the price for emission allowances showed, that the Option 2 is an interesting solution to substitute natural gas if the price level rises above 54 €/t_{CO2} and to substitute coal above 132 €/t_{CO2}.

A realization of the created production concept would support the strategic goals of the European energy policy. The installation of the created plant layout could be used to generate a positive impulse for development of a region, if used wood chips are supplied from local suppliers. Further realization steps would need to watch feed stock price development to maintain financial risks at a low level. At the same time, also alternative methods to reduce fossil energy consumption of iron ore reduction need to be observed and compared with the presented solution.

8.11. Results and Findings

Iron and steel production is one of the main industrial sources for fossil CO_2 emissions. Within **Chapter 8** experimental results and mass and energy balances for the production of a reducing agent from biomass by sorption enhanced reforming have been presented.

- Biomass gasification by sorption enhanced reforming enables a product gas composition which consists of a high share of components which are favorable for the chemical reduction of iron oxide (Fe_xO_y). Therefore, product gas from sorption enhanced reforming offers suitable characteristics for the usage as reducing agent.

- Sorption enhanced reforming experiments have been conducted with "KS_1_09_12" in September and October 2012. "KS_1" is a limestone type which is used as additive for the raw iron production enhancing slag formation in blast furnaces. As a part of the present work, sorption enhanced reforming experiments have been carried out with "KS_1_09_12" to provide specific data for present investigations.

- The creation of a plant layout for the supply of a reducing agent for the raw iron production set the foundation for a plant simulation model. The created plant layout is based on a gasifier system operating the sorption enhanced reforming process, gas cooling enabling electricity production by the aid of a steam power cycle and gas cleaning based on a regular product gas filter combined with a RME-scrubber.

- The calculation of mass- and energy balances showed that **100 MW** reducing agent can be produced from **133 MW** of biomass. The expected product gas composition contains around 63 vol.-$\%_{db}$ of hydrogen (H_2), 9 vol.-$\%_{db}$ of carbon monoxide (CO) and 12 vol.-$\%_{db}$ of methane (CH_4). The produced gas stream can be used to reduce fossil resource consumption based on coal or natural gas.

- Sorption enhanced reforming has already been investigated in experimental facilities before. Within the present work, a novel plant concept for the integration of sorption enhanced reforming into raw iron production was elaborated for the first time in detail. Further experimental investigations are recommended to expose the practical long time performance of considered bed materials like "KS_1" to ensure adequate process efficiency.

- An extension of the created plant layout by the oxyfuel combustion process would enable a further improvement of the emission balance. Oxyfuel combustion modifies the exhaust gas stream into a gas stream containing a high share of CO_2. Therefore, the resulting exhaust gas stream offers improved properties for an efficient disposal and storage as a part of a carbon capture and storage concept. Additional cost for oxygen and electricity can only be justified by an adequate price level of emission allowances. The investigated business case showed that a price level above 54 $€/t_{CO2}$ is necessary to favor the oxyfuel combustion process. The overall concept could be used to induce a significant reduction of the overall fossil CO_2 emissions of raw iron production.

- Fuel prices dominate the feasibility of the created plant concept. Investment costs can only be justified if the price gap between coal, natural gas and wood leads to a favorable price development towards wood. The investigated business case showed that a wood price below 12 €/MWh and a coal price above 26 €/MWh is necessary with respect to a natural gas price of 29 €/MWh.

- Sorption enhanced reforming has so far not been operated continuously within large-scale gasifier systems. Further scale-up steps need to be accompanied by theoretical and experimental investigations focusing on the long time performance of used bed materials as well as on existing tradeoffs in the area of bed material circulation, CO_2 transport, and efficiency vs. product gas composition.

The created plant concept for the production of a reducing agent represents a first plant of its kind and a mature possibility to reduce the fossil energy consumption of raw iron production. An installation of the created plant layout using biomass as feedstock is a possibility to increase the share of local available feedstock and reduces necessary energy imports for end products of heavy energy intensive industry. For an economic operation of a new plant an adequate price relation between wood, natural gas and coal is necessary.

9. Discussion: Advantages of Sorption Enhanced Reforming Over Conventional Gasification for the Production of a Reducing Agent

Chapter 7 and **Chapter 8** illustrated two different cases in industry with high hydrogen demand. Both chapters described innovative concepts for the industrial production of hydrogen. And both concepts were set up supported by

- a literature review,
- experimental data,
- plant operation data,
- and process simulation.

Conventional dual fluid gasification using olivine as bed material has been modeled by the aid of operational data from existing large-scale plants. Whereas, modeling of a large-scale sorption enhanced reforming plant can only be established as predictive calculation based on results from lab scale.

Fig. 63 depicts a comparison of the modeled gasifier for a refinery from **Chapter 7** with the modeled gasifier operating sorption enhanced reforming for iron production from **Chapter 8**. Both gasifier systems have been fed with the same ratio of steam to fuel. Within the product gas stream hydrogen atoms can be found in

- water (H_2O – blue),
- gaseous hydrogen (H_2 – red),
- or in remaining hydrocarbons (C_xH_y – white).

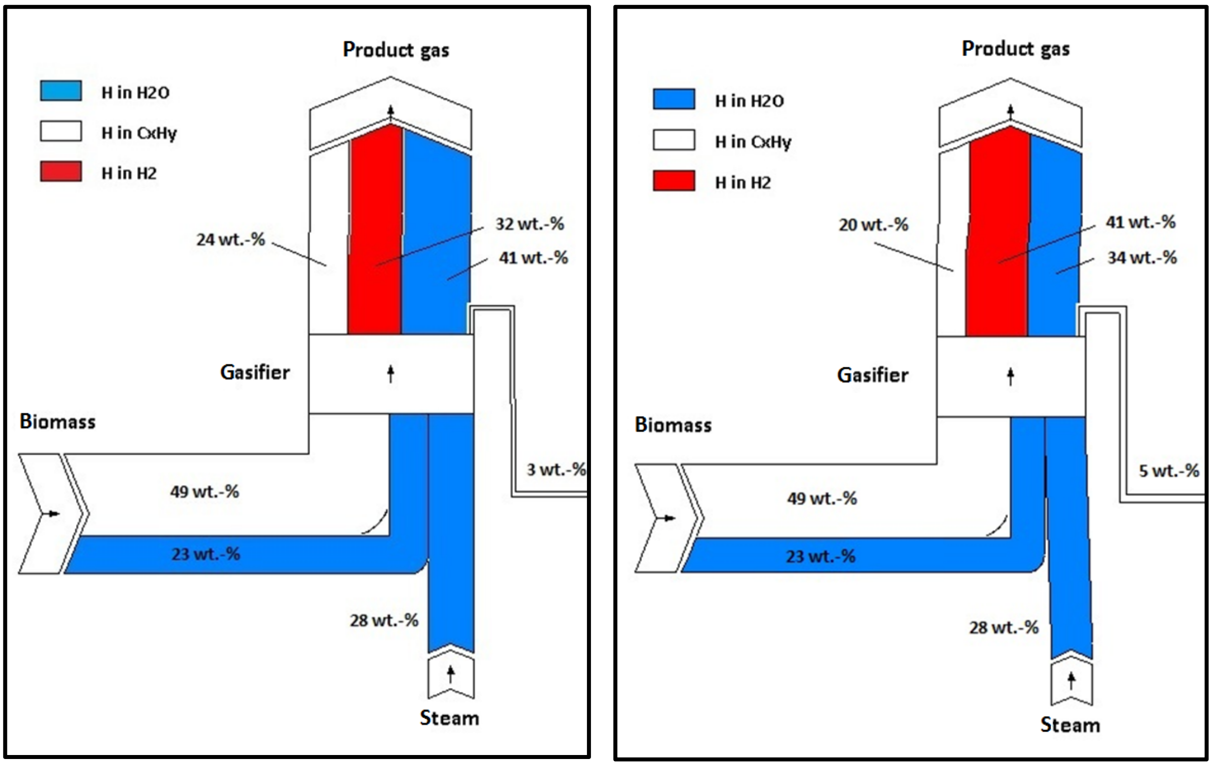

Fig. 63: Hydrogen mass flow chart of the modeled gasifier: conventional hydrogen production for a refinery (left - P_{th} = 50 MW) compared to the SER based production of a reducing agent for raw iron production (right - P_{th} = 100 MW)

The comparison in **Fig. 63** highlights, that sorption enhanced reforming in a large-scale plant is expected to provide ~ 30% more of gaseous hydrogen (H_2 – red - 41:32 wt.-%) in the final product gas stream than conventional gasification. Hydrogen (H_2) from conventional gasification mainly arises from the conversion of biomass. Whereas sorption enhanced reforming generates additional hydrogen (H_2) from water conversion.

Another main difference is the amount of remaining char, which is transported from the gasifier to the combustor. Low gasification temperatures slow char gasification down. Sorption enhanced reforming therefore implies that a higher share of wood char is transported from the gasifier to the combustor. At this stage, the transport is also dependent on the operated circulation rate. Char gasification at low temperatures requires:

- sufficient gas-solid contact
- and sufficient residence time.

If sufficient residence times are provided by the gasification system, char gasification is encouraging the favored conversion of water and increased hydrogen production as already shown by **Eq. 3.3** from **Chapter 3**.

Eq. 3.3 $$C + H_2O \leftrightarrow CO + H_2 \qquad \Delta H = +118.5\ kJ/mol$$

In addition to the hydrogen mass flow analysis, key figures are used to describe the behavior of the dual fluid gasifier system. Within **Chapter 6** several key figures have already been introduced, described and discussed. **Fig. 64** and **Fig. 65** show now a comparison of important key figures for dual fluid systems which were modeled as a part of the present work. Required values for the illustration were taken:

- for "sorption enhanced reforming" from literature and experimental results,
  (cf. **Tab. 13** ; **Tab. 27**, **Tab. 43**, **Tab. 47**)
- for the "reference plant" from literature,
  (cf. **Tab. 22**)
- and for "refinery" & "iron production" from simulation results achieved.
  (cf. **chapter 7.4** , **8.6**)

Fig. 64 shows key figures for sorption enhanced reforming. Whereas **Fig. 65** contains a comparison of large-scale plants investigated. Discussed key figures are, cold gas efficiency, absolute water conversion rate, hydrogen productivity and CO_2 load.

All calculations showed that the **cold gas efficiency** of novel plants is predicted with ~ 70 %. The efficiency of large-scale facilities at the same time is dependent on the required bed material renewal rate. The **absolute water conversion** of systems operating sorption enhanced reforming is higher than that of conventional gasification systems. This also has been proven by experimental results on a lab-scale.

The **hydrogen productivity** describes the relation between elementary hydrogen fed to the gasifier and gaseous hydrogen within produced gas. Sorption enhanced reforming at a large scale will enable an improved water conversion and an improved hydrogen productivity.

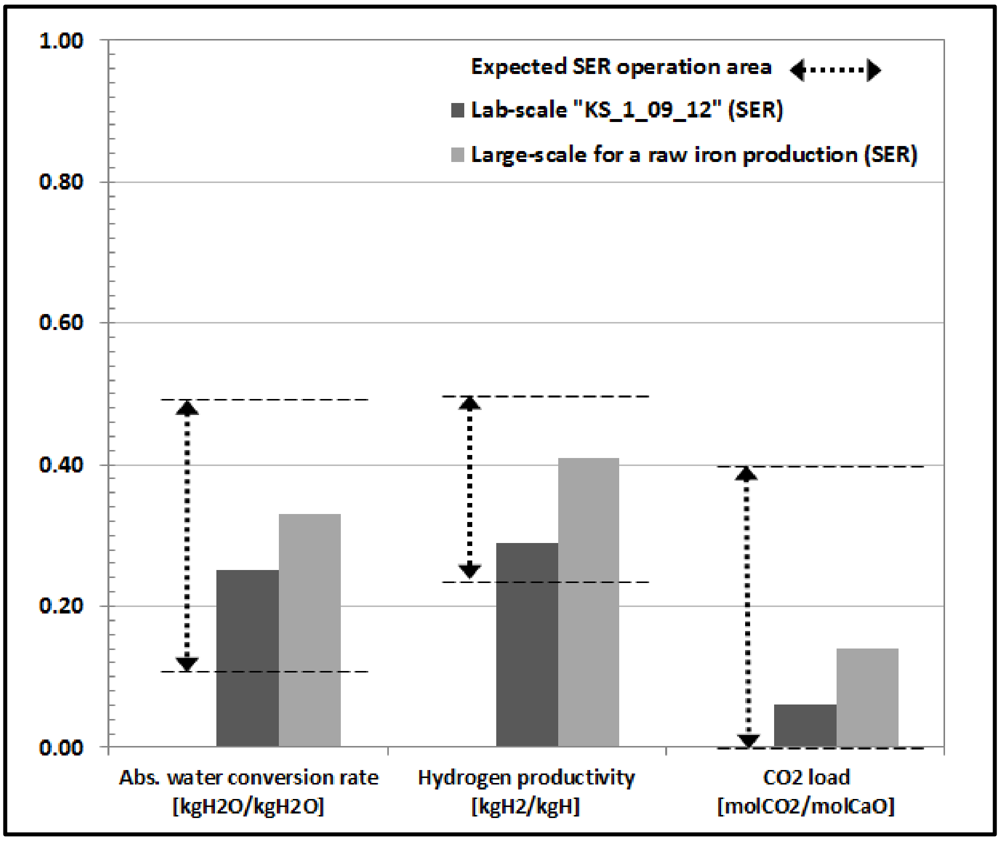

Fig. 64: Comparison of key figures of sorption enhanced reforming

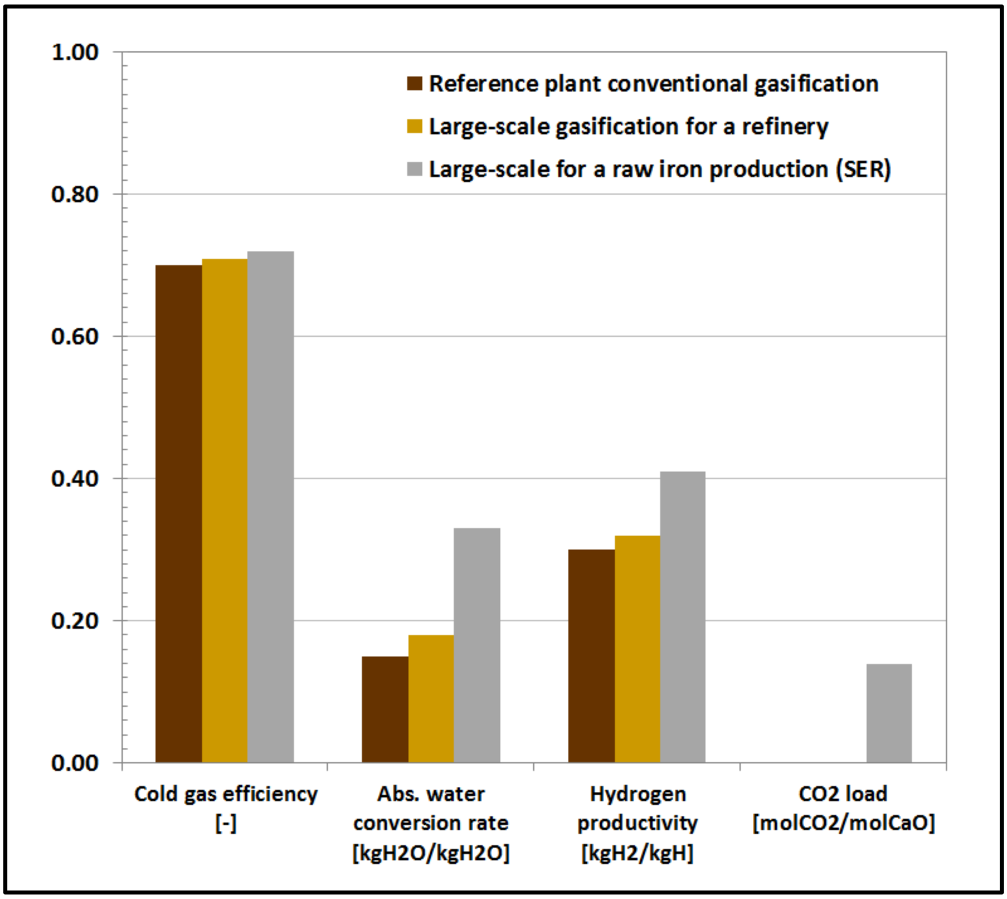

Fig. 65: Comparison of key figures of large scale dual fluid gasifier systems

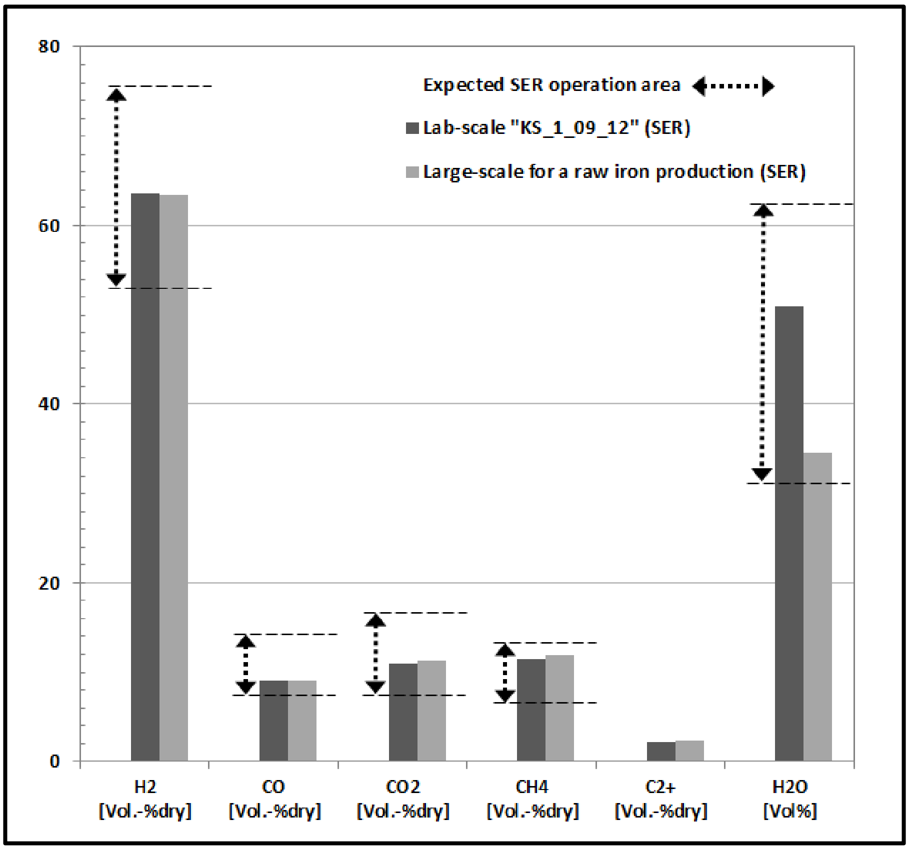

Fig. 66: Comparison of the product gas composition of sorption enhanced reforming

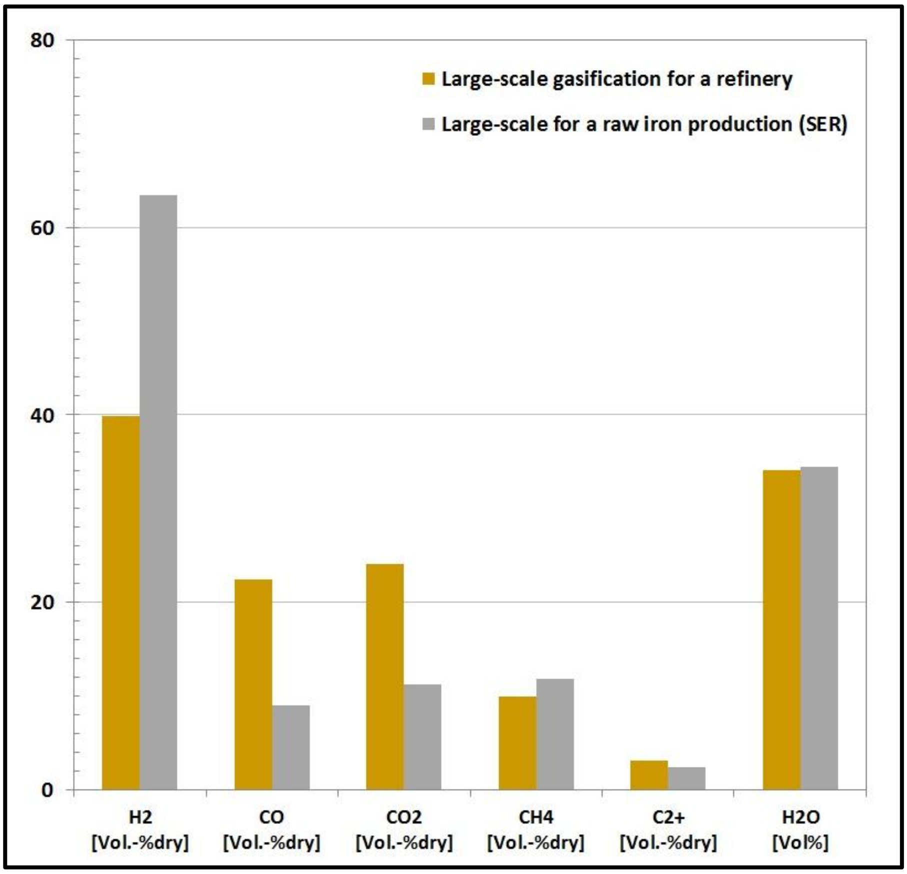

Fig. 67: Comparison of the product gas composition for large scale dual fluid gasifier systems

The impact of the **CO_2 load** of used particles has been discussed before within present work several times. Long time experiments need to be performed to proof the capability of specific bed materials.

Beside the discussed key figures, the product gas composition achieved is an important aspect for the application. **Fig. 66** and **Fig. 67** show a comparison of the gas composition for the different investigated cases.

Sorption enhanced reforming is known as a process which enables high hydrogen content. As it can be seen in **Fig. 66,** the water content of the gas produced is calculated lower than observed on a lab-scale. The water content is calculated on a low level because of the preset low steam to fuel ratio of 0.55 $kg_{H2O}/kg_{fuel,waf}$. The findings of Pröll T. 2004 recommend a low steam to fuel ratio because of several benefits like increased cold gas efficiency due to less heat demand in the gasifier or reduced gas mass flows in the plant.

Finally, **Tab. 52** illustrates now different advantages of sorption enhanced reforming in comparison with conventional dual fluid gasification for the production of a reducing agent. Higher water conversion rate leads to a higher share of hydrogen (H_2) in the produced gas. Higher reducing potential achieved is mainly based on hydrogen (H_2) which could be accounted as an advantage with respect to the carbon dioxide (CO_2) balance of the subsequent blast furnace. This is especially the case, if the gasifier is operated in combination with oxyfuel combustion aiming on carbon capture and storage purposes. Following advantages of sorption enhanced reforming can be summarized:

- lower bed material price,
- bed material can be reused in blast furnace,
- increased conversion of water is contributing to reducing potential,
- the produced reducing agent is mainly hydrogen based whereas conventional dual fluid gasification is also based on carbon monoxide,
- smaller gas volume flows due to the selective removal of CO_2 have a positive effect on equipment size,
- less carbon content in product gas improves the CO_2 balance of the blast furnace,
- and the gasifier could be used to prepare CCS by oxyfuel combustion.

Conventional gasification is operated since many years on a large-scale. Sorption enhanced reforming so far was mainly operated on lab-scale. Listed advantages endorse the operation of sorption enhanced reforming on a large-scale.

Comparison criterion	Unit	Conventional dual fluid gasification	Sorption enhanced reforming	Source
Bed material	-	**olivine**	**limestone**	-
Process characteristics				
Absolute water conversion rate	kg_{H2O}/kg_{H2O}	**0.18**	**0.33**	cf. Chapter 7 & 8: Tab. 34 , Tab. 47
Reducing potential [1,2,X] (calculated with IPSEpro excl. C_xH_y, tar, char)	$(H_2/(H_2+H_2O))$ [vol.-%/vol.-%]	**0.44**	**0.54**	cf. Chapter 7 & 8: Tab. 32; Tab. 45
	$(CO/(CO+CO_2))$ [vol.-%/vol.-%]	**0.48**	**0.45**	
Lower heating value [X]	MJ/Nm³	**12.75**	**13.75**	cf. Chapter 7 & 8: Tab. 32; Tab. 45
Plant operation characteristics*				
Gas volume flow [X] (calculated with IPSEpro for T = 675°C)	m³/h	**175 000**	**145 000**	cf. Chapter 7 & 8: Fig. 49; Fig. 59
Carbon content in product gas [X] (calculated with IPSEpro)	t_C/h	**12.3**	**5.6**	cf. Chapter 7 & 8: Fig. 49; Fig. 59
Bed material consumption	t/h	**0.3**	**5**	cf. Chapter 7 & 8: Tab. 34 , Tab. 47
State of technology development	-	**commercial**	**experimental**	cf. Chapter 3.3 & 4.5
Economic considerations				
Costs for fresh bed material	€/t	**185**	**30**	cf. Chapter 6.3, Tab. 24
Bed material recycling within the iron production process	-	**olivine is used as supplement material for pelletizing of iron ore**	**limestone is reused within the blast furnace**	cf. Chapter 8.1, Fig. 54

colors: green (advantage); yellow (disadvantage);
[X] values calculated for the product gas composition at the exit of the gasifier system;
* values of conv. gasification from Chapter 7 are adapted from 53 MW to thermal gasifier power of 141 MW

Tab. 52: Essential parameters describing the advantages of sorption enhanced reforming over conventional dual fluid gasification for the production of a reducing agent

---

1 cf. Baur E., 1903, p354-p368; 2 cf. Ruge J., 2007, p194

10. Summary and Outlook

The present work was carried out to investigate the industrial hydrogen production from biomass by the use of dual fluid gasification. For that reason, the structure of present work was established with respect to the following research questions:

- How can "**conventional dual fluid gasification**" be deployed to produce pure hydrogen for a refinery on a large scale from biomass?
- How can "**sorption enhanced reforming**" be applied to provide a hydrogen rich gas for iron production on a large scale from biomass?
- What are the technological and economic advantages of **sorption enhanced reforming** over **conventional dual fluid gasification** for the production of a reducing agent?
- Are the hydrogen production costs achieved, sufficiently low to justify a further step aiming at the realization of large-scale plants?

As a result, the carried out work was finalized in form of two new innovative concepts for the production hydrogen from biomass:

1. Pure hydrogen for a refinery (cf. **chapter 7**),
2. Hydrogen-rich gas for iron production (cf. **chapter 8**).

A comprehensive state of knowledge analysis proofed that "**conventional dual fluid gasification**" is a mature technology for the production of hydrogen from biomass. Conventional dual fluid gasification is operated since many years on a large scale. The produced gas has a hydrogen content of ~40 vol.-%$_{db}$. Furthermore, the produced gas enables the production of pure hydrogen by the application of proofed equipment known from natural gas steam reforming. The elaborated hydrogen production process is based on a conventional dual fluid gasification system in combination with a CO-shift step, pressure swing adsorption and steam reforming.

The state of knowledge in the field of **sorption enhanced reforming** so far was mainly based on experimental results. The experimental results verified a favorable product gas composition for iron ore reduction, quite similar to the composition of coke oven gas. First-time experiments with limestone "KS_1" were conducted to gain additional data for a large-scale plant. "KS_1" is already well known as an additive of iron production. The experimental results achieved, enabled the elaboration of a large-scale production of a reducing agent via sorption enhanced reforming.

Present work furthermore illustrated essential steps of process development for both processes. This included:

1. Process idea
2. Illustration of the current state of knowledge
3. Process design
4. Plant layout
5. Mass- and energy balances for overall plants
6. Illustration of main production parameters
7. Economic evaluation
8. Initiating of further development steps

Process simulation was used as an essential tool to support the described process development steps.

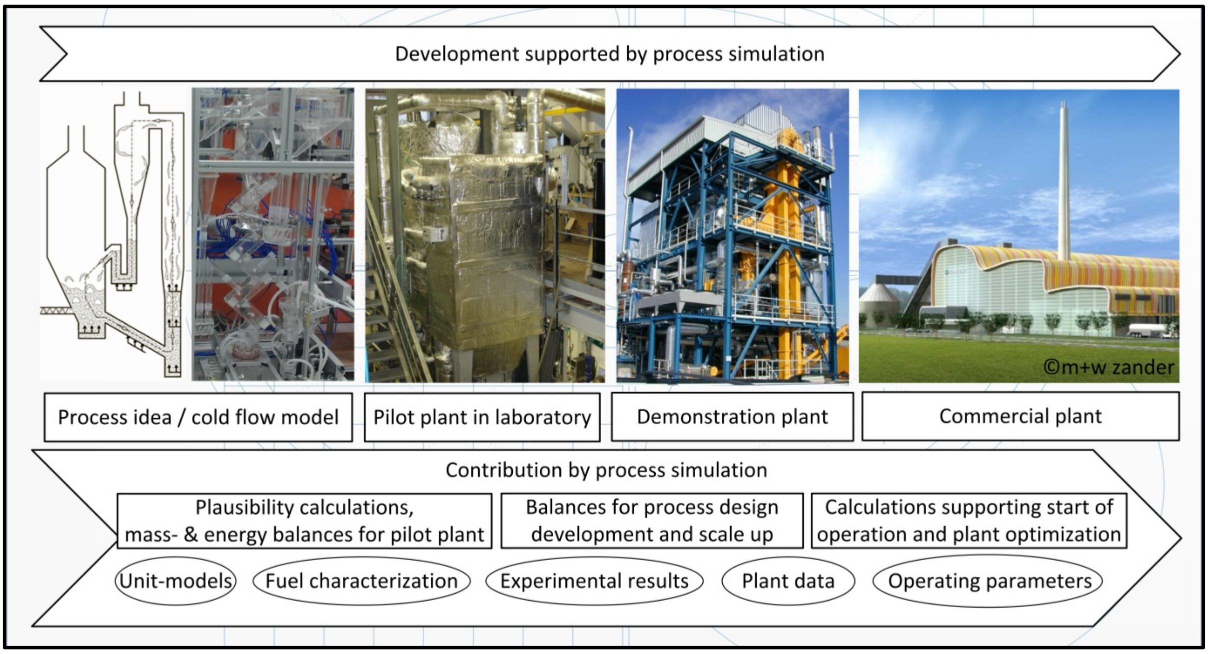

Fig. 68: Contribution of process simulation software during the plant development

Fig. 68 shows an overview about the contribution of process simulation during process development which were used as a part of the present work to investigate hydrogen from biomass for industrial application.

Within the present work, two detailed plant concepts based on dual fluid gasification systems have been setup for the large-scale hydrogen production from biomass. The results show that hydrogen can be produced from biomass on an industrial scale. The calculation of the two plants with a different scale was carried out according to the local demands of a refinery and an iron production. The first case presented shows that **30 MW** of pure hydrogen can be produced from **50 MW** of biomass for a refinery. The second case presented shows that **100 MW** of a hydrogen-rich gas can be produced from **133 MW** of biomass for a raw iron production by sorption enhanced reforming.

Main advantages of sorption enhanced reforming for the production of a reducing agent are that in case of iron production the used bed material can be reused in the blast furnace and increased water conversion is contributing to a hydrogen based reducing potential. Sorption enhanced reforming in a large-scale plant is expected to provide ~ 30% more of gaseous hydrogen in the final product gas stream than conventional gasification. Furthermore, the process could be used to prepare carbon capture and storage in combination with oxyfuel combustion technology. But at the same time, it has to be said that further efforts are necessary to reach the same state of development like conventional dual fluid gasification has already reached.

The results of the economic evaluation showed that the hydrogen production costs are mainly dependent on price development of biomass. The price development of biomass has to be observed in relation to the price development of other fuels such as natural gas, coal and oil. The current price level of biomass (~22,5 €/MWh, wood chips) in comparison to the price level of natural gas (~29 €/MWh) is not supporting a hydrogen production from biomass.

An adequate price relationship or a supportive funding framework would encourage the implementation of one of the proposed plants. An economic operation of hydrogen from biomass for a **refinery** could be established by supportive funding as it was proposed through the NER 300 funding framework by the European Commission. In the case of an **iron production**, an economic parameter analysis shows, that a biomass price below 12 €/MWh or a CO_2 emission allowance price above 54 €/t_{CO2} would create preferable economic precondition for the realization of the proposed plant.

Further technological improvement of a hydrogen production from biomass is ensured by several research activities:

1. a pilot plant for pure hydrogen (BioH2 4Industries),
2. experimental SER tests (ERBA),
3. SER process simulation (master thesis Reinhard Jentsch),
4. and a 100 kW dual fluid pilot plant (G-volution II).

In summer 2012, the construction works for a new pilot plant in Güssing (Austria) started. This pilot plant will produce pure hydrogen from biomass as a part of the research project **BioH2 4Industries**. Furthermore, the facility can be used to investigate the dynamic behavior of the proposed **hydrogen production process for a refinery**.

Further experimental **sorption enhanced reforming** tests will be carried out as a part of the research project **ERBA**. The experimental tests will provide data with respect to bed material performance, CO_2 transport and char decomposition. The experiments are accompanied by process simulation as a part of the master thesis of Reinhard Jentsch. His master thesis investigates sorption enhanced reforming within the next generation gasifier design.

At the same time, the detail engineering for the **next generation dual fluid gasifier system** is carried out as a part of the research project **G-volution II**. The construction of the new 100 kW pilot plant in Vienna will enable further experimental campaigns investigating **sorption enhanced reforming**. The engineering of the new pilot plant was influenced by the results of the present work. This new experimental facility will provide comprehensive data from additional measuring points and bed material sampling points which will result in an extended and deeper understanding of the sorption enhanced reforming process.

In the end it has to be said, that at our present time, **biomass gasification can be found at a turning point**. Within the next 20 years it will turn out if our energy system offers space for gasification technology. European society is demanding for high quality clean energy carriers from sustainable energy sources, such as hydrogen. At that point, biomass gasification could be a key energy conversion technology fulfilling the set expectations. But at the same time, biomass gasification is struggling today with high feed stock prices and missing support from existing funding frameworks. Research and development can only focus on the demanded high overall conversion efficiencies. Further research activities need to concentrate on low price feedstock from biogenic waste, industrial waste materials as well as municipal waste. Because it would by a great opportunity for gasification technology, if these types of feedstock could be used for the generation high quality clean energy carriers like hydrogen, kerosene, diesel fuel, gasoline, or other valuable petrochemical products.

List of Figures

List of Tables

References

Abanades J.C., Alvarez D.;
Conversion Limits in the Reaction of CO_2 with Lime, in: Energy & Fuels, 17, 2003

Abu El-Rub Z., Bramer E.A., Brem G.;
Review of Catalysts for Tar Elimination in Biomass Gasification Processes, in: Industrial Engineering Chem., Res. 43, 2004

Air Liquide;
1x1 der Gase – Physikalische Daten für Wissenschaft und Praxis, Düsseldorf, 2006

Balasubramanian B., Ortiz A.L., Kaytakoglu S., Harrison D.P.;
Hydrogen from methane in a single-step process in: Chem. Eng. Sci., 54(15-16), 1999

Baur E., Glassner A.;
Gleichgewicht der Eisenoxide mit Kohlenoxid und Kohlensäure in Z. phys. Chemie, 43, 1903

Benthaus F., Beyer H.D., Hodek W., Jimeson M., Leininger D., et al;
Kohle, in: Benthaus F. (Ed.): Rohstoff Kohle, Eigenschaften, Gewinnung, Veredlung – 1.Auflage, Weinheim, New-York, 1978

BMELV – Bundesministerium für Ernährung, Landwirtschaft und Verbraucherschutz;
Schriftenreihe "Nachwachsende Rohstoffe" – Analyse und Evaluierung der thermochemischen Vergasung von Biomasse, Münster, 2006

Bolhar-Nordenampf M.;
Techno-Economic Assessment on the Gasification of Biomass on the Large Scale for Heat and Power Production, Disseration, Institute of Chemical Engineering, Vienna University of Technology, 2004

BP;
BP Statistical Review of Word Energy – June 2011, www.bp.com/statisticalreview (accessed August 17th, 2011), London, 2011

Brundtland G., Khalid M., et. al.;
Our common future, Report of the World Comission on Environment and Development, United Nations, Oslo, 1987

Chase M.W.Jr., Davies C.A., Davie J.R.Jr., Fulrip D.J., Mc Donald R.A., Syverud A.N.;
JANAF thermochemical tables, 3rd edition, Journal of Physical and Chemical Reference Data, 1985

Curran G.P., Fink C., Gorin E.;
The CO_2 acceptor gasification process, American Chemical Society., Div. Fuel Chem., Preprints 8, 1964

EN ISO 6976;
Erdgas – Berechnung von Brenn- und Heizwert, Dichte, relativer Dichte und Wobbeindex aus der Zusammensetzung, DIN Deutsches Institut für Normung e.V., Berlin, 2005

Ehrig R., Wörgetter M.;
Biomasseverfügbarkeit zur Versorgung einer Biowasserstoffanlage am Standort Wien, Disclosure Report Work Package 1, FFG-Project BioH2 4Refineries, 2010

European Commission;
Hydrogen Energy and Fuel Cells – A vision of our future, Final Report of the High Level Group, Directorate-General for Research, Brussels, 2003

Eurostat;
Energy, transport and environment indicators – Pocketbook 2010, European Commission/Eurostat, Luxemburg, 2011

Eurostat;
Forestry in the EU and the World – 2011 edition, Publication Office of the European Union, Luxemburg, 2011a

Fischer Taschenbuch Verlag;
Der Fischer Weltalmanach 2009 – Zahlen, Daten, Fakten, Fischer Taschenbuch Verlag, Frankfurt am Main, 2008

Florin N. H., Harris A.T.;
Hydrogen production from biomass coupled with carbon dioxide capture: The implications of thermodynamic equilibrium in: International Journal of Hydrogen Energy, 32(17), 2007

Florin N. H., Harris A. T.;
Enhanced hydrogen production from biomass with in situ carbon dioxide capture using calcium oxides sorbents in: Chemical Engineering Science, 63, 2008

Fuchs M.;
Polygeneration – Applied Gas Cleaning and Gas Analytics for Syngas Application, Dissertation, Institute of Chemical Engineering, Vienna University of Technology, 2010

Fürnsinn S.;
Outwitting the dilemma of scale – Cost and energy efficient scale-down of the Fischer-Tropsch fuel production from biomass, Dissertation, Institute of Chemical Engineering, Vienna University of Technology, 2007

Grasa G.S., Abanades, J.C.;
CO_2 Capture Capacity of CaO in Long Series of Carbonation/Calcination Cycles, in: Ind. Eng. Chem. Res., 45, 2006

Grübler A.;
A Comparison of Global and Regional Energy Emission Scenarios, Working Paper of the International Institute for Applied System Analysis, Laxenburg, 1994

Haas G.;
Best Practice - Beschaffungsmanagement, Gernsbach, 2005

Haider M., et al.;
Technische, wirtschaftliche und ökologische Grundlagen der CO_2-Abscheidung für Österreich, Technische Universität Wien & Universität Stuttgart, 2009

Hawthorne C., Poboss N., Dieter H., Gredinger A., Zieba M., Scheffknecht G.;
Operation and results of a 200 kW dual fluidized bed pilot plant gasifier with adsorption-enhanced reforming, in: Biomass Conversion and Biorefinery, Volume 2, Issue 3, 2012

Hlubleck W., Schilling H.-D.;
Potentiale der Forschung und Entwicklung in der Kraftwerkstechnik, Energiewirtschaftliche Tagesfragen Heft 1-2, 1996

Hofbauer H.;
Brennstoff- und Energietechnologie – Lehrbehelf für das Sommersemester 2007, Institute of Chemical Engineering, Vienna University of Technology, 2007

Hofbauer H.;
Thermische Biomasse Nutzung I und II – Unterlagen zu Vorlesung für das Sommersemester 2007, Institute of Chemical Engineering, Vienna University of Technology, 2007a

Hofbauer H.;
Biomassedampfvergasung – eine Erfolgsstory, in: Nachwachsende Rohstoffe Nr.58 – Dezember 2010, http://blt.josephinum.at (accessed November 30th, 2011), 2010

Hofbauer H.;
Wirbelschichttechnik – Unterlagen zur Vorlesung Sommersemester 2010, Institute of Chemical Engineering, Vienna University of Technology, 2010a

Höftberger, E.;
In Situ CO_2 Adsorption in a Dual Fluidized Bed Biomass Steam Gasifier to Produce a Hydrogen Rich Gas, Dissertation, Institute of Chemical Engineering, Vienna University of Technology, 2005

Hubacek H, Pesek A.;
Chemie und Umwelttechnik, Wien, 1994

Holdren J., Smith K.;
Energy, the environment, and health, in: UNDP (Ed.): World Energy Assessment – Energy and the challenge of sustainability, United Nations Development Programme, New York, 2000

Höltl W.;
OxyFuel-Verbrennung in einer zirkulierenden Wirbelschicht – Auslegung, Konstruktion und Inbetriebnahme einer 100 kW_{th} Versuchsanlage, Dissertation, Institute of Chemical Engineering, Vienna University of Technology, 2010

International Energy Agency (IEA);
World Energy Outlook 2010, OECD/IEA, Paris, 2010

Intergovernmental Panel on Climate Change (IPCC);
Climate Change 2007: Synthesis Report, an Assessment of the Intergovernmental Panel on Climate Change, November 12-17th, Valencia, 2007

Johnsen K., Ryu H.J., Grace J.R., Lim C.J.;
Sorption-enhanced steam reforming of methane in a fluidized bed reactor with dolomite as CO_2-acceptor, in: Chem. Eng. Sci., 61(4), 2006

Jünger C.;
Grundlagenuntersuchungen zur Biomassetrocknung und Entwicklung eines Verfahrens zur Niedertemperaturtrocknung von Hackschnitzel, Dissertation, Institute of Chemical Engineering, Vienna University of Technology, 2008

Kaiser S.;
Simulation und Modellierung von Kraft-Wärme-Kopplungsverfahren auf Basis Biomassevergasung, Dissertation, Institute of Chemical Engineering, Vienna University of Technology, 2001

Kaltschmitt M., Hartmann H., Hofbauer H.;
Energie aus Biomasse – Grundlagen, Techniken und Verfahren, 2. neu bearbeitete und erweiterte Auflage, Springer-Verlag, Berlin Heidelberg, 2009

Kast W.;
Adsorption aus der Gasphase – Ingenieurwissenschaftliche Grundlagen und technische Verfahren, Basel, Cambridge, New York, 1988

Kirnbauer F., Hofbauer H.;
Investigations on Bed Material Changes in a Dual Fluidized Bed Steam Gasification Plant in Güssing, Austria, in: Energy & Fuels, 25, 2011

Kirnbauer F., Kotik J., Hofbauer H.;
Investigations of Inorganic Matter in DFB Biomass Steam-Gasification Plants in Güssing/Austria and Oberwart/Austria, in: Proceedings of the 19th European Biomass Conference, Berlin, 2011a

Kirnbauer F., Wilk V., Kitzler H., Kern S., Hofbauer H.;
The postitive effects of bed material coating on tar reduction in a dual fluidized bed gasifier, Fuel, Vol. 95, 2012

Klaus T., Loreck C., Müschen K.;
Klimaschutz und Versorgungssicherheit – Entwicklung einer nachhaltigen Stromversorgung, Umweltbundesamt, Dessau-Roßlau, 2009

Knautz H.;
Gasreinigung mittels Nasselektrofilter, Master Thesis, Institute of Chemical Engineering, Vienna University of Technology, 2003

Konstantin P.;
Praxisbuch Energiewirtschaft – Energieumwandlung, -transport und –beschaffung im liberalisierten Markt, 2. bearbeitete und aktualisierte Auflage, Springer-Verlag Berlin Heidelberg, 2009

Koppatz S., Pfeifer C., Rauch R., Hofbauer H., Marquard-Moellenstedt T., Specht M.;
H_2 rich product gas by steam gasification of biomass with in situ CO_2 absorption in a dual fluidized bed system of 8 MW fuel input, in: Fuel Processing Technology, 90, 2009

Koppatz S., Pfeifer C., Kreuzeder A., Soukup G., Hofbauer H.;
Application of CaO-based bed material for dual fluidized bed steam biomass gasification", in: Proceedings of the 20th International Conference on Fluidized Bed Combustion, Xi`an, Voll. II, China, 2009a

Koppatz S., Schmid J.C., Pfeifer C., Hofbauer H.;
The effect of bed particle inventories with different particle sizes in a dual fluidized bed pilot plant for biomass steam gasification, Industrial & Chemical Engineering 51, 2012

Kotik J.;
Über den Einsatz von Kraft-Wärme-Kopplungsanlagen auf Basis der Wirbelschicht-Dampfvergasung fester Biomasse am Beispiel des Biomassekraftwerks Oberwart, Dissertation, Institute of Chemical Engineering, Vienna University of Technology, 2010

Kreuzeder A.;
Fluidynamische Untersuchungen zur Optimierung des Zyklons der Wirbelschicht-Vergasung des BHKW Güssing an einem Kaltmodell, Master Thesis, Institute of Chemical Engineering, Vienna University of Technology, 2005

Levenspiel O.;
Chemical Reaction Engineering, John Wiley & Sons, Third edition, 1999

Lin S. Y., Suzuki Y., Hatano H., Harada M.;
Developing an innovative method, HyPr-RING, to produce hydrogen from hydrocarbons, in: Energy Convers. Manag., 43, 2002

Mayer T.;
Über die Aufbereitung biogener Gase mittels Adsorption, Dissertation, Institute of Chemical Engineering, Vienna University of Technology, 2012

McGranahan G., Jacobi P., Songsore J., Surjadi C., Kjellen M.;
Citizens at Risk: From Urban Sanitation to Sustainable Cities, London, 2000

McKelvey V.E.;
Mineral resource estimates and public policy, American Scientist, v.60, 1972

McMurry J, McDonald A.;
Fundamentals of Organic Chemistry, 5th edition, Belmont, USA, 2003

Medek R.;
85 Jahre städtisches Gaswerk Wien – Simmering – Kommunale Gasversorgung seit 1899, Wiener Stadwerke-Gaswerke, Wien, 1984

Meerman J.C., Ramirez A., Turkenburg W.C., Faaij A.P.C.;
Economic potential of feedstock flexible integrated gasification cogeneration facilities, in: Hofbauer, H. (Ed.): Proceedings of the International Conference on Polygeneration Strategies (ICPS11), Vienna, 2011

Minchener A.;
Coal gasification for advanced power generation, in: Fuel, 84, 2005

Müller S., Stidl M., Pröll T., Rauch R., Hofbauer H.;
Hydrogen from Biomass - Large Scale Hydrogen Production Based on a Dual Fluidized Bed Steam Gasification System, in: Biomass Conversion and Biorefinery, 1, 2011

Müller S., Pröll T., Hofbauer H.;
A Thermodynamic Investigation of Dual Fluidized Bed Biomass Gasification with Sorption Enhanced Reforming, in: Proceedings of the 21st International Conference on Fluidized Bed Combustion (FBC), 3.-6. June, Naples, Italy, 2012

Nakicenovic N., Haas R.;
Skriptum zur Vorlesung mit Übung Energieökonomie, Institut für Elektrische Anlagen und Energiewirtschaft, Vienna University of Technology, 2010

Pascalowska B., Whysall M., Narasimhan M.V.;
Improve Hydrogen Recovery from Refinery Off gases, Hydrocarbon Process 75, 1996

Pfeifer C., Soukup A., Kreuzeder A., Cuadrat C., Hofbauer H.;
In-Situ CO_2 Capture in a dual fluidized bed biomass steam gasifier: bed Material and fuel variation, in: J. Werther, et al., (Ed.), Circulating Fluidized Bed Technology IX, TuTech, Hamburg, 2008

Pfeifer C., Puchner B., Hofbauer H.;
Comparison of dual fluidized bed steam gasification with and without selective transport of CO_2, in: Chemical Engineering Science, 64, 2009

Pfeifer C., Koppatz S., Hofbauer H.;
Catalysts for dual fluidised bed biomass gasification – an experimental study at the pilot plant scale, in: Biomass Conversion and Biorefinery, 1, 2011

Poboss N.;
Experimental results on hydrogen production from biomass applying the adsorption enhanced reforming (AER) process in a 200kWth dual fluidized bed, in: Hofbauer, H. (Ed.): Proceedings of the International Conference on Polygeneration Strategies (ICPS11), Vienna, 2011

Pröll T.;
Potenziale der Wirbelschichtdampfvergasung fester Biomasse – Modellierung und Simulation auf Basis der Betriebserfahrungen am Biomassekraftwerk Güssing, Dissertation, Institute of Chemical Engineering, Vienna University of Technology, 2004

Pröll T., Hofbauer H.;
H_2 rich syngas by selective CO_2 removal from biomass gasification in a dual fluidized bed system – process modeling approach, in: Fuel Processing Technology, 89, 2008

Pröll T., Hofbauer H.;
Development and Application of a Simulation Tool for Biomass Gasification Based Processes, in: International Journal of Chemical Reactor Engineering, Vol. 6, A89, 2008a

Rauch R., Hofbauer H.;
Zweibett-Wirbelschichtvergasung in Güssing mit 2MWe/4,5MWt, Conference contribution to the: 7. HolzenergieSymposium, Zurich, October 18th, 2002

Rauch R.;
"Thermochemical Biorefineries - R&D in Austria", oral presentation at the 19th BEPS Annual Meeting, September 28-30th, Vienna, 2011

Reddy A.;
Energy and Social Issues, in: UNDP (Ed.): World Energy Assessment – Energy and the challenge of sustainability, United Nations Development Programme, New York, 2000

Rehling B., Hofbauer H., Rauch R., Tremmel H.,
Aichernig C., Schildhauer T., Biollaz S., Ulrich D., Schaub M.;
Bio-SNG – First results of the 1 MW pilot and demonstration unit at Güssing, in: Proceedings 1st International Conference on Polygeneration Strategies, Vienna, 2009

Rehling B., Hofbauer H., Rauch R., Aichernig C.;
BioSNG-process simulation and comparison with first results from a 1 MW demonstration plant, in: Biomass Conversion and Biorefinery, 1, 2011

Ringhofer T.;
Evaluierung des Biomassetrockners der Kraft-Wärme-Kopplungsanlage Oberwart, Bachelor Thesis, Institute of Chemical Engineering, Vienna University of Technology, 2011

Rogner H.;
Energy Resources, in: UNDP (Ed.): World Energy Assessment – Energy and the challenge of sustainability, United Nations Development Programme, New York, 2000

Ruge J., Wohlfahrt H.;
Technologie der Werkstoffe – Herstellung, Verarbeitung, Einsatz, 8., überarbeitete und erweiterte Auflage, Wiesbaden, 2007

Sauciuc A., Potetz A., Weber G., Rauch R., Hofbauer H., Dumitrescu L.;
Synthetic diesel from biomass by Fischer-Tropsch synthesis, in: Proceedings International Conference of Renewable Energies and Power Quality ICREPQ '11, Las Palmas de Gran Canaria, Spain, 2011

Sauciuc A., Abosteif Z., Weber G., Potetz A.,
Rauch R., Hofbauer H., Schaub G., Dumitrescu L.;
Influence of pressure on the performance of biomass based Fischer-Tropsch synthesis, in: Hofbauer, H. (Ed.): Proceedings of the International Conference on Polygeneration Strategies (ICPS11), Vienna, 2011a

Scala F., Montagnaro F., Salatino P.;
Attrition of limestone by impact loading in dual fluidized beds, in: Energy Fuels, 21 (5), 2007

Schmid J.C., Pröll T., Pfeifer C., Hofbauer H.;
Improvement of gas-solid interaction in dual circulating fluidized bed systems, in: Reis, A. et al. (Ed.), Proceedings of the 9th European Conference on Industrial Furnances and Boilers (INFUB-9), 26 - 29 April, Estoril, Portugal, 2011

Schmid J.C., Wolfesberger U., Koppatz S., Pfeifer C., Hofbauer H.;
Variation of feedstock in a dual fluidized bed steam gasifier – Influence on product gas, tar content and composition, Environmental Progress & Sustainable Energy Vol. 31, 2012

Schmid J.C., Pröll T., Kitzler H., Pfeifer C., Hofbauer H.;
Cold flow model investigations of the countercurrent flow of dual circulating fluidized bed gasifier, Biomass Conversion and Biorefinery, 2(3), 2012a

Schuster G., Löffler G., Weigl K., Hofbauer H.;
Biomass steam gasification – an extensive parametric modeling study, Bioresource Technology, 77, 2001

Shimizu T., Hirama T., Hosada H., Kitano K., Inagaki M., Tejima K.;
A Twin Fluid-Bed Reactor for Removal of CO_2 from Combustion Processes, in: Transactions of the Institution of Chemical Engineers, 77, Part A, 1999

Simtech:
IPSEpro Process Simulator – Model Development Kit, User Manual, 2003

Sircar S., Golden T.C.;
Pressure Swing Adsorption Technology for Hydrogen Production, in Liu K. (Ed.): Hydrogen and Syngas Production and Purification Technologies, John Wiley & Sons, Hoboken, USA, 2009

Soukup G.;
Der AER – Prozess, Weiterentwicklung in einer Technikumsanlage und Demonstration an einer Großanlage, Dissertation, Institute of Chemical Engineering, Vienna University of Technology, 2009

Soukup G., Pfeifer C., Kreuzeder A., Hofbauer H.;
In - Situ CO_2 - Capture in a Dual Fluidized Bed Biomass Steam Gasifier: Bed Material and Fuel Variation, Chemical Engineering & Technology, 32, 2009a

Spath P., Mann M.;
Life cycle assessment of hydrogen via natural gas steam reforming, National Renewable Energy Laboratory, US Department of Energy, Colorado, 2001

Stidl M.;
Ersatz fossiler Brennstoffe durch die Zweibett-Wirbelschicht-Dampfvergasung fester Biomasse, Dissertation, Institute of Chemical Engineering, Vienna University of Technology, 2012

Strauß K.;
Kraftwerkstechnik zur Nutzung fossiler, nuklearer und regenerativer Energiequellen, 6., aktualisierte Auflage, Heidelberg, Dordrecht, London, New York, 2009

Sutton D., Kelleher B., Ross J.R.H.;
Review of literature on catalysts for biomass gasification, in: Fuel Processing Technology, Volume 73, 2001

Tessie Du Motay M., Marechal M.;
Bulletin de la Societe Chimique de Paris, 1868

Tondl G.;
Oxyfuel-Verbrennung alternativer Brennstoffe, Dissertation, Institute of Chemical Engineering, Vienna University of Technology, 2013

Tretter H.;
k:a energieholz – Marktanalyse des Bundesministeriums für Land- und Forstwirtschaft, Umwelt und Wasserwirtschaft, http://www.energieholz.klimaaktiv.at (accessed Septermber 07th, 2011), Wien, 2011

Urban W., Lohmann H., Kai G.;
Abschlussbericht für das BMBF-Verbundprojekt „Biogaseinspeisung" – Beseitigung technischer, rechtlicher und ökonomischer Hemmnisse bei der Einspeisung biogener Gase in das Erdgasnetz zur Reduzierung klimarelevanter Emissionen durch Aufbau und Anwendung einer georeferenzierten Datenbank, in: Band 4 Technologien und Kosten der Biogasaufbereitung und Einspeisung in das Erdgasnetz, Ergebnisse der Markterhebung 2007-2008, Fraunhofer UMSICHT, Oberhausen, 2009

UNDP;
World Energy Assessment – Energy and the challenge of sustainability, United Nations Development Programme, New York, 2000

U.S. Energy Information Administration;
Annual Energy Review 2009 – DOE/EIA-0384(2009), U.S. Energy Information Administration, U.S. Department of Energy, Washington D.C., 2009

VDI;
Guideline 3633 – Simulation von Logistik-, Materialfluss- und Produktionssystemen, Richtlinie 3633, Verein Deutscher Ingenieure, Düsseldorf, 1993

Voestalpine;
Environmental Report – Measures, Developments, Results, Linz and Steyrling Locations, 2010

Wagner W., Kruse A.;
Properties of water and steam – Zustandsgrößen von Wasser und Wasserdampf, IAPWS-IF97, Springer, Berlin, 1998

Walter H.;
Fortschrittliche Energieanlagen – Lehrveranstaltungsunterlagen zu VU Fortschrittliche Energieanlagen Sommersemester 2011, Institut für Energietechnik und Thermodynamik, Vienna University of Technology, 2011

Weimer T., Berger R., Hawthorne C., Abanades J.C.;
Lime enhanced gasification of solid fuels - Examination of a process for simultaneous hydrogen production and CO_2 capture in: Fuel, 87, 2008

Wildemann, H.;
Risikomanagement und Rating, 1.Auflage, TCW Transfer-Centrum GmbH & Co KG, München, 2006

Wilk V., Kern S., Kitzler H., Koppatz S., Schmid J.C., Hofbauer H.;
"Gasification of plastic residues in a dual fluidized bed gasifier- Characteristics and performance compared to biomass", in: Proceedings of the International Conference on Polygeneration Strategies (ICPS11), Vienna, 2011

in total: 111 References

Abbreviations

AER	Absorption enhanced reforming
ARGE DKWF	Joint venture steam power
Aspen Hysys	Software for process simulation
Aspen Plus	Software for process simulation
bbl.	Oil barrel equals 159 liters
BG_Lib	Biomass gasification library of simulation models
Bioenergy 2020+	Bioenergy 2020+ GmbH, Austrian bioenergy research company
BioH2 4Refineries	National research project in Austria investigating hydrogen production from biomass for refineries
BioSNG	Synthetic natural gas from biomass
BK Güssing	Biomasse-Kraftwerk Güssing GmbH & Co KG, company operating the CHP plant Güssing
BMLEV	Federal Ministry of Food, Agriculture and Consumer Protection (Germany)
BP	British Petrol, oil company
CCS	Carbon capture and storage
cet. par.	From Latin: "all other things held constant"
cf.	From Latin: confer, compare
CHEMASIM	Software for process simulation
ChemCAD	Software for process simulation
CHP	Combined heat and power plant
CIP	Competitiveness and Innovation Framework Programme
CO-shift	Reactor enhancing the water gas shift reaction
CO2	Carbon dioxide
DFB	Dual fluidized bed
DFB_comb_AERgas	Model of associated combustion reactors for sorption enhanced reforming
DFB_comb_standard	Model of associated combustion reactors for sorption enhanced reforming
DFB_gsf_AERGas_std	Extended gasifier model including chemical reactions of sorption enhanced reforming
DFB_gsf_AERGasCO2capt	Extended gasifier model including chemical reactions of sorption enhanced reforming
DFB_gsf_bal	Simple gasifier model based on mass- and energy balance
DFB_gsf_char_kin	Extended gasifier model reflecting char kinetics
DFB_gsf_char_kin II	Extended gasifier model reflecting residence times
DFB_gsf_char_kin_OW	Extended gasifier model reflecting geometries
DFB_gsf_wgshift	Extended gasifier model including water-gas shift reaction
dll	Dynamic link libary
Ed.	Editor
EJ	Exajoule
EN	European standard
Energie Burgenland	Energie Burgenland AG, Austrian energy provider
EON	E.ON SE, energy provider from Germany
ERBA	National research project in Austria investigating sorption enhanced reforming
et al.	From Latin: et alii, and others
EU	European Union

EU-15	Former 15 member states of the European Union
EU-27	27 member states of the European Union
EUR	Euro (currency)
Eurostat	Statistical office of the European Union
FAME	Fatty acid ethyl esters (biodiesel)
ff.	Following pages
First Solar	First Solar GmbH, German photovoltaic manufacturer
FT	Fischer Tropsch process, chemical reactions for the production of synthetic fuel
GDP	Gross domestic product
GLV	Glowing loss
G-volution II	National research project in Austria for the construction of a Next generation dual fluid gasifier
HSC Sim - Chemistry	Software for process simulation
H2 SIM GUO	Research project investigating hydrogen production from residues of palm oil industries
IAPWS-IF97	International Association for Properties of Water and Steam, Industrial Formulation 1997
IC	Investment costs
IEA	International Energy Agency
IGCC	Integrated gasification combined cycle
IPCC	International Panel on Climate Change
IPSEpro	Process simulation software
ISO	International Organization for Standardization
JANAF-tables	Joint, Army, Navy, Air Force, publication of property data for ideal gases
Juwi	Juwi AG, German renewable energy technology company
KS	German "Kalksplitt", limestone chips
KWK	"Kraft-Wärme-Kopplung" German for combined heat and power
lhv	Lower heating value
MAN	MAN (Maschinenfabrik Augsburg-Nürnberg) SE, German mechanical engineering company
MCFC	Molten carbonate fuel cells
Metso	Metso Cooperation, chemical engineering company
Mtoe	Million tons oil equivalent
NASA	National Aeronautics and Space Administration
n.a.	Not available
NER300	Funding framework by the European Commission for renewable energy technology and CCS in the EU
n.n.	Not named
Nm^3	Gas cubic meter according to standard conditions (1.01325 bar, 0.001001 °C)
NPV	Net present value
OECD	Organisation of Economic Co-operation and Development
OMV	OMV AG, refinery operator in Austria
ORC	Organic rankine cycle
ORTNER	Ortner GmbH, Austrian engineering company
POP	Population

ppb	Parts per billion
ppm	Parts per million
PRIMINREP	National research project in Austria for the reduction of primary energy sources in the field of raw iron production
PSA	Pressure swing adsorption
PSE	Process simulation environment
PTFE	Polytetrafluoroethylen
REPOTEC	Repotec Umwelttechnik GmbH, Austrian engineering company
RES	Renewable energy sources
RL	In German “Rücklauf”, outlet flow
RME	Rapeseed methyl ester
SCA	SCA Hydiene Products GmbH, paper mill operator in Austria
SEM	Scanning electron microscope
SER	Sorption enhanced reforming
SET-Plan	Strategic energy technology plan
Siemens	Siemens AG, German multinational industrial conglomerate company
Simtech	SimTech GmbH, software company, Austria
SNG	Synthetic natural gas
SP	Steam power cycle
SST	Product abbreviation for Siemens steam turbines
System 7	Software for process simulation
Tauernkraftwerke AG	Former company operating the hydropower plant in Kaprun, Austria
TECON	Tecon Engineering GmbH, Austrian engineering company
TGA	Thermo gravimetric analysis
TOE	Tons oil equivalent
Trianel	Trianel GmbH, German energy provider
UNDP	United Nations Development Programme
UniSim	Software for process simulation
UOP	UOP LLC (Universal Oil Products), multi-national company for petroleum refining technology
USA	United States of America
USD	US dollar (currency)
Vattenfall	Vattenfall AB, Swedish energy provider
VDI	German society of engineers
Verbund	Verbund AG, Austrian energy provider
Vestas	Vestas Wind Systems A/S, Danish wind turbine manufacturer
VL	German “Vorlauf”, inlet flow
VOEST	Voestalpine Stahl Gmbh, Austrian iron producer
vol.-%$_{db}$	Volume percent on dry basis
waf	Water and ash free
wf	Water free
wt.-%$_{db}$	Weight percent on dry basis
Wien Energie	Wien Energie GmbH, Austrian energy provider

Symbols

A	Expenses	[€/a]
BWSF	Cumulative present value factor	[-]
C	Costs	[€/a]
$C_{Opt,X}$	Costs option X	[€/a]
c_p	Specific heat	[kJ/kg K]
C(x)	Concentration of gaseous reactant	[mol/mol]
ΔC_X	Cost savings	[€/a]
d_p	Particle diameter	[mm]
d_{p10}	Particle size of the 10% quantile (sieve analysis)	[mm]
d_{p50}	Mean particle size (sieve analysis)	[mm]
d_{p90}	Particle size of the 90% quantile (sieve analysis)	[mm]
d_{sv}	Sauter diameter	[mm]
E	Earnings	[€/a]
h	Specific enthalpy	[kJ/kg]
H*	Total enthalpy	[kJ/mol]
ΔH	Enthalpy of reaction	[kJ/mol]
i	Interest rate	[%]
I_0	Investment costs	[€]
$I_{Opt,X}$	Investment costs option X	[€]
ΔI_X	Additional investment costs	[€]
$K_p(T)$	Equilibrium constant	[-]
l	Heat loss rate	[-]
$lhv_{add\ fuel}$	Lower heating value of additional fuel	[kJ/kg]
lhv_{fuel}	Lower heating value of fuel (biomass)	[kJ/kg]
lhv_{PG}	Lower heating value of product gas	[kJ/kg]
$\dot{m}$	Mass flow	[kg/h]
$\dot{m}_{add\ fuel}$	Additional fuel mass flow	[kg/h]
$\dot{m}_{air}$	Air mass flow	[kg/h]
$\dot{m}_{bed,fresh}$	Fresh bed material ($CaCO_3$) entering circulation loop	[kg/h]
$\dot{m}_{bed,G,in}$	Mass flow of bed material entering the gasifier from combustor	[kg/h]
M_{CaCO3}	Molar weight of $CaCO_3$	[g/mol]
M_{CaO}	Molar weight of CaO	[g/mol]
$\dot{m}_{char,bed}$	Char mass flow from gasifier to combustor	[kg/h]
M_{CO}	Molar weight of carbon monoxide (CO)	[kg/mol]
M_{CO2}	Molar weight of CO_2	[g/mol]
$\dot{m}_{CO2,capt}$	Mass flow of CO_2 absorbed by bed material in gasifier	[kg/h]
$\dot{m}_{flue,g}$	Flue gas mass flow	[kg/h]
$\dot{m}_{fuel}$	Fuel mass flow (e.g. biomass to gasifier)	[kg/h]
$\dot{m}_{fluid}$	Fluidization mass flow gasifier (steam)	[kg/h]
$m_{gasifier}$	Amount of bed material within gasifier	[kg]
$m_{inventory}$	Total bed material within system	[kg]
M_{O2}	Molar weight of oxygen (O_2)	[kg/mol]
$\dot{m}_{PG}$	Product gas mass flow	[kg/h]
$\dot{m}_{PGre}$	Product gas recycle mass flow	[kg/h]
n	Lifetime	[a]
N	Mean cycles of particle within system	[-]
$\dot{n}$	Molar flow rate	[mol/s]
$\dot{n}_{CaO}$	Present CaO	[mol]

$\dot{n}_{\mathrm{CaCO3}}$	Present $CaCO_3$	[mol]
$\dot{n}_{\mathrm{CO2}}$	Absorbed CO_2	[mol]
NPV	Net present value	[€]
ΔNPV_X	Advantageous net present value	[€]
p	Pressure	[bar]
P	Mechanical power	[W]
$P_{\mathrm{chem,pg}}$	Chemical power in product gas	[W]
p_{CO}	Partial pressure of CO in product gas	[Pa]
p_{CO2}	Partial pressure of CO_2 in product gas	[Pa]
p_{df}	Particle diameter frequency	[-]
$P_{\text{€}}$	Profit	[€/a]
$P_{\mathrm{el,cons}}$	Electricity consumption	[W]
$P_{\mathrm{el,gr}}$	Gross electricity output	[W]
$P_{\mathrm{el,net}}$	Net electricity output	[W]
p_{H2}	Partial pressure of H2 in product gas	[Pa]
p_{H2O}	Partial pressure of H2O in product gas	[Pa]
P_{th}	Thermal power based on fuel power	[W]
$\dot{Q}$	Heat output, heat flow	[W]
$\dot{Q}_{\mathrm{loss}}$	Heat loss	[W]
R	Radial position	[m]
r_{circ}	Bed material circulation rate	$[\mathrm{kg}/\mathrm{kg}_{\mathrm{fuel.waf}}]$
T	Temperature	[°C]
T_G	Gasification temperature	[°C]
T_R	Combustion temperature	[°C]
U	Superficial gas velocity	[m/s]
U_{mf}	Minimum fluidization gas velocity	[m/s]
U_t	Terminal velocity	[m/s]
$w_{\mathrm{ash,fuel}}$	Ash content of biomass	[-]
$w_{\mathrm{H.fluid}}$	Elementary hydrogen content of gasifier fluidization	[-]
$w_{\mathrm{H.fuel}}$	Elementary hydrogen content of biomass	[-]
$w_{\mathrm{H2.PG}}$	Hydrogen content of product gas	[-]
$w_{\mathrm{H2O,fuel}}$	Water content of biomass	[-]
$w_{\mathrm{H2O.fluid}}$	Water content of gasifier fluidization	[-]
$w_{\mathrm{H2O.PG}}$	Water content of product gas	[-]
X_{CaO}	CO_2 load	$[\mathrm{mol}_{\mathrm{CO2}}/\mathrm{mol}_{\mathrm{CaO}}]$
X_{CH4}	Methane (CH_4) conversion rate	[%]
X_{CO2}	Carbon monoxide (CO) conversion rate	[%]
X_{CxHy}	Conversion rate of C_xH_y	[%]
$X_{\mathrm{H2O.abs}}$	Absolute water conversion rate	$[\mathrm{kg}_{\mathrm{H2O}}/\mathrm{kg}_{\mathrm{H2O}}]$
$X_{\mathrm{H2O.rell}}$	Relative water conversion rate	$[\mathrm{kg}_{\mathrm{H2O}}/\mathrm{kg}_{\mathrm{fuel,waf}}]$
X_m	Carbon conversion associated with microporosity	[-]
X_W	Carbon conversion associated with grain boundaries	[-]
Z	Number of connected streams	[-]

δ_{CaO}	Calcium circulation rate	$[s^{-1}]$
$\delta_{Eq.,WGS\text{-}shift}$	Logarithmic distance to equilibrium (water-gas-shift reaction, gasifier)	[-]
ε_m	Porosity around micrograins	[-]
ε_W	Propsity around large pores	[-]
η_{chem}	Simplified chemical efficiency	[-]
η_{el}	Electric efficiency	[-]
η_g	Cold gas efficiency	[-]
η_{H2}	Hydrogen productivity rate	$[kg_{H2}/kg_H]$
η_Q	Thermal efficiency	[-]
η_u	Utilization rate	[-]
κ_{CaO}	Bed material renewal rate	$[h^{-1}]$
λ	Air ratio	[-]
$\mu_{O2,adf}$	Oxygen content in additional fuel	$[kg_{O2}/kg]$
$\mu_{O2,air}$	Oxygen content in combustion air	$[kg_{O2}/kg]$
$\mu_{CO,fluegas}$	Carbon monoxide content in flue gas stream	$[kg_{CO}/kg]$
$\mu_{O2,fluegas}$	Oxygen content in flue gas stream	$[kg_{O2}/kg]$
σ_{CO}	CO / CO_2 in combustor exhaust gas	[mol/mol]
τ_{CaO}	Mean time of particle within system	[s]
φ_{CaO}	CO_2 load	$[kg_{CO2}/kg_{CaO}]$
φ_{char}	Char combusted in combustion chamber	$[kg_{char}/kg_{fuel,waf}]$
φ_{SF}	Steam to fuel ratio	$[kg_{H2O}/kg_{fuel,waf}]$
$\omega_{CaCo3,bed,fresh}$	$CaCO_3$ in fresh material	$[kg_{CaCO3}/kg_{bed,fresh}]$
$\omega_{CaCo3,bed,G,in}$	$CaCO_3$ in bed material to gasifier from combustor	$[kg_{CaCO3}/kg_{bed}]$
$\omega_{CaCo3,inventory}$	$CaCO_3$ in bed material inventory	$[kg_{CaCO3}/kg_{bed}]$
$\omega_{CaO,bed,fresh}$	CaO in fresh bed material	$[kg_{CaO}/kg_{bed,fresh}]$
$\omega_{CaO,bed,G,in}$	CaO in bed material to gasifier from combustor	$[kg_{CaO}/kg_{bed}]$
$\omega_{CaO,inventory}$	CaO in bed material inventory	$[kg_{CaO}/kg_{bed}]$

Appendices

Reviewed paper published

I. Müller, S., Stidl, M., Pröll, T., Rauch, R., Hofbauer, H., 2011, "Hydrogen from Biomass - Large Scale Hydrogen Production Based on a Dual Fluidized Bed Steam Gasification System", Biomass Conversion and Biorefinery, (2011) 1, 55-61.

II. Müller, S., Kotik, J., Pröll, T., Rauch, R., Hofbauer, H., 2011, "Hydrogen from Biomass for Industry - Biomass Gasification for Integration in Refineries", in: Proceedings of the International Conference on Polygeneration Strategies (ICPS11), 30 August - 1 September 2011, Wien, Austria.

III. Müller, S., Pröll, T., Hofbauer, H., 2012, "A Thermodynamic Investigation of Dual Fluidized Bed Biomass Gasification with Sorption Enhanced Reforming", in: Proceedings of the 21st International Conference on Fluidized Bed Combustion (FBC), 3.-6. June 2012, Naples, Italy, pp.781-788, ISBN978-88-89677-83-4

Paper I

Müller, S., Stidl, M., Pröll, T., Rauch, R., Hofbauer, H.,

"Hydrogen from Biomass - Large Scale Hydrogen Production Based on a Dual Fluidized Bed Steam Gasification System"

Biomass Conversion and Biorefinery, 1, pp. 55-61, **2011.**

Biomass Conv. Bioref. (2011) 1:55–61
DOI 10.1007/s13399-011-0004-4

REVIEW ARTICLE

Hydrogen from biomass: large-scale hydrogen production based on a dual fluidized bed steam gasification system

Stefan Müller · Martin Stidl · Tobias Pröll · Reinhard Rauch · Hermann Hofbauer

Received: 20 September 2010 / Revised: 17 January 2011 / Accepted: 20 January 2011 / Published online: 8 February 2011

Abstract Hydrogen is used as an important feedstock for the chemical industry. Common production technologies for the production of hydrogen from fossil fuels today cause relevant CO_2 emissions. Hydrogen from renewable energy sources is discussed as an alternative option to replace traditional feedstock and can therefore be part of a low-carbon energy system. This paper describes the results of a simulation of a concept for the production of hydrogen with biomass as feedstock. The described investigations include a possible process design, the process simulation using the software IPSEpro, a description of the operation characteristics, and a profitability analysis of the applied hydrogen production concept. The simulation result shows that 61 MW of hydrogen can be produced from 100 MW wood chips and 6 MW of electricity. As a result, hydrogen production costs of 54 €/MWh can be estimated. For the investigated concept, the wood chip price is the most important factor for the hydrogen production cost followed by investment costs for the plant and the realized plant operation time per year.

Keywords Biomass · Gasification · Hydrogen · Membrane · Plant simulation

1 Introduction

The world's energy system today is facing increasing challenges regarding its environmental, economical, and social sustainability. Continuation of our current way of energy consumption would lead to a catastrophic and irreversible damage to the global climate by increasing the global mean temperature by 6°C in 2100 compared to 1850. Such an increase would imply major economical and social crises all over the world. To avoid such a scenario in the future, a rapid transformation to a low-carbon, efficient, and environmentally benign system of energy supply is required [1].

For the realization of a low-carbon energy system, the development of new energy carriers is needed because most energy carriers today are based upon fossil energy sources. For this reason, hydrogen produced from renewable energy sources is discussed as an alternative to fossil energy carriers. Hydrogen can be used as an energy carrier, for energy storage applications, as fuel for fuel cells and as fuel for combustion engines. Furthermore, hydrogen is used as an important feedstock for the chemical industry. Common production technologies for the production of hydrogen today cause relevant CO_2 emissions. The combustion process of hydrogen itself is free of CO_2 emission and can therefore be a part of a low-carbon energy system. It is important to note that there is still some research required to meet the challenges regarding the storage of hydrogen and the production from renewable energy sources [2].

For the production of hydrogen so far, mainly natural gas and naphtha are used as feedstock. The most common production technology is the steam reforming of natural gas. But also production technologies like partial oxidation or autothermal reforming of fossil fuels are used for industrial applications [3, 4]. All of the so-far mentioned production technologies have in common that they cause relevant CO_2 emissions. To meet the goal of a "low-carbon energy system," hydrogen can only be an option if it is produced from renewable energy sources. The production

---

S. Müller (✉) · M. Stidl · T. Pröll · R. Rauch · H. Hofbauer
Institute of Chemical Engineering-Future Energy Technology,
Vienna University of Technology,
Getreidemarkt 9/166,
1060 Vienna, Austria
e-mail: stefan.mueller@tuwien.ac.at

of hydrogen by applying the electrolysis of water can at this point only be considered as an opportunity if the used electricity is supplied by renewable resources like wind or sunlight. Promising ways for the production of hydrogen are biomass-based production technologies. These production technologies are still under development, and only few data about plants and their operation are available up to now. Therefore, it is difficult for energy policy decision makers to identify the advantages and disadvantages of production technologies based on biomass feedstock [5].

In this area, more research is necessary to be able to quantify the disadvantages and advantages of hydrogen production from biomass. Can hydrogen from biomass be produced at affordable costs? Which improvements of the production technology would be necessary to reach affordable costs? Which production method can achieve the best efficiency and the highest hydrogen output? Previous studies have shown that alkaline electrolysis shows high energy efficiency among the renewable production technologies. But also the reforming of biomass gasification gas shows good production efficiencies [5].

Gasification of biomass is the thermochemical conversion of solid biomass to combustible gases with significant hydrogen content. Therefore, gasification is an appropriate process step for the production of hydrogen from solid biomass [6]. The following research results should help to answer the mentioned questions around hydrogen production from biomass and quantify the characteristics of a hydrogen production plant from biomass basing on a dual fluidized bed steam gasification system and a gas permeation membrane. The following chapters include:

- the process simulation,
- the process design,
- the operation characteristics, and
- a profitability analysis

of a hydrogen production plant concept.

2 Concept and methodology

The following investigations describe the evaluation of a hydrogen production concept with 100 MW biomass as feedstock. The results of the investigations should quantify the advantages and disadvantages of the analyzed production concept. A useful tool for the evaluation of a power plant concept is process simulation. For the calculation of the hydrogen plant parameters, the simulation software IPSEpro has been used. IPSEpro has been part of several successful development processes at the Vienna University of Technology and has proven its reliability in many process design simulations in the past. IPSEpro enables an efficient and quick calculation of mass and energy balances for a modeled process design. The applied process design for the production of hydrogen is basing on the experiences made with biomass gasification in Güssing, Austria. In Güssing, the gasification of biomass with a dual fluidized bed has been successful demonstrated.

The process design plays a crucial role for the performance of a plant configuration. Figure 1 illustrates a general overview over the chosen process design for the simulation of the hydrogen production plant. The starting point of the hydrogen production is the gasification of biomass in a dual fluidized bed steam gasification system. Two separate gas streams are the product of the gasification system. The product gas stream contains the chemical energy of the gasified wood chips. After further gas treatment steps, the product gas contains a high amount of hydrogen which can be separated from the main product gas stream. The evaluated process design contains a dual fluidized bed steam gasification system with olivine as bed material. This gasification system has been chosen because it offers the possibility to produce a product gas with high energy density and high hydrogen content and this technology has already been successfully demonstrated on a larger scale. A promising way for a further future development of the evaluated process design would be the implementation of a dual fluidized bed steam gasification system using lime as bed material to selectively transport CO_2. This would lead to a higher hydrogen content of the product gas at the exit of the gasification system and reduce therefore the necessary gas treatment [7].

The flue gas stream is the result of a separate combustion process which delivers the necessary heat for the gasification and can be used for the recovery of process heat. Figure 2 illustrates the applied process design more in detail. The treatment of the product gas stream should ensure a high share of hydrogen. In a first step, the gas stream gets reformed in a steam reformer at a temperature between 750°C and 850°C. In a second step, the product gas gets converted in a CO-shift reactor at a temperature of 350°C. Table 1 shows the development of the product gas stream at the different stages.

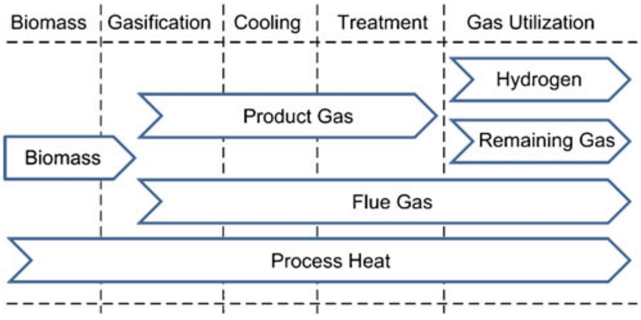

Fig. 1 Process design

Fig. 2 Detailed process design

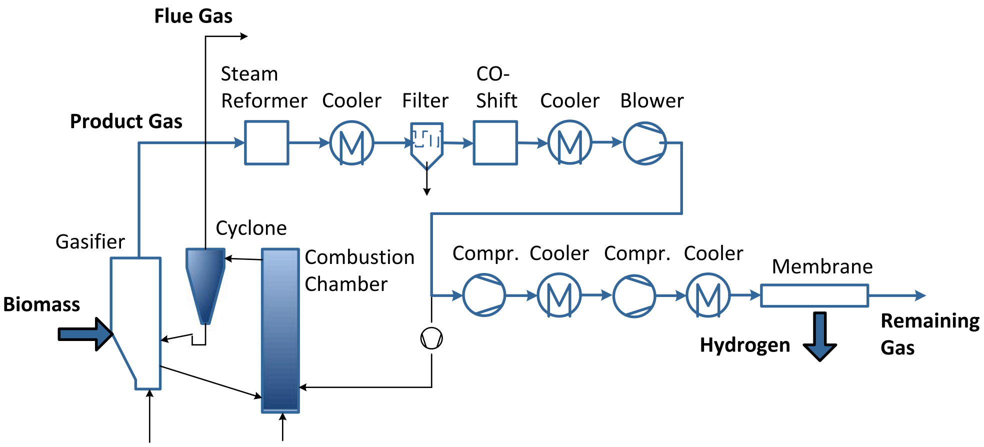

After the CO-shift reactor, the product gas stream contains a high amount of hydrogen. The hydrogen needs to be separated from the other fractions in the product gas stream. For the separation of hydrogen from the remaining gas, the application of a hydrogen purification technology is necessary. There are different purification systems available:

- Cryogenic separation
- Pressure swing adsorption (PSA)
- Membrane separation

The different hydrogen purification systems are basing on different separation principles. So, the process characteristics differ significantly. The selection of the appropriate separation method depends not only on the economics but also on process flexibility, reliability, and the way of the hydrogen utilization [8].

In the investigated case, a polyamide gas permeation membrane has been implemented in the process design. The behavior of the membrane is currently under experimental investigation together with a scientific cooperation partner, and the simulation results of the plant concept should give feedback about the characteristics of the implementation of such a membrane in a 100-MW plant configuration. The low pressure of the hydrogen product is a disadvantage of the separation with membranes because for most hydrogen utilization cases, the hydrogen is needed at high pressure. To reach this pressure, another compression is necessary which leads to higher electricity consumption. An alternative method for the separation of hydrogen from the product gas would be by applying PSA processes. PSA systems offer high separation efficiencies and design flexibility [9]. PSA systems are common for the industrial production of hydrogen from natural gas and in small-scale configurations like oxygen production from air and biogas separation. On the other hand, the complexity of PSA systems can be a disadvantage for the application in small- and medium-scale plant configurations. The decision between a membrane and a PSA system depends on the utilization of the hydrogen. If high purity of the hydrogen is needed, PSA devices deliver better results regarding purity and energy efficiency. The membrane has been chosen for the hydrogen separation process because it is a simple system and well established in the production of hydrogen from natural gas and in different fermentation gas separation processes [10].

Table 1 Product gas composition

Product gas after…	Gasifier (%)	Steam reformer (%)	CO-shift reactor (%)	Membrane separation (hydrogen) (%)
H_2 (wf)	40.9	55.0	62.9	87.0
CO (wf)	25.0	30.0	7.3	0.2
CO_2 (wf)	19.6	12.5	27.8	12.8
CH_4 (wf)	9.9	1.4	1.1	0.01
Other (wf)	4.6	1.1	0.9	0.19

wf water free

The applied process design should ensure high efficiency with high hydrogen output and low biomass and electricity consumption. This way, low hydrogen production cost should be achieved. The process simulation software IPSEpro should quantify the advantages and disadvantages of the designed hydrogen production concept. Therefore, the detailed process design for the production of hydrogen has been modeled in an IPSEpro Project.

3 Results and discussion

Figure 3 gives an impression of the IPSEpro model for the simulation of the described hydrogen production concept with 100 MW of biomass as feedstock. The calculation of the model with IPSEpro delivers the results for mass and energy balances of the modeled process design. These results demonstrate the possible hydrogen output for the modeled concept. The results show that 61 MW hydrogen (basis lower heating value) can be made from 100 MW biomass (basis lower heating value). Additionally, there is

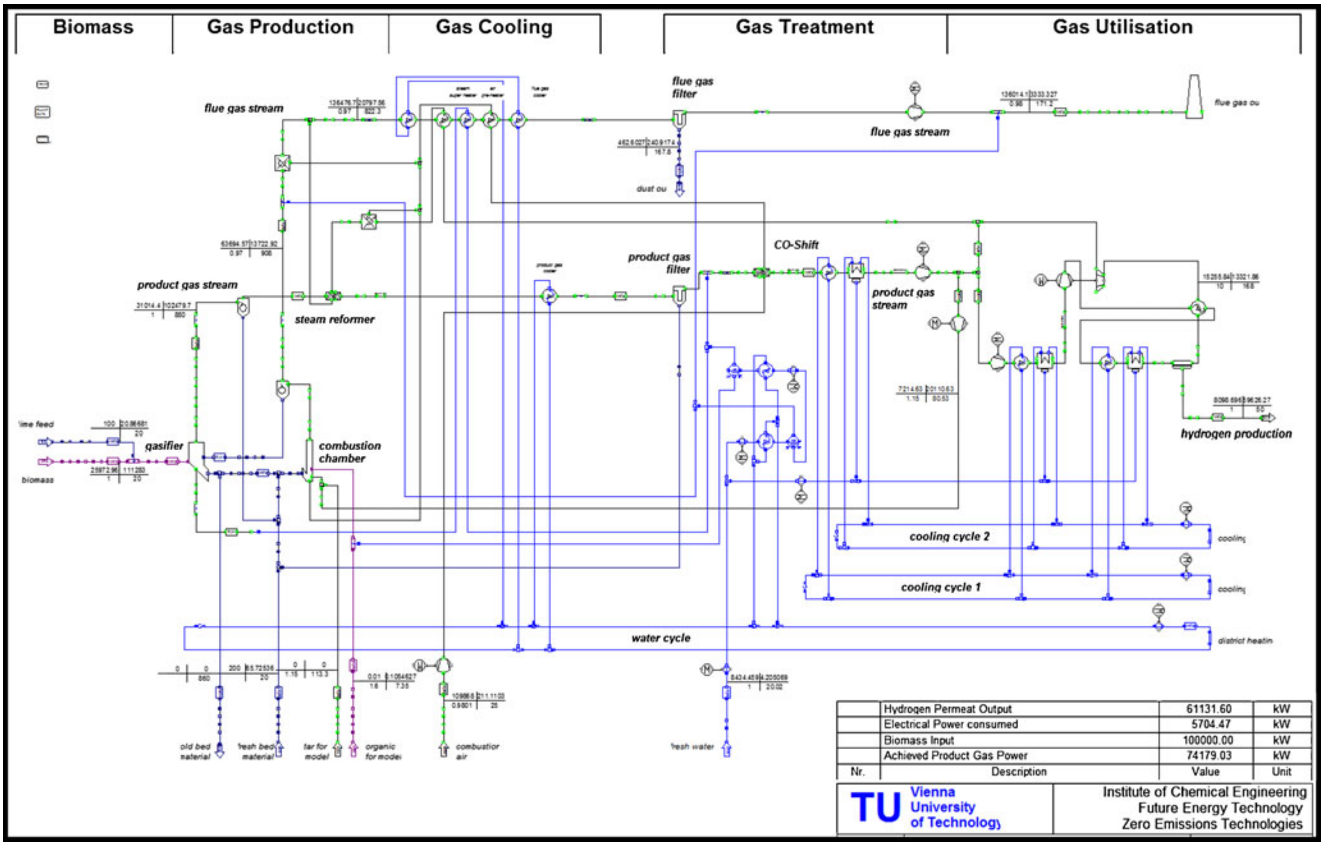

Fig. 3 IPSEpro project—concept for the hydrogen production from 100 MW biomass

6 MW of electricity necessary for the production process. As well as hydrogen process heat is also generated. This process heat could be used, for example, for district heating if there is local demand beside the plant. The results also show that 17.5 MW of heat could be used for district heating with a feed temperature of 142°C (10 bar) and a return flow temperature of 100°C (8 bar). Tables 2 and 3 show the final results of the mass and energy balances for the modeled hydrogen plant. The feed for this plant is wood chips with a water content of 20 wt.%. The wood chips get gasified in a dual fluidized steam gasification system.

After the gasification process, the produced product gas exits the gasifier with a temperature of 850°C. The produced product gas gets cleaned, cooled, and reformed as shown in Fig. 2 and Table 1. For the hydrogen separation from the remaining gas, the gas gets compressed to a pressure of 10 bar. For this compression, 3.5 MW of electricity is used and electricity is therefore a main production factor which needs to be considered. Table 2 illustrates the electricity consumption of the plant which includes the remaining pumps and blowers. The remaining gas of the hydrogen separation process is used for the generation of process heat for the gas reforming process. The gas reforming process can be heated only by the combustion of the remaining gas independently. In the case of power fluctuation, the performance of the

Table 2 Plant input

Plant input		
Biomass (wood chips)	kg/h	25 972
Biomass—water content	wt.%	20
Biomass—lower heating value	MJ/kg	13.86
Biomass—chemical energy	kW	100 000
Electricity—consumption	kW	5 714
Water	kg/h	8 434
Air	Nm³/h	85 752

Table 3 Plant output

Plant output		
Hydrogen	Nm³/h	23 782
Hydrogen—production costs	€/MWh	54
Hydrogen—lower heating value	MJ/kg	27.17
Hydrogen—chemical energy	kW	61 131
District heating	kW	17 666
Ash	kg/h	462
Flue gas	Nm³/h	102 689

steam reformer can be adjusted by additional combustion of product gas.

With the simulation of the described hydrogen production plant, the mass and energy balance of the concept have been quantified. A further perspective for the evaluation of the achieved results arises by looking at the possible profitability of the plant concept. Tables 2 and 4 show the values of the main parameters which have been considered for the cost analysis. The most important factors for the production cost of hydrogen are the wood chip price, the investment costs for the plant, and the realized operation time per year. A calculation with the illustrated values in Table 4 shows that the hydrogen production cost are 54 €/MWh.

The represented values in Table 4 refer to a simple cost calculation model for the calculation of the hydrogen production costs. The calculation results refer to the hydrogen purity shown in Table 1 at atmospheric pressure. A higher purity of the produced hydrogen and the compression of the hydrogen for transport and storage would lead to higher investment and operational costs. An evaluation of different hydrogen production plants using the methodology of a net present value calculation would need to consider alternative options with similar plant output conditions. The main purpose of this cost calculation is not to estimate the production costs exactly. The purpose is to find out about the main factors which have the most impact on the overall production cost. These factors are the critical success factors for the evaluated plant concept, and they enable a significant optimization of the process design. At this point, values for costs and prices always involve insecurity about their future development of the different cost parameters. For the evaluated plant concept, the main factors for the hydrogen production costs are the wood chip price, the investment costs, and the operational hours per year of the plant. A change of these main factors is shown in Fig. 4. This figure illustrates a possible change of investment costs, operation time, and wood chip price and their impact on the hydrogen production costs. Other cost factors like electricity consumption, nitrogen, olivine, etc., have also been included in the calculation of hydrogen production costs, but their impact is less compared to the mentioned main cost factors. The most likely expected price change would be a change of the wood chip price.

Table 4 Cost analysis

Cost analysis		
Operating hours	h/a	7 000
Wood chip costs	€/MWh	20
Electricity costs	€/MWh	90
Nitrogen costs	€/Nm³	0.06
Olivine costs	€/t	150
Lime costs	€/t	15
Labor costs	€/a pers.	45 000
Plant investment costs	€	50 000 000
Maintenance costs	%/a	0.5
Operating time	a	10
H_2 production costs	€/MWh	54

The circle in Fig. 4 marks the estimated case with a “wood chip price” of 20 €/MWh [11], 50 000 000 € “investment cost” for the plant, and an estimated “operation time per year” of 7 000 h. A change of the wood chip price has the biggest impact on the production cost of the applied production concept. Thus, the relation between wood chip price and the price of an alternative feedstock like natural gas is a critical success factor for hydrogen production concepts. This underlines the impact of energy policy decision makers by taxing and subsidizing different feedstock. Investment cost and the plant operation hours also have a major impact on the production costs.

To cover the impact of economic modeling uncertainties, different price scenarios have been calculated and illustrated in Fig. 4. Further realization steps for the evaluated hydrogen production plant need to include adequate economic methodology for the precise prediction of the costs and earnings for the first years of plant operation. The biggest uncertainties for this calculation would be the exact prediction of realized investment cost for the plant and the realized wood chip purchase price in the future. To achieve low hydrogen production cost, the plant operator needs an excellent management of the planning, construction, and operation phase of the hydrogen production plant. This would also ensure a high availability of the plant in the first years of operation. To address technical modeling uncertainties, it is important to validate the implemented model units. The implemented models have been validated in the past with experimental data from the 8–10 MW plants in Güssing and Oberwart. Especially the long time behavior of units in the process design, which have not been part of the demonstrated plants before, and their reaction on the long time application in a gasifier product gas stream need to be considered before further realization steps of the plant concept. Therefore, the data regarding the behavior of the “membrane system” and the “CO-shift reactor” need to be approved by experiment at relevant operating conditions.

The evaluated hydrogen production plant is based on a dual fluidized bed steam gasification system. This system is an indirect gasification system which has been successfully demonstrated on a large scale in Güssing and in Oberwart. A dual fluidized bed steam gasification system produces a nitrogen-free product gas with high hydrogen content and can be compactly build without the need of an air separation unit. Disadvantages compared to direct gasification systems are that the plant has to operate two separate

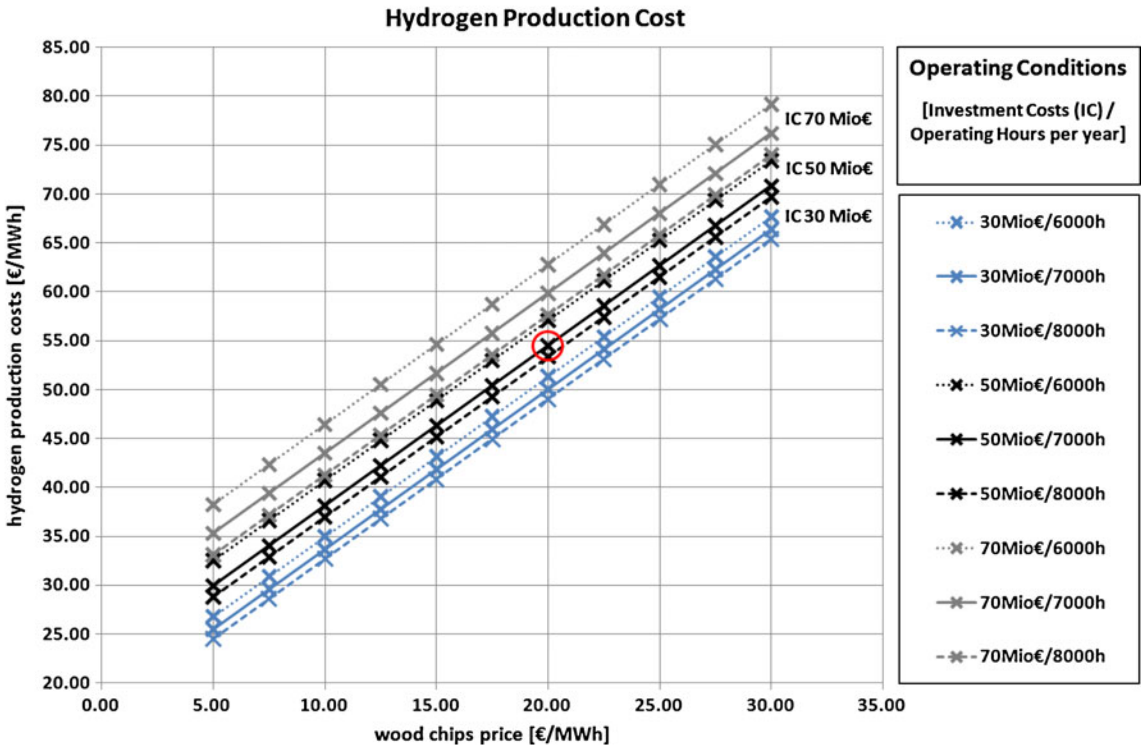

Fig. 4 Hydrogen production costs

gas streams and that it is so far demonstrated on a larger scale just at atmospheric pressure. The dual fluidized bed steam gasification technology offers good properties for the integration into a hydrogen production concept. For the further development of the hydrogen production concept, gasification using lime as bed material to selectively transport CO_2 could be an interesting option because of the higher hydrogen content of the produced product gas. The higher hydrogen content and improved product gas quality would reduce the necessary amount of gas treatment and gas cleaning. A dual fluidized bed steam gasification system using lime as bed material to selectively transport CO_2 has so far not been demonstrated on a larger scale. Also, pressurized gasification is an interesting option which could reduce the electricity consumption of the plant. Further research and development is necessary to gain the benefits of the mentioned principles.

4 Conclusion and outlook

Continuing our current way of energy consumption would lead to a catastrophic damage to the global climate. Hydrogen from renewable energy sources is discussed as an alternative option to replace traditional energy carriers and can therefore be part of a low-carbon energy system. For the production of hydrogen so far, in most cases, fossil fuels are used as feedstock. This paper describes the results of the simulation of a concept for the production of hydrogen with biomass as feedstock. The investigated concept is basing on a dual fluidized bed steam gasification system and a gas permeation membrane.

The results of the simulation with the process simulation software IPSEpro show that 61 MW of hydrogen can be produced from 100 MW wood chips. Additionally, there is 6 MW of electricity necessary for this hydrogen production concept. Furthermore, all mass and energy balances have been quantified for the modeled hydrogen production plant. The applied process design plays a major role for the performance of the plant.

In the case investigated, the process design was based on a dual fluidized bed steam gasification system, a steam reformer, a “CO-shift” reactor, and a gas permeation membrane. In this process design, the following weaknesses have been identified and need be considered before further project development. The hydrogen separation with a gas permeation membrane leads to a certain electricity consumption because of the necessary product gas compression. After the separation process, the hydrogen is delivered at a low pressure and the purity of the hydrogen product is relatively low for further utilization. Depending on the hydrogen utilization, PSA units could also deliver good overall results. At this point, further investigations are necessary to identify the advantages of the different separation processes and their overall plant operation behavior regarding performance and harmful substances for the different process steps.

Additional to the simulation of mass and energy balances, a profitability analysis of the modeled hydrogen production plant has been carried out. This analysis shows that the wood chip price is the most important factor for the hydrogen production cost followed by investment costs for the plant and realized plant operation time per year. The hydrogen production costs are expected with 54 €/MWh of hydrogen. Because of the insecurity about future costs and price development, additional scenarios have also been quantified. The additional scenarios also underline the big impact of the wood chip price on the production costs. If hydrogen can be produced from biomass at affordable costs, it strongly depends on the relation between biomass price and the price of traditional feedstock. Therefore, energy policy decision makers play a major role by taxing and subsidizing different feedstock. To achieve low hydrogen production costs, the plant operator needs an excellent management of the planning, construction, and operation phases.

Acknowledgments We would like to thank Professor Michael Harasek and Aleksander Makaruk from the Vienna University of Technology for their support and their contribution.

References

1. OECD/IEA (2008) World energy outlook 2008. International Energy Agency, Paris, pp 37–40, 401
2. Claasen P, Vrije T, Koukious E, Niel E, Eroglu I, Modigell M, Friel A, Wukovits W, Ahrer W (2010) Non-thermal production of pure hydrogen from biomass—hyvolution. J Clean Prod 18:1–5
3. Corbo P, Migliardini F (2007) Hydrogen production by catalytic partial oxidation of methane and propane on Ni and Pt catalyst. Int J Hydrogen Energy 32(1):55–66
4. Corbo P, Migliardini F (2009) Natural gas and biofuel as feedstock for hydrogen production on Ni catalysts. J Nat Gas Chem 18(1):9–14
5. Miltner A, Wukovits W, Pröll T, Friedl A (2010) Renewable hydrogen production—a technical evaluation based on process simulation. J Clean Prod 18:1–12
6. Kaltschmitt M, Hartmann H, Hofbauer H (2009) Energie aus Biomasse – Grundlagen, Techniken und Verfahren; 2.Auflage, Springer Verlag; 4
7. Pröll T, Hofbauer H (2008) H_2 rich syngas by selective CO_2 removal from biomass gasification in a dual fluidized bed system—process modelling approach. Fuel Process Technol 89:1207–1217
8. Pacalowska B, Whysall M, Narasimhan M. V. (1996) Improve Hydrogen Recovery from Refinery Offgases. Hydrocarbon Process 75:55–59
9. Waldron W, Sircar S (2000) Parametric study of a pressure swing adsorption process. Adsorption 6:179–188
10. Baker R (2002) Future directions of membrane gas separation technology. Ind Eng Chem Res 41:1393–1411
11. Schönberger C, Hofbauer H (2008) FT-Treibstoffe aus Biomasse in Österreich, Biomassepotential, Technologien und ökonomische und ökologische Relevanz; BMVIT – Energiesysteme der Zukunft; 18

Paper II

Müller, S., Kotik, J., Pröll, T., Rauch, R., Hofbauer, H.,

"Hydrogen from Biomass for Industry - Biomass Gasification for Integration in Refineries"

in: *Proceedings of the International Conference on Polygeneration Strategies (ICPS11)*, 30th August – 1st September, Vienna, Austria, **2011**

Hydrogen from Biomass for Industry – Biomass Gasification for Integration in Refineries

S.Müller[1], J.Kotik[1], T.Pröll[1], R.Rauch[1] and H.Hofbauer[1]

1. Vienna University of Technology, Institute of Chemical Engineering - Future Energy Technology, Getreidemarkt 9/166, 1060 Vienna, Austria

Abstract

This paper shows results of a simulation of a plant for the production of hydrogen with high purity for the direct integration in a refinery. The hydrogen production of the investigated case is based on a dual fluidized bed steam gasification system, a CO-shift step, CO_2-separation with a pressurized water scrubber, a PSA system, a steam reformer and advanced gas cleaning components. The implemented process configuration delivers hydrogen with a purity according to the demands of a modern refinery. The results show that 30 MW of hydrogen can be produced from 50 MW of wood chips. The main process steps of the simulated hydrogen production plant have been successfully demonstrated in industrial scale the past. The overall process configuration is the starting point for the basic engineering of a prototype plant. Crucial process components have been identified and are currently under investigation to prepare for demonstration at relevant scale in the near future.

Keywords: biomass, gasification, hydrogen, refinery, plant simulation

1. Introduction

Industrial production processes today are facing increasing challenges regarding their environmental, economical and social sustainability. Especially, the energy intensive industry is forced to look for new innovative solutions to cope the necessary reduction of CO_2 emissions, rising energy prices, and energy supply security. For the **reduction of CO_2 emissions** new approaches together with new concepts and new technologies need to aim at high energy efficiency and an efficient utilization of a rising share of renewable resources [1]. **Hydrogen** is an important commodity for production processes in a refinery. The production of hydrogen itself is therefore usually integrated into a refinery and fossil feedstocks such as natural gas or naphtha are typically used [2]. Most common method for the generation of hydrogen is production via natural gas steam reforming as shown in **Figure 1** [3]. This production process is based on a steam reformer, a CO-shift step and pressure swing adsorption (PSA). **Table 1** and **Table 2** show input and output data of a common hydrogen production plant. As can be seen hydrogen production via natural gas steam reforming leads to a significant consumption of natural gas and therewith of fossil resources. This conventional pathway of hydrogen production causes significant fossil CO_2 emissions on the site of a refinery. New concepts for the integration of renewable resources are investigated and should lead to a significant reduction of fossil CO_2 emissions. Previous efforts in this research area have focused on an increase of efficiencies of different existing concepts for the production of hydrogen from renewable resources.

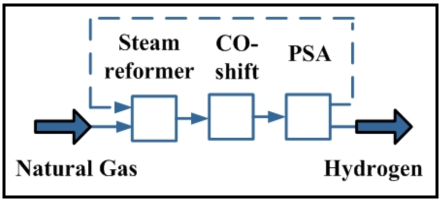

Fig. 1: Simplified H_2 production via natural gas steam reforming [3]

Plant input *		
Natural Gas**	Nm^3/h	3 822
Natural Gas (lhv)	MJ/Nm^3	36.91
Natural Gas (chem. en.)	MW	39.2
Electricity	MW	0.3
Steam (26 bar_{abs})	t/h	8.7
*Plant size [4] reduced to 30 MW H_2 Output (~16%)		
** Electricity for compressed natural gas 0.76 MW		

Tab. 1: Input H_2 production [4]

Plant output *		
Hydrogen	Nm^3/h	10 040
Hydrogen (lhv)	MJ/Nm^3	10.79
Hydrogen (chem. ener.)	MW	30
Steam (48 bar_{abs})	t/h	12.4

Tab. 2: Output H_2 production [4]

So far none of the concepts has been convincing enough to be realized in the scale of a large industrial demonstration plant. Possible methods for the production of hydrogen from renewable resources are alkaline electrolysis using green electricity, the reforming of biogas, coupled dark and photo fermentation, coupled dark and biogas fermentation as well as thermal gasification of biomass. From these processes alkaline electrolysis and thermal biomass gasification offer high energy efficiencies. But the electricity used in case of electrolysis is very valuable and can be used in many other ways. Thermal gasification of biomass has shown good production efficiencies and could be an efficient way for the production of hydrogen from renewable feedstock. At that point the choice for the proper production technology is strongly dependent on the local availability of raw materials [5]. In the past several research activities have demonstrated that biomass gasification is adequate for the production of hydrogen rich synthesis gas [6]. Furthermore, detailed simulation models have shown that hydrogen production based on biomass gasification can reach reasonable production efficiencies [7].

For the utilization in a refinery large amounts of hydrogen with high purity are needed. So far no large scale hydrogen production process from renewable resources, which would allow satisfying the needs of a refinery, has been demonstrated. Therefore, more research is necessary to develop such hydrogen production technologies and answer the following questions: Is it possible to meet the specifications of a refinery regarding hydrogen purity with renewable feedstocks on long term reliable basis? What are the production costs that can be achieved with such a technology?

Advanced gasification technologies combined with advanced gas cleaning strategies have shown appropriate characteristics which should technically allow meeting the high demands of a refinery. As a part of a precise evaluation this paper discusses

- a proper **process design**,
- the **simulation** of the whole production plant
- the analysis of the plant performance according to the **plant operation figures** and
- a **comparison** with hydrogen production via natural gas steam reforming.

2. Methodology and process description

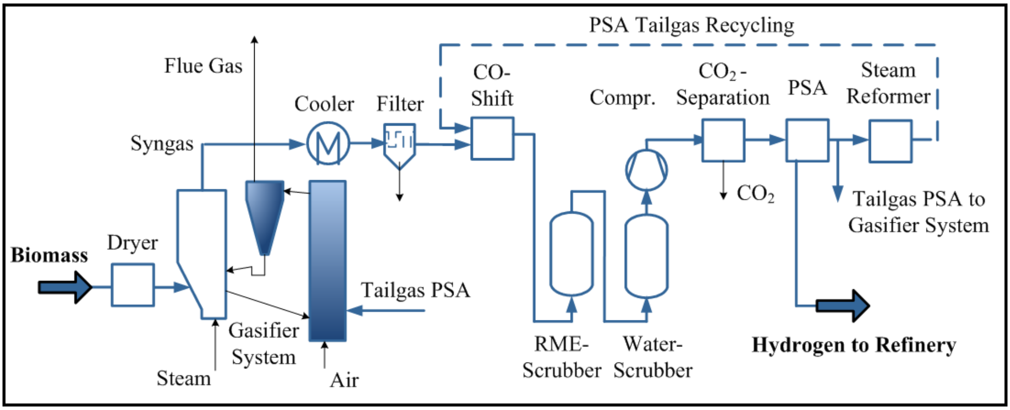

Fig. 2: Process design

For the evaluation of the developed hydrogen production process the plant simulation software IPSEpro has been used for the calculation of mass and energy balances. This allows a detailed insight into the plant performance and allows predictions regarding the operating behavior of the plant.

Figure 2 shows the process design for generation of high purity hydrogen for integration in a refinery. The displayed process design is based on a **dual fluidized bed steam gasification system** which converts solid biomass into syngas with high hydrogen content of about 40 vol% db. Wood chips with a water content of 40 wt% are used as fuel for the gasification unit. Before the wood chips enter the gasifier they are dried in a biomass dryer to a water content of 20 wt%. Low temperature process heat is used for the biomass dryer.

Downstream of the gasifier the produced syngas is cooled in a heat exchanger and cleaned in a bag filter where the dust is separated from the syngas stream. After that, the syngas is mixed with the recycled PSA tail gas. Subsequently, the gas stream is heated up to a temperature of about 300°C before entering a CO-shift unit. Herein, the CO content of the syngas is converted with steam to hydrogen and CO_2 on a CO-shift-catalyst. As CO-shift catalyst a sulfur resistant type is used.

$$CO + H_2O \leftrightarrow CO_2 + H_2$$
$$\Delta H^0_{R\,298} = -40.6 \text{ kJ/mol}$$

When the syngas has passed the shift stage the gas stream enters a scrubber operated with rape seed oil methyl ester (RME) followed by a scrubber operated with water. In these steps, condensable hydrocarbons (tars) are removed and water is condensed. The scrubber fluids are to be cooled to low temperatures to ensure the necessary separation efficiencies and to protect the subsequent PSA unit against condensing tars. After that, the syngas is compressed and CO_2 is removed in a pressurized water scrubber unit. After all these steps, hydrogen is recovered from the syngas using pressure swing adsorption (PSA). PSA units reach high separation efficiencies [8] and deliver hydrogen with high purity at high pressure. Furthermore, PSA units are relatively robust with respect to impurities like H_2S, HCN, NH_3 in the incoming gas stream. The PSA delivers hydrogen according to the demands of the refinery, which expects hydrogen with purity > 99.9 vol% and max. concentrations of

- CO < 10ppm,
- O_2 < 2.5ppm,
- H_2O < 2.5ppm and
- N_2 < 50ppm.

Syngas composition		
Syngas …	Gasifier exit	H_2-PSA exit
H_2 (vol%db)	40.2	99.9
CO (vol%db)	22.5	0.0
CO_2 (vol%db)	22.7	0.0
CH_4 (vol%db)	9.0	0.0
C_2H_4 (vol%db)	3.0	0.0
C_2H_6 (vol%db)	0.5	0.0
C_3H_8 (vol%db)	0.5	0.0
Other (vol%db)	1.6	0.1
H_2O (vol%)	34.7	0.0

Tab. 3: Syngas composition

An important aspect for high overall plant efficiency is the utilization of the left over tail gas from the PSA unit. The remaining tail gas has a high content of CH_4, C_2H_6 and C_3H_8. As can be seen in the displayed process design, a part of the tail gas is used as additional fuel for the combustion chamber of the gasification system.

The main part of the tail gas is fed into a steam reformer and recycled before the CO-shift unit to raise the overall hydrogen output of the plant. In most hydrogen production plants the steam reformer is arranged at the beginning of the syngas reforming. In this case the steam reformer is arranged at the end of the process as there are no steam reformers available for syngas with high dust content. Furthermore, after the PSA system the steam reformer has to operate smaller volume flows and smaller amounts of gas need to be heated up above 750°C.

The steam reforming of the PSA tail gas needs 3.5 MW of process heat which is mainly supplied by the combustion of a small share of the recycled PSA tail gas. In the detailed simulation model heat exchangers arrange the heat transfer of process heat between flue gas cooling, syngas cooling, steam production, combustion air pre heating, wood chips dryer and district heating.

Each single gas treatment step aims at a continuous, efficient and stable operation of the hydrogen production. Therefore, crucial gas and operating parameters have to be controlled. Crucial process parameters are:

- stable syngas composition,
- tar content and dust content in the syngas,
- nitrogen content, and
- chlorides, sulfur, etc. which influence the conversion efficiency of catalytic steps.

The dimensioning and the size of the PSA unit is, among other parameters, strongly dependent on the nitrogen content of the syngas. Therefore, CO_2 instead of N_2 is used as inertisation media in the gasification section, to suppress e.g. reflux of syngas into the biomass feeding system. This is done to keep the nitrogen content as low as possible. For stable operation of the plant it is important that the influence of the mentioned crucial process parameters stays within the allowed operation limits. Therefore, certain process components are currently under experimental investigation and long term performance tests.

3. Results and discussion

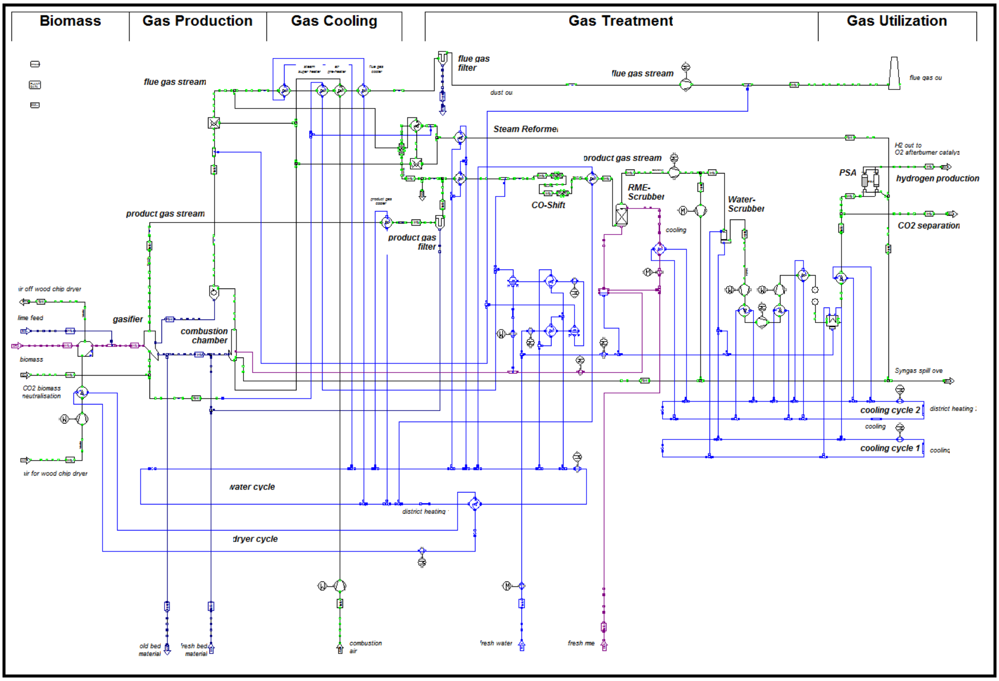

Fig. 3: Flow sheet of the hydrogen production plant in IPSEpro

Figure 3 displays the flow sheet of the whole hydrogen production plant. The process configuration as well as the predefinition of many operational parameters is strongly based on the experiences made in the past on industrial biomass gasification systems, gas cleaning and gas separation technologies as well as during experimental investigations in these fields. For the whole hydrogen production plant detailed mass and energy balances have been calculated.

The results show that **30 MW of hydrogen** with high purity can be produced from **50 MW of biomass** (based on the lower heating value) together with additional electricity and operational resources like lime and biodiesel (RME). In **Table4** and **Table5** the most important data obtained from the calculations are summarized. The produced 30 MW of hydrogen are delivered to the refinery. 18.8 tons/h of wood chips with a water content of 40 wt% are used as fuel for the gasification unit. Additionally to the fuel power of biomass 6.6 MW of electricity are needed.

The main share of this electricity is used for the compression of the syngas before entering the CO_2 scrubber and the PSA system. More investigations are necessary to determine the desired cooling temperatures and the achievable efficiency of CO_2 separation from syngas with the pressurized water scrubber. So far the already performed calculations give a good impression of the expected performance of the whole hydrogen production plant.

Plant input		
Biomass (wood chips)	kg/h	18 760
Biomass (water content)	wt%	40
Biomass (lhv)	MJ/kg	9.59
Biomass (chem. energy)	MW	50
Electricity *	MW	6.58
Air	Nm^3/h	57 400
Water	kg/h	3 327
* excl. Electricity for cooling and CO_2 separation		

Tab. 4: Plant input

Plant output		
Hydrogen	Nm^3/h	10 040
Hydrogen (lhv)	MJ/Nm^3	10.79
Hydrogen (chem. energy)	MW	30
Pure CO_2 (from separ.)	Nm^3/h	5 923
District heating	MW	8.9
Ash	kg/h	1 036
Flue gas	Nm^3/h	61 800

Tab. 5: Plant output

Besides 30 MW of hydrogen additional 8.9 MW of district heating can be provided. This process heat could also be employed in other ways like for the production of steam or for generation of electricity. The utilization of the valuable byproducts of the hydrogen production process at this stage strongly depends on the location of the plant and on the local demand. The results allow a comparison with the already well known and well described hydrogen production technology form natural gas via steam reforming (e.g**Table1** and **Table2**).

Figure 4 displays a comparison of the main production factors. Instead of 39.1 MW of natural gas 50 MW of wood chips are needed for the production of 30 MW of hydrogen. High syngas volume flows and the necessary compression of the syngas within the hydrogen production plant lead to 6.6 MW electricity consumption which reduces the overall plant efficiency. The comparison in **Figure 4** shows that hydrogen production via natural gas steam reforming is already a very efficient production method. Therefore, it is very hard to reach similar production efficiencies with technologies based on renewable solid feedstock. The high feedstock and electricity consumption contribute to the hydrogen production costs and may be critical to the process.

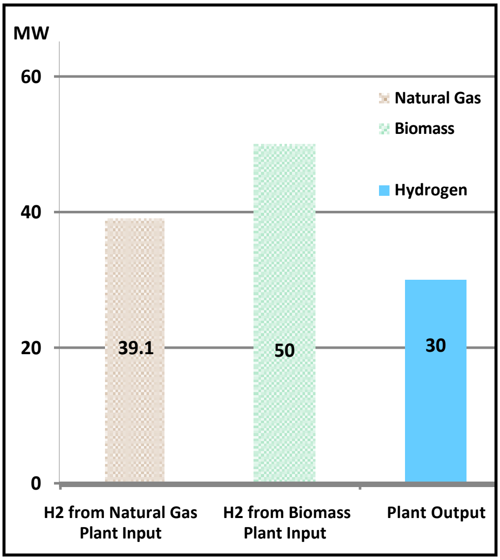

Fig. 4: Comparison of hydrogen production methods by primary feedstock input

4. Conclusion and outlook

This paper described a possibility for the production of hydrogen from renewable feedstock for the integration in a refinery. The described production method would enable the production of large amounts of hydrogen with high purity. The presented process configuration based on solid feedstock cannot reach production efficiencies similar to hydrogen production via natural gas steam reforming. Nonetheless, the results describe a pathway for the production of hydrogen from renewable feedstock according to the demands of a refinery. This would contribute to a reduction of CO_2 emissions and possibly raise the energy supply security by the utilization of local available feedstocks. At the same time wood is a scarce resource and has to be used with care in the most reasonable way. The possible achievements which can be made with the analyzed production technology are also highly depending on the local availability of adequate raw materials. Whether hydrogen can be produced from biomass at affordable costs will strongly depend on the relation between biomass price and the price of traditional feedstock [7]. Although main parts of the developed hydrogen production plant have been successfully demonstrated in the past the overall process configuration as described in this paper would represent a first plant of its kind.

In the upcoming months the overall concept will be investigated in more detail. Furthermore, a calculation of the expected production costs will be done as a part of a business case analysis.

5. Acknowledgements

The authors thank the “FFG & Klima und Energiefonds” and our project partners OMV AG, Repotec Umweltechnik GmbH, and Bioenergy2020+ for their support and their contribution.

6. References

[1] OECD/IEA (2010); World Energy Outlook 2010, IEA, Paris, pp. 435–437

[2] Corbo P., Migliardini F. (2009); Natural gas and biofuel as feedstock for hydrogen production on Ni catalysts. J Nat Gas Chem 18(1):9–14

[3] Spath P., Mann M. (2001); Life cycle assessment of hydrogen via natural gas steam reforming, National Renewable Energy Laboratory, pp. 3-5

[4] Spath P., Mann M. (2001); Life cycle assessment of hydrogen via natural gas steam reforming, National Renewable Energy Laboratory, Table 1

[5] Miltner A., Wukovits W., Pröll T., Friedl, A. (2010); Renewable hydrogen production - a technical evaluation based on process simulation. J Clean Prod 18:1–12

[6] Kaltschmitt M., Hartmann H., Hofbauer H. (2009); Energie aus Biomasse, Springer, Berlin Heidelberg, pp. 618-621

[7] Müller S., Stidl M., Pröll T., Rauch R., Hofbauer H. (2011); Hydrogen from Biomass – large-scale hydrogen production based on a dual fluidized bed steam gasification system; J Biomass Conv. Bioref. 1: 55-61

[8] Waldron W., Sircar S. (2000); Parametric study of a pressure swing adsorption process. Adsorption 6:179–188

Paper III

Müller, S., Pröll, T., Hofbauer, H.,

"A Thermodynamic Investigation of Dual Fluidized Bed Biomass Gasification with Sorption Enhanced Reforming"

in: *Proceedings of the 21st International Conference on Fluidized Bed Combustion (FBC)*, 3.-6. June 2012, Naples, Italy, pp.781-788, **2012**

A THERMODYNAMIK INVESTIGATION OF DUAL FLUIDIZED BED BIOMASS GASIFICATION WITH SORPTION ENHANCED REFORMING

S. Müller*, T. Pröll, H. Hofbauer

Institute of Chemical Engineering, Vienna University of Technology, Vienna, Austria
**Corresponding author, e-mail: stefan.mueller@tuwien.ac.at*

Abstract: A mass and energy balance model of a dual fluidized bed system for steam gasification of solid biomass is presented. The process model includes a description of solid streams and thermodynamic aspects of solids CO_2 transport capacity for selective CO_2 transport from the gasification zone to the combustion zone through a $CaO/CaCO_3$ system (sorption enhanced reforming). The model is able to verify experimental data with high hydrogen content in the product gas if adequate temperatures are operated in gasification and combustion zone. Parameter variations using the model show that there is a critical trade-off between CO_2 transport potential and global heat integration potential depending on the solids circulation rate operated. Based on typical CO_2 transport capacity values for calcium based sorbents dependent on cycle number, an optimum bed material renewal rate can be found. If a high H_2 content in the product gas is the main aim, high renewal rates and lower energy efficiency must be taken into account. Such a configuration may be suitable in combination with industrial units processing large amounts of limestone or lime.

Keywords: gasification, sorption enhanced reforming, modeling, biomass, thermodynamic limits

INTRODUCTION

Biomass steam gasification in a dual fluidized bed allows conversion of solid fuel into a medium calorific gaseous fuel mainly consisting of hydrogen, carbon monoxide, methane, carbon dioxide and water. The subsequent production of synthesis products like synthetic natural gas, liquid hydrocarbon fuels or even pure hydrogen, is currently investigated by several research groups around the world. So far demonstrated dual fluidized bed gasification units mainly used olivine as bed material and focused on the production of heat and electricity in gas engines (Hofbauer 2007). The application of limestone as bed material instead of olivine has been well known as a part of the sorption enhanced reforming process for many years and promises an improvement of the achievable gas composition by selective elimination of CO_2 from the product gas mixture (Koppatz 2008). But the achievable performance of limestone as bed material in a dual fluidized bed for sorption enhanced reforming is limited. In addition limiting key operation parameters like **reaction temperatures**, **solids circulation rate**, **bed material renewal rate** and **decay of CO_2-transport capacity** are significantly influencing the **cold gas efficiency.**

Discussions about the achievable efficiency of sorption enhanced reforming often lead to a situation where thermodynamic limitations are not adequately considered. The main limitation of the process results from the dilemma of suitable solids circulation rate. If the solids circulation rate is low, the sorbent capacity limits the amount of CO_2 transported from the gasifier to the combustor. If the solids circulation rate is high and provides enough transport capacity, the necessary temperature difference between gasifier (carbonator) and combustior (calcinator) cannot be kept. A precise description of the thermodynamics allows to direct specific experimental investigations based on the presented results. Activities of research and development already illustrated main limiting factors for sorption enhanced reforming in the past. Abanades (2002) showed an approach for the calculation of maximum CO_2 capture efficiency at the sorption enhanced reforming process. In a further step Abanades et al. (2003) demonstrated conversion limits in the reaction of CO_2 with lime by experimental investigations. Followed by Grasa et al. (2006) who illustrated the behavior of the CO_2 capture capacity of CaO in long series of sorption enhanced reforming by experimental investigations. The outcome of these works is a good basis for the assessment of achievable performance of CaO particles within the sorption enhanced reforming process. Limitations for the practical application of sorption enhanced reforming in a dual fluidized bed biomass gasification system were investigated by Soukup et al. (2009). Pfeifer et al. (2009) showed the results of experimental investigations with a 100 kW gasifier operating sorption enhanced reforming. Furthermore, Koppatz et al. (2009) showed the results of a large scale experiment with an 8 MW biomass gasification plant in Güssing, Austria. While the results of mentioned research activities showed promising aspects (Koppatz et al. 2009), the demonstration of large scale gasification systems using the sorption enhanced reforming still implies risks. Major risks for the process are loss of CO_2 transport capacity and high bed material consumption due to attrition (Soukup 2009). Both risks have a significant impact on the achievable process performance which is often underestimated. The question which overall plant performance could be theoretically achieved, has not been satisfactorily answered so far. The present work tries to find an answer to this question. Based on the earlier work of Pröll et al. (2008) the main objective of the present work is to illustrate the theoretical limitations of gasification supported by sorption enhanced reforming. Therefore, the thermodynamic limitations are investigated with a process modeling approach reflecting previous published experimental data. Existing limitations are investigated with a special focus on the theoretical achievable performance of lime stone particles. A thermodynamic variation of the performance of used solid particles is made while reaction temperatures and a constant describing the distance to water-gas-shift equilibrium are set as fixed values. Achieved findings and results should reveal fundamental relationships influencing the achievable energetic efficiency and enable a concise prediction of main relationships for the design of experimental facilities.

METHODOLOGY AND THEORETICAL BACKGROUND

The process simulation software IPSEpro is used for the calculation of the thermodynamic limits of gasification combined with sorption enhanced reforming. IPSEpro calculates mass- and energy balances for a created simulation model. **Fig. 1** (a) shows a schematic description of the investigated process configuration. This process configuration is modeled for a reference case. The reference case, shown in **Table 1**, reflects key operation parameters and should represent a starting point for variations investigating the theoretical limit for the process performance. Based on thermodynamic equilibrium calculations and achievable solid particles performance, the reachable energy efficiency is investigated. Data for solid particles performance are taken from experimental results of Grasa et al. (2006). Experimental results implemented in a validated simulation model should provide solid figures about the maximum achievable process performance.

The pictured reference case is the starting point for variations reflecting key operation parameters relevant for the design of experimental facilities as well as future industrial facilities. Key operation parameters are reaction temperatures, the solids circulation rate, the bed material renewal rate and the decay of CO_2-transport capacity. As already mentioned in the introduction, carried out variations are made with a special focus on the thermodynamic performance of used solid particles. During the variations **reaction temperatures** are defined as **constant values** which enhance the carbonation and calcination reaction. Lower gasification temperatures favor selective transport of CO_2 from the gasifier to the combustor due to the equilibrium of the carbonation reaction. Additionally, this leads to a higher H_2

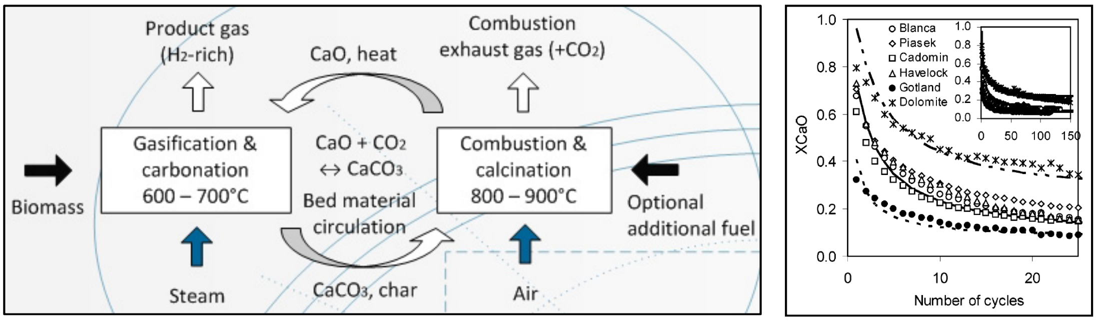

Fig. 1: (a - left) Steam gasification with selective transport of CO_2 (sorption enhanced reforming) by Pröll et al. (2008), (b - right) Molar transport capacity of CaO particles (X_{CaO}) after N numbers of carbonation-calcination cycles based on experimental results for different lime stones by Grasa et al. (2006)

Table 1: Reference case for variations within the created IPSEpro simulation model

Constant parameters during simulation runs	Symbol	Unit	Reference case value
Thermal fuel power (LHV of biomass, water content 20%)	P_{th}	kW	10 000
Optional additional fuel power	P_A	kW	0
Heat loss of overall system	Q_{loss}	kW	225
Gasification temperature	T_G	°C	645
Combustion temperature	T_R	°C	900
Air ratio for combustion	λ_R	-	1.1
Share of CO in relation to CO_2 in combustor exhaust gas	σ_{CO}	mol/mol	0
Fluidization air temperature	$T_{fluid,R}$	°C	450
Fluidization steam temperature	$T_{fluid,G}$	°C	450
Fluidization mass flow gasifier (steam)	$\dot{m}_{fluid,G}$	kg/h	600
Share of CaO in bed material entering the gasifier from combustor	$\omega_{CaO,bed,G,in}$	kg_{CaO}/kg_{bed}	0.85
Share of $CaCO_3$ in bed material entering the gasifier from combustor	$\omega_{CaCo3,bed,G,in}$	kg_{CaCo3}/kg_{bed}	0.15
Total amount of bed material within the system	$m_{inventory}$	kg	3 000
Amount of bed material within gasifier	$m_{gasifier}$	kg	1 500
Cross-sectional area of gasifier	A_G	m²	2.95
Logarithmic distance to equilibrium (water-gas-shift reaction, gasifier)	$\delta_{Eq.,WGS\text{-}shift}$	-	0.0

content in the product gas stream. But at the same time, lower gasification temperatures reduce a favorable gasification process constraining char gasification reactions due to short residence times of solid fuel particles at low gasification temperatures (Florin 2008). Therefore set values for reaction temperatures are based on experimental results which demonstrated a stable operation of gasification by sorption enhanced reforming (Koppatz et al. 2009). Lower combustion temperatures would increase the cold gas efficiency while higher combustion temperatures favor the calcination reaction which is especially important when low residence times occur or oxyfuel combustion is applied. The combustion temperature (900°C) has been set on a quite high level and favors calcination reactions at low residence times. Solids circulation rate is investigated by the calculation of the introduced parameter **calcium circulation rate**. The calcium circulation rate is introduced with respect to the performance of solid CaO particles. Therefore, following equation is used:

$$(1) \qquad \delta_{CaO} = \frac{\dot{m}_{bed,G,in} \cdot \left(\frac{\omega_{CaO,bed,G,in}}{M_{CaO}} + \frac{\omega_{CaCO_3,bed,G,in}}{M_{CaCO3}}\right)}{m_{inventory} \cdot \left(\frac{\omega_{CaO,inventory}}{M_{CaO}} + \frac{\omega_{CaCO_3,inventory}}{M_{CaCO3}}\right)}; \qquad [s^{-1}]$$

The solids circulation rate describes the transition of a potentially active mol of CaO on its way between carbonation and calcination within the overall gasifier system. The **bed material renewal rate** is a further important key figure for the overall process performance. Following equation is used for the calculation of the bed material renewal rate:

$$(2) \qquad \kappa_{CaO} = \frac{\dot{m}_{bed,fresh} \cdot \left(\frac{\omega_{CaO,bed,fresh}}{M_{CaO}} + \frac{\omega_{CaCO_3,bed,fresh}}{M_{CaCO3}}\right)}{m_{inventory} \cdot \left(\frac{\omega_{CaO,inventory}}{M_{CaO}} + \frac{\omega_{CaCO_3,inventory}}{M_{CaCO3}}\right)}; \qquad [s^{-1}]$$

Additional fresh bed material is necessary to maintain the **CO_2 transport capacity** of CaO particles because of the decay of transport capacity after N cycles as shown in **Fig. 1**. Therefore, fresh $CaCO_3$ is fed to the bed material circulation loop just before the combustion and calcination step. A high bed material renewal rate raises the CO_2 transport capacity of the bulk bed material in circulation, increases the selective transport of CO_2 from the gasifier but at the same time reduces the cold gas efficiency. The CO_2 transport capacity of the bed material is therefore a further central key figure for the process. The following equations are used for the calculation of the CO_2 transport capacity based on a mass and molar perspective:

$$(3)\qquad \varphi_{CaO} = \frac{\dot{m}_{CO2,capt}}{\dot{m}_{bed,G,in} \cdot \left(\omega_{CaO,bed,G,in} + \omega_{CaCO_3,bed,G,in} \cdot \frac{M_{CaO}}{M_{CaCO3}} \right)}; \qquad \left[\frac{kg_{CO2}}{kg_{CaO}}\right]$$

$$(4)\qquad X_{CaO} = \frac{\frac{\dot{m}_{CO2,capt}}{M_{CO2}}}{\dot{m}_{bed,G,in} \cdot \left(\frac{\omega_{CaO,bed,G,in}}{M_{CaO}} + \frac{\omega_{CaCO_3,bed,G,in}}{M_{CaCO3}} \right)}; \qquad \left[\frac{mol_{CO2}}{mol_{CaO}}\right]$$

High CO_2 transport capacity improves the selective transport of CO_2 from the gasifier to the combustion chamber and therefore, increases the product gas quality by reducing the CO_2 content of the product gas. The described equations have been implemented in IPSEpro and enable a discussion of relevant parameters within the process simulation environment based on existing experimental data.

Fig. 2 shows the approach of the used simulation model. Within the created simulation model relevant mass streams are modeled as represented by arrows in **Fig. 2**. Variations should show the energetic behavior of biomass steam gasification by sorption enhanced reforming. The variation steps are carried out with respect to achievable cold gas efficiency, product gas composition, bed material consumption and key parameters for the design of experimental facilities.

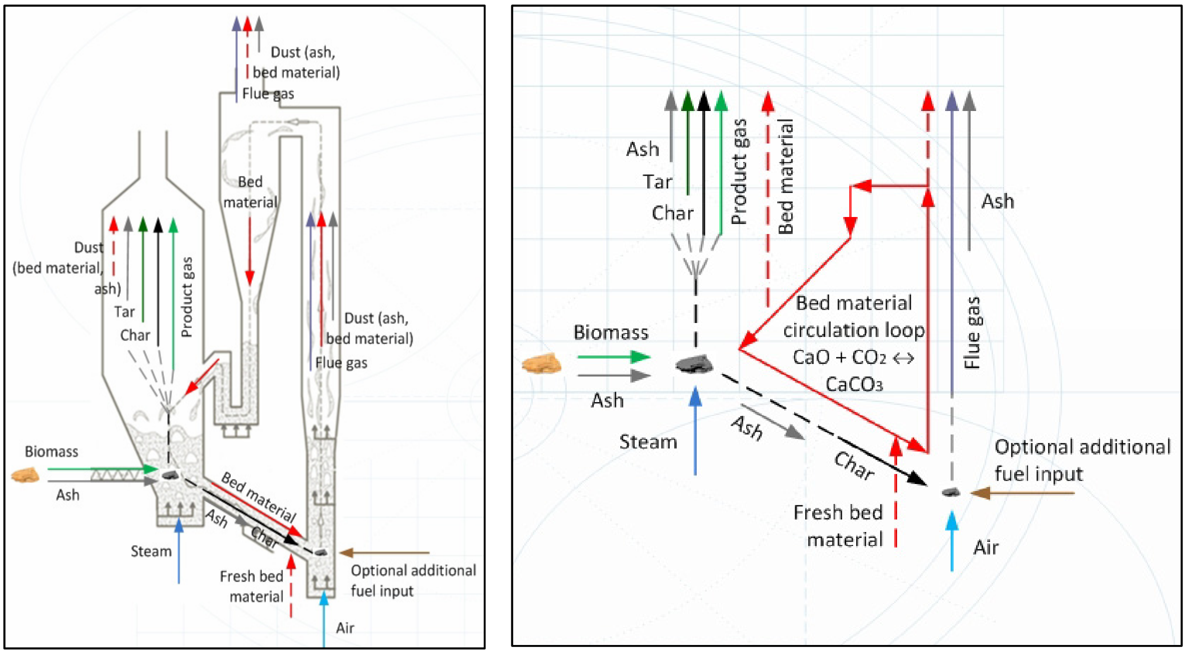

Fig. 2: Schematic representation of mass streams calculated within the IPSEpro simulation model of gasification by sorption enhanced reforming. Illustration based on Schmid, J.C. (2012)

The following important equations have been used additionally within the simulation model:

$$(5)\qquad 10^{\delta_{Eq.WGS-shift}} \cdot K_p(T) = \frac{p_{co2} \cdot p_{H2}}{p_{co} \cdot p_{H2O}} \text{ [-]}; \qquad (6)\qquad \tau_{CaO} = \frac{1}{\kappa_{CaO}} \text{ [s]};$$

$$(7)\qquad N = \tau_{CaO} \cdot \delta_{CaO} \text{ [-]}; \qquad (8)\qquad \eta_{chem} = \frac{P_{pg}}{P_{th}} \text{ [-]};$$

Table 2: Variations carried out within the created simulation model

Nr.	Variation parameters	Sym.	Unit	Values	Results	Additional constants[1]
1	CO_2 transport capacity	X_{CaO}	$[mol_{CO2}/mol_{CaO}]$	0.0 - 0.55	Fig. 4 (b), Fig. 5 (b), Fig. 6 (a), Fig. 6 (b)	κ_{CaO} = 0.065* *equals $\dot{m}_{bed,fresh}$ = 200 kg/h
2	CO_2 transport capacity bed material renewal rate	X_{CaO} κ_{CaO}	$[mol_{CO2}/mol_{CaO}]$ $[h^{-1}]$	0.1 - 0.8 0.0 - 1.0	Fig. 4 (a)	-
3	CO_2 transport capacity mean cycle number	X_{CaO} N	$[mol_{CO2}/mol_{CaO}]$ [-]	0.0 - 0.85 5 – 100	Fig. 5 (a)	-

[1] Variations are based on reference case in Table 1. Additional constants are added for a single variation to enable a specific investigation case

RESULTS AND DISCUSSION

Fig. 3 shows the flow chart of the created simulation model based on the simplified modeling approach shown in **Fig. 2**. Several variations illustrated in **Table 2** based on the reference case shown in **Table 1** were carried out.

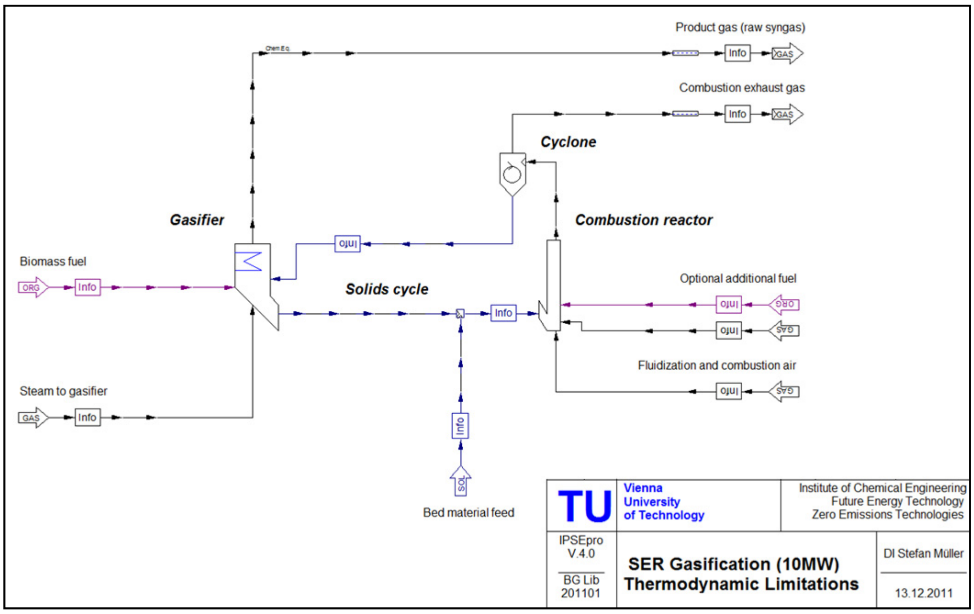

Fig. 3: Simulation model of sorption enhanced reforming in dual fluidized bed gasification system

Cold Gas Efficiency & Product Gas Composition

Achievable cold gas efficiency is strongly determined by temperatures, fuel composition, fuel water content and heat losses. Cold gas efficiency is furthermore depending on the bed material renewal rate as shown in **Fig. 4** (a). Large amounts of fresh $CaCO_3$ entering the system raise the heat demand in the combustion chamber for calcination and maintaining the necessary temperatures. Furthermore, low CO_2 transport capacity of the circulating bed material raises the necessary amount of circulating bed material to maintain the process. According to the described relationships bed material renewal rates should be kept on a low level with in terms of cold gas efficiency. The composition of the product gas is strongly depending on the selective transport of CO_2 from the gasifier to the combustion chamber. Therefore, the CO_2 transport capacity of the circulating bed material has a major influence on the product gas composition. This dependency is shown in **Fig. 4** (b). The equilibrium of the water-gas-shift reaction has

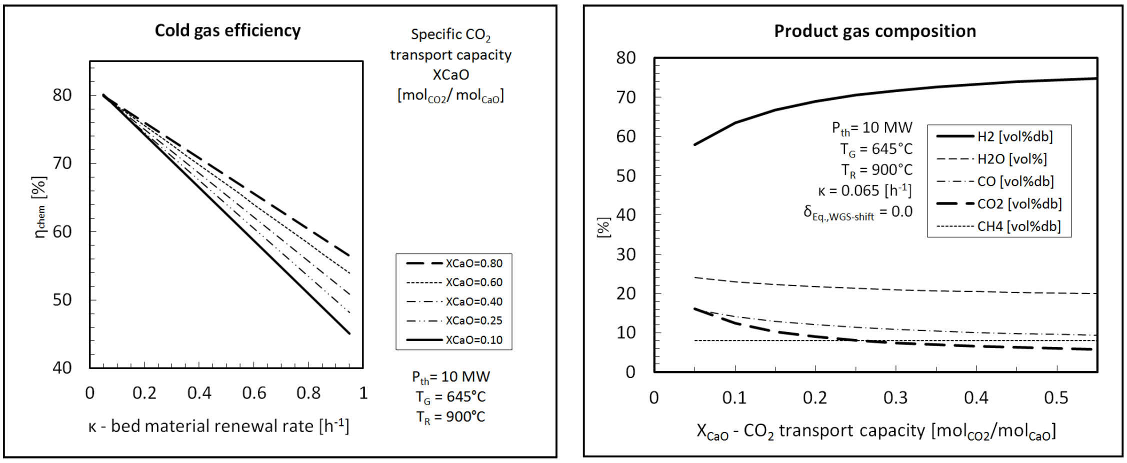

Fig. 4: (a - left) Cold gas efficiency depending (η_{chem}) on bed material renewal rate, (b - right) Product gas composition depending on CO_2 transport capacity of circulating bed material.

been an important precondition for the calculation of the composition of the product gas at the exit of the gasifier. Solid particles with high CO_2 transport capacity would raise the H_2 content in the product gas. At the same time high bed material renewal rates would be necessary to keep the transport capacity at high levels with respect to the findings of Grasa et al. (2006) shown in **Fig. 1**. Favorable product gas compositions and high cold gas efficiency can therefore be identified as an important trade-off of gasification with sorption enhanced reforming. An improvement of product gas composition by the operation of higher bed material renewal rates leads to a reduction of cold gas efficiency. In specific cases this reduction of the cold gas efficiency can be prevented by arranging the process along industrial processes involving a certain lime and/or limestone throughput.

Bed Material Consumption

CO_2 transport capacity of circulating solid particles is a limiting parameter for the overall process. The practical performance of different lime stones has a strong influence on **bed material consumption**. Low transport capacity after low cycle numbers (N) leads to a high demand for bed material renewal. The practical performance of solid particles directly influences bed material consumption and cold gas efficiency. **Fig. 5** (a) shows necessary bed material renewal rates for different transport capacities of lime stone particles after different mean cycle numbers completed. A real system includes bed material inventory which consist of different fractions of solid particles which experienced a different number of cycles. Within the simulation model the occurring cycle number distribution of the operating bed material is represented by the parameter N (mean cycle number). Furthermore, it has been assumed that solid particles are ejected at random and old solid particles are not discharged selectively from the operating bed material. This simplified approach has to be acknowledged at the evaluation of the results.

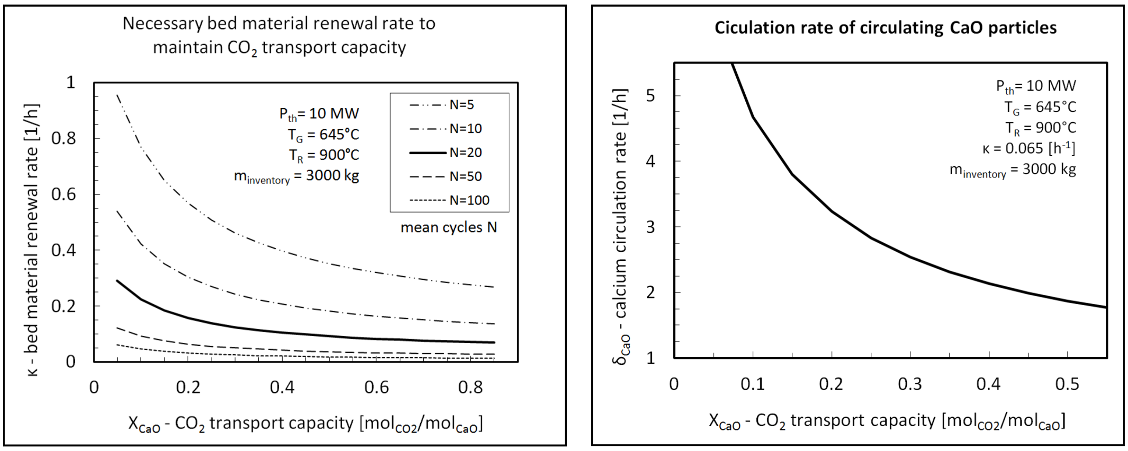

Fig. 5: (a - left) Necessary bed material renewal for constant CO_2 transport capacity,
(b - right) Circulation rate of CaO particles

As it can be seen, low CO_2 transport capacity of a certain lime stone after low cycle numbers, leads to a high demand for bed material renewal. High bed material renewal rates at the same time reduce the cold gas efficiency. This relationship underlines once more the long time performance of circulating solid particles as a key factor for the overall process. Lime stones with a low decay of CO_2 transport capacity after long time operation are needed for high cold gas efficiency and a desired product gas composition. Otherwise high bed material consumption could be a significant disadvantage for the realization of sorption enhanced reforming. **Fig. 5** (b) additionally shows the calcium circulation rate for solid CaO particles with different transport capacity. High CO_2 transport capacities enable a lower cycling rate because necessary heat for the gasification is transported in form of latent heat together with bound reaction energy of the carbonation reaction. Simulation results shown in **Fig. 5** (b)show necessary circulation rates which were calculated for a fixed bed material renewal rate of $\kappa = 0.065$ per hour. This value equals 200 kg of fresh bed material per hour according to the set reference case. A low bed material renewal rate is desired to keep cold gas efficiency high and bed material consumption low. Attrition and or decay of CO_2 transport capacity can be limiting parameters which demand for higher bed material renewal rates. This tradeoff therefore has a strong influence at the necessary circulation rate depend on solids particle performance. The attrition of solid particles is at the same time strongly dependent on the used solids separation systems, the mechanical stability of used bed material and velocities maintained within the dual fluidized bed system.

Key Parameters for the Design of Experimental Facilities

Relevant key parameters for the design of facilities operating the investigated process are **volume flows** and **bed material circulation** in kg/h. Volume flows need to be considered during the dimensioning of the dual fluidized bed system hosting the process. **Fig. 6** (a) shows the influence of the selective transport of CO_2 from the gasification reactor to the combustion reactor.

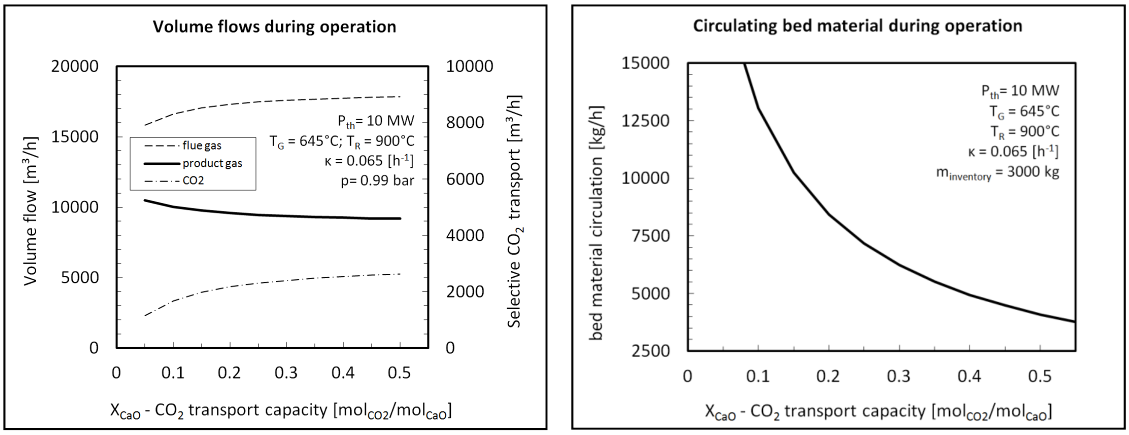

Fig. 6: (a) Volume flows during operation, (b) Amount of circulating bed material during operation

As it can be seen, selective transport of CO_2 has only a small impact on the operational volume flows. Nevertheless, changes of volume flows need to be considered regarding the influence on the fluid dynamics within the system. **Fig. 6** (b) shows the necessary bed material circulation for the gasification by sorption enhanced reforming for different CO_2 transport capacities of the operating bed material. As can be seen from **Fig. 6** (b), the bed material circulation is strongly influenced by CO_2 transport capacity. This relationship should be considered before the design of experimental facilities.

CONCLUSIONS

The achieved results highlight main relationships within the process of gasification by sorption enhanced reforming. A simple model reveals important aspects of the process. The decay of CO_2 transport capacity with an increased number of carbonation/calcinations cycles has been previously identified as a key factor for the performance of gasification by sorption enhanced reforming. The optimum bed material circulation rate is determined by the energy balance of the system requiring the temperature levels for carbonation and calcination. As a consequence, the transport capacity of the sorbent directly determines the achievable product gas composition. In order to compensate the decay of CO_2 transport capacity after several calcination and carbonation cycles, continuous addition of fresh bed material is necessary to maintain a certain desired product gas composition. Significant bed material make-up rates, however, reduce in most cases the cold gas efficiency. It is important to note that the use of lime/limestone in biomass gasification shows advantages such as low tar content even if the selective CO_2 transport is moderate. A certain make-up rate will always be required in order to compensate for attrition. Low mechanical stability of the used bed material therefore can be a further constraint for the process which would lead to reduced cold gas efficiency. Mechanical stability of different lime stones itself (Koppatz et al. 2009) has been beyond the focus of present work. But, the effect of necessary bed material renewal on cold gas efficiency due to attrition can be estimated with the results shown in **Fig. 4**. Further research should identify realistic process scenarios considering both, capacity decay and attrition. Additional, reduced cold gas efficiency can be prevented in specific cases. If high H_2 contents are the primary aim, the process could be arranged along with industrial processes involving a certain limestone throughput.

ACKNOWLEDGEMENT

The authors acknowledge financial support by the Austrian government through the "Klima- und Energiefonds" financed Project ERBA within the “Neue Energien 2020” funding scheme, in cooperation with voestalpine Stahl GmbH and voestalpine Stahl Donawitz GmbH & Co KG.

ABBREVATIONS

A_G	[m²]	Cross-sectional area of gasifier
$K_p(T)$	[-]	Equilibrium constant
$\dot{m}_{bed,fresh}$	[kg/h]	Fresh bed material ($CaCO_3$) entering bed material circulation loop
$\dot{m}_{bed,G,in}$	[kg/h]	Massflow of bed material entering the gasifier from combustor
M_{CaCO3}	[g/mol]	Molar weight of $CaCO_3$
M_{CaO}	[g/mol]	Molar weight of CaO
M_{CO2}	[g/mol]	Molar weight of CO_2
$\dot{m}_{CO2,capt}$	[kg/h]	Massflow of CO_2 absorbed by bed material within gasifier
$\dot{m}_{fluid,G}$	[kg/h]	Fluidization mass flow gasifier (steam)
$m_{gasifier}$	[kg]	Amount of bed material within gasifier
$m_{inventory}$	[kg]	Total bed material within system
N	[-]	Mean cycles of particle within system
P_A	[kW]	Optional additional fuel power
p_{CO}	[Pa]	Partial pressure of CO in product gas
p_{CO2}	[Pa]	Partial pressure of CO_2 in product gas
p_{H2}	[Pa]	Partial pressure of H_2 in product gas at
p_{H2O}	[Pa]	Partial pressure of H_2O in product gas
P_{PG}	[kW]	Product gas power, LHV based, (Boie)
P_{th}	[kW]	Thermal fuel power, LHV based
Q_{loss}	[kW]	Heat loss of overall system
$T_{fluid,G}$	[°C]	Fluidization steam temperature

$T_{fluid,R}$	[°C]	Fluidization air temperature
T_G	[°C]	Gasification temperature
T_R	[°C]	Combustion temperature
X_{CaO}	[mol_{CO2}/mol_{CaO}]	CO_2 transport capacity
δ_{CaO}	[s^{-1}]	Calcium circulation rate
$\delta_{Eq.,WGS-shift}$	[-]	Logarithmic distance to equilibrium (water-gas-shift reaction, gasifier)
η_{chem}	[-]	Cold gas efficiency
κ_{CaO}	[s^{-1}]	Bed material renewal rate
λ_R	[-]	Air ratio for combustion
σ_{CO}	[mol/mol]	CO / CO_2 in combustor exhaust gas
τ_{CaO}	[s]	Mean time of particle within system
φ_{CaO}	[kg_{CO2}/kg_{CaO}]	CO_2 transport capacity
$\omega_{CaCo3,bed,fresh}$,	[$kg_{CaCO3}/kg_{bed,fresh}$],	$CaCO_3$ in fresh material
$\omega_{CaCo3,bed,G,in}$,	[kg_{CaCO3}/kg_{bed}],	$CaCO_3$ in bed material to gasifier from combustor
$\omega_{CaCo3,inventory}$,	[kg_{CaCO3}/kg_{bed}],	$CaCO_3$ in bed mat. inventory
$\omega_{CaO,bed,fresh}$,	[$kg_{CaO}/kg_{bed,fresh}$],	CaO in fresh bed material
$\omega_{CaO,bed,G,in}$,	[kg_{CaO}/kg_{bed}],	CaO in bed material to gasifier from combustor
$\omega_{CaO,inventory}$,	[kg_{CaO}/kg_{bed}],	CaO in bed mat. inventory

REFERENCES

Abanades, J.C.: The maximum capture efficiency of CO_2 using carbonation/calcinations cycle of CaO/$CaCO_3$; Chemical Engineering Journal 90, pp.303-306, 2002

Abanades, J.C., Alvez, D.: Conversion Limits in the Reaction of CO_2 with Lime; Energy & Fuels 17, pp. 308-315, 2003

Florin H.F, Harris A.T: Review – Enhanced hydrogen production from biomass with in situ carbon dioxide capture using calcium oxide sorbents, Chemical Engineering Science 63, pp.287-316, 2008

Grasa G.S., Abanades, J.C.: CO2 Capture Capacity of CaO in Long Series of Carbonation/Calcination Cycles, Ind. Eng. Chem. Res., 45, p8856-8851, 2006

Hofbauer, H.: Conversion technologies: gasification overview, Proceedings of the 15th European Biomass Conference & Exhibition, pp. 5–10., Berlin, Germany, 2007

Koppatz, S.: Insitu Produktgaskonditionierung durch selektive CO_2-Abscheidung bei Wirbelschicht Dampfvergasung von Biomasse: Machbarkeitsnachweis im industriellen Maßstab; master thesis,Vienna University of Technology, 2008

Koppatz, S., Pfeifer, C., Rauch, R., Hofbauer H., Marquard-Moellenstedt, T., Specht, M.: H_2 rich product gas by steam gasification of biomass with in situ CO_2 absorption in dual fluidized bed system, Fuel Processing Technology, 90, pp.914–921, 2009

Pfeifer, C., Puchner, H., Hofbauer, H.: Comparison of dual fluidized bed steam gasification with and without selective transport of CO_2, Chemical Engineering Science 64, pp.5073 – 5083, 2009

Pröll, T., Hofbauer, H.: H_2 rich syngas by selective CO_2 removal from biomass gasification in a dual fluidized bed system – Process modeling approach; Fuel Processing Technology, 89, pp.1207-1217, 2008

Schmid, J.C., Wolfesberger, U., Koppatz, S., Pfeifer, C., Hofbauer, H.; Variation of Feedstock in a Dual Fluidized Bed Steam Gasifier – Influence on Product Gas, Tar Content, and Composition; Environmental Progress & Sustainable Energy, to be published, 2012

Soukup, G.: Der AER Prozess, Weiterentwicklung in einer Technikumsanlage und Demonstration an einer Großanlage, PHD Thesis, Institute of Chemical Engineering, Vienna University of Technology, 2009

Soukup, G., Pfeifer, C., Kreuzeder, A., Hofbauer, H.: In Situ CO_2 Capture in a Dual Fluidized Bed Biomass Steam Gasifier – Bed Material and Fuel Variation; Chem. Eng. Technol. 32, No.3, pp.348-354, 2009

Curriculum Vitae

Personal Data

Name:	Ing. Dipl.-Ing. Stefan Müller
Birthday:	27.3.1984
Place of birth:	Vienna
Nationality:	Austria

Education

since 10/2009	**Vienna University of Technology** PhD - student of chemical engineering Research area: “Future Energy Technology” PhD thesis: „ Hydrogen from Biomass for Industry – Industrial Application of Hydrogen Production Based on Dual Fluid Gasification”
10/2004 – 10/2009	**Vienna University of Technology** Student of industrial engineering with focus on production and product management Master thesis: „Acquisition Analysis for Wheel Loader Components within the US$-market”
10/2004 – 02/2005	**Vienna University** Student of law (1 semester)
09/1998 – 06/2003	**TGM Vienna** Higher School of Technology Student of industrial engineering with focus on environmental economics Final thesis: „Outsourcing of Logistics Services”

Job Experience

since 03/2010	**Vienna University of Technology** Researcher at the Institute of Chemical Engineering, with focus on "Future Energy Technology", Development of energy supply concepts for industrial applications, Research partners: OMV, VOEST, SCA Member of the team for the development and the construction of the "Next Generation Dual Fluid Gasifier"
03/2009 – 06/2009	**Liebherr-Werk Bischofshofen Gmbh, Bischofshofen** Department of Strategic Purchase, Procurement market research, Supply chain logistics
04/2006 – 12/2006	**Fraunhofer & Vienna University of Technology** Institute for Management Sciences, Project group Production Management und Logistics, Scientific employee
07/2006 – 09/2006, 07/2005 – 09/2005	**Kosciuszko Thredbo Pty Ltd, Thredbo - Australia** Snow sports department, snow sports coach Award-winner: Instructor of the year 2005
05/2004 – 07/2004	**Syscom Emirates LLC, Dubai - United Arabic Emirates** Assistant to chief executive officer (CEO)
2000 – 2013	**Schi- und Snowboardschule Zell am See** Ski instructor for all ages and levels

Obligatory Military Service

07/2003 – 02/2004	**Austrian Military** Paramedic

Non-Academic Engagement

21.05.2000	Marathon finisher, Vienna City Marathon
10/2001 – 10/2002	TGM, deputy of student representative (3000 pupils)
10/2002 – 10/2003	TGM, student representative of the department "Industrial Engineering" (600 pupils)
08/2004 – 06/2008	FC DSG Weasel United (soccer), player, official
10/2006 – 10/2012	EHC Wolfersberg (ice hockey), player, official
26.08.2012	Ironman Finisher – 70.3 Zell am See, Kaprun

Languages

German	Native speaker
English	Fluent written and spoken

Special Knowledge

Office, Catia, Autocad, Mathcad, MS Project,

Certified project manager, IPMA D

Approved delegate in waste management, Approved safety management consultant

Approved ski and snowboard instructor, Salzburg, Austria

Approved ski instructor for disabled people, Australia

Driver license B

Interests

Reading, music, technology, sport, skiing, ice hockey, running, triathlon, fitness

Vienna, April 15th, 2013

Ing. Dipl.-Ing. Stefan Müller